Characterization of the Molecular Basis of Regulation of Gene Expression by Metals in Methanotrophs

by

Christina S. Kang-Yun

A dissertation submitted in partial fulfillment
of the requirements for the degree of
Doctor of Philosophy
(Environmental Engineering)
in the University of Michigan
2021

Doctoral Committee:

Professor Jeremy D. Semrau, Chair
Professor Alan A. DiSpirito
Professor Peter F. Dunfield
Associate Professor Brian R. Ellis
Professor Patrick D. Schloss
Professor Thomas M. Schmidt

Christina S. Kang-Yun

csrkang@umich.edu

ORCID iD: 0000-0001-5536-3253

Acknowledgements

I would like to thank my advisor, Professor Jeremy D. Semrau, who put faith in me when I most doubted myself. He guided me through my PhD research and provided life and career advice that was truly invaluable. He is and will be my inspiration in research and teaching, and I hope to be able to also inspire future generation of researchers and students.

I also extend my gratitude to my dissertation committee members, Professors Alan A. DiSpirito, Peter F. Dunfield, Brian R. Ellis, Patrick D. Schloss, and Thomas M. Schmidt. I am grateful for the comments and feedback that improved my thesis, as well as encouragements that reassured me of my progress and achievements.

I would also like to take this opportunity to thank my lab mates who helped me throughout my study. Dr. Wenyu Gu helped me settle in the lab and continued to support me even after leaving UM. My fellow lab mates Katy Teske, Dr. Peng Peng, Dr. Jin Chang, and Junwon Yang all had a hand in taking measurements and harvesting samples at times when I could not be in the lab myself.

Last but not least, I would like to thank my family. I thank my parents and in-laws who provided financial and emotional support from afar. I would not have been able to complete my studies without the support of my husband, Chan-Young Yun, who always put family first. I am grateful for my understanding son Lyle Yun, who motivated me to put in a 110% effort. I am also thankful for my youngest son, Theo Yun, who accompanied me on my journey to finishing my thesis and was my personal cheerleader. I am grateful for the experience I have had at UM and will forever cherish the memories.

Table of Contents

List of Tables

List of Figures

Abstract

Methane-oxidizing bacteria, or methanotrophs, can use methane as their sole carbon and energy source, and have a wide range of applications including: (1) methane removal from the atmosphere, (2) pollutant degradation, and (3) valorization of methane. Such applications are strongly dependent on copper and rare earth elements (REEs) due to their central role in regulating the metabolism of methanotrophs. To fully utilize these intriguing microbes for various applications, the genetics and biochemistry of metal uptake systems in methanotrophs must thus be identified and characterized.

To address this general goal, this work first sought to characterize the evolution of methanotrophs to glean insights into potential uptake systems of copper and REEs, and to develop strategies to optimize their production for industrial and medical applications. Bioinformatic analyses suggested that methylotrophs with preexisting copper uptake system(s) may have evolved into methanotrophs with the lateral gene transfer of methane monooxygenase, the critical enzyme that oxidizes methane to methanol in methanotrophs. In addition, lateral gene transfer events of methanol dehydrogenase (MeDH) with a REE active site (Xox-MeDH) were more prevalent than those of MeDH with Ca^{2+}. This may be attributable to the higher catalytic efficiency of the former MeDH, which consequently increased the fitness of methanotrophs with multiple copies.

Second, competition between methanotrophs for copper was investigated to identify "cheating" behavior amongst methanotrophs and determine how the collective activity of methanotrophs is affected. Some methanotrophs produce methanobactin (MB), a chalkophore

that can strongly bind and deliver copper. It was found that methanotrophs *Methylomicrobium album* BG8 and *Methylocystis* sp. strain Rockwell, both non-MB producers, can take up MB, while *Methylococcus capsulatus* Bath cannot. In addition, *Mmb. album* BG8 was found to produce a novel chalkophore yet to be characterized. Moreover, *Mmb. album* BG8 and *Methylocystis* sp. strain Rockwell could also take up methylmercury-MB (MeHg-MB) complex and subsequently demethylate MeHg into the less toxic inorganic mercury. The results of this study provide insight into copper competition between methanotrophs and potential applications exploiting such interaction, such as MeHg remediation.

Finally, the mechanism of methanotrophic-mediated MeHg demethylation was investigated. It has been found that MB serves as a delivery mechanism for MeHg into the cell of methanotrophs, where Xox-MeDH contributes to demethylating MeHg. The genes encoding for organoarsenical lyase (ArsI), responsible for cleaving the carbon-arsenic bond, and lanmodulin (LanM), a periplasmic REE-binding protein, were each knocked out in wildtype *Methylosinus trichosporium* OB3b. Deletion of *arsI* did not affect MeHg degradation in the *Msn. trichosporium* OB3b Δ*arsI* mutant. However, the Δ*lanM* mutant was unable to degrade MeHg under all conditions tested, suggesting *lanM* to be critical for MeHg degradation. In addition, a spheroplast prepared from *Msn. trichosporium* OB3b Δ*mbnT* mutant exhibited decreased MeHg degradation, whereas greater MeHg degradation was observed in the extract containing the periplasm and outer membrane debris. These results suggest that MeHg degradation occurs in the periplasm, where both Xox-MeDH and LanM reside.

The results of this study are anticipated to contribute to our ability to utilize methanotrophy for a wide range of applications.

Chapter 1 Introduction

1.1. Ecological significance and phylogeny of methanotrophs

Methanotrophs can use methane as their sole source of carbon and electron and are ubiquitous in both natural and engineered environments. Methanotrophy can be carried out using a wide variety of terminal electron acceptors, including dioxygen, nitrate, nitrite, sulfate, as well as oxidized metals, and by both bacteria and archaea (Timmers et al., 2017). This study, however, focuses on aerobic methane-oxidizing bacteria and the term methanotroph(y) as used here will pertain to only this group.

Kaserer (1905) and Söhngen (1906) were the first of many researchers to study methanotrophs. *Methylomonas methanica* (formerly *Bacillus methanicus*), *Pseudomonas methanitrificans*, *Methanomonas methanooxidans*, and *Methylococcus capsulatus* were the first methanotrophs to be isolated (Söhngen, 1906; Davis et al., 1964; Brown et al., 1964; Foster & Davis, 1966). Whittenbury et al. (1970b) significantly expanded this list by isolating more than 100 methanotrophs and classifying them based on their morphology, membrane structure, carbon assimilation pathway, and type of resting stage, amongst other characteristics (Whittenbury et al., 1970a).

Methanotrophs have been found in many different environments, including but not limited to landfill soils, freshwater and marine sediments, forest soils, paddy fields, peat bogs, and hot springs (Wise et al., 1999; Lidstrom, 1988; Dianou & Adachi, 1999; Dedysh et al., 1998; Tsubota et al., 2005). Despite found in diverse habitats, methanotrophs have to date only been found in the following phyla: Proteobacteria, Verrucomicrobia, and candidate phylum NC10.

The majority of identified methanotrophs belong to the Proteobacteria phylum, consisting of *Gamma*- and *Alphaproteobacteria* methanotrophs (Table 1.1). *Gammaproteobacteria* methanotrophs consist of the families *Methylococcaceae*, *Methylothermaceae*, and *Crenotrichaceae*, each with sixteen, three, and two genera, respectively, at the time this thesis was submitted. Alkaliphilic and/or halophilic methanotrophs belonging to the *Gammaproteobacteria* class that can tolerate pH values up to 11 have been found in soda lakes (Khmelenina et al., 1997; Sorokin et al., 2000; Kaluzhnaya et al., 2001). Some *Gammaproteobacteria* methanotrophs are psychrophilic, especially *Methylosphaera hansonii*, which was isolated from Antarctic meromictic lakes and can grow at temperatures as low as 0 °C (Bowman et al., 1997). Contrariwise, thermophilic methanotrophs of genera *Methylococcus*, *Methylocaldum*, *Methylothermus*, and *Methylomarinovum* with optima varying from 37 – 60 °C have been isolated from silage and thermal springs (Foster & Davis, 1966; Eshinimaev et al., 2004; Tsubota et al., 2005; Hirayama et al., 2014). Members of the *Crenotrichaceae* family are filamentous methanotrophs that may have a significant role in methane consumption in stratified aquatic environments, have yet to be cultured in the lab (Stoecker et al., 2006; Vigliotta et al., 2007; Oswald et al., 2017). *Alphaproteobacteria* methanotrophs include two families, *Methylocystaceae* and *Beijerinckiaceae*, composed of two and four genera, respectively. Some moderate acidophiles that belong to class *Alphaproteobacteria* with optimum growth pH around 5.5 have also been isolated (Dedysh et al., 2002; Dunfield et al., 2003).

Methanotrophic members of the Verrucomicrobia phylum are characterized by their extremely low growth pH optima, varying between 1 – 3.5, and consist of meso- and thermophiles (Dunfield et al., 2007; Islam et al., 2008; Pol et al., 2007; van Teeseling et al., 2014). Whereas most Proteobacteria methanotrophs use methane as both carbon and electron

source, Verrucomicrobia methanotrophs lead an autotrophic lifestyle by utilizing carbon dioxide as the carbon source via the Calvin-Benson-Bassham cycle (Khadem et al., 2011; van Teeseling et al., 2014). Verrucomicrobia methanotrophs possess polyhedral structures that resemble carboxysomes found in cyanobacteria and other chemoautotrophs (Islam et al., 2008; Op den Camp et al., 2009; Khadem et al., 2011). Carboxysomes harbor ribulose 1,5-bisphosphate carboxylase/oxygenase (RuBisCO), a critical enzyme for carbon fixation, and concentrate carbon dioxide for efficient carbon fixation. However, RuBisCO is not densely packed in the carboxysome-like structures in Verrucomicrobia methanotrophs and these methanotrophs are able to grow in high concentrations of carbon dioxide, which are typical in volcanic regions from which these methanotrophs were isolated (Khadem et al., 2011). In addition, most methanotrophs of the Proteobacteria and some of the Verrucomicrobia phyla produce intricate intracytoplasmic membrane (ICM) structures that host the particulate methane monooxygenase (pMMO) critical for the initial oxidation of methane (Kalyuzhnaya et al., 2019). Typically, *Gammaproteobacteria* methanotrophs contain stacks or bundles of ICM that are coordinated orthogonally with respect to the cytoplasmic membrane, whereas in *Alphaproteobacteria* methanotrophs these ICMs are lined around the periphery of the cell. An exception to these two ICM configurations is that found in *Methylocapsa acidiphila* B2 of the *Beijerinckiaceae* family, which is stacked to only one side of the cell (Figure 1.1; Dedysh et al., 2002). The ICM found in some species of Verrucomicrobia methanotrophs resembles that in *Gammaproteobacteria* methanotrophs (van Teeseling et al., 2014).

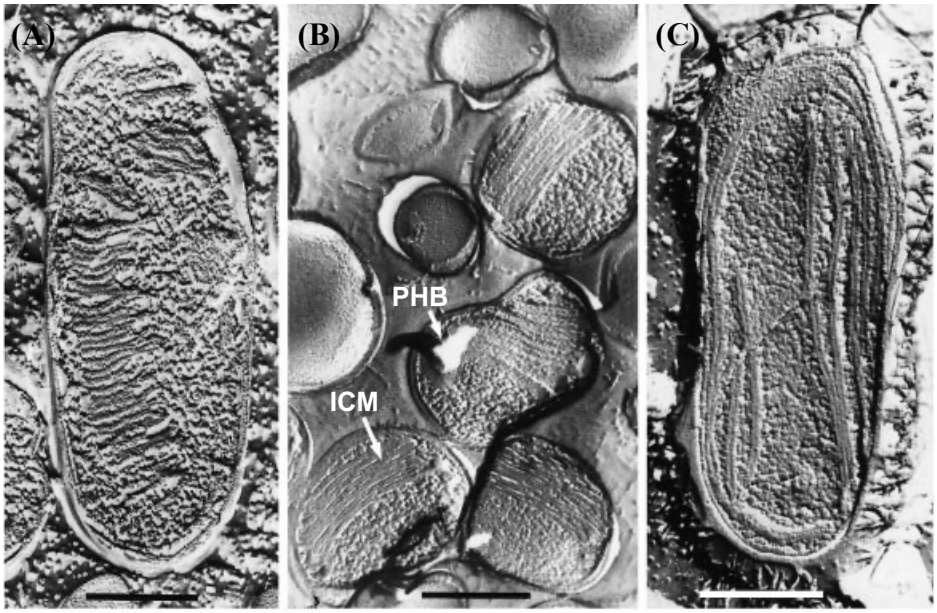

Figure 1.1. Freeze-fractured cells of methanotrophs (A) *Methylobacter luteus* (formerly *M. bovis*), (B) *Methylocapsa acidiphila* B2, and (C) *Methylosinus trichosporium* 19 (Dedysh et al., 2002). ICM, intracytoplasmic membrane; PHB, poly-β-hydroxybutyrate. Scale bar is 0.5 μm.

An anaerobic methane oxidizing bacterium "*Candidatus* Methylomirabilis oxyfera" of the candidate phylum NC10 has also been isolated. Anaerobic methane oxidation was generally believed to be solely carried out by consortia of archaea and bacteria, where archaea perform reverse methanogenesis and the resulting electrons are transferred to bacteria that carry out sulfate or nitrate reduction before the discovery of "*Ca.* Methylomirabilis oxyfera" (Caldwell et al., 2008). Ettwig et al. (2008) detected methanotrophic activity in anaerobic enrichment cultures apparently coupled to nitrite reduction, suggesting the presence of a hitherto unknown strategy of methane oxidation. Indeed, a significant portion (30 – 80%) of the enrichment cultures consisted of bacteria of the candidate phylum NC10 (Wu et al., 2011). The authors identified and sequenced "*Ca.* Methylomirabilis oxyfera" as a novel anaerobic methane oxidizing bacterium (Ettwig et al., 2010). Interestingly, despite growing under anaerobic conditions where nitrite serves as the electron acceptor, "*Ca.* Methylomirabilis oxyfera" actually performs aerobic methane oxidation via dismutation of nitric oxide into O_2 and N_2 (Ettwig et al.,

2010), and the generated dioxygen is then used to drive methane oxidation. Thus, "*Ca.* Methylomirabilis oxyfera" can be considered an aerobic methanotroph despite not being able to tolerate high levels of dioxygen (Ettwig et al., 2009; Wu et al., 2011). It is important to note, however, that "*Ca.* Methylomirabilis oxyfera" has yet to be purified and its putative nitric oxide dismutase still has not been characterized (Ettwig et al., 2010; Versantvoort et al., 2018). "*Ca.* Methylomirabilis oxyfera" also lacks ICMs that are characteristic to methanotrophs utilizing pMMO, most likely due to its low growth rate and high cost of producing ICMs (Wu et al., 2012). "*Ca.* Methylomirabilis oxyfera" can also be distinguished by its unique polygon shape and content of a novel fatty acid (Figure 1.2; Wu et al., 2012; Kool et al., 2012). "*Ca.* Methylomirabilis limnetica" and "*Ca.* Methylomirabilis lanthanidiphila", other species of this candidate division, have also been sequenced recently (Graf et al., 2018; Versantvoort et al., 2018).

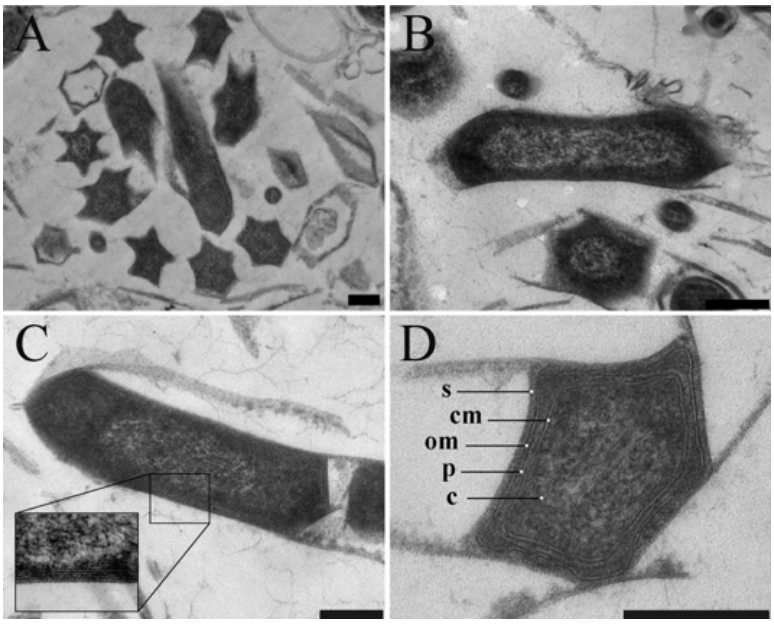

Figure 1.2. Transmission electron micrographs of chemically fixed and resin-embedded "*Ca.* Methylomirabilis oxyfera" cells (Wu et al., 2011). (A) Overview showing the star-like cell shape caused by dehydration and cell wall collapse. Longitudinal (B and C) and transverse (D) sections show the Gram-negative cell envelope and the presence of a putative S-layer on the top of the outer membrane. om, outer membrane; p, periplasm; cm, cytoplasmic membrane; c, cytoplasm; s, putative S-layer. Scale bars, 200 nm.

The origin of methanotrophy has been a subject of some debate, but it is believed that aerobic methanotrophs derived from methylotrophs (i.e., methanol-utilizing microbes), since a critical constraint is the effective handling of the initial product of methane oxidation, i.e. methanol (Tamas et al., 2014; Osborne & Haritos, 2018). Methanol oxidation is critical to prevent methanol from accumulating to toxic levels, to allow carbon assimilation from downstream products (formaldehyde) and to regenerate reducing equivalents consumed in methane oxidation (Im et al., 2011; Farhan Ul Haque et al., 2017; Semrau et al., 2018). This conclusion was supported by phylogenetic study of genes encoding methylotrophy and methanotrophy in the *Alphaproteobacteria*, which indicated that methanotrophic groups are nested within a much larger lineage of bacteria sharing vertical inheritance of methylotrophy genes (Tamas et al., 2014). Subsequent bioinformatic interrogation demonstrated that genes encoding pMMO (*pmoCAB*) in most proteobacterial methanotrophs have significantly different compositional biases than their host genomes, suggesting that these genes were obtained via recent lateral gene transfer (LGT) events (Khadka et al., 2018). That is, methane oxidation may have occurred as the result of LGT of ammonia monooxygenase from nitrifying bacteria to methylotrophs (Khadka et al., 2018). Indeed, it has been reported that when genes encoding ammonia monooxygenase are inserted in the methylotroph *Methylorubrum extorquens* AM1 (formerly *Methylobacterium extorquens* AM1), the microbe can subsequently grow on methane (Crossman et al., 1997). It has also been concluded that the soluble MMO (sMMO) was also the result of a LGT in at least some *Alphaproteobacteria* methanotrophs (Tamas et al., 2014). Given that methanotrophy possibly arose via transfer of MMO to methylotrophs and copper has a crucial role in regulating pMMO vs sMMO, it may be of interest to bioinformatically examine genes involved in methanol oxidation as well as those involved in copper uptake.

Table 1.1. Classification of genera of aerobic methanotrophs. (modified from Khmelenina et al., 2018a)

Genus	Species[a]	C_1 assimilation	ICM type[b]	N_2 fixation	Trophic niche	Reference
Class *Gammaproteobacteria*						
Family *Methylococcaceae*						
Methylobacter	*Mbt. luteus, Mbt. marinus, Mbt. psychrophilus, Mbt. tundripaludum, Mbt. whittenburyi*	RuMP[c]	Stacked	No	Some psychrophilic	Whittenbury et al., 1970a
Methylocaldum	*Mcd. marinum, Mcd. szegediense*	RuMP[c]/CBB[e]/Serine	Stacked	No	Thermophilic	Bodrossy et al., 1997
Methylococcus	*Mcc. capsulatus*	RuMP[c]/CBB[e]/Serine	Stacked	Yes	Thermophilic	Foster & Davis, 1966
Methylogaea	*Mga. oryzae*	RuMP[c]	Stacked	*nifH*[+f]	Mesophilic	Geymonat et al., 2011
Methyloglobulus	*Mgb. morosus*	RuMP[c]	Stacked	Yes	Psychrotolerant	Deutzmann et al., 2014
Methylomagnum	*Mmg. ishizawai*	RuMP[c]/CBB[e]	Stacked	No	Mesophilic	Khalifa et al., 2015
Methylomarinum	*Mmr. vadi*	RuMP[c]	Stacked	No	Halotolerant	Hirayama et al., 2013
Methylomicrobium	*Mmc. agile, Mmc. album, Mmc. lacus*	RuMP[c]	Stacked	No	Mesophilic	Bowman et al., 1995
Methylomonas	*Mmn. aurantiaca, Mmn. fodinarum, Mmn. koyamae, Mmn. methanica, Mmn. paludis, "Mmn. rubra", Mmn. scandinavica*	RuMP[c]	Stacked	Varies	Some psychrophilic	Davis et al., 1964
Methyloparacoccus	*Mpc. murrellii*	RuMP[c]	Stacked	No	Mesophilic	Hoefman et al., 2014
Methyloprofundus	*Mpf. sediment*	RuMP[c]	Stacked	Yes	Psychrotolerant	Tavormina et al., 2015
Methylosarcina	*Msc. fibrate*	RuMP[c]	Stacked	No	Mesophilic	Wise et al., 2001
Methylosoma	*Msm. difficile*	Unknown	Stacked	Yes	Mesophilic	Rahalkar et al., 2007
Methylosphaera	*Msr. hansonii*	RuMP[c]	ND[d]	Yes	Psychrophilic	Bowman et al., 1997
Methyloterricola	*Mtr. oryzae*	RuMP[c]/CBB[e]	Stacked	*nifH*[+f]	Mesophilic	Frindte et al., 2017
Methylotuvimicrobium	*Mtv. alcaliphilum, Mtv. buryatense, Mtv. japanense, Mtv. pelagicum, Mtv. kenyense*	RuMP	Stacked	Varies	Halotolerant/Alkaliphilic	Orata et al., 2018
Methylovulum	*Mvl. miyakonense*	RuMP[c]	Stacked	*nifH*[+f]	Psychrotolerant	Iguchi et al., 2011

Table 1.1. Continued

Genus	Species[a]	C_1 assimilation	ICM type[b]	N_2 fixation	Trophic niche	Reference
Family *Methylothermaceae*						
Methylohalobius	*Mhl. crimeensis*	RuMP[c]	Stacked	No	Halophilic	Heyer et al., 2005
Methylomarinovum	*Mmv. caldicuralii*	RuMP[c]	Stacked	No	Thermophilic/Halotolerant	Hirayama et al., 2014
Methylothermus	*Mtm. subterraneus*	RuMP[c]	Stacked	No	Thermophilic	Tsubota et al., 2005
Family *Crenotrichaceae*						
Clonotrix	*Clo. fusca*	-	Stacked	-	Mesophilic	Vigliotta et al., 2007
Crenothrix	*Cre. polyspora*	RuMP[c]	Stacked	-	Mesophilic	Stoecker et al., 2006
Class *Alphaproteobacteria*						
Family *Methylocystaceae*						
Methylocystis	*Mct. echinoides, Mct. heyeri, Mct. hirsuta, Mct. parvus, Mct. rosea, Mct. bryophila*	Serine	Periphery	Yes	Some acidophilic	Whittenbury et al., 1970a
Methylosinus	*Msn. sporium, Msn. trichosporium*	Serine	Periphery	Yes	Mesophilic	Whittenbury et al., 1970a
Family *Beijerinckiaceae*						
Methylocella	*Mcl. palustris, Mcl. silvestris, Mcl. tundrae*	Serine	None	Yes	Acidophilic	Dedysh et al., 2000
Methylocapsa	*Mcs. acidiphila, Mcs. aurea*	Serine	Stacked on one side only	Yes	Acidophilic	Dedysh et al., 2002
Methyloferula	*Mfr. stellata*	CBB[e]/Serine	None	Yes	Acidophilic	Vorobev et al., 2011
Methyloceanibacter	*Mon. caenitepidi*	Serine	None	Yes	Mesophilic	Takeuchi et al., 2014

Table 1.1. Continued

Genus	Species[a]	C_1 assimilation	ICM type[b]	N_2 fixation	Trophic niche	Reference
Phylum Verrucomicrobia						
Candidate Family *Methylacidiphilaceae*						
"*Candidatus* Methylacidimicrobium"	"*Ca.* Methylacidimicrobium cyclopophantes", "*Ca.* Methylacidimicrobium *fagopyrum*", "*Ca.* Methylacidimicrobium *tartarophylax*"	CBB[e]	Stacked/ None	-	Acidophilic	van Teeseling et al., 2014
"*Candidatus* Methylacidiphilum"	"*Ca.* Methyloacidiphilum *fumariolicum*", "*Ca.* Methyloacidiphilum *Infernorum*", "*Ca.* Methyloacidiphilum *kamchatkense*"	CBB[e]	None	Yes	Acidophilic/Thermophilic	Dunfield et al., 2007a
Candidate Phylum NC10						
"*Candidatus* Methylomirabilis"	"*Ca.* Methylomirabilis oxyfera", "*Ca.* Methylomirabilis lanthanidiphila", "*Ca.* Methylomirabilis limnetica"	CBB[e]	None	-	Anaerobic	Ettwig et al., 2010

[a] Validated species
[b] ICM: Intracellular membrane
[c] RuMP: ribulose monophosphate
[d] ND: not determined
[e] CBB: Calvin-Benson-Bassham
[f] *nifH*$^+$: *nifH* detected but no nitrogen fixation activity observed

1.2. Metabolism in methanotrophs

1.2.1. Methane oxidation

1.2.1.1. Methane monooxygenase

Methane oxidation is initiated by alternative forms of methane monooxygenase (MMO) – particulate MMO (pMMO) or soluble MMO (sMMO) (Figure 1.3). This initial step requires oxygen and two electrons and produces water. The vast majority of methanotrophs possess pMMO, some are able to express both pMMO and sMMO, and a small fraction only express sMMO (Table 1.2; Semrau et al., 2018). Though these two enzymes have identical function, they are structurally, biochemically, and evolutionarily very distinct.

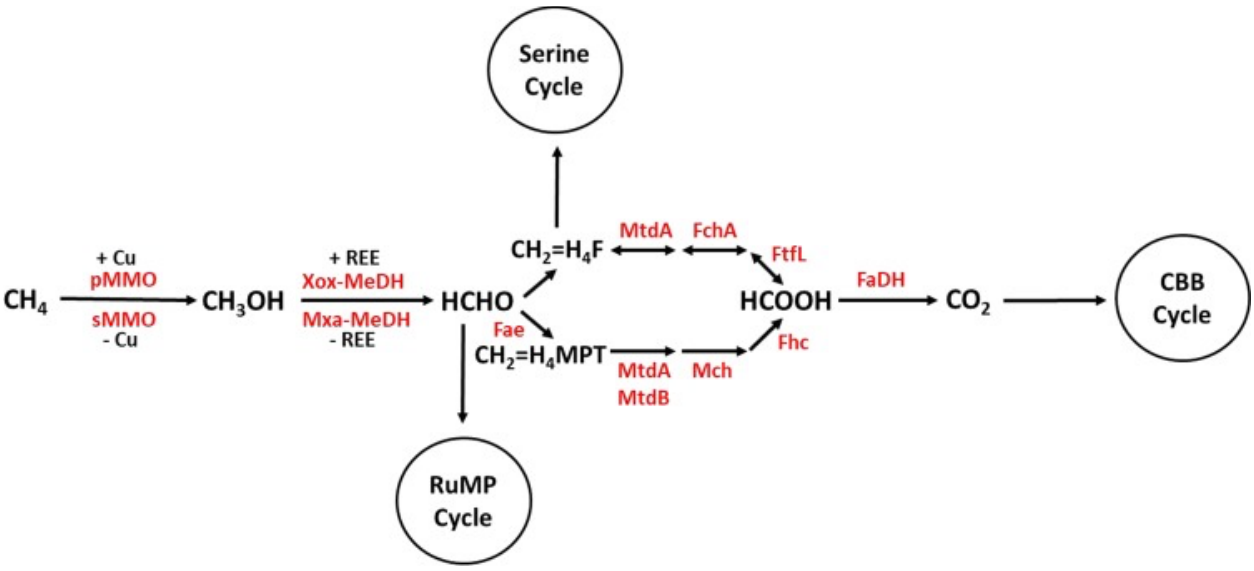

Figure 1.3. General pathway of methane oxidation by aerobic methanotrophs (Semrau et al., 2018). Enzymes are noted in red. pMMO, particulate methane monooxygenase; sMMO, soluble methane monooxygenase; Xox-MeDH, Xox-methanol dehydrogenase; Mxa-MeDH, Mxa-methanol dehydrogenase; Fae, formaldehyde-activating enzyme; H_4MPT, tetrahydromethanopterin; MtdB, NADP-dependent methylene-H_4MPT dehydrogenase; Mch, methenyl-H_4MPT cyclohydrolase; Fhc, formyltransferase-hydrolase complex; H_4F, tetrahydrofolate; MtdA, NADP-dependent methylene-H_4F–methylene-H_4F dehydrogenase; FchA, methenyl H_4F-cyclohydrolase; FtfL, formate tetrahydrofolate ligase; FaDH, formate dehydrogenase; CBB, Calvin-Benson-Bassham; RuMP, ribulose monophosphate.

The pMMO is located in the ICM and is part of the copper-containing membrane monooxygenase (CuMMO) family along with ammonia monooxygenase and some short-chain alkane and alkene monooxygenases (Tavormina et al., 2011; Khadka et al., 2018). Members of the CuMMO family follow the canonical gene order of C-A-B in bacteria, though a sequence-divergent pMMO (pXMO) has also been found in several methanotrophs with the operon organized as *pxmABC* (Table 1.2; Tavormina et al., 2011). The importance of pXMO, however, is unclear. Several studies have examined *pxmABC* expression *in situ* and in pure cultures (Tavormina et al., 2011; Saidi-Mehrabad et al., 2013; Kits et al., 2015b, 2015a), and its expression is quite low, suggesting it may have limited importance. It should be stressed, however, that little work has been done to elucidate the function of pXMO, and so its relevance is still open to debate.

Multiple operons encoding for pMMO polypeptides (*pmo*) are often found in many methanotrophs as highly similar sequence copies, indicative of gene duplication, (Tavormina et al., 2011; Khmelenina et al., 2018a). Some of these operons appear to encode for pMMOs with different properties (Stolyar et al., 1999; Dunfield et al., 2002). Stoylar et al. (1999) found two complete *pmoCAB* operons in *Mcc. capsulatus* Bath with near identical intergenic and coding sequences but divergent flanking sequences. Divergent sequences around the operons led the authors to speculate that the two copies could be differentially expressed and thus relevant under varying growth conditions such as stress commonly encountered in the organism's natural habitat. They later found that the two operons are controlled under similar σ^{70} promoters but "copy 2" is expressed predominantly under normal copper concentrations (~5 μM) and expression of "copy 1" is comparable to "copy 2" at higher concentrations of copper (~50 μM), indicating redundant function yet possibly a different role in the environment (Stolyar et al.,

2001). In *Methylocystis* sp. SC2, there are three complete *pmoCAB* operons – two operons that are different only by a single silent nucleotide (*pmoCAB1*), and another that has lower identity to the other two at both the nucleotide (67.4–70.9%) and derived amino acid (59.3–65.6%) sequence levels (*pmoCAB2*) (Dunfield et al., 2002; Baani & Liesack, 2008). Baani & Liesack (2008) found that both copies of *pmoCAB1* are expressed and pMMO1 contributes to methane oxidation at high methane concentrations (> 600 ppmv), whereas *pmoCAB2* is constitutively expressed and is critical for methane oxidation at concentrations less than 600 ppmv. pMMO2 has a significantly lower apparent half-saturation constant as compared to pMMO1 ($K_{m(app)}$ = 0.12 μM vs 9.30 μM), and is even capable of oxidizing atmospheric methane (1.75 ppmv). These results indicate that some methanotrophs can survive extended periods of starvation by utilizing pMMO2 and can contribute to methane consumption at sites with limited and/or fluctuating methane concentrations, e.g. upland soils, natural wetlands, rice paddies. It is also important to note that pMMO2 is found to date only in *Alphaproteobacteria* methanotrophs, possibly providing them with an advantage over other methanotrophs in these specific environments (Baani & Liesack, 2008; Tveit et al., 2019). In the Verrucomicrobia methanotroph "*Ca.* Methylacidiphilum kamchatkense" Kam1, there are three complete copies of *pmoCAB* that have varying degrees of similarity at the nucleotide (56.7–70.3%) and derived amino acid (41.2–75.7%) sequence levels (Erikstad & Birkeland, 2015). *pmoA* expression analysis of the three complete *pmoCAB* operons showed that one copy was the predominant transcript (Erikstad et al., 2012). Suboptimal growth conditions did not affect gene expression pattern in this methanotroph, whereas changing growth substrate from methane to methanol decreased the expression of all *pmoA* copies examined. In addition, transcriptomic analysis of "*Ca.* Methylacidiphilum fumariolicum" SolV grown under varying conditions indicated differential

expression of two of the three *pmoCAB* operons (Khadem et al., 2012a). That is, it was found that under "normal" growth conditions, i.e., excess ammonium and oxygen, copy 2 was predominantly expressed, whereas under oxygen limitation (<0.03% dissolved oxygen), copy 1 was predominant and expression of copy 2 decreased 40-fold.

pMMO is a heterotrimer ($\alpha_3\beta_3\gamma_3$) composed of predominantly transmembrane subunits PmoA (24 kDa) and PmoC (22 kDa), and a transmembrane subunit with a large periplasmic domain, PmoB (42 kDa) (Figure 1.4; Ross & Rosenzweig, 2017). Despite its clear importance in methanotrophy, much is still unknown about pMMO, e.g., the metal cofactors and active sites associated with it. That is, it has been long known that copper is required for the expression and activity of pMMO (Stanley et al., 1983). However, various models have been proposed for the composition of the active site of pMMO with one, two or three copper atoms as well as a di-iron moiety postulated to be involved.

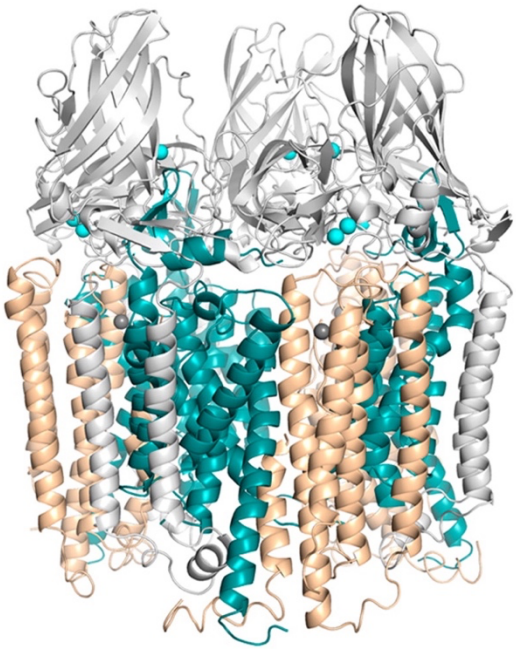

Figure 1.4. Overall $\alpha_3\beta_3\gamma_3$ structure of pMMO in *Methylocystis* sp. strain M with PmoB, PmoA, and PmoC subunits in gray, teal, and wheat, respectively (Sirajuddin & Rosenzweig, 2015) (PDB ID 3RGB). Copper and zinc ions are shown as cyan and gray spheres.

Lieberman et al. (2003) initially proposed the presence of a mononuclear copper site and copper-containing cluster in the pMMO of *Mcc. capsulatus* Bath, then incorrectly calculated to be a dimer of $\alpha_2\beta_2\gamma_2$ (Lieberman & Rosenzweig, 2005b), based on X-ray absorption and electron paramagnetic resonance (EPR) spectroscopic analyses. They later identified a mononuclear copper site and di-nuclear copper cluster in the PmoB subunit of *Mcc. capsulatus* Bath via X-ray crystallography (Lieberman & Rosenzweig, 2005a). The mononuclear copper site was proposed to be coordinated with two histidine ligands, His^{48} and His^{72} (Lieberman & Rosenzweig, 2005a; Wang et al., 2017). However, His^{48} is not conserved in other methanotrophs and copper was not observed at this site in the crystal structures of PmoB from *Methylosinus trichosporium* OB3b, *Methylocystis* sp. strain M, or *Methylocystis* sp. strain Rockwell (Lieberman & Rosenzweig, 2005a; Wang et al., 2017). In addition, replacing His^{48} with asparagine, the residue observed in *Msn. trichosporium* OB3b at this position, in a soluble recombinant PmoB from *Mcc. capsulatus* Bath did not affect its specific activity (Balasubramanian et al., 2010). Therefore, it was concluded that this mononuclear copper site did not serve as the catalytic site for methane oxidation. Lieberman & Rosenzweig (2005a) also proposed a second copper-containing site – a di-nuclear copper site. Here, one copper ion is coordinated by the sidechain δ nitrogen and the N-terminal amino nitrogen of His^{33} and the other copper by His^{137} and His^{139}. When His^{137} and His^{139} were replaced with alanine, the methane oxidation activity was abolished, suggesting that these residues were critical for pMMO activity (Balasubramanian et al., 2010).

Though these residues appeared to be necessary for pMMO activity and are highly conserved in pMMO and ammonia monooxygenase (Lieberman & Rosenzweig, 2005a; Balasubramanian et al., 2010), they are absent in Verrucomicrobia pMMOs (Liew et al., 2014). In addition, the well-known suicide inhibitor, acetylene, binds to PmoA and not PmoB (Prior &

Dalton, 1985; Semrau et al., 2018). These results collectively suggest that methane oxidation may not occur at this di-nuclear copper site.

The di-iron site was originally observed as occupied with a single zinc ion coordinated by Asp^{156}, His^{160}, and His^{173} from PmoC and Glu^{195} from PmoA, all of which are highly conserved (Lieberman & Rosenzweig, 2005a; Wang et al., 2017). However, as the authors pointed out, this zinc occupancy was likely due to an artefact introduced by the zinc in the crystallization buffer (Lieberman & Rosenzweig, 2005a; Balasubramanian et al., 2010). A later study utilizing Mössbauer spectroscopy to characterize the iron components of pMMO from *Mcc. capsulatus* Bath indicated that there were components within pMMO that had identical spectral characteristics as the di-iron center in sMMO (Martinho et al., 2007). Moreover, when pMMO was prepared with iron, it showed the highest specific activity, much higher than those of other preparations (160 $nmol \cdot min^{-1} \cdot mg$ pMMO $protein^{-1}$ vs 0.469 – 130 $nmol \cdot min^{-1} \cdot mg$ pMMO $protein^{-1}$), suggestive but not conclusive that it is a di-iron site responsible for methane oxidation in pMMO (Zahn & DiSpirito, 1996; Takeguchi et al., 1998; Basu et al., 2003; Choi et al., 2003; Lieberman et al., 2003; Martinho et al., 2007). In addition, the 1:1 di-iron center per $\alpha\beta\gamma$ trimer ratio and the close agreement between site occupancy and specific activity of purified pMMO further supported this model of di-iron center.

The third and last model involves a putative tri-copper $Cu(II)Cu(II)(\mu\text{-}O)_2Cu(III)$ complex site located in the hydrophilic cavity composed of His^{38}, Met^{42}, Asp^{47}, Asp^{49}, and Glu^{100} from PmoA and Glu^{154} from PmoC, residues which are highly conserved (Chan et al., 2004, 2007; Wang et al., 2017). The authors proposing this model demonstrated that tri-copper complexes can oxidize methane to methanol under biologically relevant conditions using peptides derived from *Mcc. capsulatus* Bath pMMO (Chan et al., 2013).

Recently, the research group postulating the di-nuclear copper site model revisited their solved structures of PmoB from *Mcc. capsulatus* Bath and *Methylocystis* sp. strain M to perform quantum refinement via quantum mechanical calculations (Cao et al., 2018). Their results indicate that this site can be reasonably modeled only as a mononuclear copper site. In addition, they now argue that the "zinc" site in PmoC contains copper and is in fact the active site where substrate binding and oxidation occur (Ross et al., 2019). Collectively, given so many different models, especially corrections to previous assessments, indicates that there is still less known than unknown regarding pMMO structure.

Much like the active site of pMMO, the electron donor required for pMMO to break a stable C-H bond in methane (bond dissociation energy of 104 kcal/mol) is still unclear due to difficulties in purifying the enzyme and measuring its activity *in vitro* (Ross & Rosenzweig, 2017; Lieven et al., 2018). Three modes of electron transfer have been previously presented (Figure 1.5 and Figure 1.6):

(1) Redox-arm mode: the electrons collected from methanol oxidation to formaldehyde by methanol dehydrogenase (MeDH) is linked to a redox-arm, where electrons are transferred to either AA_3- or CBD-type terminal oxidase (Cyt AA_3 or Cyt CBD) via cytochrome *c*555 and cytochrome *c*553, contributing to establishing a proton motive force and synthesis of ATP (Anthony, 1992; Dawson & Jones, 1981; de la Torre et al., 2015; DiSpirito et al., 2004a; Larsen & Karlsen, 2016; Lieven et al., 2018). The electrons required for methane oxidation is provided through ubiquinone (Q8H2) and the Q8 pool is replenished by reactions downstream of MeDH.

(2) Direct coupling mode: MeDH directly passes electrons to the pMMO via cytochrome *c*555 (Leak & Dalton, 1983; Culpepper & Rosenzweig, 2014). This mode is supported

by a study where pMMO of *Mcc. capsulatus* Bath was found as a complex with MeDH via cryoelectron microscopy (Myronova et al., 2006).

(3) Uphill electron transfer: the electrons from cytochrome *c*553 can be directly transferred to the Q8 pool via ubiquinol-cytochrome-*c* reductase (CYOR-q8) instead of being expended for ATP synthesis. This mode can explain the reduced efficiency of methane oxidation observed when only considering the direct coupling mode (Leak & Dalton, 1986b).

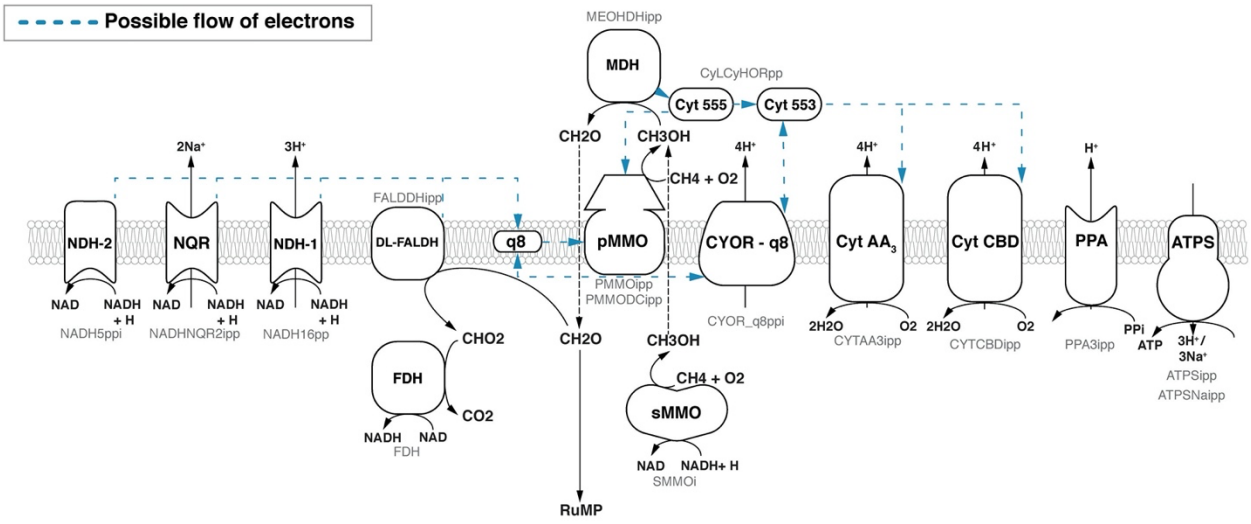

Figure 1.5. Respiratory chain in *Methylococcus capsulatus* Bath (Lieven et al., 2018). Blue dotted arrows indicate possible flow of electrons between respiratory components.

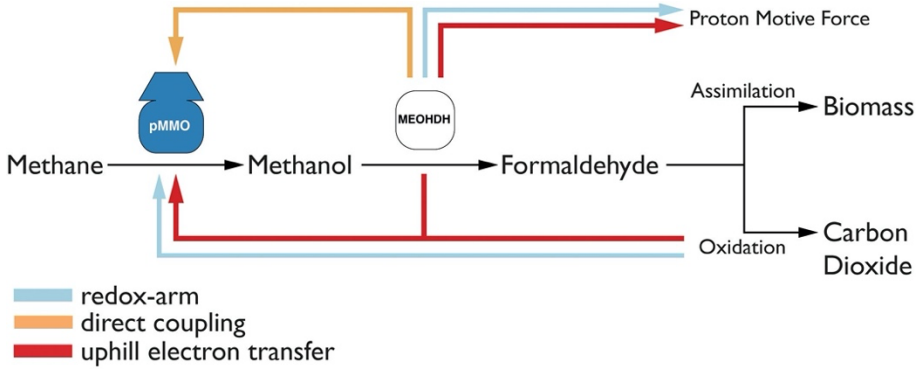

Figure 1.6. The three possible modes of electron transfer to pMMO (Lieven et al., 2018).

There have been several investigations to clarify the mode of electron transfer to pMMO using genome-scale metabolic modeling of various methanotrophs (de la Torre et al., 2015; Lieven et al., 2018; Bordel et al., 2019a; Bordel et al., 2019b; Naizabekov & Lee, 2020). In *Gammaproteobacteria* methanotrophs, the direct coupling mode with reduced efficiency and uphill electron transfer mode best explained stoichiometric flux balance models of *Methylotuvimicrobium buryatense* 5GB1 and *Methylotuvimicrobium alcaliphilum* 20Z (de la Torre et al., 2015; Akberdin et al., 2018), both formerly classified as genus *Methylomicrobium*, and also of *Mcc. capsulatus* Bath (Lieven et al., 2018). In *Alphaproteobacteria* methanotrophs *Methylocystis parvus* OBBP (Bordel et al., 2019a), *Methylocystis hirsuta* CSC1, *Methylocystis* sp. SB2, *Methylocystis* sp. SC2 (Bordel et al., 2019b), and *Msn. trichosporium* OB3b (Naizabekov & Lee, 2020), the redox-arm mode seem to best fit the respective metabolic models.

Aside from the computational investigations above, it has been experimentally shown that pMMO forms a stable complex with MeDH in a *Gammaproteobacteria* methanotroph *Mcc. capsulatus* Bath, providing evidence for the direct coupling mode (Myronova et al., 2006). This pMMO-MeDH complex may provide an efficient way of methane oxidation in methanotrophs growing in copper replete conditions, where the ICM generation and pMMO expression/activity are increased.

Table 1.2. Presence of select genes in the genomes of methanotrophs. Number of operons is indicated in parenthesis.

Strain	Family	*pmoCAB*	*pxmABC*	*mmo XYBZDC*	*mxaFJGI*	*xoxFJ*	*mbnABCM*	MCA2590 + *mopE/corAB*	*copCD*	*sgaA*	*fdhBA*	*fdsBA*	*lanM*
Class *Gammaproteobacteria*													
Methylobacter sp. BBA5.1[a]	*Methylococcaceae*	Yes (1)	Yes (1)	No	Yes (1)	Yes (2)	No	No	Yes (1)	Yes (1)	Yes (1)	Yes (1)	No
Mbt. marinus A45[a]	*Methylococcaceae*	Yes (1)	Yes (1)	No	Yes (1)	Yes (2)	No	No	Yes (1)	Yes (1)	Yes (1)	Yes (1)	No
Mbt. tundripaludum SV96[a]	*Methylococcaceae*	Yes (1)	Yes (1)	No	Yes (1)	Yes (1)	No	No	Yes (1)	Yes (1)	No	Yes (1)	No
Mbt. whittenburyi ACM 3310[a]	*Methylococcaceae*	Yes (1)	Yes (1)	No	Yes (1)	Yes (2)	No	No	Yes (1)	Yes (1)	Yes (1)	Yes (1)	No
Mcd. szegediense O-12[a]	*Methylococcaceae*	Yes (1)	No	No	Yes (1)	Yes (2)	No	No	Yes (1)	Yes (1)	No	Yes (1)	No
Mcc. capsulatus Bath	*Methylococcaceae*	Yes (2)	No	Yes (1)	Yes (1)	Yes (1)	No	Yes (1)	Yes (1)	Yes (1)	Yes (1)	Yes (1)	No
Mcc. capsulatus Texas[a]	*Methylococcaceae*	Yes (1)	No	Yes (1)	Yes (1)	Yes (1)	No	Yes (1)	Yes (1)	Yes (1)	Yes (1)	Yes (1)	No
Mgb. morosus KoM1[a]	*Methylococcaceae*	Yes (1)	Yes (2)	No	Yes (1)	No	No	No	Yes (1)	Yes (1)	No	Yes (1)	No
Mmg. ishizawai 175	*Methylococcaceae*	Yes (2)	No	Yes (1)	Yes (1)	Yes (1)	No	Yes (1)	Yes (1)	No	No	Yes (1)	No
Mmc. agile ATCC 35068[a]	*Methylococcaceae*	Yes (1)	Yes (1)	No	Yes (1)	Yes (1)	No	Yes (1)	Yes (1)	Yes (1)	No	Yes (1)	No
Mmc. album BG8[a]	*Methylococcaceae*	Yes (1)	Yes (1)	No	Yes (1)	Yes (1)	No	Yes (1)	Yes (1)	Yes (1)	No	Yes (1)	No
Mmc. lacus LW14	*Methylococcaceae*	Yes (1)	No	No	Yes (1)	Yes (1)	No	Yes (1)	Yes (1)	Yes (1)	No	Yes (1)	No
Mtv. alcaliphilum 20Z	*Methylococcaceae*	Yes (1)	No	No	Yes (1)	Yes (1)	No	Yes (1)	Yes (1)	Yes (1)	Yes (1)	No	No
Mtv. buryatense 5G[a]	*Methylococcaceae*	Yes (1)	No	Yes (1)	Yes (1)	Yes (1)	No	Yes (1)	Yes (1)	Yes (1)	Yes (1)	Yes (1)	No
Mmn. methanica MC09	*Methylococcaceae*	Yes (1)	No	Yes (1)	Yes (1)	Yes (1)	No	No	Yes (1)	Yes (1)	No	Yes (1)	No
Methylomonas sp. 11b[a]	*Methylococcaceae*	Yes (1)	Yes (1)	Yes (1)	Yes (1)	Yes (1)	No	No	Yes (1)	Yes (1)	No	Yes (1)	No
Methylomonas sp. LW13[a]	*Methylococcaceae*	Yes (1)	Yes (1)	Yes (1)	Yes (1)	Yes (1)	No	No	Yes (1)	Yes (1)	No	Yes (1)	No
Methylomonas sp. MK1[a]	*Methylococcaceae*	Yes (1)	Yes (2)	Yes (1)	Yes (1)	Yes (1)	No	No	Yes (1)	Yes (1)	No	Yes (1)	No
Msc. fibrata AML-C10[a]	*Methylococcaceae*	Yes (1)	No	No	Yes (1)	Yes (1)	No	Yes (1)	Yes (1)	Yes (1)	No	Yes (1)	No
Mvl. miyakonense HT12[a]	*Methylococcaceae*	Yes (1)	No	Yes (1)	Yes (1)	No	No	Yes (1)	Yes (1)	Yes (1)	No	Yes (1)	No
Mhl. crimeensis 10Ki[a]	*Methylothermaceae*	Yes (2)	No	No	Yes (1)	No	No	No	Yes (1)	Yes (1)	No	Yes (1)	No

Table 1.2. Continued.

Strain	Family	*pmoCAB*	*pxmABC*	*mmo XYBZDC*	*mxaFJGI*	*xoxFJ*	*mbnABCM*	MCA2590 + *mopE/corAB*	*copCD*	*sgaA*	*fdhBA*	*fdsBA*	*lanM*
Class *Alphaproteobacteria*													
Mcs. acidiphila B2[a]	*Beijerinckiaceae*	Yes (1)	No	No	Yes (1)	Yes (1)	No	No	Yes (1)	Yes (1)	Yes (1)	Yes (1)	Yes (1)
Mcs.aurea KYG[a]	*Beijerinckiaceae*	Yes (1)	No	No	Yes (1)	Yes (1)	No	No	Yes (2)	Yes (1)	Yes (1)	Yes (1)	Yes (1)
Mcl. silvestris BL2	*Beijerinckiaceae*	No	No	Yes (1)	Yes (1)	Yes (3)	No	No	Yes (1)	Yes (1)	No	Yes (1)	Yes (1)
Mfr. stellata AR4	*Beijerinckiaceae*	No	No	Yes (1)	Yes (1)	Yes (2)	No	No	Yes (1)	Yes (1)	Yes (1)	Yes (1)	Yes (1)
Methylocystis sp. LW5[a]	*Methylocystaceae*	Yes (3)	No	Yes (1)	Yes (1)	Yes (1)	Yes (2)	No	Yes (1)	Yes (1)	Yes (1)	Yes (1)	Yes (1)
Mct. parvus OBBP[a]	*Methylocystaceae*	Yes (2)	No	No	Yes (1)	Yes (1)	Yes (2)	No	Yes (1)	Yes (1)	No	Yes (1)	Yes (1)
Methylocystis sp. strain Rockwell[a]	*Methylocystaceae*	Yes (1)	No	No	Yes (1)	Yes (2)	No	No	Yes (2)	Yes (1)	No	Yes (1)	Yes (1)
Mct. rosea SV97[a]	*Methylocystaceae*	Yes (2)	Yes (1)	No	Yes (1)	Yes (2)	Yes (1)	No	Yes (2)	Yes (1)	No	Yes (1)	Yes (1)
Methylocystis sp. SB2[a]	*Methylocystaceae*	Yes (1)	Yes (1)	No	Yes (1)	Yes (1)	Yes (1)	No	Yes (2)	Yes (1)	No	Yes (1)	Yes (1)
Methylocystis sp. SC2	*Methylocystaceae*	Yes (3)	No	No	Yes (1)	Yes (2)	Yes (1)	No	Yes (2)	Yes (1)	No	Yes (1)	Yes (1)
Methylosinus sp. LW3[a]	*Methylocystaceae*	Yes (3)	No	Yes (1)	Yes (1)	Yes (1)	Yes (2)	No	Yes (2)	Yes (1)	Yes (1)	Yes (1)	Yes (1)
Methylosinus sp. LW4[a]	*Methylocystaceae*	Yes (3)	No	Yes (1)	Yes (1)	Yes (1)	Yes (1)	No	Yes (2)	Yes (1)	No	Yes (1)	Yes (1)
Msn. trichosporium OB3b[a]	*Methylocystaceae*	Yes (2)	No	Yes (1)	Yes (1)	Yes (2)	Yes (1)	No	Yes (2)	Yes (1)	No	Yes (1)	Yes (1)
Candidate phylum NC10													
"Ca. Methylomirabilis oxyfera"	-	Yes (1)	No	No	Yes (1)	Yes (2)	No	No	Yes (1)	Yes (1)	Yes (1)	Yes (1)	No
Phylum *Verrucomicrobia*													
"*Ca.* Methylacidimicrobium cyclopophantes" 3C[a]	"*Ca.* Methylacidiphilaceae"	Yes (1)	No	No	No	Yes (1)	No	No	No	Yes (1)	No	Yes (1)	No
"*Ca.* Methylacidimicrobium" sp. LP2A	"*Ca.* Methylacidiphilaceae"	Yes (2)	No	No	No	Yes (1)	No	No	No	Yes (1)	No	Yes (1)	No
"*Ca.* Methylacidiphilum fumariolicum" SolV	"*Ca.* Methylacidiphilaceae"	Yes (3)	No	No	No	Yes (1)	No	No	No	Yes (1)	No	Yes (1)	No
"*Ca.* Methylacidiphilum infernorum" V4	"*Ca.* Methylacidiphilaceae"	Yes (3)	No	No	No	Yes (1)	No	No	No	Yes (1)	No	Yes (1)	No

The sMMO is located in the cytoplasm and is a member of the multicomponent soluble di-iron monooxygenase family found in diverse bacteria for oxidation of aliphatic and aromatic hydrocarbons (Leahy et al., 2003). sMMO consists of three components – a hydroxylase (MMOH), reductase (MMOR), and a regulatory protein (MMOB) (Merkx et al., 2001; Ross & Rosenzweig, 2017). The MMOH is an $\alpha_2\beta_2\gamma_2$ homodimer of 251 kDa with a di-iron active site where methane oxidation occurs (Figure 1.7; Woodland & Dalton, 1984; Fox et al., 1989; Lipscomb, 1994). MMOR is approximately 40 kDa and consists of three domains – [2Fe-2S] ferredoxin domain, FAD-binding domain, and an NADH binding domain, and is responsible for transferring electrons from NADH to the active site of MMOH (Lund & Dalton, 1985). The regulator MMOB is a 16 kDa α/β protein that couples MMOH and MMOR (Brazeau et al., 2001).

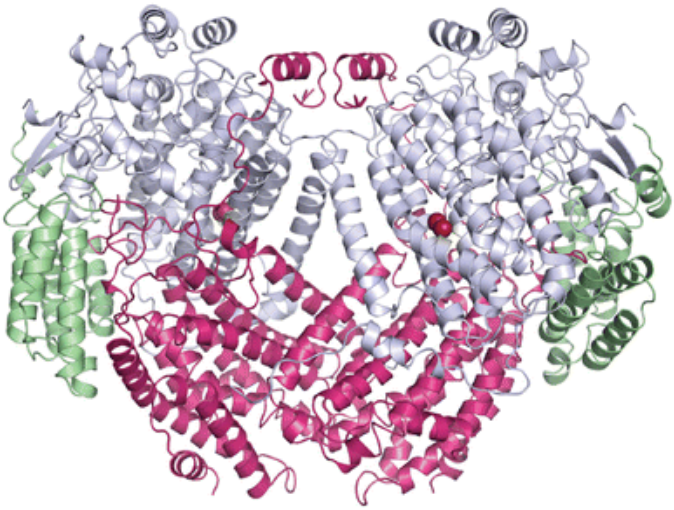

Figure 1.7. Structure of MMOH from *Methylococcus capsulatus* Bath. α, β, and γ subunits are shown in gray, magenta, and green, respectively. (Ross & Rosenzweig, 2017)

Unlike the ambiguous active site and electron donor of pMMO, those of sMMO have been extensively validated (Merkx et al., 2001). In sMMO, NADH serves as the electron donor for methane oxidation, where the reducing equivalents are used to split the O-O bond of O_2, and

subsequently passed to one of the oxygen atoms to form H_2O and the other incorporated into methane with the remaining oxygen atom to form methanol via homolytic oxygen cleavage (Colby & Dalton, 1976; Lipscomb, 1994). A μ-hydroxo-bridged di-iron center is located in each MMOH of the $\alpha_2\beta_2\gamma_2$ homodimer, where both oxygen and methane are activated (Rosenzweig et al., 1993; DeRose et al., 1993; Leahy et al., 2003). This di-iron center is coordinated by four glutamate residues, two histidine residues, and a water molecule through various stages of the catalytic cycle (Rosenzweig et al., 1993; Elango et al., 1997). In the *Gammaproteobacteria* methanotroph *Mcc. capsulatus* Bath, the resting state active site ($MMOH_{ox}$) contains two Fe(III) ions, of which the first ion is coordinated by Glu^{114}, His^{147}, and a water molecule, and the other by Glu^{209}, Glu^{243}, and His^{246}. In *Msn. trichosporium* OB3b, an *Alphaproteobacteria* methanotroph, the di-iron center is coordinated similarly with the exception of Asp^{209} instead of Glu^{209} (Elango et al., 1997). The iron ions are also bridged by two water molecules and Glu^{144} to form a pseudo-octahedral structure (Rosenzweig et al., 1993, 1995; Ross & Rosenzweig, 2017). Interestingly, two conserved His and carboxylate residues, each, in conjunction with nearby residues in the "Zn site" of pMMO from the same methanotroph are highly similar to the coordinating residues of sMMO and may serve as ligands to accommodate the proposed di-iron site-mediated reaction (Martinho et al., 2007).

MMOR transfers two electrons from NADH to $MMOH_{ox}$ di-iron site, where the distance between Fe(II)-Fe(II) increases and one of the water molecules is displaced by Glu^{243} through the process carboxylate shift (Figure 1.8) (Rosenzweig et al., 1995). The resulting $MMOH_{red}$ readily reacts with dioxygen to form intermediate O, then the peroxo intermediates P* (Fe(II)) and P (peroxo-bridged Fe(III)), and finally the Fe(IV)-Fe(IV) intermediate Q (Lee et al., 1993; Lee & Lipscomb, 1999; Banerjee et al., 2013; Lawton & Rosenzweig, 2016). The intermediate Q then

reacts with methane to form the product complex T (Banerjee et al., 2015). One oxygen atom from dioxygen is associated with T, and the other incorporated into the substrate to form methanol (Banerjee et al., 2015). The intermediate P can also be formed via H_2O_2 activation of $MMOH_{ox}$ (Andersson et al., 1991; Jiang et al., 1993; Ross & Rosenzweig, 2017).

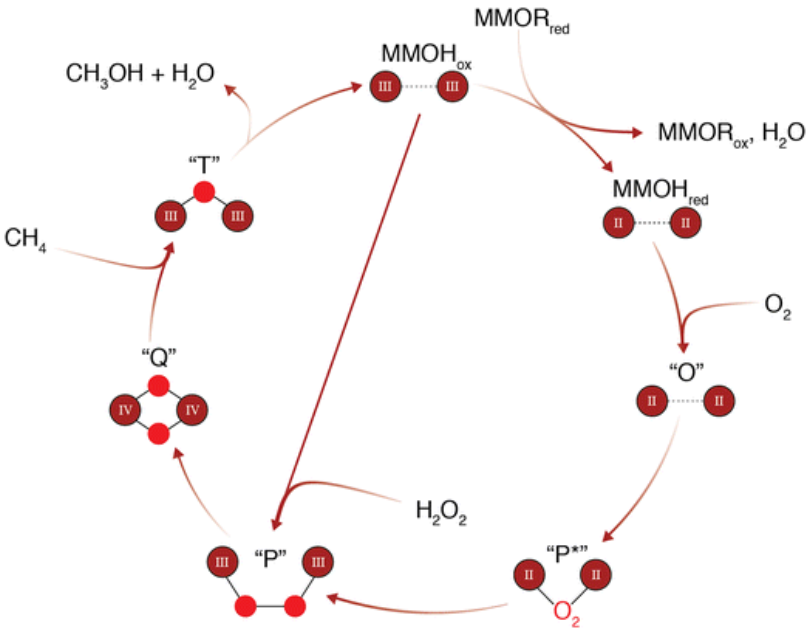

Figure 1.8. The catalytic cycle of sMMO with stable species MMOHox and MMOHred, and transient species O, P*, P, Q, and T (Ross & Rosenzweig, 2017). Iron ions are shown as red-brown spheres labeled with oxidation state. Oxygen atoms are shown as red spheres except for P*, for which oxygen and di-iron active site binding mode is unknown. The peroxide shunt, a mechanism by which intermediate P is generated from reaction between $MMOH_{ox}$ and H_2O_2 is shown.

The MMOH dimer interface produces a "canyon" region with a hydrophilic opening in the center of the molecule known as the "pore", controlled by residues Thr^{213}, Asn^{214}, and Glu^{240} (Rosenzweig et al., 1993; Lee et al., 2013; Wang et al., 2015; Ross & Rosenzweig, 2017). Separate from the pore, there are also three hydrophobic pockets that have also been found in another multicomponent soluble di-iron monooxygenase (Whittington et al., 2001; Sazinsky et al., 2004; Sazinsky & Lippard, 2005). It has been shown that both MMOR and MMOB dock at

the canyon of MMOH (MacArthur et al., 2002; Kopp et al., 2003; Chatwood et al., 2004; Sazinsky & Lippard, 2006). In addition, MMOB significantly enhances the reaction by changing the conformation of MMOH upon binding in order to moderate oxygen, methane, and proton access to the di-iron center (Liu et al., 1995; Lee et al., 2013; Srinivas et al., 2020).

There are currently two models of substrate access to the active site (Ross & Rosenzweig, 2017). In one model, the authors propose that the substrates oxygen and methane travel through the hydrophobic cavities that lead to the active site and products exit via this passage, while protons, electrons, and water are transported via the pore facilitated by residue Glu^{240} (Lee et al., 2013; Wang et al., 2015). However, the movement through each cavity would follow zero order kinetics with respect to substrate, contrary to previous findings demonstrating the reaction between intermediate Q and the substrates to have a linear relationship (Lee et al., 1993; Tinberg & Lippard, 2010; Ross & Rosenzweig, 2017). In an alternative model, substrates are thought to access the active site via the pore. Mutation of MMOB residues near the pore significantly affects the rate of reaction between intermediate Q and the substrates in a substrate-dependent manner, supporting the model of pore entry (Wallar & Lipscomb, 2001; Brazeau & Lipscomb, 2003; Lee et al., 2013).

sMMO is encoded by the *mmo* operon, consisting of structural genes *mmoXYZBC*, encoding for the α, β, γ subunits of MMOH, MMOB, and MMOR, respectively, and regulatory genes *mmoR*, *mmoG*, and *mmoD* (Figure 1.9) (Stainthorpe et al., 1990; Cardy et al., 1991; Merkx et al., 2001; Csáki et al., 2003; Stafford et al., 2003; Semrau et al., 2013). The order of core genes *mmoXYBZDC* is conserved in the *mmo* operons identified thus far, with other genes of the operon occurring in different orientations with respect to the core genes (Figure 1.9). In *Msn. trichosporium* OB3b, expression of the *mmoXYBZDC* is regulated by the σ^{54} and σ^{70} promoters

upstream of *mmoX* and *mmoY*, respectively (Nielsen et al., 1997). *mmoR* and *mmoG* encode for a σ^{54}-dependent transcriptional activator and a putative GroEL-like chaperone (Csáki et al., 2003; Stafford et al., 2003; Scanlan et al., 2009). It has been shown that activation of the σ^{54} promoter is dependent on *rpoN* (encoding for σ^{N}), *mmoR*, and *mmoG* (Csáki et al., 2003; Stafford et al., 2003).

The *mmo* operon occur as a single copy and the gene arrangement is conserved in most methanotrophs (Table 1.2). The position of the regulator genes *mmoR* and *mmoG*, though, can vary (Figure 1.9), and a putative two-component sensor regulator system, *mmoS* and *mmoQ*, can be found in the *mmo* gene cluster in *Mcc. capsulatus* Bath (Csáki et al., 2003; Ukaegbu & Rosenzweig, 2009). It has been suggested that this system senses copper levels and transmit the signal to MmoR, though it does not seem critical for expression of sMMO as its knockout had little effect (Csáki et al., 2003).

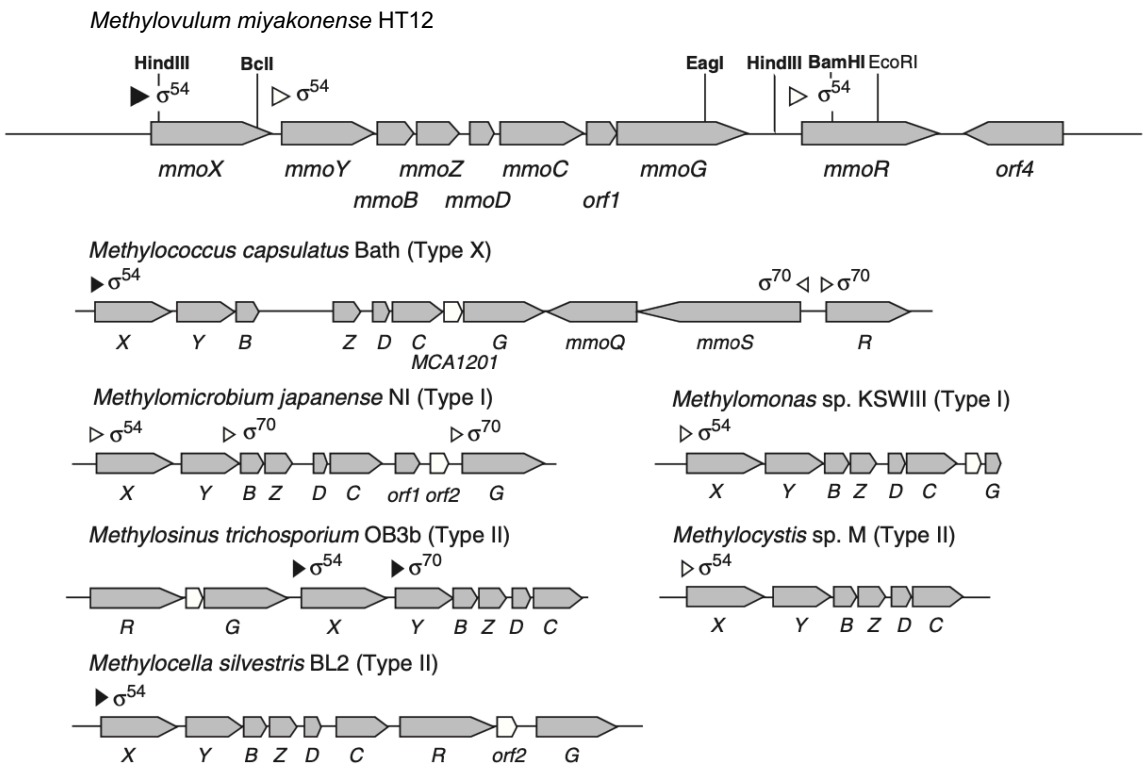

Figure 1.9. *mmo* operon map of various methanotrophs (Iguchi et al., 2010). Open triangles indicate putative promoter sites, and closed triangles indicate the promoter sites that have been experimentally validated.

As mentioned earlier, the pMMO and sMMO, despite carrying out the same function, have many distinct differences. Perhaps not surprisingly, these two enzymes have very different substrate ranges and kinetics – pMMO has higher affinity for methane, while sMMO has higher maximum methane turnover rate (Lee et al., 2006; Semrau et al., 2018). In addition, sMMO has a wider substrate range and has been found to oxidize alkanes up to C_8, ethers, cyclic alkanes, and aromatic carbons (Colby et al., 1977; Burrows et al., 1984), while pMMO is able to oxidize alkanes up to C_5, but not aromatic compounds (Burrows et al., 1984). sMMO was also found to degrade chlorinated ethenes at significantly faster rates than pMMO (Oldenhuis et al., 1991; Lee et al., 2006). Therefore, sMMO has received more interest in application to bioremediation of various organic pollutants. However, as mentioned earlier, most methanotrophs express pMMO

and those that do have the ability to express sMMO only do so at very low copper concentrations (Hanson & Hanson, 1996; Choi et al., 2003). That is, a "copper switch" controls the expression and activity of pMMO and sMMO. There is also competition between methane and halogenated organic pollutants for binding to MMO and these pollutants and their products can have toxic effects and lower the efficiency overall (Oldenhuis et al., 1989, 1991; Lontoh et al., 1999; Han et al., 1999). It has been shown that pMMO may be more advantageous in the long term and/or at extremely high concentrations of pollutants due to its greater specificity for methane that supports growth and viability (Lee et al., 2006; Yoon & Semrau, 2008). Therefore, it is important to understand the target pollutant, site characteristics (i.e. copper availability), and the required timeframe of bioremediation processes in order to fully utilize pMMO or sMMO.

1.2.1.2. Methanol dehydrogenase

There are two alternative enzymes that oxidize methanol in the central one-carbon metabolism of methanotrophs – a Ca^{2+}-dependent MeDH (Mxa-MeDH) and rare earth element (REE)-dependent MeDH (Xox-MeDH) (Pol et al., 2014). Both MeDHs are localized in the periplasm and intra-ICM space and are dependent on pyrroloquinoline quinone cofactor (Fassel et al., 1992; Brantner et al., 2002). These MeDHs belong to the class of eight-bladed β-propeller quinoproteins, which include other alcohol and aldehyde dehydrogenases (Anthony & Ghosh, 1998; Khmelenina et al., 2018a). Expression of the two MeDHs are regulated by the presence of REE, indicative of an "REE switch," to be discussed in a different section to follow.

In methanotrophs and non-methanotrophic methylotrophs – the latter being microorganisms that utilize reduced one-carbon substrates other than methane – methanol is oxidized by MeDH to formaldehyde, which is further oxidized to carbon dioxide or serves as a starting substrate for carbon assimilation (Khmelenina et al., 2018a). Mxa-MeDH was first described in a pink facultative methylotroph, *Mrr. extorquens* AM1 more than 50 years ago (Anthony, 1993; Anthony & Zatman, 1964a, 1964b). Subsequently, the PQQ prosthetic group was characterized and the divalent cation required for Mxa-MeDH activity identified as Ca^{2+} (Anthony & Zatman, 1967; Duine et al., 1978; Duine & Frank, 1980; Salisbury et al., 1979; Richardson & Anthony, 1992; Adachi et al., 1990). Mxa-MeDH structures from a number of methylotrophs have been solved via X-ray crystallography to reveal the $\alpha_2\beta_2$ tetrameric structure consisting of the catalytic α subunit with PQQ (66 kDa) and the small β subunit (8.5 kDa) (Figure 1.10) (Xia et al., 1992, 1996, 2003; White et al., 1993; Anthony et al., 1994; Ghosh et al., 1995; Anthony & Ghosh, 1998; Zheng et al., 2001; Afolabi et al., 2001; Williams et al., 2005; Nojiri et al., 2006; Choi et al., 2011). The two αβ subunits are arranged so that the eight-blade

propellers are approximately perpendicular to each other. The PQQ resides in the funnel-shaped internal cavity of the α subunit, between the indole ring of Trp^{237} and the disulfide bridge spanning Cys^{103}-Cys^{104} (Ghosh et al., 1995). The single Ca^{2+} ion present in the active site is coordinated by C_5 quinone oxygen, one oxygen of C_7 carboxylate, and N_6 ring atom of the PQQ and residues Glu^{177} and Asn^{261} (Ghosh et al., 1995). In addition, the C_4 and C_5 oxygen atoms of PQQ, which are reduced during the catalytic cycle, are associated with Arg^{331} via hydrogen bond, a residue of which the NH_2 is hydrogen bonded with the carboxylate of Asp^{303}, the base postulated to be required for catalytic mechanism (Anthony & Williams, 2003). The exact function of the small β subunit is still unknown, but it has been speculated that it stabilizes the MeDH structure (Ghosh et al., 1995) or facilitates proper Ca^{2+} coordination (Keltjens et al., 2014).

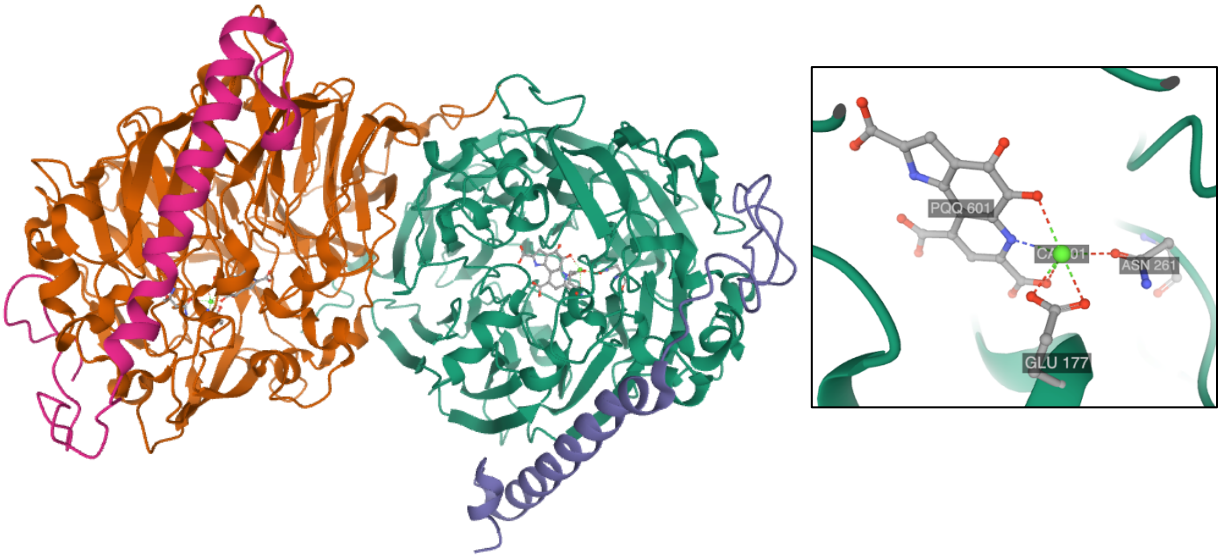

Figure 1.10. Structure of Mxa-MeDH from *Methylorubrum extorquens* (PDB ID 1H4I) (Ghosh et al., 1995; Sehnal et al., 2018). α subunits are shown in orange and green, β subunits in magenta and purple (left). PQQ cofactor and residues coordinating Ca^{2+} is depicted as a ball and stick model and Ca^{2+} is represented as a green sphere (right).

Methanol oxidation by Mxa-MeDH is initiated by abstraction of the proton from the alcohol group by the base, most likely Asp^{303}. (Afolabi et al., 2001). Then there is a direct hydride transfer from the methyl group of methanol to the C_5 of PQQ, proposed to be facilitated by the Ca^{2+} ion acting as a Lewis acid to stabilize the electrophilic C_5 for attack by the hydride, forming $PQQH_2$ and the product formaldehyde (Anthony, 1993, 2004). Ammonia activation and higher pH is required for this rate-limiting step using an artificial electron acceptor *in vitro* (Anthony, 1993; Anthony & Ghosh, 1998; Pol et al., 2014).

The role of Ca^{2+} ions has been studied by substituting Ca^{2+} in the growth medium with Sr^{2+} or reconstituting metal-free Mxa-MeDH with Ca^{2+}, Sr^{2+}, or Ba^{2+} (Adachi et al., 1990; Goodwin et al., 1996; Goodwin & Anthony, 1996). In these studies, replacing Ca^{2+} ions with a stronger Lewis acid (e.g. Sr^{2+}, Ba^{2+}) resulted in increased activity, but much lower affinity for the substrate, most likely due to altered structure to accommodate the different metal ions.

The reduced $PQQH_2$ then passes the two electrons down the electron transport chain consisting of cytochrome c_L, then cytochrome c_H, both named based on their isoelectric points (low vs high), and finally to terminal oxidases that establish the proton motive force and contribute to the subsequent ATP synthesis (Anthony, 1992; DiSpirito et al., 2004a; Nojiri et al., 2006). In a *Gammaproteobacteria* methanotroph *Mcc. capsulatus* Bath, cytochromes *c*555 and *c*553 pass the electrons to the terminal oxidase of types CBD and AA_3. (Larsen & Karlsen, 2016; Lieven et al., 2018) (Figure 1.5).

Xox-MeDH was first noticed as an Mxa-MeDH-like putative PQQ-dependent dehydrogenase based on the sequence similarity between the genes (Chistoserdova & Lidstrom, 1997a; Keltjens et al., 2014). Its importance, however, was unclear, as an *mxa* insertion mutant of a facultative methylotroph *Paracoccus denitrificans* rendered the organism incapable of

growing on methanol, despite the existence of the genes for Xox-MeDH (van Spanning et al., 1991). Further, disruption of the gene encoding for Xox-MeDH did not lead to a clearly different phenotype (van Spanning et al., 1991; Chistoserdova & Lidstrom, 1997a). On the contrary, it was shown that an *xox*-disrupted mutant of *Mrr. extorquens* AM1 was less competitive than the wild-type during colonization *in planta* (Schmidt et al., 2010). In addition, no significant expression of *xox* was detected in the lab, though high expression was observed *in situ* (Delmotte et al., 2009; Sowell et al., 2011). To further complicate matters, some methanotrophs and methylotrophs, such as Verrucomicrobia methanotrophs (Pol et al., 2007; Hou et al., 2008; Anvar et al., 2014), *Methylotenera* methylotrophs (Bosch et al., 2009; Lapidus et al., 2011), and phototroph *Rhodobacter sphaeroides* (Mackenzie et al., 2001), were found to have Xox-MeDH, but not the canonical Mxa-MeDH (Chistoserdova, 2011; Keltjens et al., 2014). Thus, the role of Xox-MeDH remained elusive for quite some time. This was largely due to the requirement of rare earth elements (REE) in place of Ca^{2+}. REEs are abundant in the environment but not commonly added to growth media (Pol et al., 2014). This is not surprising, as REEs have extremely low solubility and thus low bioavailability, and were previously thought to have a minimal, if any role in biochemical reactions (Franklin, 2001; Lim & Franklin, 2004; Pol et al., 2014).

Kawai research group originally hypothesized that REEs such as lanthanum and cerium may induce Xox-MeDH via an unknown regulatory mechanism based on observations of Xox-MeDH and its enhanced specific activity in the presence of REEs (Hibi et al., 2011; Fitriyanto et al., 2011). They later found that Xox-MeDH was in fact activated by and contained La^{3+}, and that La^{3+} may facilitate the dimerization to the α_2 structure (Nakagawa et al., 2012). In addition,

the growth of an *mxa*-deficient mutant of methylotroph *Mrr. extorquens* AM1 was only supported by the supplementation of La^{3+} and not Ca^{2+}.

Furthermore, it has been suggested that the isolation and identification of acidophilic Verrucomicrobia methanotrophs has been delayed due to presence of Xox-MeDH and absence of the Ca^{2+}-dependent Mxa-MeDH in this group of methanotrophs (Pol et al., 2014). Sufficient growth of "*Ca.* Methylacidiphilum fumariolicum" SolV, a Verrucomicrobia methanotroph, was only supported when mudpot water from its original habitat was supplemented. The authors found 2 – 3 μM of REEs in these mudpot water samples, and addition of REEs instead of the mudpot water to the mineral growth medium could also support growth. The structure of the Xox-MeDH was subsequently solved via X-ray crystallography (Figure 1.11). Xox-MeDH is an α_2 homodimer that resembles the large subunit of Mxa-MeDH, also supported by previous observations of purified protein via gel electrophoresis and chromatography (Hibi et al., 2011; Fitriyanto et al., 2011). The electron density and distances to coordinating atoms indicated that calcium, zinc, magnesium, or copper cannot reside in the metal binding site, but cerium or lanthanum ions satisfy the structural constraints of the model. All of the amino acids that coordinate PQQ and the metal ion in Mxa-MeDH were found to be conserved in Xox-MeDH, with the exception of an additional residue, Asp^{301}, coordinating the REE ion. In addition, two other residues in Xox-MeDH were different in order to accommodate the larger REE ion – Pro^{259} and Ala^{176}, both conserved in Mxa-MeDH, are instead replaced with the smaller threonine and glycine, respectively (Pol et al., 2014).

Xox-MeDH from methanotrophs "*Ca.* Methylomirabilis oxyfera" of the NC10 candidate phylum and *Mtv. buryatense* 5GB1C of the *Gammaproteobacteria* class were also characterized (Wu et al., 2015; Deng et al., 2018). It is interesting to note that Xox-MeDH from "*Ca.*

Methylomirabilis oxyfera" was found to form a heterotetrameric enzyme with the small subunit of Mxa-MeDH (Wu et al., 2015), and that from *Mtv. buryatense* 5GB1C was observed as a monomer in solution (Deng et al., 2018).

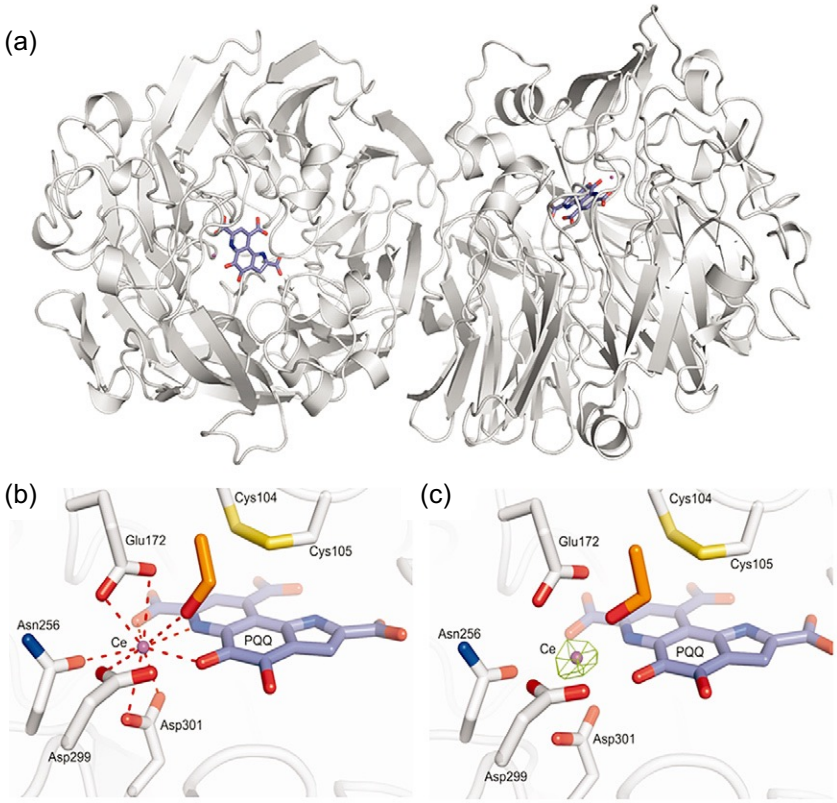

Figure 1.11. X-Ray crystal structure of "*Ca*. Methyloacidiphilum fumariolicum" SolV Xox-type methanol dehydrogenase (Pol et al., 2014). (a) Dimer structure with PQQ cofactor in blue and cerium ion in purple. (b) Active site of Xox-MeDH with PQQ in blue and cerium in purple, water molecule in orange and coordination of cerium ion represented by red dashed lines. (c) Anomalous difference density (green mesh) supporting presence of cerium ion in the active site of Xox-MeDH.

As mentioned before, Ca^{2+} acts as a Lewis acid to facilitate the attack on the electrophilic C_5 atom of the PQQ by the hydride of the substrate methyl group. REEs are much stronger Lewis acids than Ca^{2+}, and therefore can make the C_5 atom more electrophilic. This can explain the higher rates and affinity of Xox-MeDH compared with Mxa-MeDH reported thus far (Keltjens et al., 2014), and also the high activity of Xox-MeDH at circumneutral pH, whereas Mxa-MeDH require ammonia activation at higher pH (Pol et al., 2014). Both Mxa- and Xox-

MeDH can oxidize several primary alcohols, but Xox-MeDH can convert methanol directly to formate rather than formaldehyde via a four-electron oxidation (Keltjens et al., 2014). This mode of methanol oxidation can explain the lack of complete methanopterin- or folate-dependent enzymes required for formaldehyde oxidation in Verrucomicrobia methanotrophs, and also the need for these methanotrophs to rely on the Calvin-Benson-Bassham cycle to assimilate carbon dioxide (Khadem et al., 2012b; Pol et al., 2014; Keltjens et al., 2014). There is an exception to the direct conversion of methanol to formate via Xox-MeDH, i.e., Xox-MeDH of the facultative methylotroph *Mrr. extorquens* AM1 has been found to oxidize methanol to formaldehyde rather than formate, implying species-dependent role of Xox-MeDH that can affect downstream oxidation and/or assimilatory pathways in methanotrophs (Semrau et al., 2018; Good et al., 2019).

1.2.1.3. Formaldehyde oxidation

In methanotrophs, methanol is transformed to formaldehyde or formate via two- or four-electron oxidation by MeDH. Formaldehyde produced by the two-electron oxidation of methanol is transported into the cytoplasm and can be further oxidized to carbon dioxide for additional reducing power or serve as the starting substrate for assimilation into biomass via the ribulose monophosphate (RuMP) cycle or serine pathway (Figure 1.3, pg. 10) (Keltjens et al., 2014). Oxidation of formaldehyde is particularly important, because formaldehyde not only serves as the substrate required for ATP generation but is also a potent toxin that requires careful control *in vivo* (Chistoserdova, 2011). There are three pathways for formaldehyde oxidation:

(1) Oxidation via dye-linked formaldehyde dehydrogenase (DL-FalDH).

(2) Tetrahydrofolate (H_4F)- and tetrahydromethanopterin (H_4MPT)-dependent oxidation.

(3) Oxidation via dissimilatory RuMP (dRuMP) cyclic pathway.

The DL-FalDH has received little attention as a method of formaldehyde oxidation in methanotrophs due to its low substrate specificity and activity (Anthony, 1982; Vorholt, 2002; Chistoserdova & Lidstrom, 2013). DL-FalDH purified from *Msn. trichosporium* OB3b and methylotroph *Hyphomicrobium* X exhibited activity with a wide range of aldehydes including straight-chain C_1 – C_{10} aldehydes (Patel et al., 1980; Attwood, 1990). Moreover, DL-FalDH is not inducible by growth on C_1 compounds and its activity is unable to account for the formaldehyde oxidation rates in methanotrophs (Anthony, 1982; Vorholt, 2002). A membrane-bound DL-FalDH containing a PQQ was also purified from the *Gammaproteobacteria* methanotroph *Mcc. capsulatus* Bath (Zahn et al., 2001). It has been suggested that this protein is in fact a member of a new type of PQQ formaldehyde/quinone reductase based on sequence

similarity with sulfide/quinone reductase and wide distribution amongst methanotrophs (Keltjens et al., 2014).

H_4F is an important coenzyme that functions as a C_1 carrier in various biochemical reactions and found in all three domains of life (Maden, 2000). In methanotrophs, the H_4F-dependent formaldehyde oxidation is initiated by the spontaneous condensation of formaldehyde with H_4F to form N^5,N^{10}-CH_2=H_4F. This intermediate is oxidized to N^5,N^{10}-CH≡H_4F^+ by NADP-specific methylene-H_4F/H_4MPT dehydrogenase (MtdA), and can also serve as a substrate that enters the serine cycle for carbon assimilation (Figure 1.12) (Vorholt et al., 1998; Hagemeier et al., 2001). N^5,N^{10}-CH≡H_4F^+ is then transformed to N^{10}-CHO-H_4F catalyzed by methenyl-H_4F cyclohydrolase (Fch) through a reversible reaction (Pomper et al., 1999). Alternatively, these two reactions can be catalyzed by bifunctional methylene-H_4F dehydrogenase/cyclohydrolase (FolD) (Studer et al., 2002). Finally, the intermediate is transformed to formate and H_4F is released through a reversible reaction by formyl-H_4F synthetase/ligase (Fhs/FtfL) or irreversible reaction by formyl-H_4F deformylase (PurU) (Nagy et al., 1995). It is important to note that N^5,N^{10}-CH_2=H_4F can be formed via condensation of formate with H_4F following the reductive direction of the H_4F-dependent pathway, and benefits methanotrophs that exploit the serine cycle for carbon assimilation (Figure 1.13) (Crowther et al., 2008). Indeed, the enzymes of this pathway are found at high levels during methylotrophic growth in serine cycle methylotrophs (Marison & Attwood, 1982; Vorholt, 2002). Characterization of a methylotroph mutant deficient in FtfL also supported a model in which the H_4F-dependent pathway provides the substrate for the serine cycle from formate via the reductive direction (Marx et al., 2003; Crowther et al., 2008). MtdA and Fch are present in all *Alpha*- and *Gammaproteobacteria* methanotrophs, but, as mentioned before, absent in Verrucomicrobia methanotrophs, which utilize the FolD instead

(Khadem et al., 2012b; Khmelenina et al., 2018a). In addition, "*Ca.* Methylomirabilis oxyfera" has PurU instead of Fhs/FtfL for the final, irreversible release of H_4F (Chistoserdova, 2011), which would have little consequence on this methanotroph because it fixes carbon via Calvin-Benson-Bassham cycle rather than serine cycle.

In addition to the well-known H_4F-dependent pathway, the H_4MPT-dependent pathway was proposed based on genes found in the methylotroph *Mrr. extorquens* AM1 that closely resembled those involved in carbon metabolism from methanogenic and sulfate-reducing archaea and subsequent characterization of these gene products (Chistoserdova et al., 1998; Vorholt et al., 1998). The H_4MPT-dependent formaldehyde oxidation is initiated by the condensation of formaldehyde and the pterin cofactor to form N^5,N^{10}-CH_2=H_4MPT through a spontaneous reaction, accelerated by the formaldehyde activation enzyme (Fae) (Figure 1.12) (Vorholt et al., 2000). NAD(P)-dependent methylene-H_4MPT dehydrogenase (MtdB), a distant homolog of MtdA, catalyzes the oxidation of N^5,N^{10}-CH_2=H_4MPT to N^5,N^{10}-CH≡H_4MPT^+ (Hagemeier et al., 2000), which is then transformed to N^5-CHO-H_4MPT by methenyl-H_4MPT cyclohydrolase (Mch) (Pomper et al., 1999). Then, with the help of another C_1 carrier methylofuran (Hemmann et al., 2016, 2019), the H_4MPT is released by the formyltransferase/hydrolase complex (Fhc) and formate is produced (Pomper et al., 2002). It has been proposed that in the methylotroph *Mrr. extorquens* AM1, the H_4MPT-dependent pathway is the dominant formaldehyde oxidation pathway, whereas the H_4F-dependent pathway mainly serves in the reductive direction to produce substrates for carbon assimilation via the serine cycle (Crowther et al., 2008), which can also be true in serine cycle methanotrophs.

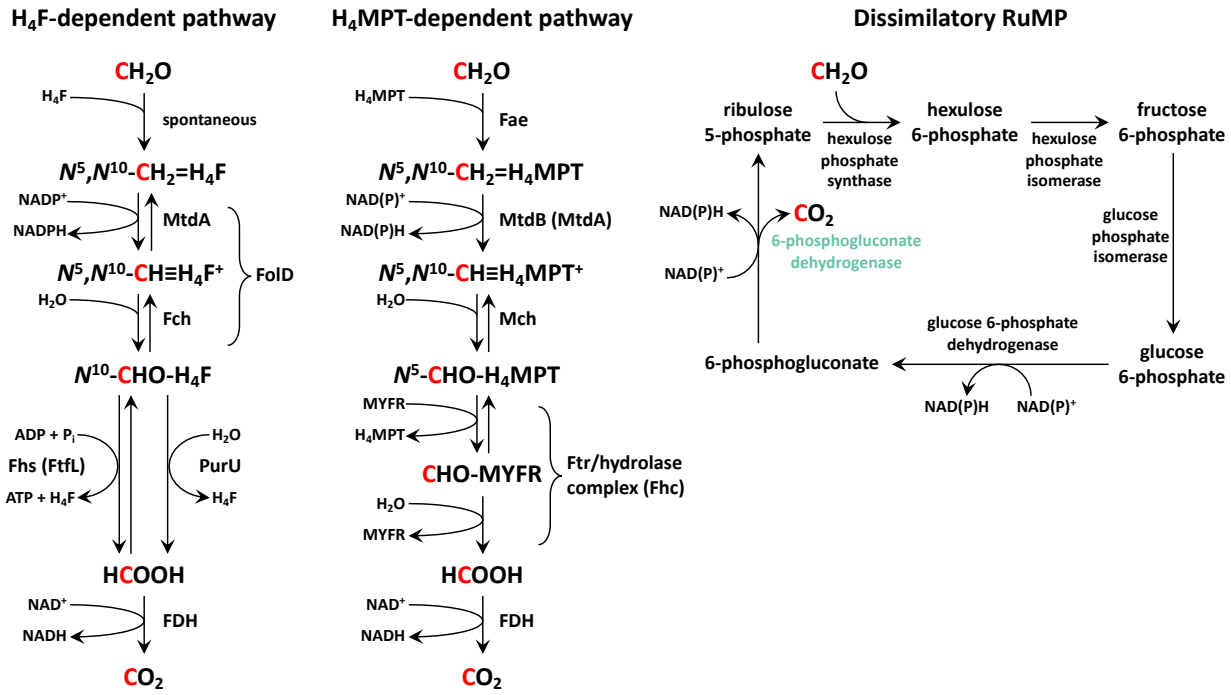

Figure 1.12. Formaldehyde oxidation pathways in methanotrophs (slightly modified from C. Anthony, 1982; Vorholt, 2002). C_1 is noted in red. The enzyme responsible for closing the dissimilatory RuMP cycle is noted in green. H_4F, tetrahydrofolate; H_4MPT, tetrahydromethanopterin; MYFR, methylofuran. Enzymes involved in H_4F- and H_4MPT-dependent pathways are described in Table 1.3.

Table 1.3. Enzymes involved in H_4F- and H_4MPT-dependent formaldehyde oxidation pathways.

Pathway	Enzyme	Function	Reference
H_4F-dependent	FolD	bifunctional methylene-H_4F dehydrogenase/cyclohydrolase	Studer et al. (2002)
H_4F-dependent / H_4MPT-dependent	MtdA	NADP-specific methylene-H_4F / H_4MPT dehydrogenase	Vorholt et al. (1998)
H_4F-dependent	Fch	methenyl-H_4F cyclohydrolase	Pomper et al. (1999)
H_4F-dependent	Fhs (FtfL)	formyl-H_4F synthetase (formyl-H_4F ligase)	Marx et al. (2003)
H_4F-dependent / H_4MPT-dependent	FDH	formate dehydrogenase	
H_4F-dependent	PurU	formyl-H_4F deformylase	Nagy et al. (1995)
H_4MPT-dependent	Fae	formaldehyde activating enzyme	Vorholt et al. (2000)
H_4MPT-dependent	MtdB	NAD(P)-dependent methylene-H_4MPT dehydrogenase	Hagemeier et al. (2000)
H_4MPT-dependent	Mch	methenyl-H_4MPT cyclohydrolase	Pomper et al. (1999)
H_4MPT-dependent	Ftr	formyltransferase	Pomper and Vorholt (2001)
H_4MPT-dependent	Fhc	Ftr/hydrolase complex	Pomper et al. (2002)

Gammaproteobacteria methanotrophs, which typically use the RuMP pathway to fix carbon, can also carry out dRuMP to oxidize formaldehyde (Kalyuzhnaya et al., 2019). The dRuMP cycle involves 6-phosphogluconate dehydrogenase, which releases CO_2 and produces reducing equivalents as NAD(P)H from the six-carbon intermediate, in addition to the enzymes required to fix formaldehyde (Figure 1.12) (Anthony, 1982). However, the activities of glucose-6-phosphate and 6-phosphoglucoante dehydrogenases are low in *Gammaproteobacteria* methanotrophs, and thus the significance of dRuMP in these organisms is unclear (Zatman, 1981; Chistoserdova & Lidstrom, 2013).

1.2.2. Carbon assimilation

Methanotrophs utilize the RuMP, serine, or CBB cycles to fix carbon largely depending on their classification. That is, methanotrophs belonging to the *Gammaproteobacteria* class mainly fix carbon via RuMP cycle, those of *Alphaproteobacteria* class the serine cycle, and those of the phylum Verrucomicrobia and candidate phylum NC10 the CBB cycle (Figure 1.13). The point of entry for carbon assimilation varies for each pathway, where formaldehyde, $CH_2=H_4F$, and CO_2 enters the RuMP, serine, and CBB cycles, respectively. In the RuMP and serine pathways of carbon assimilation, the C_1 compound is condensed with multicarbon compounds, and the cycles are completed through production of C_3 compounds and regeneration of the acceptor molecules (Chistoserdova & Lidstrom, 2013).

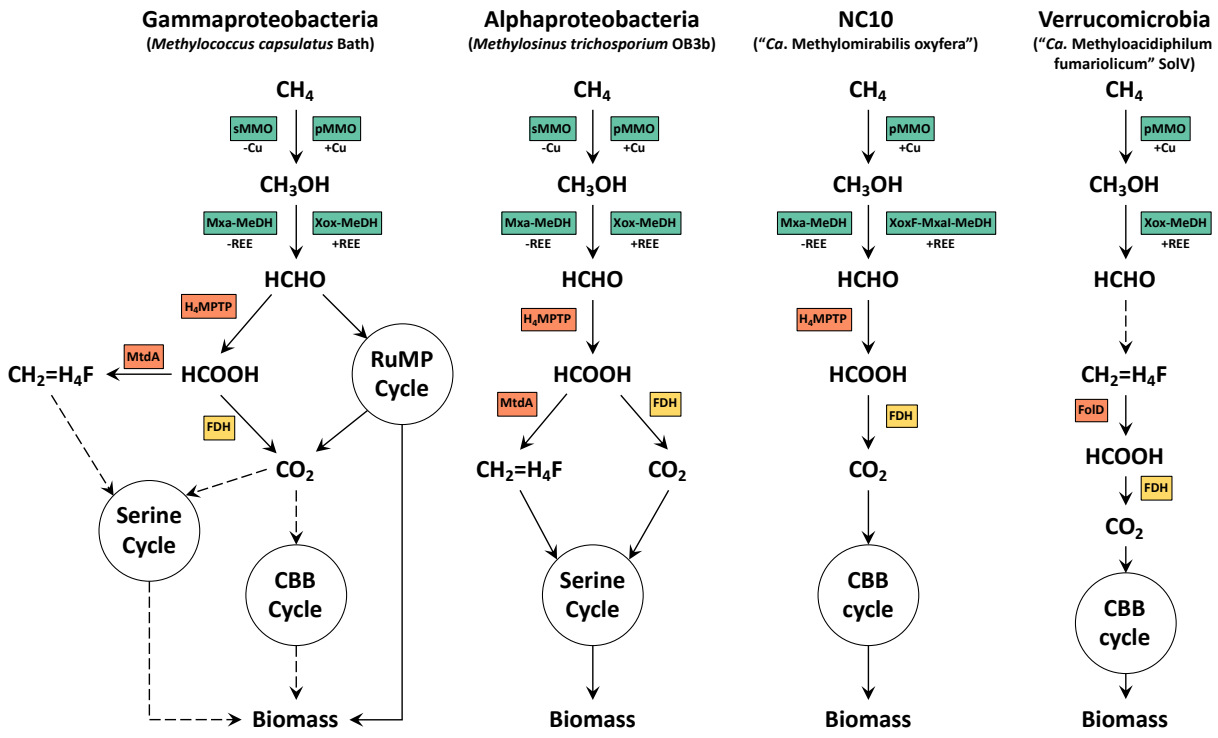

Figure 1.13. A simplified diagram depicting major substrates, intermediates, and methanotrophy metabolic modules (modified from Chistoserdova, 2011). Primary oxidation modules are shown in green, formaldehyde-related modules in red, formate dehydrogenase module in yellow, and assimilation modules in circle. Dashed lines represent lack of biochemical knowledge or lack of knowledge of significance during methanotrophic growth.

1.2.2.1. Ribulose monophosphate cycle

Gammaproteobacteria methanotrophs mainly fix carbon via the RuMP cycle, where formaldehyde is the entry point. The RuMP cycle is initiated by formaldehyde fixation via condensation with ribulose-5-phosphate by 3-hexulosephosphate synthase (Hps) (Figure 1.14) (Kemp, 1972, 1974; Anthony, 1982; Khmelenina et al., 2018a). The resulting (D-arabino)-3-hexulose-6-phosphate is very unstable and is immediately isomerized to fructose-6-phosphate, catalyzed by 6-phospho-3-hexulose isomerase (Phi/Hpi) (Ferenci et al., 1974). The genes encoding for Hps and Phi/Hpi are found in all RuMP methanotrophs, and in some, fused *hps-phi*

genes have been identified (Rozova et al., 2017). It is interesting to note that *hps-phi* is not found in any nonmethanotrophic methylotrophs.

In the second part of the cycle, fructose-6-phosphate is eventually cleaved to C_3 molecules via three alternative pathways – the Entner-Doudoroff (ED) pathway, Embden-Meyerhof-Parnas (EMP) glycolysis, and phosphoketolase pathway (Khmelenina et al., 2018a). In the ED pathway, fructose-6-phosphate is transformed to glucose-6-phosphate, 6-phosphogluconate, then to 2-keto-3-deoxy-6-phosphogluconate (KDPG), which is then cleaved to pyruvate and glyceraldehyde-3-phosphate (GAP) by KDPG-aldolase (Anthony, 1982). In the EMP glycolysis pathway, fructose-6-phosphate is phosphorylated to fructose-1,6-biphosphate by pyrophosphate-dependent 6-phosphofructokinase (Anthony, 1982), which is subsequently cleaved to GAP and dihydroxyacetone phosphate (DHAP). Here, PPi, a by-product of various anabolic reactions, is reutilized instead of ATP, which increases the energy efficiency of carbon fixation (Khmelenina et al., 2018b). In the phosphoketolase (Xfp) pathway, Xfp cleaves fructose-6-phosphate to erythrose-4-phosphate and acetyl-phosphate, which is then transformed to acetate via reversible acetate kinase (Ack) (Sánchez et al., 2010; Rozova et al., 2015; Khmelenina et al., 2018a). The phosphoketolase pathway increases the efficiency of C_2 production by preserving the C-C bond formed during C_1 fixation, as it bypasses the traditional glycolytic pathway that inevitably cleaves this C-C bond (Rozova et al., 2015; Khmelenina et al., 2018a). Interestingly, *xfp* and *ack* are found in nearly all methanotrophs and in many other C_1-utilizing bacteria (Rozova et al., 2015). In the final part of the RuMP cycle, three molecules of ribulose-5-phosphate is regenerated from rearranging two molecules of fructose-6-phosphate and one of GAP via reactions similar to those in the CBB cycle (Anthony, 1982). The RuMP cycle is

thermodynamically the most efficient carbon fixation pathway in methanotrophs (Anthony, 1982; Kalyuzhnaya et al., 2019).

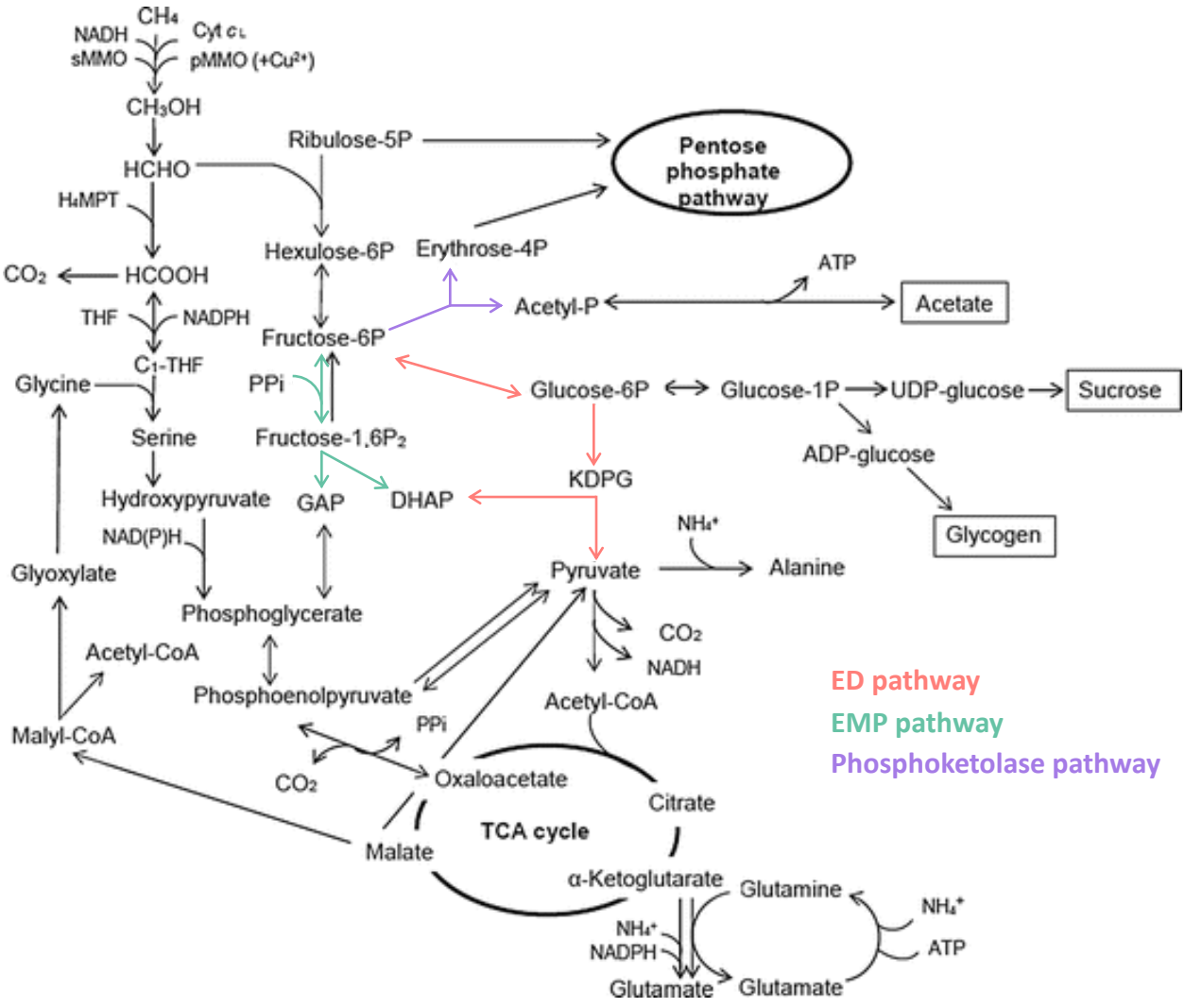

Figure 1.14. Pathways of carbon metabolism in *Gammaproteobacteria* methanotrophs (modified from Khmelenina et al. (2018a)). DHAP, dihydroxyacetone phosphate; ED, Entner-Doudoroff; EMP, Embden-Meyerhof-Parnas; KDPG, 2-keto-3-deoxy-6-phosphogluconate; GAP, glyceraldehyde- 3-phosphate; pMMO, particulate methane monooxygenase; sMMO, soluble methane monooxygenase; TCA, tricarboxylic acid; THF, tetrahydrofolate; H_4MPT, tetrahydromethanopterin.

Initially, the ED pathway was hypothesized to be the major contributor for carbon fixation via the RuMP cycle in *Gammaproteobacteria* methanotrophs due to high activities of 6-phosphogluconate dehydratase and KDPG-aldolase (Strøm et al., 1974; Kalyuzhnaya et al., 2013). However, some *Gammaproteobacteria* methanotrophs lack genes encoding for the complete ED pathway (Khmelenina et al., 2018a). In *Mcc. capsulatus* Bath, enzymes involved in both ED and EMP pathways were found to be expressed based on proteomics studies (Kao et al., 2004). In addition, ^{13}C-labeling analysis indicated carbon fixation via the EMP pathway in the halophilic *Gammaproteobacteria* methanotroph *Mtv. alcaliphilum* 20Z grown with methane under laboratory conditions (Kalyuzhnaya et al., 2013). Recently, it has been proposed that the ratio between the two pathways depend on the growth substrate and consequent need to balance the production and consumption of ATP and NADH (Fu et al., 2019). That is, when *Mtv. buryatense* 5GB1 was grown with either methane or methanol as the substrate, flux through the EMP and ED pathways were increased, respectively. As mentioned before, electrons are provided for pMMO activity via direct coupling with methanol oxidation in this organism (de la Torre et al., 2015), and growth on methanol would force the transfer these electrons instead to the electron transport chain to produce ATP, resulting in less NADH and ATP produced via oxidative phosphorylation from NADH as compared to growth on methane (Fu et al., 2019). Whichever pathway is used in the RuMP cycle, the results of the study conducted by Fu et al. (2019) suggest that RuMP methanotrophs with complete ED and EMP pathways may tune their metabolism to maintain a constant ATP and NADH pool.

1.2.2.2. Serine cycle

Alphaproteobacteria methanotrophs typically fix carbon via the serine cycle (Figure 1.15), though some methanotrophs of the *Beijerinckiaceae* family also possess full gene sets for the CBB pathway (Table 1.1) (Chen et al., 2010; Chistoserdova & Lidstrom, 2013; Miroshnikov et al., 2017). Carbon dioxide and N^5,N^{10}-CH_2=H_4F, both products of methane oxidation, are the substrates for the serine cycle (Large et al., 1962a), the latter is produced either via spontaneous condensation of formaldehyde with H_4F followed by oxidation, or the reverse/reductive direction of formaldehyde oxidation (Crowther et al., 2008).

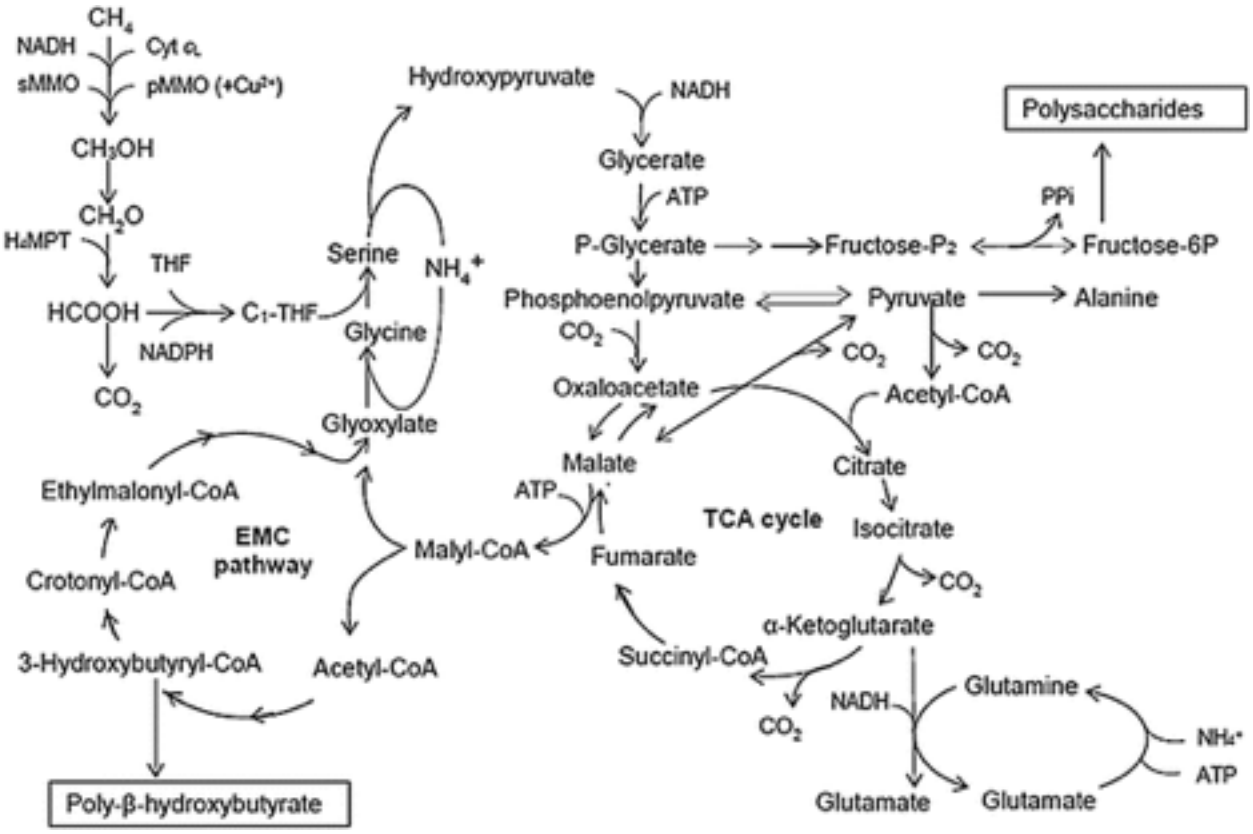

Figure 1.15. Pathways of carbon metabolism in *Alphaproteobacteria* methanotrophs (modified from Khmelenina et al. (2018a)). EMC, ethylmalonyl-CoA; TCA, tricarboxylic acid; THF, tetrahydrofolate; H_4MPT, tetrahydromethanopterin.

Much of the serine cycle was elucidated by the 1970s by Quayle and colleagues using radio-labeled substrates and subsequent evaluation of labeled biomass and intermediates (Large et al., 1961, 1962b, 1962a; Large & Quayle, 1963; Salem et al., 1973), and its genetics in the 1990s by Lidstrom and colleagues (Arps et al., 1993; Chistoserdova & Lidstrom, 1992, 1994c, 1994a, 1994b, 1997b, 1997a).

In the serine pathway, glyoxylate, a C_2 molecule, is transaminated to glycine, which is then condensed with N^5,N^{10}-CH_2=H_4F to produce serine, initiating the serine cycle for C_1 assimilation (Large et al., 1962a; Anthony, 2011). The amino group of serine is then transferred to glyoxylate, forming glycine and hydroxypyruvate (Large & Quayle, 1963; Khmelenina et al., 2018a). Hydroxypyruvate is transformed to glycerate, which is subsequently phosphorylated to 2- or 3-phosphoglycerate (Large & Quayle, 1963; Khmelenina et al., 2018a). Phosphoglycerate is then isomerized to phosphoenolpyruvate, which is then carboxylated to oxaloacetate (Large et al., 1962b). Oxaloacetate is reduced to malate, then transformed to malyl-CoA, which is then cleaved into acetyl-CoA and glyoxylate (Salem et al., 1973). In the serine cycle, this acetyl-CoA must be converted to glyoxylate to replenish glyoxylate for continued C_1 assimilation, however, the mechanism of such reaction has been unclear for about half a century (Anthony, 2011). It was initially hypothesized that the same mechanism used for replenishing intermediates of the tricarboxylic acid (TCA) cycle were employed for glyoxylate regeneration in serine cycle methanotrophs, i.e. the glyoxylate cycle (Kornberg & Madsen, 1957). Though a limited number of methanotrophs including *Methylocella silvestris* BL2 do possess and use the critical enzyme isocitrate lyase that transforms isocitrate to glyoxylate and succinate in this pathway (Bordel et al., 2020; Chen et al., 2010), most obligate methanotrophs do not (Trotsenko & Murrell, 2008). The glyoxylate regeneration cycle (GRC) involving 18 intermediates was proposed based on

genomic, mutant, and radiolabeled intermediate analyses of the methylotroph *Mrr. extorquens* AM1 (Korotkova et al., 2002a; Anthony, 2011). Though some of the intermediates were later found to be involved in glyoxylate regeneration, most were not involved (Anthony, 2011).

The ethylmalonyl-CoA (EMC) pathway was first verified in phototrophic purple non-sulfur bacteria lacking isocitrate lyase with the discovery of three novel enzymes, crotonyl-CoA carboxylase/reductase, ethylmalonyl-CoA mutase, and methylsuccinyl-CoA dehydrogenase (Meister et al., 2005; Alber et al., 2006; Erb et al., 2007, 2008, 2009). The EMC pathway in serine cycle methanotrophs share intermediates, reactions, and/or enzymes with the serine cycle, TCA cycle, polyhydroxybutyrate cycle, fatty acid biosynthesis pathway, and other metabolic pathways (Khmelenina et al., 2018a). In the EMC pathway, two molecules of acetyl-CoA are condensed to form acetoacetyl-CoA, which is then reduced to 3-hydroxybutyryl-CoA (Korotkova et al., 2002b). 3-Hydroxybutyryl-CoA is transformed to crotonyl-CoA, which is then transformed to the C_5 molecule EMC via reductive carboxylation by crotonyl-CoA carboxylase/reductase (Erb et al., 2007). EMC is transformed to β-methylmalyl-CoA via methylsuccinyl-CoA and mesaconyl-CoA, and is cleaved to produce glyoxylate and propionyl-CoA (Chistoserdova et al., 2003; Meister et al., 2005; Erb et al., 2008, 2009), thus replenishing the glyoxylate and closing the gap in C_1 assimilation via the serine cycle. The fate of propionyl-CoA determines the overall carbon balance, i.e. $3C_1 + 3CO_2 = 2C_3$ vs $3C_1 + 4CO_2 = 1C_3 + 1C_4$ (Peyraud et al., 2009; Anthony, 2011). The EMC pathway was further experimentally confirmed through investigating intermediates and their flux via ^{13}C metabolomics of *Mrr. extorquens* AM1 (Peyraud et al., 2009). The results of this study ruled out GRC as a contributor for glyoxylate regeneration and closed the serine cycle during methylotrophic growth. It is also interesting to note that some *Gammaproteobacteria* methanotrophs, e.g. *Mcc. capsulatus* Bath, have the

complete gene set for the serine cycle, but not for the EMC cycle or the glyoxylate cycle (Chistoserdova et al., 2005; Kalyuzhnaya et al., 2015b, 2019).

1.2.2.3. Calvin-Benson-Bassham cycle

The activity and complete gene set for Calvin-Benson-Bassham (CBB) cycle (Figure 1.16) was first observed in the *Gammaproteobacteria* methanotroph *Mcc. capsulatus* Bath, though the main route of carbon assimilation is via the RuMP cycle and autotrophic growth is very slow and restricted to solid medium for this organism (Taylor et al., 1981; Baxter et al., 2002). The complete gene set for CBB was also found in other Proteobacteria methanotrophs, of which some exhibited activity as well (Table 1.1) (Eshinimaev et al., 2004; Chen et al., 2010; Dedysh et al., 2002, 2015; Frindte et al., 2017a). In thermophilic methanotrophs *Mcc. capsulatus* Bath and *Methylocaldum szegediense* O-12, RuBisCO activity is enhanced with temperature increase, suggesting a role of the CBB cycle in thermoadaptation (Eshinimaev et al., 2004; Khmelenina et al., 2018a). The exact role of the CBB cycle in Proteobacteria methanotrophs is yet to be identified.

Methanotrophs belonging to the phylum Verrucomicrobia and candidate phylum NC10 primarily utilize the well-known CBB cycle to assimilate carbon dioxide and use methane as the source of energy (Figure 1.13). These methanotrophs lack key genes of the Serine and RuMP pathways for carbon assimilation, and $^{13}CH_4$ and $^{13}CO_2$/bicarbonate experiments indicated that CO_2 is the sole source of carbon (Khadem et al., 2011; Rasigraf et al., 2014). The Verrucomicrobia methanotroph "*Ca.* Methylacidiphilum fumariolicum" SolV possesses a form Ie RuBisCO (Khadem et al., 2011), whereas the RuBisCO found in "*Ca.* Methylomirabilis oxyfera" of the candidate phylum NC10 is of form Ic, distinct from that found in

Verrucomicrobia methanotrophs, and is more closely related to Proteobacteria RuBisCOs such as those found in methanotrophs of the *Beijerinckiaceae* family (Rasigraf et al., 2014). Though Verrucomicrobia methanotrophs have carboxysome-like structures, methanotrophs of both phyla lack genes encoding for carboxysomes and carbon fixation seem to be cytoplasmic rather than carboxysomal (Khadem et al., 2011; Rasigraf et al., 2014).

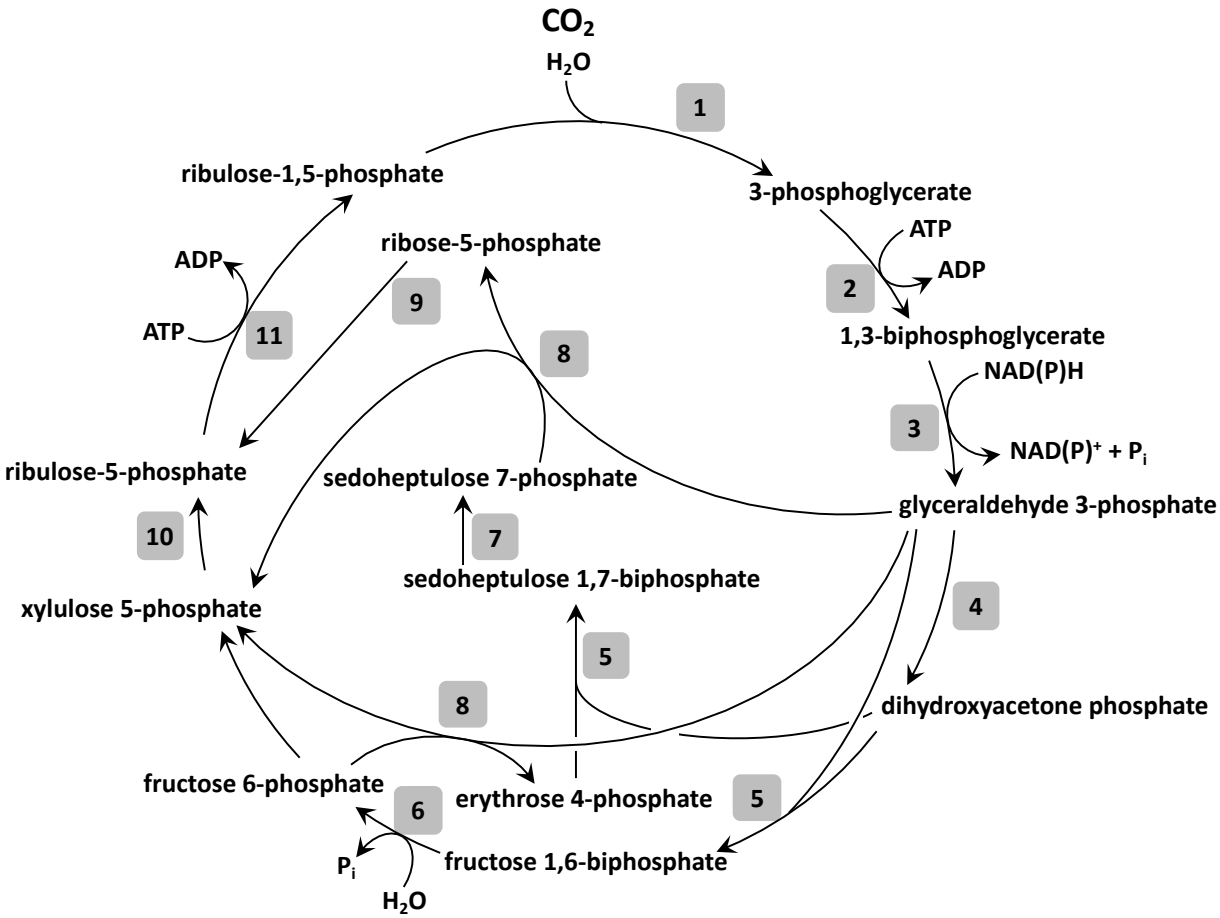

Figure 1.16. Calvin-Benson-Bassham cycle (modified from Sato and Atomi (2010) and Crumbley and Gonzalez (2018)). The corresponding enzymes are: 1: ribulose-1,5-bisphosphate carboxylase/oxygenase, 2: phosphoglycerate kinase, 3: glyceraldehyde-3-phosphate dehydrogenase, 4: triose phosphate isomerase, 5: fructose- bisphosphate aldolase, 6: fructose-1,6-bisphosphatase, 7: sedoheptulose bisphosphatase, 8: transketolase, 9: ribose-5-phosphate isomerase, 10: ribulose-5-phosphate 3-epimerase and 11: phosphoribulokinase. The directions of the arrows represent the direction of the pathway, and do not indicate that the enzyme reactions are irreversible.

1.3. Metal uptake systems

1.3.1. Copper uptake systems

Methanotrophs have several methods of acquiring copper from the environment and any single species often is found to have redundant systems (Table 1.2). For example, all methanotrophs excluding the extreme acidophiles of the Verrucomicrobia phylum contain *copCD* (copper resistance), which encode for a periplasmic copper-binding protein and inner membrane transporter (Figure 1.17) (Arnesano et al., 2003; Gu et al., 2017b). Some *Alphaproteobacteria* methanotrophs have *mbnABCM* (methanobactin), encoding for a chalkophore that is excreted, binds copper and is then taken up (Semrau et al., 2013). Some *Gammaproteobacteria* methanotrophs have *mopE* (*Methylococcus* outer membrane protein) and an associated cytochrome *c* peroxidase (Helland et al., 2008; Ve et al., 2012), or close analogs *corAB* (copper-repressible protein) (Berson & Lidstrom, 1997; Johnson et al., 2014), that both encode for outer membrane proteins that import extracellular copper. A passive porin-dependent mode of copper uptake has also been proposed based on inhibition studies (Balasubramanian et al., 2011).

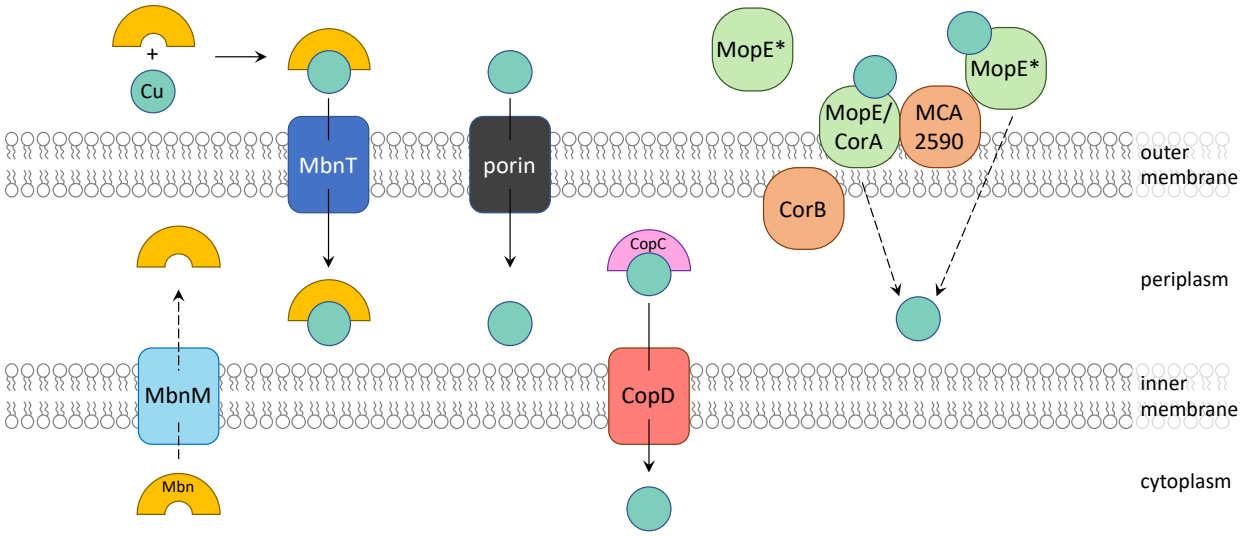

Figure 1.17. Copper uptake strategies found in methanotrophs. Cop, copper resistance; Cor, copper-repressible protein; Mbn, methanobactin; Mop, *Methylococcus* outer membrane protein.

1.3.1.1. CopCD in methanotrophs

copC and *copD* encode for a periplasmic copper-binding protein and inner membrane protein, respectively, and are part of the operon *copABCD* that is responsible for copper resistance in various bacteria (Cha & Cooksey, 1993; Koay et al., 2005). The CopC and CopD pair is one of several strategies by which methanotrophs appear to import copper. There are two binding sites in CopC, each for Cu(I) and Cu(II), that varies between organisms (Lawton et al., 2016). In methanotrophs, CopC contains one Cu(II) binding site as opposed to two binding sites observed in some nonmethanotrophs (Koay et al., 2005; Lawton et al., 2016). The copper binding affinity also varies depending on the coordination of the binding sites. In a *Gammaproteobacteria Pseudomonas syringae* pathovar *tomato*, the dissociation constants for the Cu(I) and Cu(II) binding sites are 10^{-13} and 10^{-15}, respectively (Koay et al., 2005), and in *Pseudomonas fluorescens* SBW25, $10^{-17.2}$ for the single Cu(II) binding site (Wijekoon et al., 2015).

It has been proposed that *copD* is directly involved in the copper switch that regulates the expression of pMMO and sMMO in copper replete/deplete conditions based on the disrupted *copD* found in a mutant *Msn. trichosporium* OB3b that constitutively expresses sMMO (Kenney et al., 2016b). However, deletion mutants of *Msn. trichosporium* OB3b lacking *copCD* or *copCD* and *mbnAN* still exhibited the copper switch (Gu et al., 2017b). Copper uptake by these mutants was also comparable to that of the wild-type, indicating redundancy of copper uptake systems in this organism (Gu et al., 2017b). In addition, *copCD* (ADVE02_v2_10396, ADVE02_v2_10395) is mildly upregulated in the presence of copper, indicating that *copCD* most likely has a minor role in the copper switch (Gu et al., 2017b; Gu & Semrau, 2017). In support of this conclusion, the complete *copCD* pair (MCA0808, MCA0807) in the *Gammaproteobacteria* methanotroph *Mcc. capsulatus* Bath is not differentially expressed in response to copper, though a lone *copC* (MCA2170) is upregulated in the presence of copper (Larsen & Karlsen, 2016).

1.3.1.2. MCA2590/MopE and CorAB in Gammaproteobacteria methanotrophs

Fjellbirkeland et al. (1997) found five proteins exclusive to the outer membrane fraction of a *Gammaproteobacteria* methanotroph, *Mcc. capsulatus* Bath – MopA-E (*Methylococcus* outer membrane protein). The surface-exposed MopE was later found to have a truncated form, MopE*, that consists of the C-terminal region of MopE and is excreted to the surrounding (Fjellbirkeland et al., 2001). Both forms of MopE are expressed under low copper-to-biomass conditions (Karlsen et al., 2003). MopE* contains a novel protein fold and mononuclear copper-binding site, where copper is coordinated by two imidazoles of His^{132} and His^{203}, oxygen ligand of a water molecule, and the N_1 atom of the unique $kynurenine^{130}$ formed via post-translational

oxidation of Trp^{130} (Fjellbirkeland et al., 2001; Helland et al., 2008). This mononuclear copper-binding site has copper occupancy of approximately 0.65 and binds Cu(I) with high affinity as determined via competition experiments using Bathocuproine ($K_d < 10^{-20}$ M) (Helland et al., 2008; Ve et al., 2012). MopE* can also bind up to two Cu(II) ions at the weaker mononuclear binding sites thought to be in the first 24 N-terminal amino acid residues (K_d in micromolar range) (Ve et al., 2012). The only protein identified to be similar to MopE to date is CorA, a membrane-bound copper transporter found in another *Gammaproteobacteria* methanotroph, *Methylomicrobium album* BG8 (Berson & Lidstrom, 1997). CorA is much smaller than MopE or MopE* (28.5 kDa vs 64/45 kDa), and thus shows similarity only to the C-terminal of MopE, or the secreted MopE* (Berson & Lidstrom, 1997; Fjellbirkeland et al., 2001). However, the two histidine residues and kynurenine are all conserved in CorA (His^{64}, His^{114}, Kyn^{62}) and the overall structure of CorA is similar to that of MopE* (Johnson et al., 2014). Disruption of *corA* in *Mmc. album* BG8 resulted in poor growth (Berson & Lidstrom, 1997), and in *Mtv. alcaliphilum* 20Z, lack of growth in methane that was relieved by growth on methanol (Shchukin et al., 2011). In addition, MopE and CorA are copper repressible and bind copper with high affinity ($K_d < 10^{-12}$ M – 10^{-20} M) (Helland et al., 2008; Johnson et al., 2014), all indicative of a crucial role of MopE and CorA in copper homeostasis and acquisition.

Immediately upstream of *mopE* is an open reading frame (MCA2590) encoding for a surface-associated di-heme cytochrome *c* peroxidase (SACCP), a subfamily of bacterial di-heme cytochrome *c* peroxidase (BCCP) family proteins (Karlsen et al., 2005). This SACCP is exposed to the surface rather than the periplasm and has a much longer amino acid sequence as compared to other BCCPs (Karlsen et al., 2005). A homolog, *corB*, is found immediately downstream of *corA* in *Mmc. album* BG8, which encodes for an SACCP that is associated with the outer

membrane and exposed to the periplasm (Karlsen et al., 2010). Both MCA2590 and CorB are similar to a tryptophan-modifying, methylamine utilizing protein MauG, another member of the BCCP family (Wang et al., 2003; Karlsen et al., 2005), and as such, MCA2590 was speculated to convert Trp^{130} to Kyn^{130} in MopE and CorA (Helland et al., 2008; Karlsen et al., 2010). MCA2590 with *mopE* and *corA* with *corB* comprise operons regulated under a promoter upstream of MCA2590/*corA*, and expression of these genes are upregulated under low copper-to-biomass conditions (Karlsen et al., 2005, 2010). So far, the MCA2590/MopE and CorAB homologs were only identified in methanotrophs, specifically in some *Gammaproteobacteria* methanotrophs, suggesting a specific strategy used to compete for copper (Table 1.2).

1.3.1.3. Methanobactin in Alphaproteobacteria methanotrophs

In the 1990s, researchers found evidence of peptide-based extracellular copper-binding compounds in some methanotrophs (Zahn & DiSpirito, 1996; DiSpirito et al., 1998; Téllez et al., 1998), which was later termed methanobactin (MB) (Kim et al., 2004). MB was first purified and crystallized from *Msn. trichosporium* OB3b (Kim et al., 2004). This copper-binding compound, or chalkophore, was found to be a ribosomally synthesized post-translationally modified polypeptide with two oxazolone rings, each with an associated thioamide group that collectively serve to bind copper as Cu(II) (Figure 1.18) (Choi et al., 2006; El Ghazouani et al., 2011). The copper is coordinated via the N_2S_2 ligand set with a distorted tetrahedral geometry (Kim et al., 2004; Choi et al., 2006). Upon binding to MB, Cu(II) is reduced to Cu(I), which is then bound with a higher affinity, potentially to prevent uncontrolled, toxic redox reactions within the cell (El Ghazouani et al., 2011, 2012). The reductant is as yet unidentified, although it

has been speculated that water may serve as the electron source, though it has not been experimentally proven (Krentz et al., 2010).

Later, other MBs were identified and characterized from *Methylocystis* sp. SB2 (Krentz et al., 2010), *Methylocystis hirsuta* CSC1, *Methylocystis* strain M, *Methylocystis rosea* SV97 (El Ghazouani et al., 2012), *Methylosinus* sp. LW4 (Kenney et al., 2016a), and *Methylosinus sporium* NR3K (Baslé et al., 2018), all belonging to the *Methylocystaceae* family of the *Alphaproteobacteria* class (Figure 1.19). This led to a classification of MBs based on primary and secondary structures into two general groups, i.e., Group I and Group II MBs, represented by *Msn. trichosporium* OB3b and *Methylocystis* sp. SB2, respectively (Kim et al., 2004; Krentz et al., 2010). Both Group I and II MBs have two heterocyclic rings with associated enethiol groups responsible for copper binding, and the C-terminal or B ring is always an oxazolone (DiSpirito et al., 2016). However, there are significant differences between Group I and II MBs as well. First, Group I MBs have an N-terminal oxazolone ring, or in one case (for *Msn. sporium* NR3K), a pyrazinedione ring, whereas Group II MBs have an N-terminal imidazolone or pyrazinedione ring (Figure 1.19). Second, Group I MBs form a dicyclic structure after binding copper via the internal disulfide bridge, while Group II MBs lack this bridge and form a hairpin shape (Figure 1.18) (Behling et al., 2008; Baral et al., 2014). Third, Group II MBs characterized so far are sulfonated (Krentz et al., 2010; El Ghazouani et al., 2012; DiSpirito et al., 2016; Semrau & DiSpirito, 2019), and such modification appears to enhance copper binding (El Ghazouani et al., 2012). Fourth, Group I MBs have to date only been purified/characterized from methanotrophs of the *Methylosinus* genus, while Group II MBs have only been purified/characterized from *Methylocystis* species, though bioinformatic analyses suggest that some methanotrophs have the genes to synthesize both forms of MB.

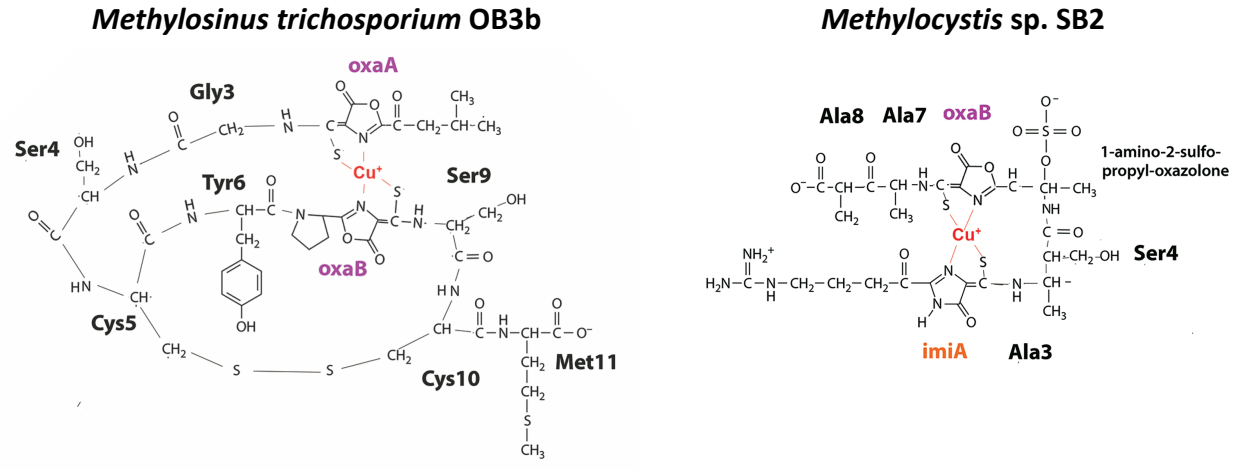

Figure 1.18. Structures of Groups I and II methanobactins (MB). Note that MB from *Msn. trichosporium* OB3b (Group I MB) has a dicyclic structure, while MB from *Methylocystis* sp. SB2 (Group II MB) has a hairpin-like form when copper is bound.

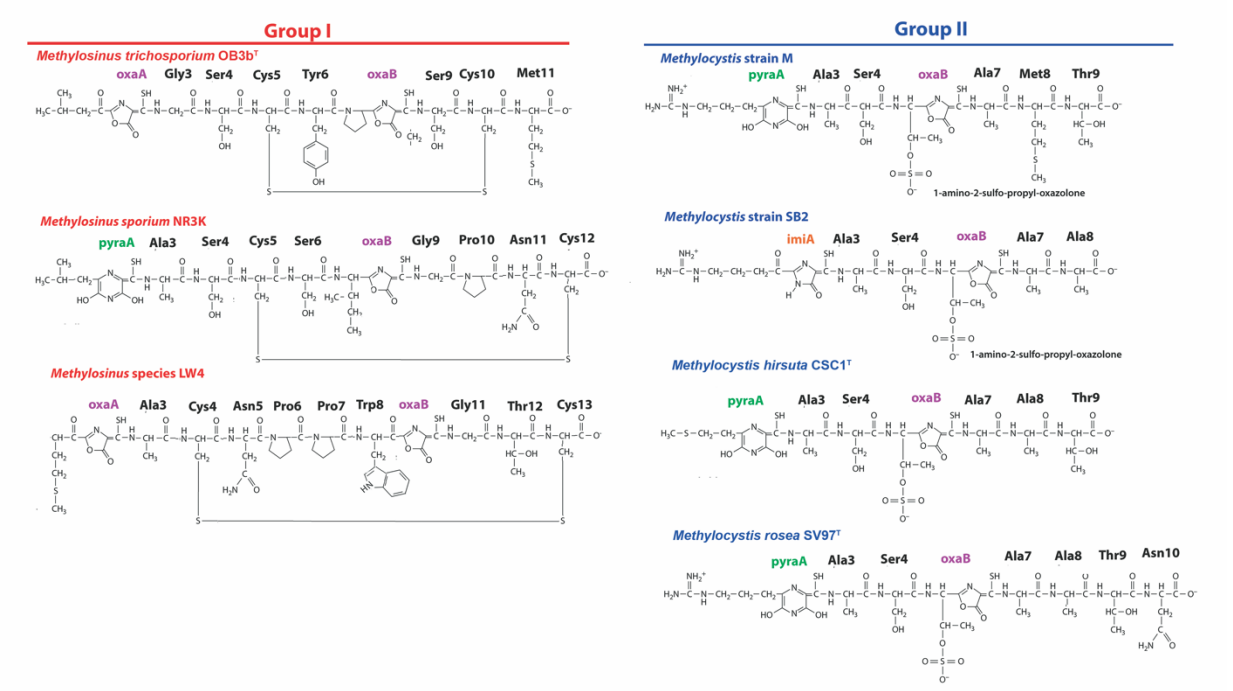

Figure 1.19. Primary structures of characterized Group I and II methanobactins. oxa, oxazolone; pyr, pyrazinedione; imi, imidazolone.

Initially, it was hypothesized that due to the presence of heterocyclic rings in MB, this modified polypeptide was created via a non-ribosomal polypeptide synthase much like how siderophores are produced (Crosa & Walsh, 2002; Balasubramanian & Rosenzweig, 2008). Subsequent acid digestion assays, however, suggested that these rings may in fact be derived from a dipeptide sequence, and that one of these amino acids was likely a cysteine (Krentz et al., 2010), i.e. MB was more likely a ribosomally synthesized post-translationally modified polypeptide. Scanning of the genome of *Msn. trichosporium* OB3b identified one gene, *mbnA*, that appeared to encode for the polypeptide precursor of mature MB. This polypeptide included both a leader and a core peptide with a potential cleavage site, indicating that the mature product was secreted. Knock-out of *mbnA* indicated that it did indeed encode for the precursor of MB as no production was observed in such a mutant (Semrau et al., 2013).

mbnA is part of gene cluster that includes many genes with functions either experimentally validated or presumed based on bioinformatic comparisons (Figure 1.20 and Table 1.4). For all identified MB gene clusters in methanotrophs, immediately adjacent to *mbnA* are two genes, *mbnBC*, that appear to encode for proteins required for the formation of the C-terminal oxazolone ring from an XC dipeptide (Kenney et al., 2018). In addition, all identified MB gene clusters in methanotrophs have *mbnM* (believed but not proven to be responsible for MB secretion) and *mbnT* (shown to encode a TonB-dependent transporter responsible for MB uptake in at least *Msn. trichosporium* OB3b) (Gu et al., 2016a).

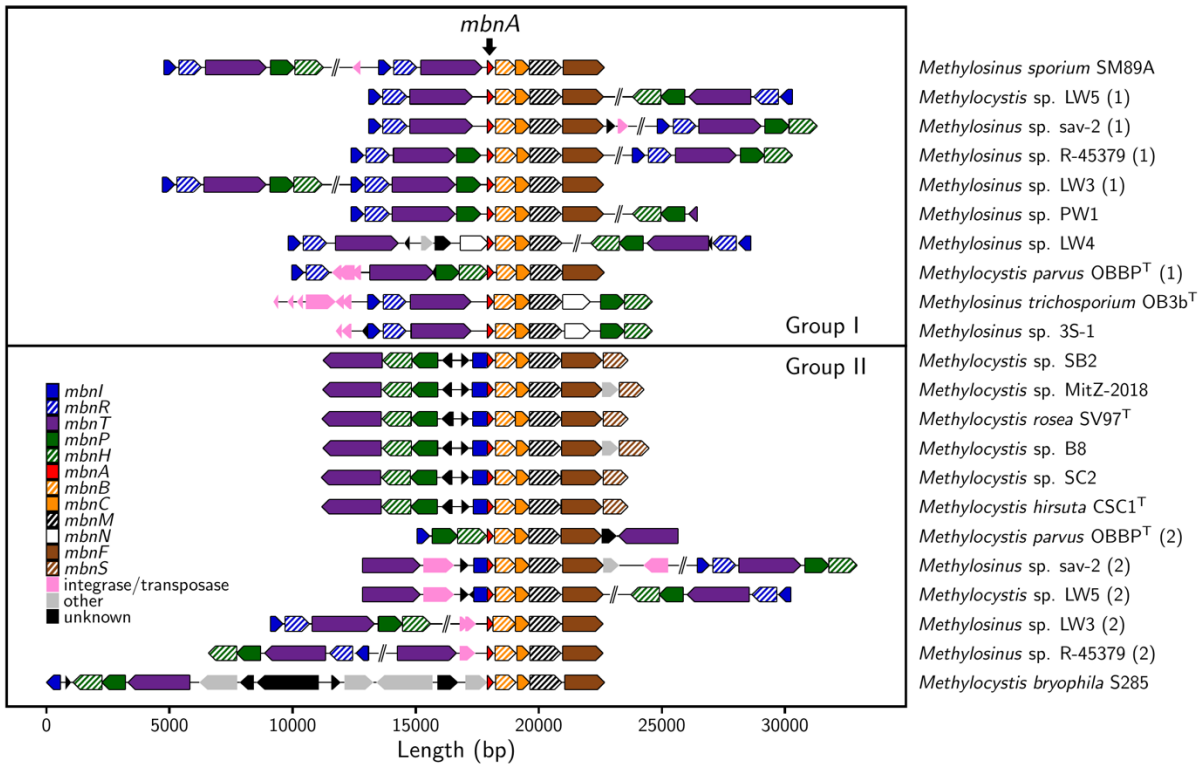

Figure 1.20. Identified methanobactin gene clusters from methanotrophs with available genome sequences. Four genes are found in each cluster with consistent synteny, i.e. *mbnA* (in red, encoding for the precursor polypeptide of MB); *mbnB* and *mbnC* (in shaded and solid orange, involved in ring synthesis); and *mbnM* (black shaded, believed to be responsible for MB secretion). A gene encoding for a TonB-dependent transporter (in purple; *mbnT*) responsible for MB uptake is also found in each cluster, but location varies. Other genes are also often found in MB gene clusters, but are not consistently co-located, including *mbnIR* (in shaded and solid blue, encoding for an extracytoplasmic sigma factor and membrane sensor protein, respectively) and *mbnPH* (in shaded and solid green, encoding for a putative diheme cytochrome c peroxidase and its partner protein). Group I MB gene clusters frequently, but not consistently include mbnN (in white, encoding for an aminotransferase). All Group II and many Group I MB gene clusters include *mbnF* (in solid brown, encoding for a putative FAD-dependent oxidoreductase). Several but not all Group II MB gene clusters have *mbnS* (in shaded brown, putatively encoding for a sulfotransferase).

Several other genes are also often found in MB gene clusters, but are not consistently co-located, including *mbnIR* (encoding for an extracytoplasmic sigma factor and membrane sensor protein, respectively) and *mbnPH* (encoding for a di-heme cytochrome *c* peroxidase and its partner protein). It has been suspected that MbnIR play a role in regulating expression of *mbn* genes via interaction with MbnT (Kenney & Rosenzweig, 2013), but experimental data cast

doubt on this conclusion (Gu et al., 2016a). Thus, the role of these two genes in MB production is still an open question. Further, it has been speculated that MbnPH may play a role in the formation of the heterocyclic rings in MB and/or aid in copper release from MB (Kenney & Rosenzweig, 2018) but this has yet to be examined in any detail. It should also be noted that several MB gene clusters lack *mbnPH* (Figure 1.20), suggesting that these two genes are either not critical for MB production/copper release or that homologs elsewhere in the genome of various methanotrophs may serve in their place.

Table 1.4. Known or putative role of various genes in methanobactin biosynthesis.

Gene	Known or putative function	Reference
mbnA	Precursor polypeptide of methanobactin	Semrau et al., 2013
mbnB	Involved in synthesis of C-terminal oxazolone ring	Kenney et al., 2018
mbnC	Involved in synthesis of C-terminal oxazolone ring	Kenney et al., 2018
mbnM	Putative mechanism of MB secretion?	
mbnP	Di-heme cytochrome oxidase; may be involved in ring formation and/or copper release?	
mbnH	Partner protein of *mbnP*	
mbnI	Extracytoplasmic sigma factor, possible role in gene regulation?	
mbnR	Membrane sensor protein, possible role in gene regulation?	
mbnT	TonB-dependent transporter, required for MB uptake	Gu et al., 2016
mbnF	Putative FAD-dependent oxidoreductase, possible role in formation of N-terminal imidazolone/pyrazinedione ring?	
mbnN	Aminotransferase, required for formation of N-terminal oxazolone ring	Gu et al., 2017
mbnS	Putative sulfotransferase, required for sulfonation of threonine in MB?	

For Group I MBs with an N-terminal oxazolone ring (e.g., *Msn. trichosporium* OB3b), an aminotransferase (E.C.2.6.1.*x*) encoded by *mbnN* is critical for the formation of this ring (Gu et al., 2017a). Not all MB gene clusters putatively encoding for a Group I MB, however, include *mbnN*, suggesting that methanotrophs with these clusters may not have an N-terminal oxazolone ring, e.g., like that found in *Msn. sporium* NR3K (Figure 1.19). However, it should be noted that the genome of this strain is not available (Baslé et al., 2018). Alternatively, homologs of *mbnN*

that could serve in its place are found in methanotrophic genomes (data not shown), and it has been shown that other aminotransferases can fulfill the function of MbnN (Park et al., 2018).

All identified Group II MB gene clusters in methanotrophs include *mbnF*, encoding for a putative FAD-dependent oxidoreductase. It is thus tempting to speculate that *mbnF* is involved in the formation of N-terminal imidazolone/pyrazinedione ring in Group II MBs, but it must be noted that no experimental data have been published showing that this is indeed the case. It has been suggested that *mbnF* is required for the formation of the N-terminal pyrazinedione ring from an oxazolone precursor (Kenney & Rosenzweig, 2018), but as *mbnN* has been shown to be necessary for formation of this ring and most Group II MB gene clusters lack *mbnN* (although methanotrophs have aminotransferases encoded elsewhere in their genome; data not shown), such a conclusion should be considered at best tentative without more explicit empirical evidence. Finally, many, but not all MB gene clusters presumed to encode for Group II MBs also have *mbnS*, encoding for a putative sulfotransferase believed (but not experimentally shown) to sulfonate threonine that is combined with a cysteine to form the C-terminal oxazolone ring.

Some methanotrophs appear to have multiple MB gene clusters encoding for both Group I and II MBs, i.e., *Mct. parvus* OBBP, *Methylocystis* sp. LW5, *Methylosinus* sp. LW3, *Methylosinus* sp. R-45379, and *Methylosinus* sav2. To date, neither expression of any of these genes nor purification of MB from any of these strains has been reported. As such, it is unknown if these methanotrophs produce either or both general forms of MB, and if so, under what conditions. It should also be stressed that *mbnIR* and *mbnPH* are not part of several of these identified MB gene clusters; rather homologs of these genes are found some distance away. It is thus unclear: (1) what role these genes have in MB production, (2) if the lack of co-localization

with *mbn* genes with clearly identified function affects the ability of these strains to produce MB, or (3) if MB made by these strains is used as a chalkophore or if it serves some other purpose as MB appears to be a "moon-lighting" protein with multiple functions.

Finally, it is important to note that to date, core genes for MB biosynthesis (i.e. *mbnABCM*) have only been found in the genomes of *Methylosinus* and *Methylocystis* species and that not all methanotrophs in these genera have these genes (Table 1.1). Indeed, *mbn* genes are only found in ~10% of sequenced methanotrophic genomes (Dennison et al., 2018). Such data indicate that MB production is a ***not*** a universal trait of methanotrophs. Rather, other methanotrophs appear to rely on alternative copper-uptake systems for copper collection, or even 'steal' MB, suggesting that there may be copper competition between methanotrophs as seen between methanotrophs and denitrifying bacteria (Chang et al., 2018). We also note that the presence of *mbn* genes is ***not*** strictly correlated with the ability to express different forms of MMO, i.e. some methanotrophs with *mbn* genes can only express pMMO, while others can express both sMMO and pMMO (Table 1.1).

For those methanotrophs shown to produce MB, it is clear that it plays an important role in copper uptake, but it has also been found that methanotrophs have remarkable redundancy in their ability to sequester copper. That is, methanotrophs defective in MB production (i.e., knock outs of either *mbnA* or the MB gene cluster from *mbnA* through *mbnN*), were still able to sense and collect copper (Semrau et al., 2013; Gu et al., 2017b). Interestingly, the ability to express MB appears to amplify the cells' response to copper (Semrau et al., 2013).

Further, a mutant where *mbnT*, encoding for a TonB-dependent transporter was knocked-out showed that this mutant, although unable to take up MB, was able to sequester copper by some alternative means (Gu et al., 2016a). If, however, exogenous MB was added to this mutant

to ‘soak-up’ all available copper, copper uptake was prevented, indicating that this transporter was indeed required for uptake of copper associated with MB. It may be that methanotrophs that express MB utilize it as a high affinity copper uptake system when copper is limiting, but have other, lower-affinity systems when it is not. The identity and nature of these low-affinity systems is still elusive. It has been hypothesized that *copCD,* encoding for an inner membrane and periplasmic copper binding protein respectively, may be involved in copper uptake (Kenney et al., 2016b). Knock-out of these genes, either alone or in conjunction with genes for MB biosynthesis, however, does not prevent copper uptake, suggesting that they are either not involved in copper uptake, or that there are other, as yet unidentified, copper uptake systems in methanotrophs (Gu et al., 2017b).

1.3.2. Rare earth element uptake system

1.3.2.1. Lanmodulin and related transporters

Recently, a periplasmic REE-binding protein lanmodulin (LanM), similar to Ca^{2+}-binding protein calmodulin (CaM), with high affinity for REE ($K_{d,app}$ ~ 5 pM) was characterized in *Mrr. extorquens* AM1 . CaM contains EF hands, which are metal-binding motifs that occur in pairs, i.e. two, four or six, and is composed of a helix-loop-helix structural unit (Gifford et al., 2007). In CaM, the residues at positions 1, 3, 5, 7, and 9 of the EF loop serve as coordinating groups, as well as the bidentate carboxylate ligand of the acidic amino acid in the exiting helix, or position 12 with respect to the EF loop (Gifford et al., 2007). In addition, the EF hand pair forms a hydrophobic core once bound to Ca^{2+} and conformation of CaM is changed, contributing to increased stability (Figure 1.21). However, there are three distinct characteristics of the metal-binding EF hands in LanM compared to canonical EF hands found in CaMs that contribute to

enhanced selectivity of REEs over Ca^{2+}: (1) aspartate residue in the ninth position, (2) asparagine rarely found in the first position, (3) proline residue in second position, and (4) relatively short intermotif sequences spanning 12 or 13 residues between each EF hand (Figure 1.22) (Cotruvo et al., 2018).

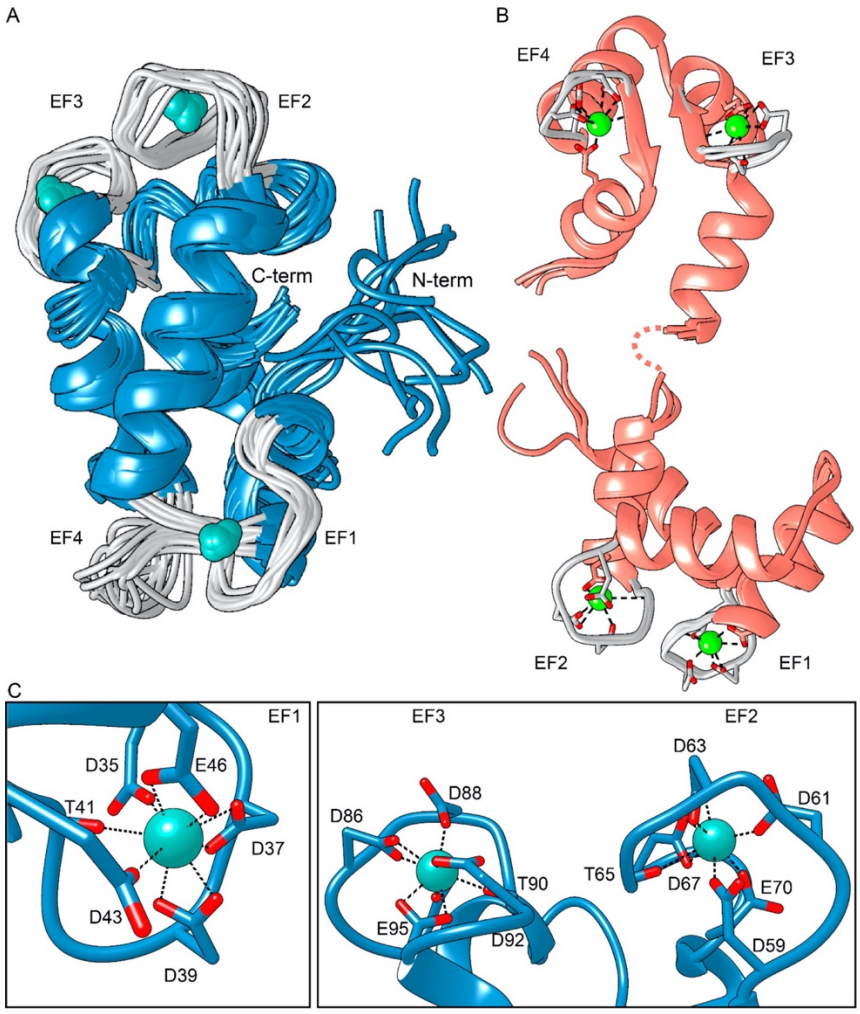

Figure 1.21. The solution structure of Y^{3+}-LanM and Ca^{2+}-CaM (Cook et al., 2019). (A) Ribbon diagrams representing the 12 lowest-energy models of Y^{3+}–LanM. Y^{3+} ions are shown as teal spheres, and EF-loops are colored gray. For the sake of clarity, the C-terminal His_6 tag is not shown. (B) Ribbon diagrams representing the three deposited models of Ca^{2+}–CaM. Ca^{2+} ions (green spheres) and coordinating residues (sticks) are shown, and the flexible linker is indicated as a dashed line. CaM's EF3/EF4 pair is shown in an orientation similar to that of LanM's EF2/EF3 pair in panel A. (C) Y^{3+} coordination by the Ln^{3+}-binding sites of EF1–EF3 in LanM. Metal-coordinating residues are labeled. Because of intermediate exchange in the ^{1}H–^{15}N HSQC spectrum, Y^{3+} was not modeled into EF4, although this site was saturated under the NMR solution conditions.

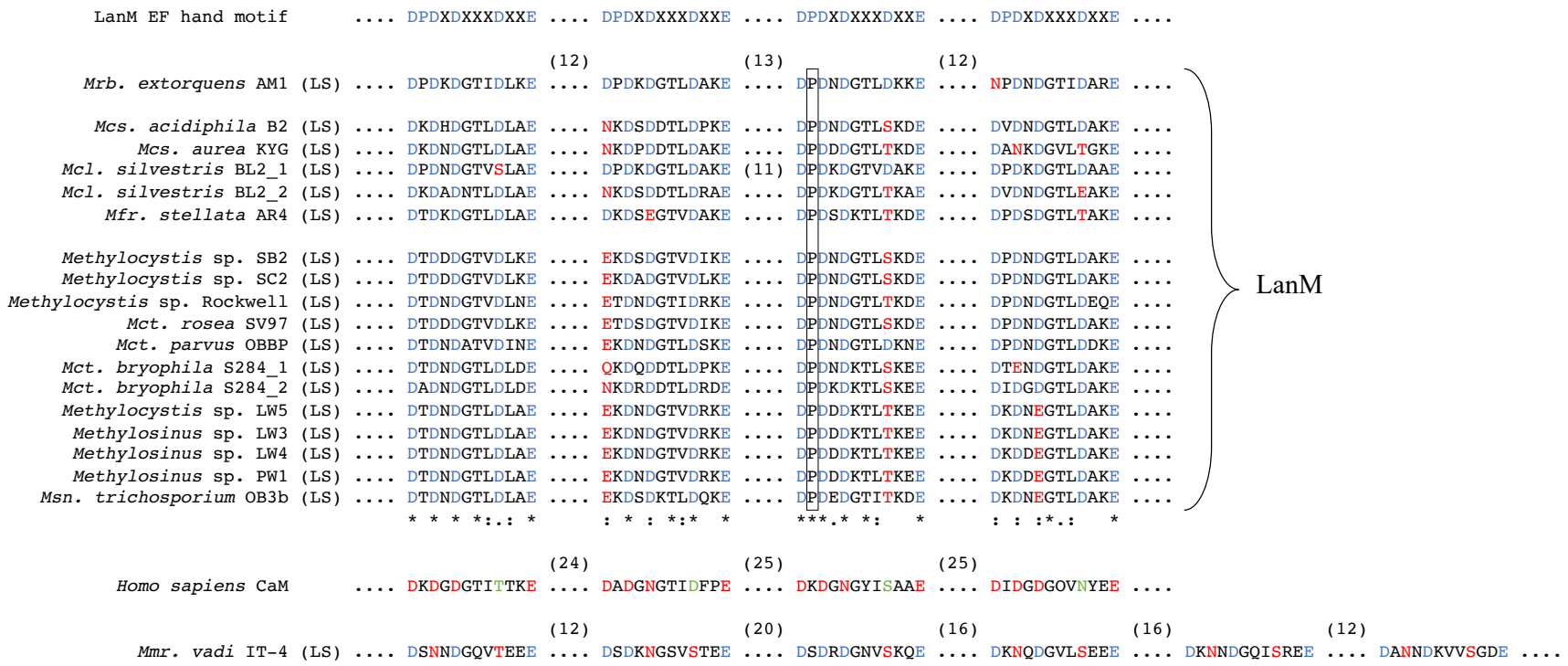

Figure 1.22. Amino acid sequence alignment of lanmodulin, human calmodulin, and an exported protein of unknown function from *Methylomarinum vadi* IT-4. In lanmodulin, aligning residues are shown in blue, differing residues in red, unique Pro residues that are completely conserved in a box. In human calmodulin, residues providing side chain Ca^{2+} ligation are shown in red and residues involved in hydrogen-bonding network to a metal-coordinated water molecule are shown in green. Number in parentheses indicates number of residues between EF-hands and LS the leader sequence.

LanM undergoes a conformational change from a disordered structure to an ordered one in a highly REE-selective manner (Cotruvo et al., 2018; Cook et al., 2019). Of the different coordinating ligands, Asp in the first and ninth positions and Pro in the second position seem to contribute to REE binding affinity and REE selectivity, respectively. That is, EF4, which lacks the Asp in the first position, has weaker affinity for REE binding (picomolar vs micromolar), and LanM exhibits extremely high selectivity for REE over Ca^{2+} (~10^8-fold selectivity), which is compromised when Pro_2 is substituted with Ala (Cotruvo et al., 2018). La^{3+}, Ce^{3+}, Pr^{3+}, Nd^{3+}, and Sm^{3+} induce conformational change in LanM at the lowest concentration, suggesting LanM may be involved in discriminating between early and late REEs (Cotruvo et al., 2018). Interestingly, La^{3+} through Nd^{3+} supports growth of *mxaF* mutant strains of *Mrr. extorquens* AM1 and *Msn. trichosporium* OB3b, and also causes differential expression of *xox* and *mxa*, whereas Sm^{3+}, a smaller/later REE does not or does so poorly (Gu et al., 2016b; Vu et al., 2016).

lanM-like genes were also found in *Methylobacterium* and *Bradyrhizobium* genomes (Cotruvo et al., 2018), and was found to be upregulated 5-fold by La^{3+} in *Methylobacterium aquaticum* 22A (Masuda et al., 2018). The deletion of *lanM* in *Mrr. extorquens* PA1 Δ*mxaF* mutant did not cause adverse effects on growth on methanol in the presence of REE, although deletion of the adjacent TonB-dependent outer membrane receptor and ABC transporter led to no or diminished growth, respectively (Table 1.5) (Ochsner et al., 2019). This was again demonstrated in *Mrr. extorquens* AM1, suggesting these uptake systems are crucial for REE-dependent growth (Roszczenko-Jasińska et al., 2020). The importance of a TonB-dependent outer membrane receptor in REE-dependent growth suggests the existence of an excreted REE chelator, a lanthanophore, as many known substrates of the transporter are organic molecules or metal ions bound to chelators (Schauer et al., 2008; Ochsner et al., 2019; Daumann, 2019).

Moreover, recent studies provide evidence for import of REEs into the cytoplasm, despite their crucial role in the periplasm with Xox-MeDH (Mattocks et al., 2019; Roszczenko-Jasińska et al., 2020). Mattocks et al. (2019) have demonstrated that early REEs, specifically La^{3+} – Nd^{3+}, are imported into the cytoplasm of *Mrr. extorquens* AM1 by using a LanM-based fluorescent sensor. La^{3+} uptake was also visualized via transmission electron microscopy in wild-type and mutant strains of the same organism, where La^{3+} was taken up and possibly stored complexed with phosphates within the cytoplasm of the wild-type, La^{3+} was not taken up by mutant lacking TonB-dependent transporter, and La^{3+} was localized in the periplasm of a mutant with disrupted ABC transporter (Roszczenko-Jasińska et al., 2020).

Table 1.5. *lut* (Ln utilization and transport) gene cluster in *Methylorubrum extorquens* AM1 (MexAM1_META1) (Roszczenko-Jasińska et al., 2020).

Accession No.	Gene	Product
p1778	*lutA*	ABC transporter-periplasmic binding component
p1779	*lutB*	Exported protein
p1781	-	Periplasmic protein
p1782	*lutE*	ABC transporter-ATP binding component
p1783	*lutF*	ABC transporter-membrane component
p1784	*lutG*	Exported protein
p1785	*lutH*	TonB-dependent receptor
p1786	*lanM*	Lanmodulin
p1787	*lutI*	Periplasmic protein of unknown function

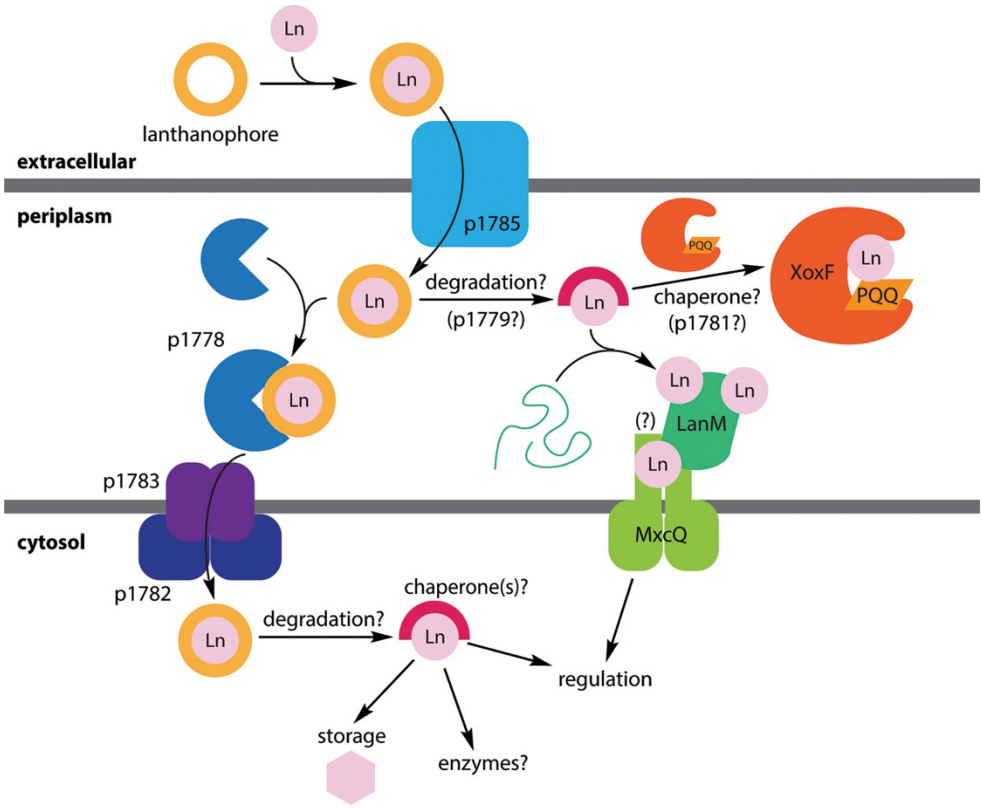

Figure 1.23. Model for REE uptake and utilization in *Methylorubrum extorquens* (Cotruvo, 2019). Unknown/postulated functions (the exact ligand for p1778, functions of p1779 and p1781, and LanM-MxcQ interaction) are indicated with parentheses and question marks.

The role of LanM in REE uptake and/or "REE switch" is not entirely clear, as it seems to serve as an auxiliary system and is not critical in REE-dependent growth of methylotrophs. Rather, the highly REE-selective conformational change of LanM suggests a role in REE sensing, potentially as part of a two-component system (Figure 1.23) (Cotruvo, 2019). In addition, as LanM was first identified as a co-eluted fraction with XoxF at a 1:1 ratio, it may be involved in the activity of Xox-MeDH (Cotruvo et al., 2018). However, it is interesting to note that not all methanotrophs that have Xox-MeDH also have LanM, though all *Alphaproteobacteria* methanotrophs do possess LanM (Table 1.2). The REE switch in *Alphaproteobacteria* methanotrophs may involve different components than those of other

methanotrophs. It is thus important to identify these components of the REE uptake and/or switch, including the putative lanthanophore.

1.4. Regulation by metals

1.4.1. Change in gene expression by copper

As briefly mentioned before, there exists a "copper switch" that regulates the expression and activity of pMMO and sMMO. That is, in methanotrophs that possess genes for both pMMO and sMMO, pMMO is expressed at high copper-to-biomass ratios, whereas sMMO is highly expressed at low copper-to-biomass ratios (Stanley et al., 1983; Green et al., 1985). Semrau et al. (2013) found that *Msn. trichosporium* OB3b deletion mutant lacking *mmoXYBZDC* (sMMO minus deletion mutant; SMDM (Borodina et al., 2007)) exhibited an inverted copper switch as compared to the wild-type, i.e. pMMO was expressed in low copper-to-biomass ratios, and expression decreased with increased copper-to-biomass ratios. Since the function of the structural genes *mmoXYBZC* were clear, it was proposed that MmoD plays a critical role in the copper switch. This was again demonstrated in a *Gammaproteobacteria* methanotroph, *Mtv. buryatense* 5GB1C, where an *mmoD* knock-out mutant exhibited lack of sMMO activity in the absence of copper (Yan et al., 2016). In addition to MmoD, MB also amplify the magnitude of the copper switch, as Δ*mbnA*::Gm^R mutants exhibited a much weaker switch (Semrau et al., 2013). The most recent model of the copper switch includes the *mmo* regulators MmoG and MmoR as well as MbnIR, hypothesized to act as a sensor and sigma factor in regulating *mbn* expression via interaction with MbnT (Figure 1.24) (Kenney & Rosenzweig, 2013; DiSpirito et al., 2016). Here, MbnI is proposed as responsible for inducing expression of the *mbn* genes. MB, MmoR, and MmoG induce expression from the σ^{54} promoter upstream of *mmoX*, and MbnI

induces expression from the σ^{70} promoter upstream of *mmoY*. In this model, *mmoD* is constitutively expressed with respect to copper, and can repress the *pmo* operon and induce *mbn* operon in the absence of copper or associate with copper in its presence. However, the copper switch may be more complex than suggested by the model and some MB-producing methanotrophs, such as *Methylocystis* sp. SB2 (Table 1.2, pg. 19), do not possess *mmoD*. Thus further investigation is required to elucidate the mechanism of the copper switch.

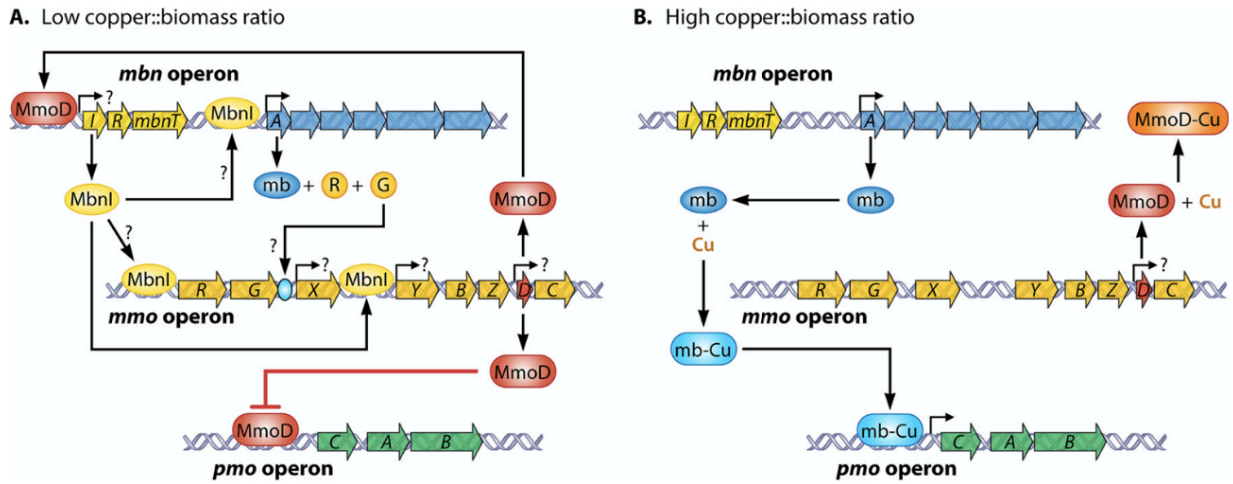

Figure 1.24. Model for the regulation of gene expression in *mmo*, *pmo*, and *mbn* gene clusters as a function of copper, MB, and MbnI (DiSpirito et al., 2016). (A) Low copper/biomass ratio; (B) high copper/biomass ratio.

1.4.2. Change in gene expression by rare earth elements

As aforementioned, two alternative enzymes exist that degrade methanol in the central C_1 metabolism of methanotrophs and nonmethanotrophic methylotrophs – Mxa-MeDH and Xox-MeDH. Both MeDHs are located in the periplasm and dependent on a pyrroloquinoline quinone cofactor. Expression of the *mxa* and *xox* operons are regulated by the presence of REE, thus

indicating the presence of an "REE switch" in methylotrophs with both operons, similar to the "Cu switch" that regulates the expression of pMMO and sMMO in methanotrophs.

The redundancy in enzymes involved in carbon metabolism by methanotrophs and nonmethanotrophic methylotrophs can be attributed to strategies for survival and competition. Either of the two MeDHs can be active depending on metal availability, and also provide a competitive advantage to those that express Xox-MeDH against those that express Mxa-MeDH. That is, Xox-MeDH exhibits higher catalytic efficiency than Mxa-MeDH due to the REE center as opposed to Ca^{2+} (Pol et al., 2014), resulting in small or no leakage of methanol from methanotrophs (Krause et al., 2017a). In addition, nonmethanotrophic methylotrophs were found to alter the REE switch in methanotrophs to repress the expression of Xox-MeDH and induce that of Mxa-MeDH as a means to cause methanol leakage from the periplasm of methanotrophs to the environment (Krause et al., 2017b), showing a critical role of REE switch in microbial competition.

The REE switch also involves other components, some of which are yet to be identified. In a nonmethanotrophic methylotroph *Mrr. extorquens* AM1, expression of the *mxa* operon is regulated by sensor-regulator two-component systems *mxcQE* and *mxbDM*, and also an orphan response regulator, *mxaB* (Springer et al., 1997, 1998). In addition, expression of this operon in *Mrr. extorquens* AM1 is dependent on the presence of *xoxF*, as deletion of both copies abolished the transcription of *mxaF* (Skovran et al., 2011), a phenomenon again demonstrated in strain PA1 (Ochsner et al., 2019). In a *Gammaproteobacteria* methanotroph *Mtv. buryatense* 5BG1C, the histidine kinase *mxaY* upregulates *mxaB* and *mxaF*, and downregulates *xoxF* in the absence of REE (Chu et al., 2016). In addition, a TonB-dependent receptor, LanA, is also required for the REE switch and regulates downstream genes in the signaling cascade (Groom et al., 2019).

In an *Alphaproteobacteria* methanotroph *Msn. trichosporium* OB3b, it was shown that the *mxa* and *xox* operons are regulated by REE, but Cu can override the REE switch whereby in the presence of both Cu and REE, expression of *mxaFI* is not repressed (Farhan Ul Haque et al., 2016; Gu et al., 2016b). Moreover, Xox-MeDH is dominant in the absence of Cu and presence of Ce, suggesting Xox-MeDH can replace Mxa-MeDH in sMMO-expressing conditions (Farhan Ul Haque et al., 2015a).

In addition, LanM was proposed as a secondary REE sensing mechanism in some methylotrophs that possess the gene encoding for this periplasmic protein (Cotruvo, 2019), and TonB-ABC transport system near the *lanM* were identified to be essential for REE-dependent growth (Ochsner et al., 2019; Roszczenko-Jasińska et al., 2020). The homologous TonB-dependent receptor is downregulated by 2.8-fold ($p = 3.6\times10^{-33}$) in the presence of REE in the *Alphaproteobacteria* methanotroph *Msn. trichosporium* OB3b (Gu & Semrau, 2017). What is more interesting is that REEs are imported into the cytoplasm where they may be stored, loaded onto Xox-MeDH, and/or directly affect the REE switch (Mattocks et al., 2019; Ochsner et al., 2019; Roszczenko-Jasińska et al., 2020). It is yet unknown whether insertion of REE into Xox-MeDH occurs in the cytoplasm or periplasm, but in the *Alphaproteobacteria* methylotroph *Mrr. extorquens*, REE must be imported into the cytoplasm in order for *xoxF* to be expressed (Roszczenko-Jasińska et al., 2020). It was also shown that an ABC transporter is crucial for REE- and ethanol-dependent growth in *Pseudomonas putida* KT2440, belonging to class *Gammaproteobacteria*, suggesting that import of REE into the cytoplasm may be a common requirement for REE-utilizing PQQ-dependent alcohol dehydrogenases (Wehrmann et al., 2019). So far, it seems the REE switch is different between members of the *Alpha*- and *Gammaproteobacteria* classes, as (1) LanM is only found in *Alphaproteobacteria* and (2) the

TonB-dependent receptor crucial for REE-dependent growth is significantly different between representatives of each class. However, it is also possible that analogous systems exist in both classes that function similarly.

1.5. Applications of methanotrophy

Methanotrophs can be used in various environmental, industrial, and medical applications. As methanotrophs use methane as its sole source of carbon and energy, methanotrophy can be stimulated to mitigate CH_4 emission and also remove atmospheric CH_4 in some cases. Also, as mentioned earlier, MMOs have been found to be nonspecific, and therefore can bind and oxidize alkanes up to C_8, ethers, cyclic alkanes, aromatic carbons, and halogenated carbons (Colby et al., 1977; Burrows et al., 1984; Hanson et al., 1990). As such, cometabolism of organic pollutants with substrate CH_4 can achieve bioremediation of contaminated sites. Methanotrophy can also be utilized to produce value-added products such as single cell protein for animal feed (Bothe et al., 2002), poly-β-hydroxybutyrate (PHB) for bioplastic (Asenjo & Suk, 1986), or lipids for biodiesel (Conrado & Gonzalez, 2014; Fei et al., 2014), due to the unique physiology and low-cost substrate – CH_4. Some important applications of methanotrophs will be discussed in detail below.

1.5.1. Mitigation of greenhouse gas emissions

Methane is a greenhouse gas (GHG) that is 28 times more effective than carbon dioxide at absorbing infrared radiation and its atmospheric concentrations are continuing to rise (IPCC, 2014). Methanotrophs can be applied to control methane emission from significant sources such as natural landfills and coal mines by stimulating methanotrophic activity (Semrau et al., 2010;

US EPA, 2020). Various engineered systems have been developed and validated to reduce CH_4 emissions. Examples include 'biocovers' and 'biofilters' that can be either applied over the surface of the landfill, or constructed as a separate unit to pass through CH_4 gas streams (Huber-Humer et al., 2008; Scheutz et al., 2009). The latter can also be applied to CH_4 emitted from animal husbandry and coal mine ventilation (Scheutz et al., 2009), all significant sources of CH_4 (US EPA, 2020).

In addition to mitigating CH_4 emission at the source, methanotrophs inhabiting unsaturated soil can also act as a significant sink for atmospheric CH_4 (Conrad, 2009). The existence of methanotrophs that can utilize atmospheric CH_4 was discovered in the 1990s (Whalen & Reeburgh, 1990; Yavitt et al., 1990; Bender & Conrad, 1992), and were subsequently identified as uncultured clades within the *Alpha-* and *Gammaproteobacteria* via radiolabeling experiments (Holmes et al., 1999; Roslev & Iversen, 1999; Knief et al., 2003). These clades were termed upland soil clusters α and γ (USCα and USCγ). Representatives of these clades were elusive for years, until recently, a pure culture of a member of the USCα clade, *Methylocapsa gorgona* MG08, was isolated and characterized (Tveit et al., 2019). Other members of this genus, *Mcs. acidiphila* and *Mcs. aurea*, were also found to utilize atmospheric CH_4, expanding our understanding of soil and methanotrophs as an atmospheric CH_4 sink.

Removal of methane at the source or from the atmosphere is important in mitigating global GHG emission. However, nitrous oxide is a GHG that is almost 10 times more potent than CH_4 (US EPA, 2020), and emission of N_2O may be affected by some methanotrophs. That is, MB can prevent other microbes (e.g. denitrifiers) from collecting copper by binding copper with high affinity, causing N_2O accumulation (Chang et al., 2018). Nitrous oxide reductase (NosZ), responsible for the conversion of N_2O to N_2 in denitrifiers, requires copper for its

activity (Brown et al., 2000). Thus, stimulating methanotrophy to decrease methane emission may inadvertently cause a copper-limited environment for denitrifiers inhabiting the same soil environment, thereby increasing N_2O emission and net GHG emission. Therefore, understanding copper competition between methanotrophs, denitrifiers, and other microbes dependent on copper will support future strategies to mitigate GHG emission.

1.5.2. Methylmercury detoxification via demethylation

Mercury methylation and demethylation in the environment is governed by biotic and abiotic processes. Mercury can be methylated into the more toxic and bioavailable form – methylmercury (MeHg) – by some anaerobic microorganisms harboring the key two-gene cluster, *hgcAB* (Figure 1.25; Gilmour et al., 2013; Parks et al., 2013; Smith et al., 2015). An equally important and significant process is the demethylation of MeHg via MerB, the canonical organomercurial lyase, of which the gene belongs to the *mer* operon that confers mercury resistance (Figure 1.26; Weiss et al., 1977; Ogawa et al., 1984; Barkay et al., 2003). Recently, it has been shown that methanotrophs may play an important role in mercury speciation as well as toxicity mediation in the environment.

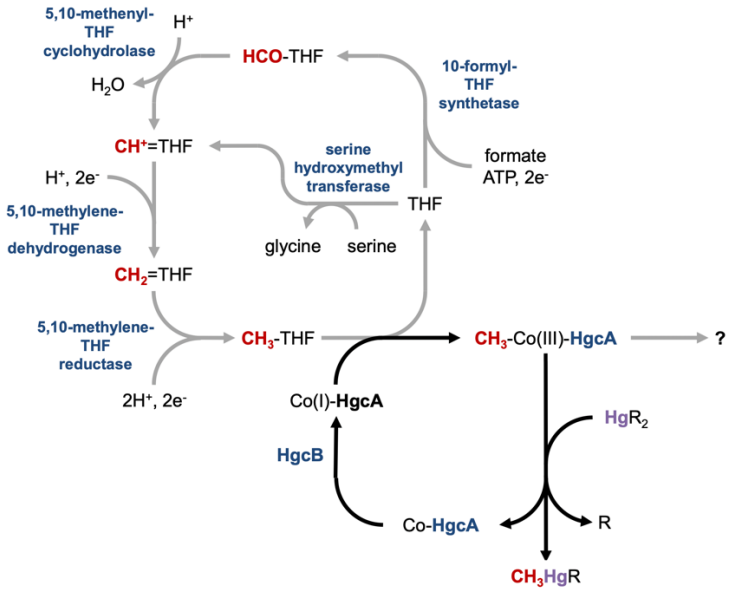

Figure 1.25. Proposed Hg methylation pathway including potential sources of C_1 units entering the reductive acetyl-CoA pathway, methyl group transfer from CH_3-H_4folate (CH_3-THF) to cob(I)alamin-HgcA, methylation of Hg(II) by HgcA, and reduction to cob(I)alamin-HgcA by HgcB (Parks et al., 2013). In the absence of Hg, the methyl group is transferred to a different unknown substrate, which may be a physiologically relevant metabolite.

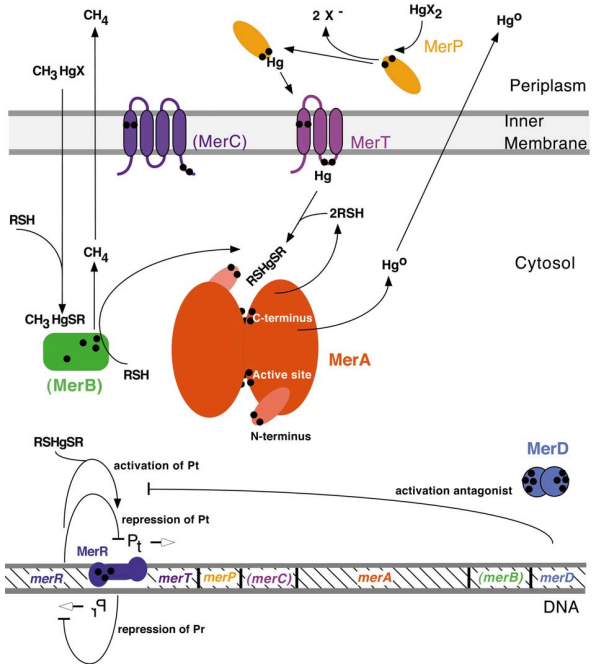

Figure 1.26. Model of a typical Gram-negative mercury resistance (*mer*) operon (Barkay et al., 2003). The symbol • indicates a cysteine residue. X refers to a generic solvent nucleophile. RSH is the low-molecular-mass, cytosolic thiol redox buffer such as glutathione. Parentheses around gene or protein designations indicate proteins/genes that do not occur in all examples of the operon.

Specifically, it has been found that MBs, in addition to strongly binding copper, can strongly bind other metals, including mercury as Hg(II). Group I and II MBs from *Msn. trichosporium* OB3b and *Methylocystis* sp. SB2 will both quickly and irreversibly bind Hg(II) even in the presence of copper (Vorobev et al., 2013; Baral et al., 2014). Hg(II) toxicity is significantly reduced when bound by MB, suggesting that MB may have a secondary role in protecting microbes from toxic effects of Hg(II) (Vorobev et al., 2013). In addition, MB enables methanotrophs to demethylate a much more toxic and bioavailable form of mercury, methylmercury (MeHg), despite the fact that methanotrophs that degrade MeHg do not have *merB* encoding for the canonical organomercurial lyase in their genome (Lu et al., 2017). Moreover, *Msn. trichosporium* OB3b can degrade MeHg at environmentally relevant concentrations unlike the canonical MerB, i.e. nanomolar vs micromolar concentrations (Lu et al., 2017). Though methanotrophs that do not have the genes encoding MB biosynthesis, such as *Mcc. capsulatus* Bath, cannot degrade MeHg, MB alone is not sufficient for MeHg degradation in methanotrophs (Lu et al., 2017). Therefore, it appears that MB acts as a delivery mechanism for methanotrophs to uptake MeHg, wherein it is degraded by an as-yet-unknown mechanism.

More interestingly, it was recently shown that MB also affects Hg(II) methylation by the mercury-methylating bacteria *Desulfovibrio desulfuricans* ND132 and *Geobacter sulfurreducens* PCA (Yin et al., 2020). Surprisingly, the Group I MB from *Msn. trichosporium* OB3b seemed to decrease the rates of sorption and internalization, but enhance Hg(II) methylation in both of these microbes to varying degrees at moderate concentrations. The Group II MB from *Methylocystis* sp. SB2 did not affect or impede Hg(II) methylation in these microbes, respectively. This difference may be attributable to the different structure of Cu-MB complex and/or varying affinity for Hg(II). Thus, methanotrophs may affect not only the demethylation of MeHg but

methylation of Hg(II) and mercury speciation in the natural habitat. Thus, understanding the mechanism of MeHg degradation by methanotrophs will provide insight into interaction with mercury and other microbes in the environment and further facilitate remediation solutions for mercury-contaminated sites.

1.5.3. Potential applications of methanobactin

In addition to binding copper and mercury, MBs will also bind and reduce Au(III), and in so doing, they have been observed to produce elemental gold nanoparticles of well-defined size distributions at room temperature (Choi et al., 2006; Baral et al., 2014). In particular, very well-defined spherical gold nanoparticles were formed with MB from *Methylocystis* sp. SB2, with the mean size of 2.0 ± 0.7 nm (Bandow, 2014). Such a finding is remarkable for typically biosynthesis of gold nanoparticles produces a wide range of particle sizes of varying shapes (Narayanan & Sakthivel, 2010; Pourali et al., 2017). Further, bacterial-mediated gold nanoparticle synthesis typically involves whole cells where a variety of electron donors are available. Here, with MB, no reductant was added, and so the source of electrons for gold reduction is unclear. This issue is particularly confounding as Au(III) was not found in solution until the Au/MB ratio was greater than two, i.e. at least six electrons were transferred per MB to Au(III). As noted above, the source of electrons has not been explicitly identified, but if it is water, it appears that MB can repeatedly oxidize it by an as-yet-unknown mechanism, although such a possibility implies that metal-MB complexes, particularly an Au-MB complex, may have a very high redox potential. The resting potential of MBs is high, 550–750 mV (El Ghazouani et al., 2012), although the redox potential of metal-bound MB has not been determined. As speculated earlier, forcing a metal such as Cu(II) or Au(III) into a non-preferential ligand

arrangement may enhance its redox potential (Krentz et al., 2010). Regardless of the source and mechanism of electron transfer, the finding that MB can produce gold nanoparticles indicates that this may be an alternative for their production especially as this occurred spontaneously in mild conditions at room temperature. Such a process could be advantageous as gold nanoparticles have many applications in medicine and industry, e.g. as an antimicrobial agent, fuel cell development, X-ray imaging, cancer treatment and electronics, among others (Daniel & Astruc, 2004; Khlebtsov & Dykman, 2010; Elahi et al., 2018).

Perhaps the most novel and meaningful application of MB, however, is its potential for use in treating copper-related diseases. That is, there are several medical conditions related to the misdistribution of copper in the human body, most notably Wilson's disease. Individuals with this congenital disorder are unable to tolerate copper due to mutations in a specific ATPase responsible for secretion of excess copper to the bile. As a result, they are unable to expel copper from the liver, leading to copper buildup that causes severe damage. Left untreated, this disease can lead to complete liver failure as well as copper spillover into brain tissue, leading to significant neurological problems. There is no cure for Wilson's disease, and current therapies only limit future damage, i.e. they do not repair damage already incurred (Schilsky, 2001; Ferenci, 2005; Ala et al., 2007; Roberts, 2011; Schilsky, 2014). Wilson's disease is also considered to be an ‘orphan’ or ‘rare’ disease according to the US Orphan Drug Act of 1983, i.e. a disease with a prevalence of <200,000 people in the United States (Wilson's disease only affects roughly 1 in 30,000 people worldwide or ~10,000 people in the United States). As a result, development and testing of alternative therapies for Wilson's disease is limited given the small market, and the US Federal Drug Administration Office of Orphan Products Development actively seeks to promote development of drugs that treat it. Initial testing in rodent model

indicates that MB is well tolerated and is also singularly effective in preventing copper buildup (Lichtmannegger et al., 2016; Zischka et al., 2017; Müller et al., 2018). Further, it can also remove pre-existing copper, leading to liver repair (Lichtmannegger et al., 2016). Such a finding is of particular interest as it indicates that MB may enable Wilson's disease patients to avoid having to undergo a liver transplant if severe liver damage occurs. As there are other copper-related diseases in humans (e.g. Alzheimer's Disease and BRAF-positive cancers; (Cherny et al., 2001; Gaggelli et al., 2006; Bush, 2008; Squitti, 2012; Brady et al., 2014; Brewer, 2014; Squitti et al., 2014; Gamez & Caballero, 2015)), there is the potential that MB may be useful for these medical conditions as well, e.g. through reducing availability of copper required for kinase activity that drives tumorigenesis in BRAF-positive cancers or limiting development of neuronal-damaging plaques in Alzheimer's disease.

Finally, one of the initial characteristics identified in MB was its antimicrobial properties, i.e. it has been found to inhibit a variety of Gram-positive microbes, including vancomycin-resistant strains of *Staphylococcus aureus*, *Bacillus thuringiensis*, *Enterococcus fecalus*, as well as *Listeria monoocytogenes* (DiSpirito et al., 2004b; Johnson, 2006). Of these, the effect of copper-MB complexes has been most extensively reported against *L. monoocytogenes* (Johnson, 2006), with the minimum inhibitory concentration of copper-MB on the order of 1-5 mM for this strain, with reductions in population ranging from ~3 to 5 orders of magnitude. Further studies suggest that copper-MB inhibits respiration of *L. monoocytogenes* through an as-yet-unidentified mechanism, but possibilities include insertion of copper-MB complexes into the cytoplasmic membrane that reduces membrane integrity and/or the generation of radicals through uncontrolled electron transfer.

1.6. Research objectives

As discussed throughout this chapter, methanotrophy is uniquely regulated by metal availability, specifically of copper and REEs. To unravel the relationship between metals and methanotrophs and its effect *in situ*, there are three specific objectives to this work:

(1) Investigate the significance of copper and REE uptake in the evolution of methanotrophy.

(2) Characterize copper competition between methanotrophs mediated by chalkophores.

(3) Investigate how methylmercury is demethylated by methanotrophs.

Chapter 2 Materials and Methods

2.1. Materials

Chemicals were purchased from Sigma-Aldrich, Inc. (St. Louis, MO) or Fisher Scientific Company LLC (Fair Lawn, NJ) as analytical grade or higher. Growth media and chemical required for nucleic acid manipulation were purchased as molecular biology grade or higher and nuclease free, respectively. All solutions and growth media were prepared in Milli-Q water (>18.2 MΩ·cm at 25 °C) and sterilized by autoclaving or filtering using 0.22-μm nylon or PVDF filters purchased from Foxx Life Sciences (Salem, NH), as appropriate. Large volumes were filtered using a 0.22-μm PES filtration unit purchased from Thermo Fisher Scientific Inc. (Waltham, MA). Enzymes were purchased from New England Biolabs, Inc. (NEB, Ipswich, MA), Invitrogen (Carlsbad, CA), and Bio-Rad (Hercules, CA).

2.2. Cultivation, maintenance, and storage of bacterial strains

2.2.1. Preparation and transformation of chemically competent *E. coli* cells

Chemically competent *E. coli* cells were prepared using $CaCl_2$ (Cohen et al., 1972; Mandel & Higa, 1970). A single colony from a plate of *E. coli* was transferred to 3 mL of Luria-Bertani (LB) medium and grown overnight in a shaking incubator at 37 °C, 220 rpm. 1 mL of the overnight culture was transferred to 100 mL of fresh LB medium in a 500-mL Erlenmeyer flask, then grown for 2-3 h. The culture was then cooled on ice for 10 min, then centrifuged at 4,000 × g for 10 min at 4 °C and washed with 10 mL of cold 0.1 M $CaCl_2$ solution. The cell pellet was harvested via centrifugation and resuspended in 0.2 mL of 0.1 M $CaCl_2$, then

distributed into pre-chilled microcentrifuge tubes in 50-μL aliquots. For long-term storage in -80 °C, the final resuspension was performed in 0.2 mL of 0.1 M $CaCl_2$ and 15% glycerol solution.

For transformation, cells were removed from -80 °C and thawed on ice and less than 50 ng of plasmid DNA or ligation mix was added to 50 μL of competent cell suspensions and gently mixed by tapping the tube. The cells were kept on ice for 10 or 30 min, heat shocked at 42 °C for 45 or 30 s, then returned to and cooled on ice for 2 or 5 min for *E. coli* TOP10 and S17-1, respectively. 5 V (250 μL) of super optimal broth with catabolite repression (SOC) medium warmed to 37 °C was added to the cells, which were incubated at 30 °C, 220 rpm for 1 h. Aliquots of various amount were spread on selective LB plates and incubated at 37 °C overnight before colony screening.

Table 2.1. Bacterial strains and plasmids used in this study. Gm^r, gentamicin resistance; Km^r, kanamycin resistance, Sp^r/Sm^r, streptomycin/spectinomycin resistance.

Strain or Plasmid	Description	Reference or Source
Escherichia coli		
TOP10	F– *mcrA* Δ(*mrr-hsdRMS-mcrBC*) Φ80*lacZ*ΔM15 Δ*lacX74 recA1 araD139* Δ(*ara leu*) *7697 galU galK rpsL* (StrR) *endA1 nupG*	Invitrogen
S17-1	*thi pro hsdR⁻ hsdM⁺ recA1* RP4 2-Tc::Mu-Km::Tn7	(Simon et al., 1983)
Methylococcus capsulatus		
Bath	Wild-type strain	
***Methylocystis* sp.**		
strain Rockwell	Wild-type strain	
SB2	Wild-type strain	
Methylomicrobium album		
BG8	Wild-type strain	
Δ*mbnT1*	Putative *mbnT* gene deleted	This study
Methylosinus trichosporium		
OB3b	Wild-type strain	
Δ*arsI*	Putative gene encoding for arsenic lyase (*arsI*) deleted	This study
Δ*lanM*	Putative gene encoding for lanmodulin (*lanM*) deleted	This study
Δ*mbnAN*	*mbnABCMN* deleted	(Gu et al., 2017a)
Δ*mbnAN* + pBE3013	Δ*mbnAN* carrying pBE3013	This study
Δ*mbnAN* + pBE3015	Δ*mbnAN* carrying pBE3015	This study
Plasmid		
pK18*mobsacB*	Km^r, RP4-mob, mobilizable cloning vector containing *sacB* from *B. subtilis*	(Schäfer et al., 1994)
pK*arsI*	pK18*mobsacB* carrying 2 ligated arms used to knock out *arsI* in *Msn. trichosporium* OB3b	This study
pK*lanM*	pK18*mobsacB* carrying 2 ligated arms used to knock out *lanM* in *Msn. trichosporium* OB3b	This study
pK*mbnT1*	pK18*mobsacB* carrying 2 ligated arms used to knock out *mbnT1* in *Mmc. album* BG8	This study
pK*xoxF1*	pK18*mobsacB* carrying 2 ligated arms used to knock out *xoxF1* in *Msn. trichosporium* OB3b	This study
pK*xoxF1*_2	pK18*mobsacB* carrying 2 ligated arms used to knock out *xoxF1* in *Msn. trichosporium* OB3b	This study
p34S-Gm	Source of Gm^r cassette	(Dennis & Zylstra, 1998)
pTJS140	Sp^r/Sm^r cloning vector	(Smith et al., 2002)
pBE3013	pTJS140 carrying *mbnABCMFS* of *Methylocystis* sp. SB2 with *Msn. trichosporium* OB3b MB promoter and Sp^r/Sm^r cassette	This study
pBE3015	pTJS140 carrying *mbnABCMFS* of *Methylocystis* sp. SB2 with *Msn. trichosporium* OB3b MB promoter and Gm^r cassette	This study

2.2.2. Stock solutions

All antibiotic solutions were sterilized using 0.22-μm filter and added to growth medium prior to cultivation. Antibiotics were added to the following final concentrations: for *E. coli* strains, ampicillin 100 $\mu g \cdot mL^{-1}$; kanamycin 25 $\mu g \cdot mL^{-1}$; gentamicin 5 $\mu g \cdot mL^{-1}$; nalidixic acid 15 $\mu g \cdot mL^{-1}$, and for methanotrophs, kanamycin 10 $\mu g \cdot mL^{-1}$; gentamicin 2.5 $\mu g \cdot mL^{-1}$; spectinomycin 20 $\mu g \cdot mL^{-1}$ and streptomycin 20 $\mu g \cdot mL^{-1}$.

Methanobactin (MB) stocks were freshly prepared by adding MB from *Msn. trichosporium* OB3b or *Methylocystis* sp. SB2 (OB3b-MB or SB2-MB) to Milli-Q water to a final concentration of 10 mM. Cu-MB stocks were prepared by adding $CuCl_2$ and either OB3b-MB or SB2-MB at 1:5 molar ratio and incubating in the dark at 30 °C, 220 rpm for 1 h (Kalidass et al., 2015). Cu-triethylenetetramine (TRIEN, a strong abiotic chelator of copper (Bandow et al., 2011)) stock was prepared by adding $CuCl_2$ and TRIEN at 1:5 molar ratio. All stock solutions were filter-sterilized before use.

2.2.3. Cultivation of methanotrophs

Initial inocula of *Mcc. capsulatus* Bath, *Methylocystis* sp. SB2, *Msn. trichosporium* strains, and *Mmc. album* strains were grown in 30 mL of nitrate mineral salt (NMS) medium in 250-mL side-arm Erlenmeyer flasks, shaken at 220 rpm in the dark (Whittenbury et al., 1970b). *Methylocystis* sp. strain Rockwell was grown under the same conditions in ammonium mineral salts (AMS) medium (Whittenbury et al., 1970b). To prevent REE precipitation, *Msn. trichosporium* wildtype and Δ*lanM* mutant were grown in modified NMS, where the phosphate buffer was substituted with 50 mM PIPES (pH 6.8), and trace element solution contributed 3.569 mg/L $FeSO_4 \cdot 7H_2O$, 0.4 mg/L $ZnSO_4 \cdot 7H_2O$, 0.02 mg/L $MnCl_2 \cdot 7H_2O$, 0.05 mg/L $CoCl_2 \cdot 6H_2O$,

0.01 mg/L $NiCl_2 \cdot 6H_2O$, 0.015 mg/L H_3BO_3, and 205.87 mg/L trisodium citrate dihydrate to the growth medium. *Mcc. capsulatus* Bath was grown at 45 °C, and all other methanotrophs at 30 °C. CH_4 was supplemented at a CH_4-to-air ratio of 1:2. The initial inocula were then washed as necessary and used to inoculate (at 1:10 dilution factor) 50 mL of fresh media for experiments. Copper, REE, MB, TRIEN, and other stock solutions were supplemented to growth medium as required. When appropriate, cultures at stationary phase were washed and used to inoculate a new set of flasks for a second growth cycle. Methanotrophic growth was non-invasively monitored by measuring the optical density at 600 nm (OD_{600}) in sidearm flasks using a Genesys 20 Visible spectrophotometer (Spectronic Unicam, Waltham, MA).

2.2.4. Isolation of methanotrophs from methylmercury contaminated stream

Biofilm samples were collected in July 2020 by our collaborators at Oak Ridge National Laboratory. Briefly, these biofilm samples were collected from mercury-contaminated East Fork Polar Creek (EFPC) located in Oak Ridge, Tennessee, with an altitude of 255 m and coordinates of N 35.990385°, W 84.317983° for strain EFPC1 and N 35.992482°, W 84.315327° for strain EFPC2. Biofilm samples were first inoculated in NMS liquid culture at 30 °C with methane as the sole carbon and energy source to enrich for methanotrophs. After visible growth on methane, samples were then streaked on NMS agar plates as described earlier (Gu & Semrau, 2017). After repeated streaking on NMS plates with purity confirmed via microscopy, Sanger sequencing of 16s rRNA gene and negative growth on nutrient agar plates, a single colony of each strain was then grown in NMS liquid medium with methane (Im et al., 2011).

2.2.5. Conjugation of methanotrophs and *E. coli*

Plasmid DNA was transferred from *E. coli* S17-1 to methanotrophic strains via conjugation following the method modified from Martin and Murrell (1995). An overnight culture of 10 mL of *E. coli* S17-1 containing the plasmid of interest and a 50-mL culture of methanotrophic strain in early exponential phase (OD_{600} = 0.2-0.3) were separately centrifuged at 4,300 × g for 10 min, then washed with 25 mL of fresh NMS medium. Both were resuspended in 1 mL NMS medium together, then 50 μL of the resuspension was spotted onto an NMS agar plate supplemented with 0.02% (w/v) proteose peptone. After incubating the plate at 30 °C for 24-48 h, the 50-μL spots were each harvested and carefully resuspended in 100 μL of fresh NMS, then spread on selective NMS plates. The plates were incubated in the presence of CH_4 and air at 30 °C. Colonies that appear after 10-20 days were screened for successful conjugation.

2.2.6. Spheroplast preparation

Spheroplast of *Msn. trichosporium* OB3b Δ*mbnT* mutant (Gu et al., 2016a) was prepared to assess the role of periplasmic enzymes and methanobactin in methylmercury demethylation using a previously established method (Coppi et al., 2007; Wang et al., 2016), further modified for methanotrophs. A 30-mL culture was harvested via centrifugation at 4,300 × g for 10 min, then washed with 5 mL of fresh 3-(*N*-morpholino)propanesulfonic acid (MOPS; pH 7.3) buffer. The cell pellet is resuspended in 10 mL MOPS buffer with 350 mM sucrose. 5 mL of the cell suspension was centrifuged at 2,000 × g for 10 min, then resuspended in 4 mL of 250 mM Tris-HCl (pH 7.5) buffer. 0.4 mL of 500 mM EDTA (pH 8.0) was added to the cell suspension. Reaction was continued for 1 min, after which 4 mL of 700 mM sucrose was added, followed by 0.56 mL of lysozyme (134 $mg \cdot mL^{-1}$). The cell suspension was homogenized by gentle shaking,

then incubated at room temperature overnight. Then, 8 mL of Milli-Q water was added to the cell suspension and centrifuged immediately at 2,000 × g for 10 min to collect spheroplasts. The spheroplasts were washed twice with 10 mL of MOPS buffer with 350 mM sucrose to remove residual lysozyme. Spheroplasts were finally resuspended in 5 mL MOPS buffer with 350 mM sucrose before methylmercury demethylation experiments. Optical microscopy of these spheroplasts indicated removal of outer cell membrane and periplasm (rounded compared to untreated cells).

2.3. Molecular biological techniques

2.3.1. Nucleic acid extraction

DNA and RNA were extracted from methanotrophs using the method modified from Griffiths et al. (2000). For DNA extraction, 50 mL of methanotroph culture in mid- to late exponential phase (OD_{600} = 0.3-0.5) was harvested via centrifugation at 4,300 × g for 10 min. The cell pellet was resuspended in 0.75 mL of extraction buffer consisting of 2.5% (w/v) hexadecyltrimethylammonium bromide (CTAB), 0.6 M NaCl, and 0.15 M phosphate buffer (pH 7.6). The cell pellet was stored at -80 °C until frozen, then thawed at 70 °5. The freeze-thaw cycle was repeated 3 times, after which 5 μL of proteinase K (10 μg/μL) was immediately added and mixed thoroughly. 40 μL of 20% SDS was added, then incubated at 70 °C for 2 h with inversion every 30 min. The samples were left to cool for 5 min, then 700 μL of phenol-chloroform-isoamylic alcohol (25:24:1) was added, followed by mixing by inversion for 10 min. The cell debris and impurities were removed via centrifugation at 18,000 × g for 10 min. The upper aqueous phase was then transferred to a clean microcentrifuge tube, to which 700 μL of chloroform-isoamyl alcohol (25:24) added. After mixing by inversion for 5 min, the sample was

centrifuged again, and the final washing step was repeated as necessary. The purified DNA-containing upper aqueous phase was transferred to another microcentrifuge tube, and 1 V of isopropanol and 0.1 V of sodium acetate was added, then left at -20 °C overnight. The DNA was collected via centrifugation at 18,000 × g for 20 min at 4 °C, then washed with 1 mL of 70% ethanol. After completely air drying the DNA pellet, 40 µL of nuclease free water was added, and the sample was stored at 4 °C before preparing for Illumina sequencing. For GridION Nanopore sequencing, DNA was extracted from 200 mL of methanotroph cultures at mid- to late exponential phase using QIAGEN Genomic-tip 500/G following the manufacturer's instructions (Qiagen, Hilden, Germany).

RNA was extracted from methanotroph cells grown to mid- or late exponential phase (OD_{600} = 0.3-0.4), harvested from 10-50 mL of cultures. The cultures were first treated with stop solution (5% buffer-equilibrated phenol (pH 7.3) in ethanol) at a 10:1 ratio (culture-to-stop solution). Cells were then collected by centrifugation at 4,300 × g for 10 min at 4 °C. Cell pellets were resuspended in 0.75 mL of extraction buffer. 35 µL of 20% SDS, 35 µL of laurylsarcosine, and 750 µL of phenol-chloroform-isoamylic alcohol (25:24:1) were then added to the cell samples and then lysed via bead beating (Mini-BeadBeater-1; Biospec Products, Bartlesville, OK) using 0.5 g of 0.1-mm zirconia silica beads at 4,800 rpm for 1 min. The samples were then centrifuged at 18,000 × g for 5 min at 4 °C and the upper aqueous phase transferred to a new tube and mixed with 0.75 mL of chloroform-isoamylic alcohol (24:1). The mixtures were centrifuged again, and the total RNA in the upper aqueous phase was precipitated in $MgCl_2$, sodium acetate, and isopropanol overnight at -80 °C. RNA was then collected by centrifugation at 18,000 × g for 45 min at 4 °C and washed with 75% ethanol. RNA was then treated with RNase-free DNase (Qiagen, Hilden, Germany) until free of DNA, followed by

purification using Zymo RNA Clean & Concentrator kit (Zymo Research, Irvine, CA) following the manufacturer's instructions. Removal of DNA was confirmed by the absence of products from polymerase chain reaction (PCR) with the universal primers 27F and 1492R targeting 16S rRNA using 1-2 μL of RNA template (Table 2.2). cDNA was synthesized from DNA-free RNA samples using Superscript III reverse transcriptase kit (Invitrogen, Carlsbad, CA) following the manufacturer's instructions.

Concentration of purified DNA and RNA were determined using a NanoDrop ND1000 (NanoDrop Technologies, Inc., Wilmington, DE).

Plasmids were maintained in *E. coli* TOP10, and plasmid extraction was performed using QIAprep Spin Miniprep Kit following the manufacturer's instructions (Qiagen, Hilden, Germany). Extracted plasmids were stored at -20 °C until use.

2.3.2. Polymerase chain reaction

PCR was performed using C1000 Touch (Bio-Rad, Hercules, CA) or T-48 Personal (Biometra) thermocyclers. PCR reactions were prepared using GoTaq Green Master Mix (Promega, Madison, WI) and Phusion High-Fidelity PCR Master Mix (NEB, Ipswich, MA) for general and cloning purposes, respectively. A standard 50-μL PCR reaction consisted of 1× master mix and 0.5 μM forward and reverse primers (Integrated DNA Technologies, Inc., Coralville, IA). Temperature cycling conditions were set according to manufacturer's recommendations. Primer annealing temperatures were estimated using OligoAnalyzer (https://www.idtdna.com/calc/analyzer).

Template for colony PCR was prepared by picking a colony from a fresh plate using pipet tips and suspending in 10 μL of nuclease-free water. 5 μL of the suspension was mixed

with 5 μL of 0.1 M NaOH solution and heated at 95 °C for 10 min to lyse the cells. 0.3-0.6 μL of the cell lysate was used for PCR reaction. Negative and positive controls were also prepared using water and plasmid/genome as templates, respectively. PCR primers used in this study are provided in Table 2.2 and the calibration curves of qPCR primers are provided in the Appendix (Figure A.1-3).

2.3.3. Gel electrophoresis and extraction

DNA fragments were separated in 0.5-1.0% (w/v) agarose gels in 1× Tris-acetate-EDTA (TAE) buffer (Invitrogen, Carlsbad, CA), supplemented with ethidium bromide (10 $\mu g \cdot mL^{-1}$). 100-bp or 1-kb DNA ladders (NEB, Ipswich, MA) were included in the gel electrophoresis run to estimate the sizes of DNA bands. The gels were visualized using Gel Logic 100 imaging system (Kodak, Rochester, NY). Specific DNA bands were excised from gels and extracted using QIAquick Gel Extraction Kit (Qiagen, Hilden, Germany), following the manufacturer's instructions.

2.3.4. Restriction digestion

Restriction digestion of arms and plasmids was carried out using restriction enzymes purchased from NEB (Ipswich, MA) for at least 15 min at 37 °C, following the manufacturer's instructions. Digested DNA was purified using QIAquick PCR Purification Kit (Qiagen, Hilden, Germany), or gel electrophoresis followed by extraction depending on size and number of DNA fragments.

Table 2.2. Primers for PCR and sequencing.

Name	Organism	Gene	Sequence (5'-3')[a]	Reference
PCR primers				
27F	Universal	16S rRNA	AGAGTTTGATCMTGGCTCAG[b]	Lane, 1991
1492R	Universal	16S rRNA	TACGGYTACCTTGTTACGACTT[b]	Lane, 1991
M13F	Universal	plasmid	GTAAAACGACGGCCAG	Invitrogen
M13R	Universal	plasmid	CAGGAAACAGCTATGAC	Invitrogen
pmoA-A189	Universal	*pmoA*	GGNGACTGGGACTTCTGG[b]	Holmes et al., 1995
pmoA-mb661	Universal	*pmoA*	CCGGMGCAACGTCYTTACC[b]	Costello & Lidstrom, 1999
mmoX206f	Universal	*mmoX*	ATCGCBAARGAATAYGCSCG[b]	Hutchens et al., 2003
mmoxX886r	Universal	*mmoX*	ACCCANGGCTCGACYTTGAA[b]	Hutchens et al., 2003
arsI_Af	*Msn. trichosporium* OB3b	*arsI*	ATTTTTGAATTCCCTTTGCCGGTGAAGAACAG	This study
arsI_Ar	*Msn. trichosporium* OB3b	*arsI*	ATTTTTGGATCCGTTGAAGGGCGAGGCTGG	This study
arsI_Bf	*Msn. trichosporium* OB3b	*arsI*	ATTTTAGGATCCGCTTCATGGGACCCTCTCG	This study
arsI_Br	*Msn. trichosporium* OB3b	*arsI*	ATTTTAAAGCTTAGAACGCACTCAATCACACG	This study
ArsI_F1	*Msn. trichosporium* OB3b	*arsI*	TCGATCACATGCGGCTCTAT	This study
ArsI_R1	*Msn. trichosporium* OB3b	*arsI*	GCTCGCCTATCTGACGGAG	This study
lanM_Af-HindIII	*Msn. trichosporium* OB3b	*lanM*	ATTTTTAAGCTTTCATCGATATTCTGGATCTGC	This study
lanM_Ar-BamHI	*Msn. trichosporium* OB3b	*lanM*	ATTTTTGGATCCATAGGCAATTCGATCCCATC	This study
lanM_Bf-BamHI	*Msn. trichosporium* OB3b	*lanM*	ATTTTTGGATCCGGCGCTTTCCTGTATGATTC	This study
lanM_Br-EcoRI	*Msn. trichosporium* OB3b	*lanM*	ATTTTTGAATTCCCATCCGTCAACAGAATAGG	This study
lanM_A_f	*Msn. trichosporium* OB3b	*lanM*	TGAAGCCCGACAATGTGATC	This study
lanM_B_r	*Msn. trichosporium* OB3b	*lanM*	CTTCCAGACGAGATATTGGG	This study
BG8_mbnT1_Af_HindIII	*Mmb. album* BG8	*mbnT*	ATTTTTAAGCTTCTTTCTGATGATGGGGCTGC	This study
BG8_mbnT1_Ar_BamHI	*Mmb. album* BG8	*mbnT*	GAGCAAGGATCCATCTTCAG	This study
BG8_mbnT1_Bf_BamHI	*Mmb. album* BG8	*mbnT*	ATTTTTGGATCCAAGTTCCTTGCCACCGACTA	This study
BG8_mbnT1_Br_EcoRI	*Mmb. album* BG8	*mbnT*	ATTTTTGAATTCATTGGCTGGCAATGCTTTCA	This study
BG8_mbnT1_F	*Mmb. album* BG8	*mbnT*	TCTATGGACGAATGGAGCCC	This study
BG8_mbnT1_R	*Mmb. album* BG8	*mbnT*	CTCCGGCAAGATCCAATTCG	This study
xoxF1Af	*Msn. trichosporium* OB3b	*xoxF1*	ATTTTTAAGCTTGGTGTTGATGACGTAGCGAA	This study
xoxF1Ar	*Msn. trichosporium* OB3b	*xoxF1*	GCGAGGATCCCTACCGAAGTCGA	This study
xoxF1Bf	*Msn. trichosporium* OB3b	*xoxF1*	ATTTTTGGATCCCTATCAGCACAAGGGCAAGC	This study
xoxF1Br	*Msn. trichosporium* OB3b	*xoxF1*	GTTCTTGACCGAATTCTTCAGCGCCG	This study
F1_Af_2_EcoRI	*Msn. trichosporium* OB3b	*xoxF1*	ATTTTTGAATTCGAAGAGAGATAATGCGGGCC	This study
F1_Ar_2_KpnI	*Msn. trichosporium* OB3b	*xoxF1*	ATTTTTGGTACCCTTCGGGTTCTTCTGGAGCT	This study
F1_Bf_2_KpnI	*Msn. trichosporium* OB3b	*xoxF1*	ATTTTTGGTACCTGTCCAAGAGCAATGAAGGC	This study
F1_Br_2_BamHI	*Msn. trichosporium* OB3b	*xoxF1*	ATTTTTGGATCCTGCGCCAATTTGTTCTCGAA	This study
xoxF1_F1	*Msn. trichosporium* OB3b	*xoxF1*	TGTCGTCAGGAGGAAAAGCT	This study
xoxF1_R1	*Msn. trichosporium* OB3b	*xoxF1*	TTCATTGCTCTTGGACAGGC	This study

Table 2.2. Continued.

Name	Organism	Gene	Sequence (5'-3')[a]	Reference
qPCR primers				
341F	*Mmb. album* BG8	16S rRNA	CCTACGGGAGGCAGCAG	Kits et al., 2015a
518R	*Mmb. album* BG8	16S rRNA	ATTACCGCGGCTGCTGG	Kits et al., 2015a
QpmoA-FWD-7	*Mmb. album* BG8	*pmoA*	GTTCAAGCAGTTGTGTGGTATC	Kits et al., 2015a
QpmoA-REV-7	*Mmb. album* BG8	*pmoA*	GAATTGTGATGGGAACACGAAG	Kits et al., 2015a
qmxaF_BG8_F	*Mmb. album* BG8	*mxaF*	CAGAGGCCAACAAAGAACTG	This study
qmxaF_BG8_R	*Mmb. album* BG8	*mxaF*	CTGCGTCATCTTGCTGAAAT	This study
qcsp3_BG8_F	*Mmb. album* BG8	*csp3*	TCAATCCATGCAGCCTTGTA	This study
qcsp3_BG8_R	*Mmb. album* BG8	*csp3*	AGCAGATCATCAGGCGAAAG	This study
qtbrec_BG8_F	*Mmb. album* BG8	*mbnT*	CCGGCATTTCTTATCGTCATACA	This study
qtbrec_BG8_R	*Mmb. album* BG8	*mbnT*	CATTCACATCCAGAACCGACTC	This study
q16S_F2	*Mcc. capsulatus* Bath	16S rRNA	GTCAAGTCATCATGGCCCTT	This study
q16S_R2	*Mcc. capsulatus* Bath	16S rRNA	CTGCAATCCGGACTAAGACC	This study
qmmoXF_MCbath	*Mcc. capsulatus* Bath	*mmoX*	GCTCACCACGACCTGTATCT	This study
qmmoXR_MCbath	*Mcc. capsulatus* Bath	*mmoX*	GCCTCGAACCACTCCATTTC	This study
qpmoA_F2	*Mcc. capsulatus* Bath	*pmoA*	GGCTGGGGTCTGATCTTCTA	This study
qpmoA_R2	*Mcc. capsulatus* Bath	*pmoA*	GTTGTAACCCTGGATGTCGG	This study
qtbrec_bath_F	*Mcc. capsulatus* Bath	*mbnT*	CACCCTTTCCCTTGACACAC	This study
qtbrec_bath_R	*Mcc. capsulatus* Bath	*mbnT*	TCTGGTCGACCGAATAGACG	This study
qmopE_F	*Mcc. capsulatus* Bath	*mopE*	AATTCACCTGGAACGCCAAG	This study
qmopE_R	*Mcc. capsulatus* Bath	*mopE*	GGGAATTGCGGCAGATTGAT	This study
qcsp1_RW_F	*Methylocystis* sp. strain Rockwell	*csp1*	CACCATCATCCGCCGAAATA	This study
qcsp1_RW_R	*Methylocystis* sp. strain Rockwell	*csp1*	GTCGTCCATCGACAACATGC	This study
qmbnT1_RW_F	*Methylocystis* sp. strain Rockwell	*mbnT1*	TTCGAGACTTCGTGAGCAAC	This study
qmbnT1_RW_R	*Methylocystis* sp. strain Rockwell	*mbnT1*	CCGAGAGATCGTGCTGATATTC	This study
qmbnT2_RW_F	*Methylocystis* sp. strain Rockwell	*mbnT2*	TGCTCTACGAGGACGGATTT	This study
qmbnT2_RW_R	*Methylocystis* sp. strain Rockwell	*mbnT2*	AGAGCGTAATTGCCGAAGAG	This study
qmxaF_RW_F2	*Methylocystis* sp. strain Rockwell	*mxaF*	CAGGAATACTGGAAGGTCGAAA	This study
qmxaF_RW_R2	*Methylocystis* sp. strain Rockwell	*mxaF*	CGATCAGCACGACATCCTTA	This study
qpmoA_RW_F	*Methylocystis* sp. strain Rockwell	*pmoA*	CTGGAAGGATCGTCGTATGTG	This study
qpmoA_RW_R	*Methylocystis* sp. strain Rockwell	*pmoA*	GAACGGAAGACGGAAGTTGA	This study
q16S_RW_F	*Methylocystis* sp. strain Rockwell	16S rRNA	GATACGTGCGAGAGCAGAAA	This study
q16S_RW_R	*Methylocystis* sp. strain Rockwell	16S rRNA	ATCATCCTCTCAGACCAGCTA	This study

[a]Restriction site follows 6-nt overhang and is underlined.
[b]Mixed bases are R(A/G); Y(C/T); M(A/C); K(G/T); S(C/G); W(A/T); H(A/C/T); B(C/G/T); V(A/C/G); D(A/G/T); N(A/C/G/T).

2.3.5. Ligation

Ligation was carried out using T4 DNA ligase purchased from NEB (Ipsqich, MA) in 20-μL reactions consisting of vector and insert(s) in 1:3 molar ratio for at least 10 min at 25 °C or overnight at 16 °C for greater efficiency, following the manufacturer's instructions.

2.3.6. Molecular cloning

PCR primers were designed with a restriction site and 6-nt overhang at 5' end to produce DNA fragments for cloning purposes (Table 2.2). Phusion High-Fidelity polymerase was used for PCR, followed by gel purification of PCR product, restriction digestion, PCR or gel purification of digested DNA, and ligation with vector. *E. coli* TOP10 was transformed with the ligation mix for selection and maintenance. Correct inserts were confirmed via colony PCR and sequencing.

2.3.7. Reverse transcription-quantitative PCR (RT-qPCR)

Expression of select genes in methanotrophs cultured under varying conditions was quantified by reverse transcription-quantitative PCR (RT-qPCR). Primer sets used for qPCR of genes of interest are listed in Table 2.2. Expression of 16s rRNA was used as an internal reference. QIAGEN PCR Cloning Kit (Qiagen, Hilden, Germany) was used to prepare a recombinant vector containing the gene of interest. Either this recombinant vector or PCR products with known copy numbers was used to produce calibration curves for each examined gene to calculate primer efficiency. qPCR reactions were performed in 96-well PCR plates in 20-μL reactions containing 0.8 μL cDNA, 1× iTaq Universal SYBR Green Supermix (Bio-Rad), 0.5 μM each of forward and reverse primers, and nuclease-free sterile water (Fisher Scientific,

Pittsburgh, PA). CFX Connect Real Time PCR Detection System (Bio-Rad, Hercules, CA) or Applied Biosystems 7900HT (Thermo Fisher Scientific Inc., Waltham, MA) was used to run a three-step qPCR program consisting of an initial denaturation at 95°C for 3 min and 40 cycles of denaturation (95°C for 10 s), annealing (55°C for 10 s) and extension (72°C for 30 s). Primers used in this study were verified for specificity by gel electrophoresis, sequencing, and melting curve. The threshold cycle (C_T) values were used to calculate relative gene expression levels with 16S rRNA as the internal standard by the comparative threshold amplification cycle method, $2^{-\Delta\Delta CT}$ (Schmittgen & Livak, 2008). Measurements were performed for at least biological duplicates for each condition.

2.3.8. Immunoblot using antibody grown against methanobactin

MB uptake by methanotrophs was determined via immunoblotting using an antibody raised against MB. First, 10 – 20 mL of cultures were harvested by centrifugation at 4,300 × g for 10 min. The spent medium was carefully decanted, and the cell pellets washed with 1 V of fresh NMS. The cell pellets were then re-suspended in 1 mL fresh NMS, and spent medium, wash, and cell pellet were stored at -20°C until immunoblotting, which was performed by our collaborators at Iowa State University.

Antibody (10B10) to MB from *Msn. trichosporium* OB3b was produced in LOU/c rats and purified as described earlier (Gu et al., 2016a; Lichtmannegger et al., 2016). 1,4-phenylene diisothiocyanate (DITC)-derivatized polyvinylidene difluoride (PVDF) membranes were prepared as previously described (Rodrigues et al., 1994), with modifications.

The 36 mm^2 DITC-derivatized PVDF membranes were first wetted with methanol, then washed in 20 mM Tris-HCl, 0.5 M NaCl, pH 8.0 (Tris-buffered saline; TBS) for 5 min. They

were then air dried for approximately 5 min. The membranes were placed on top of Whatman No. 1 filter paper, loaded into the Bio-Rad Bio-Dot dot blot cassette, and a vacuum was pulled across the membranes. Cell extracts were diluted to an optical density of 0.13 at 600 nm and 15 μL of OB3b-MB standards, cell extracts, spent medium and lysozyme standards were then added to the wells and the membrane allowed to dry completely inside the cassette (usually 2 h). The membranes were then wetted in 50% methanol and washed twice in TBS for 10 min each time. The membrane was blocked at 4°C overnight with a blocking buffer consisting of 1% nonfat dry milk in TBS. The solution was decanted and the membrane washed twice in 0.1% Tween 20 in TBS for 10 min each time. The membrane was then incubated overnight at 4°C in primary antibody buffer (500 μL of purified MB-antibody at an optical density of 2.0 at 280 nm in 50 mL blocking buffer). The solution was decanted and the membrane washed twice in TBS for 10 min each time. The membrane was then incubated for 2 h at room temperature in secondary antibody buffer (16.5 μL of Goat Anti-Rat IgG Polyclonal Antibody Alkaline Phosphatase (AP) from Immunoreagents; Raleigh, NC, USA) in 50 mL of blocking buffer. The solution was decanted and the membrane washed 3 times in TBS for 10 min each time. The membrane was removed from solution and excess liquid drained. The membrane was then incubated with 1 mL of Immun-Star AP Chemiluminescence substrate (Bio-Rad, Hercules, CA) for 5 min with gentle agitation. The membrane was removed and imaged on a ChemiDoc system (Bio-Rad, Hercules, CA) using the Chemi protocol in signal accumulation mode. Densitometric measurements were determined using ImageJ (NIH, Bethesda, MD). Samples and background measurements were made using the oval brush option. Total signal was calculated as (sample mean × area of sample) – (background mean × area of sample).

2.4. Construction of mutants in methanotrophs

2.4.1. Markerless mutagenesis in methanotrophs

Markerless mutagenesis using the suicide vector pK18*mobsacB* (Schäfer et al., 1994) was utilized to investigate the function of target genes in *Mmc. album* BG8 and *Msn. trichosporium* OB3b. pK18*mobsacB* harboring regions flanking the target gene was introduced into methanotrophs, causing homologous recombination with their chromosome. The suicide vector pK18*mobsacB* contains the broad host range transfer elements required for mobilization from *E. coli* S17-1 to methanotrophs, and also the counterselection gene *sacB* required for screening double homologous recombination. pK18*mobsacB*, derived from plasmid pBR322, is only maintained in *E. coli* (Schäfer et al., 1994), and must go through recombination in order to be replicated in methanotrophs.

In *Mmc. album* BG8, *mbnT1* (Metal_1282), the gene encoding for a putative TonB-dependent transporter with high similarity with *mbnT* from *Msn. trichosporium* OB3b, was targeted for knockout in order to assess competition for copper with MB-producing methanotrophs. Approximately 1-kb DNA fragments in the 5' (arm A, amplified using primers BG8_mbnT1_Af_HindIII and BG8_mbnT1_Ar_BamHI; Table 2.2) and 3' (arm B, amplified using primers BG8_mbnT1_Bf_BamHI and BG8_mbnT1_Br_EcoRI; Table 2.2) of *mbnT1* were ligated together using *BamHI* site and cloned into pK18*mobsacB* at *HindIII* and *EcoRI* sites to create pK*mbnT1* (Table 2.1, Figure 2.1).

The constructed plasmid pK*mbnT1* was then introduced into *Mmc. album* BG8 via conjugation with *E. coli* S17-1, and transconjugants were selected for plasmid incorporation into the chromosome via single homologous recombination. Then, selected transconjugants were grown in NMS supplemented with 2.5% (m/v) sucrose for counterselection of double

homologous recombination events (Figure 2.1). Colonies on the sucrose NMS plates were checked for kanamycin sensitivity and loss of both pK18*mobsacB* plasmid backbone and intact *mbnT1* via PCR and sequencing (using primers BG8_mbnT1_F and BG8_mbnT1_R) (Figure A.4). Approximately 1 kb of the 2.3-kb *mbnT1* was knocked out in Δ*mbnT1*.

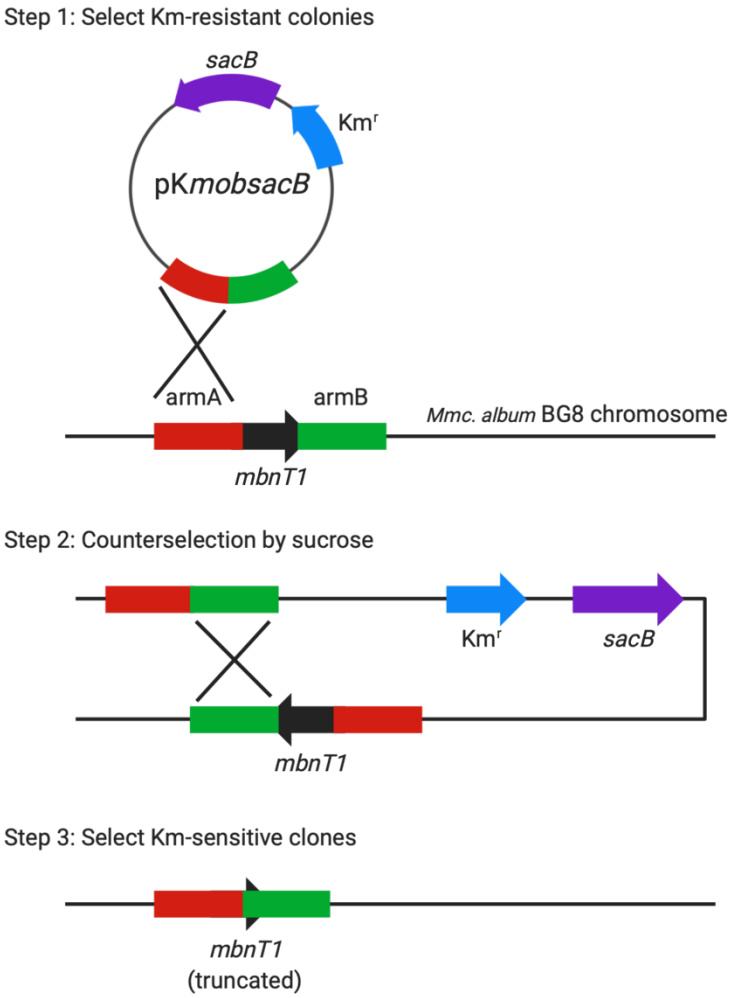

Figure 2.1. Markerless mutagenesis of *Mmc. album* BG8 Δ*mbnT1* via counterselection.

In *Msn. trichosporium* OB3b, *arsI* (ADVE02_v2_12724) encoding for an organoarsenical lyase was targeted for knockout in order to assess the role of ArsI in methylmercury demethylation. Approximately 0.8-kb and 1-kb DNA fragments upstream (arm B, amplified using primers arsI_Bf and arsI_Br; Table 2.2) and downstream (arm A, amplified using primers arsI_Af and arsI_Ar; Table 2.2) of *arsI* were ligated together using *BamHI* site and cloned into pK18*mobsacB* at *HindIII* and *EcoRI* sites to create pK*arsI* (Table 2.1). The same counterselection and verification methods as *Mmc. album* BG8 were used here to knock out *arsI*. About 0.4 kb of the 0.5-kb *arsI* was knocked out in the *Msn. trichosporium* OB3b Δ*arsI* mutant (Figure A.5).

xoxF1 (ADVE02_v2_12117) encoding for the Xox-MeDH in *Msn. trichosporium* OB3b was targeted for knockout to confirm the role of Xox-MeDH in methylmercury degradation. Two pairs of arms were used for deletion (Table 2.2). Arms A and B produced using primers xoxF1Af/xoxF1Ar and xoxF1Bf/xoxF1Br were ligated together using *BamHI* site and cloned into pK18*mobsacB* at *HindIII* and *EcoRI* sites to create pK*xoxF1*. The arms produced using primers F1_Af_2_EcoRI/F1_Ar_2_KpnI and F1_Bf_2_KpnI/F1_Br_2_BamHI were ligated together using the *KpnI* site and cloned into pK18*mobsacB* at *EcoRI* and *BamHI* sites to create pK*xoxF1*_2. The same counterselection and verification methods as *Mmc. album* BG8 were used to knock out *xoxF1*. No successful double homologous recombination was observed after multiple rounds of screening.

lanM (ADVE02_v2_11067) encoding for a periplasmic REE-binding protein in *Msn. trichosporium* OB3b was also targeted for knockout in order to assess the role of LanM in REE sensing and/or uptake. Approximately 1.1-kb DNA fragments upstream (arm A, amplified using primers lanM_Af-HindIII and lanM_Ar-BamHI; Table 2.2) and downstream (arm B, amplified

using primers lanM_Bf-BamHI and lanM_Br-EcoRI; Table 2.2) of *lanM* were ligated together using *BamHI* site and cloned into pK18*mobsacB* at *HindIII* and *EcoRI* sites to create pK*lanM* (Table 2.1). The same counterselection and verification methods as *Mmc. album* BG8 were used here to knock out *lanM*. About 0.5 kb was knocked out in the *Msn. trichosporium* OB3b Δ*lanM* mutant, including *lanM* (0.4 kb) (Figure A.6).

2.4.2. Production of modified MBs

Modified forms of MB were expressed using the *Msn. trichosporium* OB3b Δ*mbnAN* mutant as a host. Plasmids pBE3013 and pBE3015 harboring MB biosynthesis genes (*mbnABCMFS*) from *Methylocystis* sp. SB2 and the promoter found immediately upstream of *mbnA* in *Msn. trichosporium* OB3b were introduced into Δ*mbnAN* via conjugation with *E. coli* S17-1. Transconjugants were screened for resistance against spectinomycin/streptomycin or gentamicin, depending on resistance markers on plasmids.

2.5. Metal analysis

2.5.1. Metal uptake by methanotrophs

Copper and REE uptake by methanotrophs were determined via inductively coupled plasma mass spectrometry (Agilent Technologies, Santa Clara, CA). 10-20 mL of cultures were harvested by centrifugation at 4,300 × g for 10 min. The spent medium was carefully decanted, and the cell pellets washed with 1 V of fresh NMS or AMS as necessary. The cell pellets were then re-suspended in 1 mL fresh NMS or AMS, and spent medium, wash, and cell pellet were stored at -20°C until metal quantification. To prepare samples, cell pellets were acidified with 1 mL of 70% HNO_3 (vol/vol) for 2 h at 95 °C with mixing by inversion every 30 min. Fresh NMS

or AMS was added to cell samples and 70% nitric acid (vol/vol) to spent medium and wash samples to achieve a final concentration of 2% (vol/vol) nitric acid. Cell densities (as OD_{600}) were used to calculate protein concentrations using a previously established correlation (Semrau et al., 2013). Triplicate samples for every condition were analyzed.

2.5.2. Methylmercury demethylation assay

Methylmercury (MeHg) demethylation by methanotrophs were measured by our collaborators at Oak Ridge National Laboratory as described earlier (Lu et al., 2017). Briefly, these assays were conducted in 4-mL amber glass vials (National Scientific, Claremont, CA) by mixing washed cells with MeHg in 5 mM MOPS buffer under ambient conditions. A 10 nM MeHg working solution (0.5 mL) was prepared and added to 0.5 mL washed cells to give final concentrations of MeHg at 5 nM and cells at 10^8 cells mL^{-1} (Lu et al., 2016). 45 µM MB from either *Msn. trichosporium* OB3b or *Methylocystis* sp. SB2 was also added to determine if the presence of MB affected MeHg degradation by *Mmc. album* BG8 and *Methylocystis* sp. strain Rockwell. MeHg sorption was monitored by filtering samples (in triplicate) through 0.2-µm syringe filters and analyzed for remaining soluble MeHg, or soluble inorganic Hg (IHg), if any (Lin et al., 2015; Lu et al., 2016). The unfiltered samples were used to determine total Hg and MeHg, with total sorbed Hg calculated by difference. For Hg species distribution analyses, three additional samples were added with 10 µL of 2,3-dimercapto-1-propanesulfonate(DMPS) to a final concentration of 0.1 mM, and then equilibrated for an additional 15 min to wash off cell-surface-adsorbed MeHg ($MeHg_{ad}$) or IHg, as they form strong complexes with DMPS. Samples were again filtered and analyzed, so that the surface adsorbed and the intra-cellular MeHg or IHg uptake could be calculated by the difference (An et al., 2019; Liu et al., 2016).

2.6. Chalkophore purification and characterization

The putative *Mmc. album* BG8 chalkophore was purified following the method by Bandow et al (2011). The spent medium of *Mmc. album* BG8 grown in the presence of 1 μM copper and 5 μM TRIEN was centrifuged at 4,300 × g for 10 min. The supernatant was decanted, then filtered through a 0.2-μm PES filter unit (Thermo Scientific, Waltham, MA). Meanwhile, a reversed-phase C_{18} Sep-Pak cartridge (Waters Corp., Milford, MA) was sequentially conditioned with 3 mL methanol, 3 mL 60% acetonitrile, 3 mL methanol, and 6 mL H_2O, then was loaded with the filtered spent medium. The chalkophore bound to the column was washed with 6 mL H_2O, then eluted with 60% acetonitrile until the yellow band was completely collected. The eluant was then frozen at -80 °C and lyophilized to concentrate chalkophore and remove acetonitrile (FreeZone 6 Freeze Dry System, Labconco, Kansas City, MO).

Our collaborators at Iowa State University performed large scale production and isolation of *Mmc. album* BG8 chalkophore, as well as UV-visible spectroscopy and mass spectrometry analyses. First, cells were cultured in a 15-L Solida fermenter (Solida Biotechnology, Munich Germany) using the culture conditions described above. For ^{15}N labeled chalkophore, cells were cultured in 50% ^{15}N- and 50% ^{14}N- KNO_3. The chalkophore was isolated from the spent media and purified as described for methanobactin from *Methylocystis* sp. SB2, except the chalkophore from *Mmc. album* BG8 eluted from the Targa C18 column in the 65-75% methanol:H_2O fraction.

UV-visible spectroscopy was recorded on a Cary 50 (Agilent Technologies, Santa Clara, CA). Matrix-assisted laser desorption/ionization mass spectroscopy (MALDI-MS) was performed on a Shimadzu AXIMA Confidence MALDI TOF Mass Spectrometer (Shimadzu Corp., Kyoto, Japan) using a mixture of 2,5-dihydroxybenzoic acid and 2-hydroxy-5-

methoxybenzoic acid (SuperDHB) in a 1:1 matrix to sample mixture. Electrospray ionization (ESI)MS/MS was performed on an Agilent LC using a Thermo Scientific Q Exactive Hybrid Quadrupole-Orbitrap Mass Spectrometer with an HCD fragmentation cell and an Agilent 1260 Infinity Capillary Pump with an Agilent Zorbax SB-C18, 0.5 mm x 150 mm, 5 micron, part#5064-8256 using 0.1% formic acid/water and 0.1% formic acid/acetonitrile as buffers A and B, respectively.

2.7. Naphthalene assay

sMMO activity was measured via the assay developed by Brusseau et al. (1990). 1.6 mL of culture in exponential phase was incubated with a few crystals of naphthalene for 1 h at 30 °C, 220 rpm. Cells were removed via centrifugation at 5,800 × g for 10 min. 1.3 mL of the spent medium was transferred to a new microcentrifuge tube, then was added with 130 μL of 4.21 mM tetrazotized *o*-dianisidine. The mixture was immediately transferred to cuvettes for measurement of absorbance at 528 nM (ABS_{528}). The rapid development of pink/purple color indicated presence of naphthol and therefore naphthalene oxidation by sMMO.

2.8. Bioinformatic analysis

2.8.1. Genome sequences

All genomes used in this study were acquired from NCBI or MicroScope databases (NCBI Resource Coordinators et al., 2018; Vallenet et al., 2019). For the bioinformatic survey and identification of lateral gene transfer (LGT) events in methanotrophs, 39 genomes from various taxonomic families/phyla were considered – *Methylocystaceae* (9), *Beijerinckiaceae* (4),

Methylococcaceae (20), *Methylothermaceae* (1), "Methyloacidiphilaceae" (4), and candidate phylum NC10 (1).

2.8.2. Evidence for lateral gene transfer

Nucleotide bias between specific genes and the rest of the genome to detect possible lateral gene transfer was calculated using two different programs – Alien Hunter and CodonW – as described earlier (Khadka et al., 2018). Briefly, these packages determine the Kullback-Leibler divergence statistic (D_{KL}) for different DNA regions as compared to the overall genome using different criteria. Alien Hunter considers combined 2-mers through 8-mers for both specific regions and the genome using a 2500 bp window. CodonW considers codon bias between specific regions and the genome. For Alien Hunter, complete genomes in FASTA format were used as input (Vernikos & Parkhill, 2006). The D_{KL} values of operons (regions) of interest were extracted from the resulting output file to determine whether the operon fell in a region of potential LGT. For CodonW, the coding sequence of each genome was extracted from GenBank (.gbk) files using FeatureExtract 1.2L Server (Wernersson, 2005). The coding sequence of DNA regions and genomes were then uploaded to the online tool, CodonW Galaxy v1.4.4 (Peden, 1999). The frequency of all 64 codons was then counted for regions and genomes to calculate D_{KL} values. DNA regions considered here were: *pmoCAB* (for pMMO); *mmoXYBZDC* (for sMMO) *mxaFJGI* (for Mxa-MeDH), *xoxFJ* (for Xox-MeDH), *sga* (encoding serine-glyoxylate aminotransaminase), *fdhBA* and *fdsBA* (encoding the tungsten and molybdenum dependent forms of formate dehydrogenase, respectively), as well as genes for three different identified copper uptake systems in methanotrophs, i.e., (1) *mbnABCM* (encoding methanobactin; (Semrau et al., 2013)), (2) *mopE* + MCA 2590 (encoding *Methylococcus* outer

membrane protein (MopE) and its surface associated cytochrome *c* peroxidase; (Helland et al., 2008; Ve et al., 2012) as well as close analogs *corAB* (Berson & Lidstrom, 1997; Johnson et al., 2014) and; (3) *copCD* (encoding a periplasmic copper binding protein and its partner inner membrane transport protein; (Arnesano et al., 2003; Gu et al., 2017b)).

2.8.3. Phylogenetic analysis

The alignments of genes, concatenated genes, and amino acid sequences were constructed using T-COFFEE (Notredame et al., 2000). Bayesian and maximum likelihood phylogenies were generated based on these alignments using PhyML 3.1 and BEAST 1.10.4, respectively (Guindon et al., 2010; Huelsenbeck, 2001). The resulting Bayesian and maximum likelihood phylogenies were evaluated using 10^7 generations discarding a burn-in of 25% and 100 bootstrap replicates, respectively. The phylogenetic trees and alignments were visualized using ggtree 1.14.4 (Yu et al., 2017). Gene synteny maps were created using ggbio 1.36.0 (Yin et al., 2012). Sequence logos were created using ggseqlogo 0.1 (Wagih, 2017).

2.8.4. Genome assembly

Genomic DNA was extracted from two strains of methanotrophs isolated from methylmercury contaminated stream and sequenced. Libraries for Illumina sequencing were prepared using NEBNext® Ultra™ II FS DNA Library Prep Kit (New England Biolabs Inc., Ipswich, MA) with 15-min fragmentation and size selected for 275-475bp. Libraries for GridION Nanopore sequencing were prepared using Ligation Sequencing and Native Barcoding Expansion Kits (SQK-LSK109 and EXP-NBD104; Oxford Nanopore Technologies, Littlemore, UK) following the manufacturers' protocols. gDNA was sequenced using separate Nano flow

cells and 500 cycle V2 kits on an Illumina MiSeq (Illumina Inc., San Diego, CA) at the University of Michigan Advanced Genomics Core (AGC; https://brcf.medicine.umich.edu/cores/advanced-genomics/). Long-read sequencing was performed on the GridION X5 platform at the University of Michigan AGC (Oxford Nanopore Technologies, Littlemore, UK).

De novo assemblies of sequenced reads were performed. Basecalling for the GridION Nanopore sequencing reads was performed using Guppy (4.2.3) (Wick et al., 2019). The read quality was assessed using FastQC (0.11.9) (Andrews, 2010) before and after trimming. The short- and long-reads were trimmed using Trimmomatic (0.39) (Bolger et al., 2014) and Porechop (0.2.4) (Wick, 2018), respectively, then were then assembled using Unicycler (0.4.9b) with no correction (Wick et al., 2017). Assembly completeness was assessed via Benchmarking Universal Single-Copy Orthologs (BUSCO 4.1.4) (Simão et al., 2015), and also visually confirmed using Bandage (0.8.1) (Wick et al., 2015). The final contigs were annotated using National Center for Biotechnology Information (NCBI) Prokaryotic Genomes Annotation Pipeline (PGAP) (5.1) (Tatusova et al., 2016). The annotated 16S rRNA sequences were used as queries in search of the most similar organisms using the Basic Local Alignment Search Tool (BLAST; 2.11.0) (Altschul et al., 1990). Default parameters were used for all software unless otherwise specified.

2.8.5. Metabolic pathway reconstruction based on genome sequence

The deduced amino acid sequences of two strains of methanotrophs isolated from methylmercury contaminated stream were annotated using BlastKOALA (2.2) using the prokaryotes KEGG GENES database at the genus level (https://www.kegg.jp/blastkoala/)

(Kanehisa et al., 2016). The resulting list of KEGG GENES was then manually curated and mapped against KEGG databases using the Reconstruct Pathway tool of KEGG Mapper (4.3) (Kanehisa & Sato, 2020).

2.9. Statistical analysis

All statistical analysis was performed using Microsoft Excel or R (R Core Team, 2018). Data were analyzed using either the Tukey's honestly significant difference (HSD) test, Student's t-test with Bonferroni correction, or analysis of covariate (ANCOVA) to determine any significant differences between conditions. Potential outliers of biological triplicates were determined using the Grubbs' outlier test. Growth of methanotrophs was fitted to a logistic curve using the R package growthcurver (Sprouffske & Wagner, 2016). In cases of non-logistic growth of methanotrophs, the maximum growth rates were determined via linear fitting.

When assessing methylmercury (MeHg) removal by methanotrophs, the MeHg removal rate constant was determined by nonlinear regression on the basis of exponential decay with stabilization over time: $Y = (\alpha + \theta)e^{-kt} + \theta$, where Y is the amount of residual MeHg (%), k is the rate constant (h^{-1}), t is time (h), θ is residual MeHg limit (%), and $(\alpha + \theta)$ is the initial residual MeHg (%).

Chapter 3 Importance of Metal Uptake in the Evolution of Methanotrophs

3.1. Introduction

All aerobic methanotrophs utilize either a particulate methane monooxygenase (pMMO) or soluble MMO (sMMO), or both, to convert methane to methanol (Table 1.2, pg. 19). It is well-known that pMMO requires copper for its activity, and methanotrophs have multiple mechanisms for copper collection (1.3.1. Copper uptake systems Metal uptake systems, pg.49) (Chi Fru et al., 2011; El Ghazouani et al., 2012; Gu et al., 2016a, 2017b; Helland et al., 2008; Kim et al., 2004; Krentz et al., 2010; Semrau et al., 2018; Ve et al., 2012). Further, for those methanotrophs that can express both sMMO and pMMO, sMMO expression is only observed in the absence of copper, while pMMO expression increases with increasing copper, i.e., the canonical "copper-switch" (Semrau et al., 2013; Stanley et al., 1983).

Interestingly, the two forms of methanol dehydrogenase (MeDH) found in aerobic methanotrophs as well as many methylotrophs, "Mxa-MeDH" and "Xox-MeDH", are regulated via an "REE-switch" (Farhan Ul Haque et al., 2015a; Chu et al., 2016; Vu et al., 2016; Gu & Semrau, 2017). Recently, a novel periplasmic REE-binding protein, lanmodulin (LanM), with high specificity and affinity for REEs was characterized in a methylotroph, *Mrr. extorquens* AM1 (Cook et al., 2019; Cotruvo et al., 2018). It is interesting to note that *lanM* is found in all methanotrophs belonging to the *Alphaproteobacteria* class, whereas *lanM* is not found in any other methanotroph (Table 1.2, pg.19).

Several researchers have proposed the possible origin of methanotrophy, but it is generally believed that aerobic methanotrophs originated from methylotrophs, which can already

effectively handle the initial product of methane oxidation – methanol (Tamas et al., 2014; Osborne & Haritos, 2018). Specifically, methane oxidation is perceived to occur as a result of lateral gene transfer (LGT) of the ammonia monooxygenase (AMO) from nitrifying bacteria to methylotrophs (Khadka et al., 2018). Given that methanotrophy possibly arose via transfer of MMO to methylotrophs, we chose to bioinformatically examine genes involved in methanol oxidation as well as genes involved in copper and REE uptake. This is particularly relevant as methylotrophy is much more wide-spread than methanotrophy, suggesting that some methylotrophs lack essential cell machinery to be effectively transformed into methanotrophs through LGT of genes encoding MMO. As an extended focus on copper uptake systems in methanotrophs, phylogeny, sequence, and structure of methanobactins (MBs) were closely examined. The occurrence of LanM in methanotrophs and other groups of microbes as well as the composition of REE-coordinating EF hands were compared.

3.2. Evidence of LGT of methane monooxygenases

The different software packages used to detect LGT events – Alien Hunter and CodonW – gave similar trends for assessed genes (Figure 3.1), but in general greater divergence values were found using Alien Hunter than CodonW, likely due to its greater sensitivity as it uses variable order motif distributions. It should be noted that Alien Hunter does not provide numerical divergence values below a critical threshold calculated based on these distributions. These are reported as "0" in Figure 3.1.

As previously shown (Khadka et al., 2018), the *pmo* operon (*pmoCAB*) appears to be the result of a relatively recent LGT event as the nucleotide composition of this operon in most aerobic methanotrophs is significantly divergent from the genome composition of the host microbe (Figure 3.1; Table 3.1 and Table 3.2). Bayesian phylogenetic trees based either on 16S rRNA gene or concatenated *pmoCAB* gene sequences (Figure 3.2A and Figure 3.3A, respectively), however, were similar. It should be noted that D_{KL} values were not calculated for *pxm* sequences, nor are they included in the phylogenetic trees, since only a fraction of characterized methanotrophs have been found to have these genes in their genomes (Table 1.2, pg.19) and their importance or function in methanotrophic physiology is largely unknown. Maximum-likelihood phylogenetic trees based on either 16S rRNA or *pmoCAB* gene sequences (Figure 3.2B and Figure 3.3B) exhibited similar profiles as Bayesian trees.

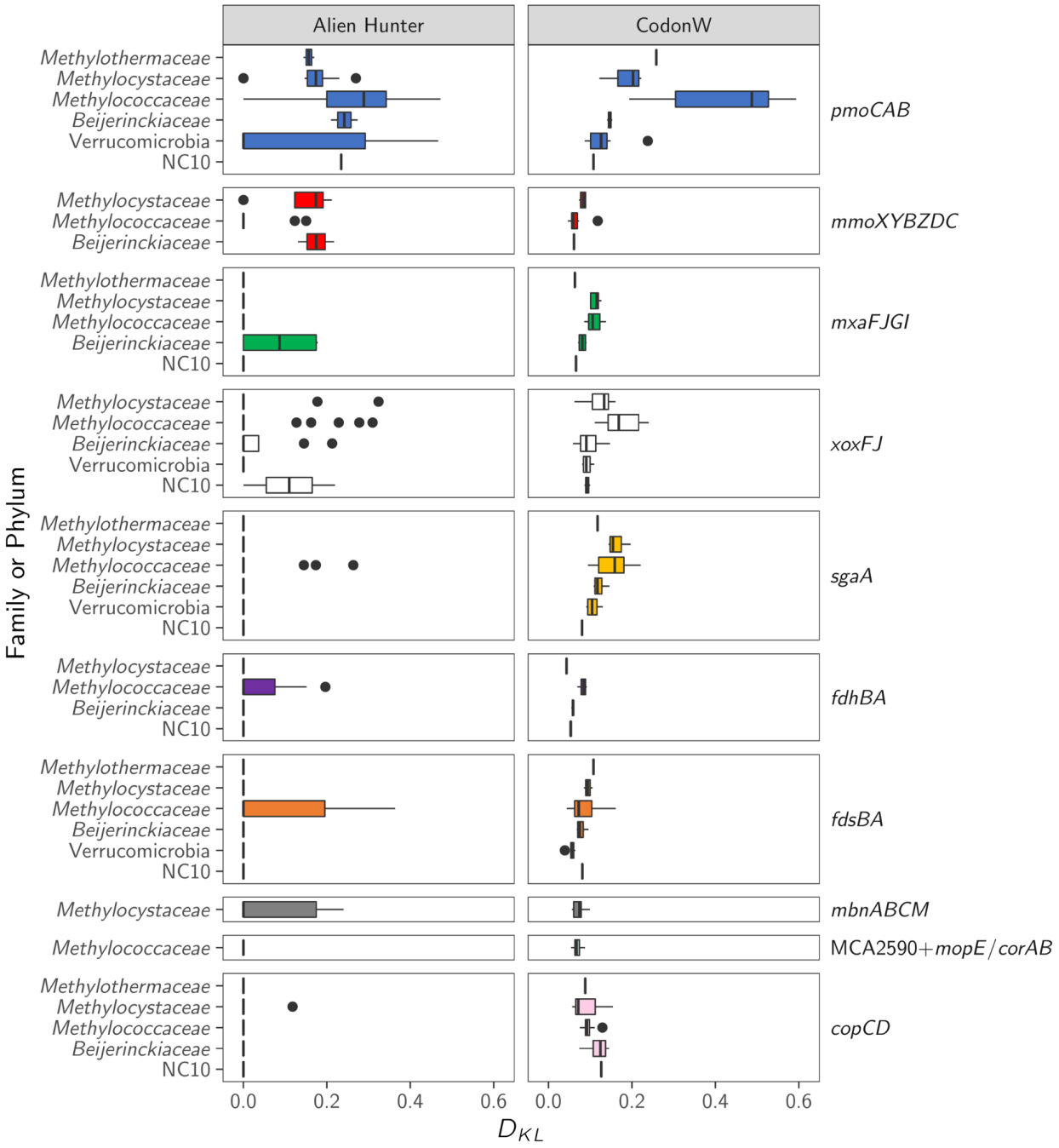

Figure 3.1. Nucleotide compositional biases (D_{KL}) of key gene clusters involved in methane oxidation (*pmoCAB* and *mmoXYBZDC*), methanol oxidation (*mxaFJGI* and *xoxFJ*), carbon assimilation (*sgaA*), formate oxidation (*fdhBA* and *fdsBA*) and copper uptake (*mbnABCM*, *corAB*, *mopE*/MCA2590, and *copCD*) in methanotrophs compared to their respective host genomes. The box indicates the interquartile range between 25th and 75th percentile, and the solid line indicates the 50th percentile. Outliers determined by the Tukey method are marked by dots. Alien Hunter D_{KL} values calculated to be below threshold are reported as "0".

Table 3.1. D_{KL} values of select genes in the genomes of methanotrophs calculated using Alien Hunter. BT indicates values below threshold.

Strain	Family	*pmoCAB*	*mmo XYBZDC*	*mxaFJGI*	*xoxFJ*	*mbnABCM*	MCA2590 + *mopE/corAB*	*copCD*	*sgaA*	*fdhBA*	*fdsBA*
Class *Gammaproteobacteria*											
Methylobacter sp. BBA5.1[a]	*Methylococcaceae*	0.268		BT	0.228			BT	BT	BT	0.255
					0.127						
Mbt. marinus A45[a]	*Methylococcaceae*	BT		BT	0.310			BT	BT	BT	0.193
					BT						
Mbt. tundripaludum SV96[a]	*Methylococcaceae*	0.395		BT	0.162			BT	BT		BT
Mbt. whittenburyi ACM 3310[a]	*Methylococcaceae*	0.285		BT	0.278			BT	BT	BT	0.203
					BT						
Mcd. szegediense O-12[a]	*Methylococcaceae*	0.186		BT	BT			BT	BT		0.197
					BT						
Mcc. capsulatus Bath	*Methylococcaceae*	0.194	0.150	BT	BT		BT	BT	0.263	BT	BT
		0.157									
Mcc. capsulatus Texas[a]	*Methylococcaceae*	BT	0.123	BT	BT		BT	BT	0.173	BT	BT
Mgb. morosus KoM1[a]	*Methylococcaceae*	0.304		BT				BT	BT		0.219
Mmg. ishizawai 175	*Methylococcaceae*	BT	BT	BT	BT		BT	BT	BT		BT
		BT									
Mmc. agile ATCC 35068[a]	*Methylococcaceae*	0.218		BT	BT		BT	BT	BT		BT
Mmc. album BG8[a]	*Methylococcaceae*	0.273		BT	BT		BT	BT	BT		BT
Mmc. lacus LW14	*Methylococcaceae*	0.284		BT	BT		BT	BT	BT		BT
Mtv. alcaliphilum 20Z	*Methylococcaceae*	0.414		BT	BT		BT	BT	BT	0.196	
Mtv. buryatense 5G[a]	*Methylococcaceae*	0.472	BT	BT	BT		BT	BT	BT	0.151	0.364
Mmn. methanica MC09	*Methylococcaceae*	0.190	BT	BT	BT			BT	BT		BT
Methylomonas sp. 11b[a]	*Methylococcaceae*	0.292	BT	BT	BT			BT	0.145		BT
Methylomonas sp. LW13[a]	*Methylococcaceae*	0.433	BT	BT	BT			BT	BT		BT
Methylomonas sp. MK1[a]	*Methylococcaceae*	0.330	BT	BT	BT			BT	BT		BT
Msc. fibrata AML-C10[a]	*Methylococcaceae*	0.318		BT	BT		BT	BT	BT		BT
Mvl. miyakonense HT12[a]	*Methylococcaceae*	0.297	BT	BT			BT	BT	BT		BT
Mhl. crimeensis 10Ki[a]	*Methylothermaceae*	0.144		BT				BT	BT		BT
		0.170									

Table 3.1. Continued.

Strain	Family	*pmoCAB*	*mmo XYBZDC*	*mxaFJGI*	*xoxFJ*	*mbnABCM*	MCA2590 + *mopE/corAB*	*copCD*	*sgaA*	*fdhBA*	*fdsBA*
Class *Alphaproteobacteria*											
Mcs. acidiphila B2[a]	*Beijerinckiaceae*	0.274		0.173	BT			BT	BT	BT	BT
Mcs. aurea KYG[a]	*Beijerinckiaceae*	0.210		0.178	BT			BT	BT	BT	BT
								BT			
Mcl. silvestris BL2	*Beijerinckiaceae*		0.131	BT	BT			BT	BT		BT
					BT						
					0.145						
Mfr. stellata AR4	*Beijerinckiaceae*		0.217	BT	0.213			BT	BT	BT	BT
					BT						
					BT						
Methylocystis sp. LW5[a]	*Methylocystaceae*	0.190	0.212	BT	BT	0.174		BT	BT	BT	BT
		0.151									
		0.154									
Mct. parvus OBBP[a]	*Methylocystaceae*	BT		BT	BT	0.240		BT	BT		BT
		0.199									
Methylocystis sp. strain Rockwell[a]	*Methylocystaceae*	0.213		BT	BT			BT	BT		BT
					0.324			BT			
Mct. rosea SV97[a]	*Methylocystaceae*	0.146		BT	BT	BT		BT	BT		BT
		0.182			0.177			BT			
Methylocystis sp. SB2[a]	*Methylocystaceae*	BT		BT	BT	BT		0.118	BT		BT
								BT			
Methylocystis sp. SC2	*Methylocystaceae*	0.189		BT	BT	BT		BT	BT		BT
		0.172			BT			BT			
		0.270									
Methylosinus sp. LW3[a]	*Methylocystaceae*	0.151	0.164	BT	BT	BT		BT	BT	BT	BT
		0.230						BT			
		0.154									
Methylosinus sp. LW4[a]	*Methylocystaceae*	0.161	BT	BT	BT	0.164		BT	BT		BT
		0.187						BT			
		0.175									
Msn. trichosporium OB3b[a]	*Methylocystaceae*	0.188	0.184	BT	BT	0.199		BT	BT		BT
		0.161			BT			BT			

Table 3.1. Continued.

Strain	Family	*pmoCAB*	*mmo XYBZDC*	*mxaFJGI*	*xoxFJ*	*mbnABCM*	MCA2590 + *mopE/corAB*	*copCD*	*sgaA*	*fdhBA*	*fdsBA*
Candidate phylum NC10											
"Ca. Methylomirabilis oxyfera"	-	0.234		BT	BT			BT	BT	BT	BT
					0.219						
Phylum *Verrucomicrobia*											
"*Ca.* Methylacidimicrobium cyclopophantes" 3C[a]	"*Ca.* Methylacidiphilaceae"	0.206			BT			BT	BT		BT
"*Ca.* Methylacidimicrobium" sp. LP2A	"*Ca.* Methylacidiphilaceae"	0.292			BT			BT	BT		BT
		0.292									
"*Ca.* Methylacidiphilum fumariolicum" SolV	"*Ca.* Methylacidiphilaceae"	BT			BT			BT	BT		BT
		BT									
		BT									
"*Ca.* Methylacidiphilum infernorum" V4	"*Ca.* Methylacidiphilaceae"	BT			BT			BT	BT		BT
		BT									
		0.467									

[a]contains assembly gaps

Table 3.2. D_{KL} values of select genes in the genomes of methanotrophs calculated using CodonW.

Strain	Family	*pmoCAB*	*mmo XYBZDC*	*mxaFJGI*	*xoxFJ*	*mbnABCM*	MCA2590 + *mopE/corAB*	*copCD*	*sgaA*	*fdhBA*	*fdsBA*
Class *Gammaproteobacteria*											
Methylobacter sp. BBA5.1[a]	*Methylococcaceae*	0.582		0.109	0.217			0.091	0.118	0.089	0.158
					0.198						
Mbt. marinus A45[a]	*Methylococcaceae*	0.593		0.106	0.217			0.089	0.123	0.087	0.145
					0.200						
Mbt. tundripaludum SV96[a]	*Methylococcaceae*	0.451		0.095	0.224			0.091	0.183		0.061
Mbt. whittenburyi ACM 3310[a]	*Methylococcaceae*	0.529		0.111	0.217			0.086	0.122	0.092	0.161
					0.133						
Mcd. szegediense O-12[a]	*Methylococcaceae*	0.288		0.101	0.111			0.075	0.097		0.052
					0.126						
Mcc. capsulatus Bath	*Methylococcaceae*	0.194	0.073	0.095	0.140		0.071	0.080	0.094	0.075	0.062
		0.198									
Mcc. capsulatus Texas[a]	*Methylococcaceae*	0.193	0.069	0.086	0.143		0.063	0.081	0.104	0.069	0.063
Mgb. morosus KoM1[a]	*Methylococcaceae*	0.352		0.088				0.088	0.113		0.058
Mmg. ishizawai 175	*Methylococcaceae*	0.235	0.118	0.137	0.167		0.066	0.111	0.113		0.069
		0.236									0.075
Mmc. agile ATCC 35068[a]	*Methylococcaceae*	0.488		0.126	0.142		0.075	0.095	0.180		0.078
Mmc. album BG8[a]	*Methylococcaceae*	0.491		0.122	0.143		0.075	0.094	0.179		0.145
Mmc. lacus LW14	*Methylococcaceae*	0.572		0.135	0.162		0.053	0.092	0.187		0.063
Mtv. alcaliphilum 20Z	*Methylococcaceae*	0.462		0.096	0.170		0.069	0.104	0.221	0.084	0.092
Mtv. buryatense 5G[a]	*Methylococcaceae*	0.417	0.050	0.105	0.160		0.063	0.096	0.202	0.080	0.072
Mmn. methanica MC09	*Methylococcaceae*	0.522	0.046	0.138	0.189			0.097	0.181		0.087
Methylomonas sp. 11b[a]	*Methylococcaceae*	0.486	0.056	0.097	0.240			0.105	0.159		0.072
Methylomonas sp. LW13[a]	*Methylococcaceae*	0.473	0.068	0.125	0.221			0.129	0.160		0.044
Methylomonas sp. MK1[a]	*Methylococcaceae*	0.489	0.059	0.102	0.214			0.102	0.135		0.115
Msc. fibrata AML-C10[a]	*Methylococcaceae*	0.490		0.085	0.132		0.062	0.092	0.163		0.066
Mvl. miyakonense HT12[a]	*Methylococcaceae*	0.535	0.056	0.109			0.087	0.092	0.137		0.058
Mhl. crimeensis 10Ki[a]	*Methylothermaceae*	0.258		0.063				0.088	0.117		0.108
		0.259									

Table 3.2. Continued.

Strain	Family	*pmoCAB*	*mmo XYBZDC*	*mxaFJGI*	*xoxFJ*	*mbnABCM*	MCA2590 + *mopE/corAB*	*copCD*	*sgaA*	*fdhBA*	*fdsBA*
Class *Alphaproteobacteria*											
Mcs. acidiphila B2[a]	*Beijerinckiaceae*	0.153		0.088	0.104			0.137	0.112	0.055	0.078
Mcs. aurea KYG[a]	*Beijerinckiaceae*	0.140		0.071	0.094			0.145	0.108	0.059	0.071
								0.074			
Mcl. silvestris BL2	*Beijerinckiaceae*		0.062	0.091	0.147			0.124	0.122		0.067
					0.073						
					0.059						
Mfr. stellata AR4	*Beijerinckiaceae*		0.060	0.074	0.142			0.107	0.146	0.060	0.095
					0.087						
					0.078						
Methylocystis sp. LW5[a]	*Methylocystaceae*	0.122	0.088	0.117	0.132	0.082		0.064	0.143	0.041	0.094
		0.219									
		0.216									
Mct. parvus OBBP[a]	*Methylocystaceae*	0.212		0.126	0.122	0.076		0.113	0.197		0.089
		0.125						0.065			
Methylocystis sp. strain Rockwell[a]	*Methylocystaceae*	0.202		0.101	0.144	0.057		0.058	0.153		0.084
		0.202			0.071			0.141			
Mct. rosea SV97[a]	*Methylocystaceae*	0.222		0.115	0.160			0.134	0.167		0.105
					0.115			0.073			
Methylocystis sp. SB2[a]	*Methylocystaceae*	0.199		0.100	0.144	0.055		0.154	0.155		0.090
								0.065			
Methylocystis sp. SC2	*Methylocystaceae*	0.202		0.100	0.073	0.062		0.112	0.145		0.086
		0.125			0.142			0.057			
		0.203									
Methylosinus sp. LW3[a]	*Methylocystaceae*	0.221	0.089	0.127	0.119	0.078		0.102	0.147	0.044	0.100
		0.124						0.066			
		0.221									
Methylosinus sp. LW4[a]	*Methylocystaceae*	0.216	0.078	0.120	0.135	0.099		0.068	0.175		0.104
		0.123						0.102			
		0.216									
Msn. trichosporium OB3b[a]	*Methylocystaceae*	0.181	0.073	0.113	0.145	0.074		0.069	0.178		0.094
		0.179			0.062						

Table 3.2. Continued.

Strain	Family	*pmoCAB*	*mmo XYBZDC*	*mxaFJGI*	*xoxFJ*	*mbnABCM*	MCA2590 + *mopE/corAB*	*copCD*	*sgaA*	*fdhBA*	*fdsBA*
Candidate phylum NC10											
"*Ca.* Methylomirabilis oxyfera"	-	0.108		0.066	0.086			0.126	0.080	0.053	0.081
					0.099						
Phylum *Verrucomicrobia*											
"*Ca.* Methylacidimicrobium cyclopophantes" 3C[a]	"*Ca.* Methylacidiphilaceae"	0.149			0.081				0.094		0.058
"*Ca.* Methylacidimicrobium" sp. LP2A	"*Ca.* Methylacidiphilaceae"	0.140			0.109				0.130		0.059
		0.136									
"*Ca,* Methylacidiphilum fumariolicum" SolV	"*Ca.* Methylacidiphilaceae"	0.108			0.085				0.116		0.039
		0.095									
		0.087									
"*Ca.* Methylacidiphilum infernorum" V4	"*Ca.* Methylacidiphilaceae"	0.126			0.096				0.104		0.064
		0.101									
		0.238									

[a]contains assembly gaps

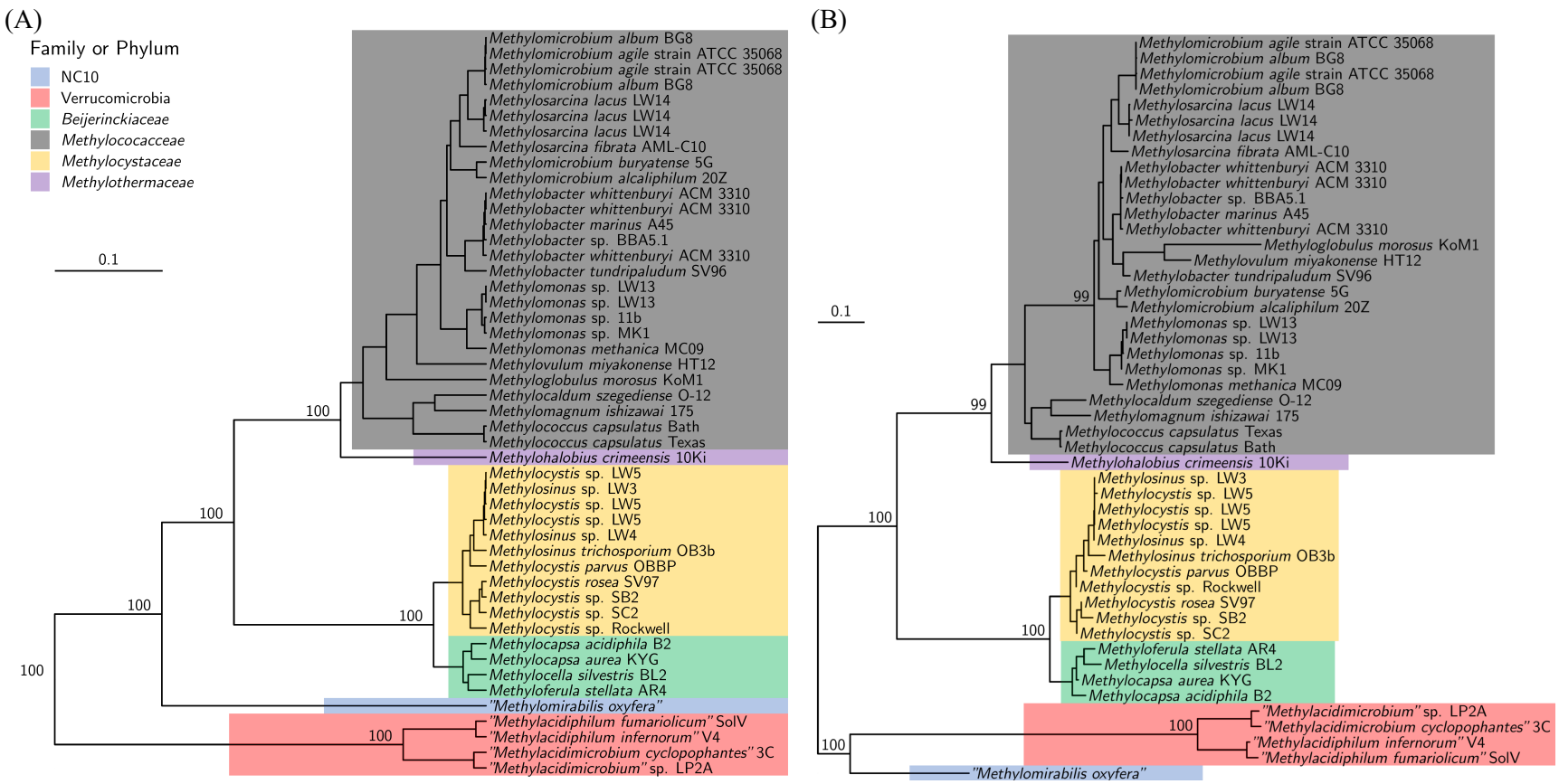

Figure 3.2. Phylogeny based on 16S rRNA gene. (A) Bayesian 16S rRNA gene based phylogeny of aerobic methanotrophs. The tree was constructed using the general time-reversible model with invariant sites and four distinct gamma categories (GTR+I+G) under a strict clock with a minimum nucleotide sequence length of 1132. Node values indicate posterior probabilities based on 10,000,000 iterations with a burn-in of 25%. The scale bar represents 0.1 changes per nucleotide position. (B) Maximum likelihood concatenated 16S rRNA gene based phylogeny of aerobic methanotrophs. The tree was constructed using the general time-reversible model with four categories in a discrete gamma model of site variability and was midpoint rooted (minimum of 1132 nucleotides). Node values are based on 100 bootstrap replicates. The scale bar represents 0.1 changes per nucleotide position.

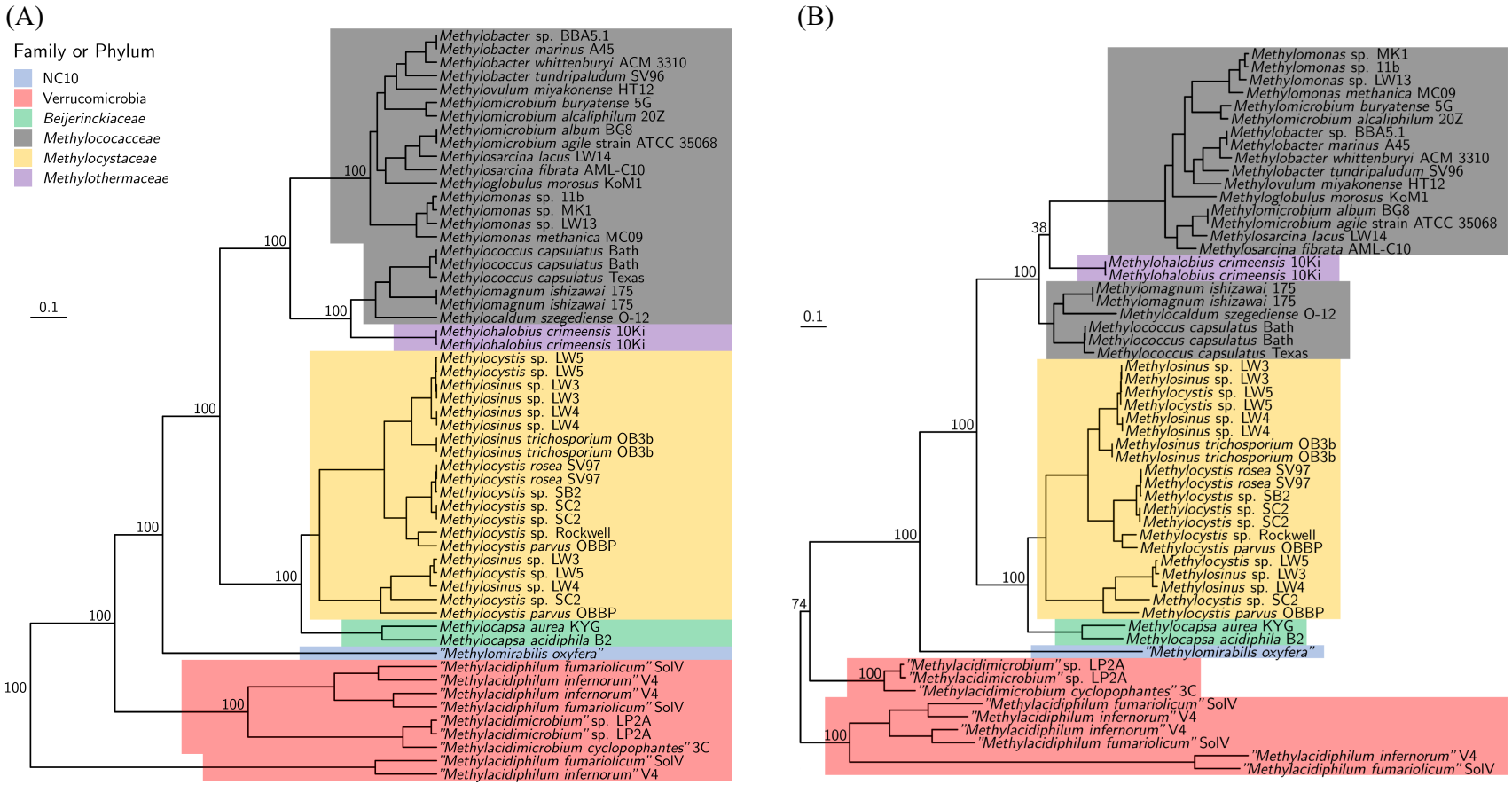

Figure 3.3. Phylogeny based on *pmoCAB*. (A) Bayesian *pmoCAB* based phylogeny of aerobic methanotrophs. The tree was constructed using the general time-reversible model with invariant sites and four distinct gamma categories (GTR+I+G) under a strict clock with a minimum nucleotide sequence length of 2085. Node values indicate posterior probabilities based on 10,000,000 iterations with a burn-in of 25%. The scale bar represents 0.1 changes per nucleotide position. (B) Maximum likelihood concatenated *pmoCAB* based phylogeny of aerobic methanotrophs. The tree was constructed using the general time-reversible model with four categories in a discrete gamma model of site variability and was midpoint rooted (minimum of 2085 nucleotides). Node values are based on 100 bootstrap replicates. The scale bar represents 0.1 changes per nucleotide position.

Evidence for LGT of the *mmo* operon (*mmoXYBZDC*), however, is not as robust as observed for *pmo* genes. That is, D_{KL} values as predicted using Alien Hunter suggest that these genes may have been incorporated into the genomes of the two considered *Beijerinckiaceae* species, as well as some *Methylococcaceae* and *Methylocystaceae* species via LGT (Figure 3.1 and Table 3.1). Many species in *Methylococcaceae*, however, had D_{KL} values for *mmo* genes below the detection threshold of Alien Hunter, unlike what was found for *pmoCAB* in these same microorganisms. D_{KL} values for *mmo* genes as determined using CodonW were low for most methanotrophs, and lower than those for *pmoCAB* in those strains that can express both forms (Table 3.2). It should be noted that relatively few methanotrophs have been found to possess *mmo* genes, limiting our ability to be as thorough in our analyses as can be done for *pmoCAB*. As a result, construction of a phylogenetic tree based on the concatenated *mmoXYBCDZ* sequence provides limited additional information as to the origin of sMMO in methanotrophy (Figure 3.4).

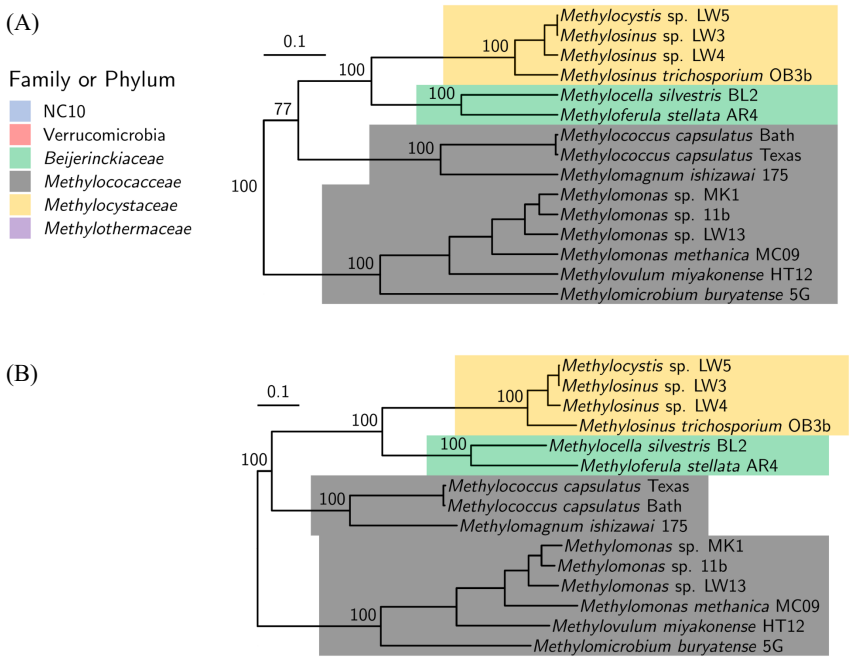

Figure 3.4. Phylogeny based on *mmoXYBZDC*. (A) Bayesian *mmoXYBZDC* based phylogeny of aerobic methanotrophs. The tree was constructed using the general time-reversible model with invariant sites and four distinct gamma categories (GTR+I+G) under a strict clock with a minimum nucleotide sequence length of 4977. Node values indicate posterior probability based on 10,000,000 iterations with a burn-in of 25%. The scale bar represents 0.1 changes per nucleotide position. (B) Maximum likelihood concatenated *mmoXYBZDC* based phylogeny of aerobic methanotrophs. The tree was constructed using the general time-reversible model with four categories in a discrete gamma model of site variability and was midpoint rooted (minimum of 4977 nucleotides). Node values are based on 100 bootstrap replicates. The scale bar represents 0.1 changes per nucleotide position.

3.3. Evidence of LGT of methanol dehydrogenases

Earlier evidence suggested that methanotrophs arose via an ancestral methylotroph procuring MMO genes via LGT (Khadka et al., 2018; Osborne & Haritos, 2018; Tamas et al., 2014). To examine this hypothesis, we calculated the D_{KL} values for operons encoding components of the PQQ-dependent Mxa-MeDH and Xox-MeDH. As shown in Figure 3.1 the composition of genes involved in formation/activity of Mxa-MeDH – *mxaFJGI* – were generally indistinguishable from the host genome for most known families of methanotrophs (it should be noted that Verrucomicrobia methanotrophs lack these genes). Relatively high D_{KL} values were

calculated for this DNA region for members of the *Beijerinckiaceae* using Alien Hunter, i.e., *Methylocapsa* species (Table 3.1), but these were lower than values calculated for *pmoCAB*. A Bayesian phylogenetic tree based on the concatenated *mxaFJGI* sequence (Figure 3.5A) is similar to the 16S rRNA phylogenetic analysis (Figure 3.2A), and comparable results were found for maximum likelihood phylogenies (Figure 3.2B and Figure 3.5B). Collectively these data indicate that in most cases the genes encoding Mxa-MeDH are more ancestral than the genes encoding MMOs, i.e. that they were present in the genomes before the MMO genes were obtained via LGT event(s).

Interestingly, there is evidence that the alternative PQQ-dependent methanol dehydrogenase – Xox-MeDH – that contains a rare earth element may have been incorporated into methanotrophic genomes via LGT. First, genes with high levels of duplication are often indicative of LGT (Wellner et al., 2007), and multiple operons of *xox* genes (as well as *pmo* genes) are commonly found in methanotrophs. *mxa* genes, however, do not exist in multiple operons for any examined methanotroph (Table 1.2, pg. 19). Second, high D_{KL} values were calculated for some copies of *xoxFJ* in several methanotrophs using both Alien Hunter and CodonW, and these were higher than those calculated for *mxaFJGI* (Figure 3.1, Table 3.1 and Table 3.2). Third, copies of *xoxFJ* in many different methanotrophs are placed differently in Bayesian and maximum likelihood trees based on *xoxFJ* as compared to 16S rRNA phylogeny, e.g., *Methylobacter* and *Methylocystis* species, Verrucomicrobia methanotrophs, as well as *Methyloferula stellata, Methylosinus trichosporium* OB3b, and *"Ca.* Methylomirabilis oxyfera*"* (Figure 3.2 and Figure 3.6).

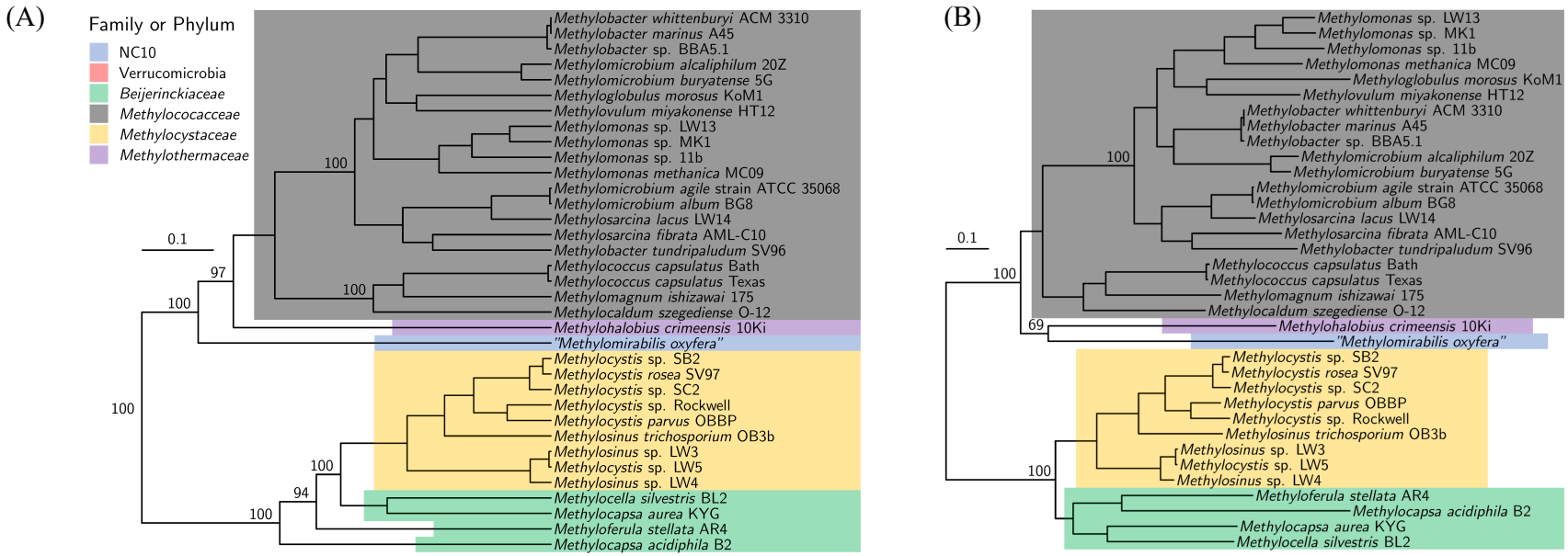

Figure 3.5. Phylogeny based on *mxaFJGI*. (A) Bayesian *mxaFJGI* based phylogeny of aerobic methanotrophs. The tree was constructed using the general time-reversible model with invariant sites and four distinct gamma categories (GTR+I+G) under a strict clock with a minimum nucleotide sequence length of 3144. Node values indicate posterior probabilities based on 10,000,000 iterations with a burn-in of 25%. The scale bar represents 0.1 changes per nucleotide position. (B) Maximum likelihood concatenated *mxaFJGI* based phylogeny of aerobic methanotrophs. The tree was constructed using the general time-reversible model with four categories in a discrete gamma model of site variability and was midpoint rooted (minimum of 3144 nucleotides). Node values are based on 100 bootstrap replicates. The scale bar represents 0.1 changes per nucleotide position.

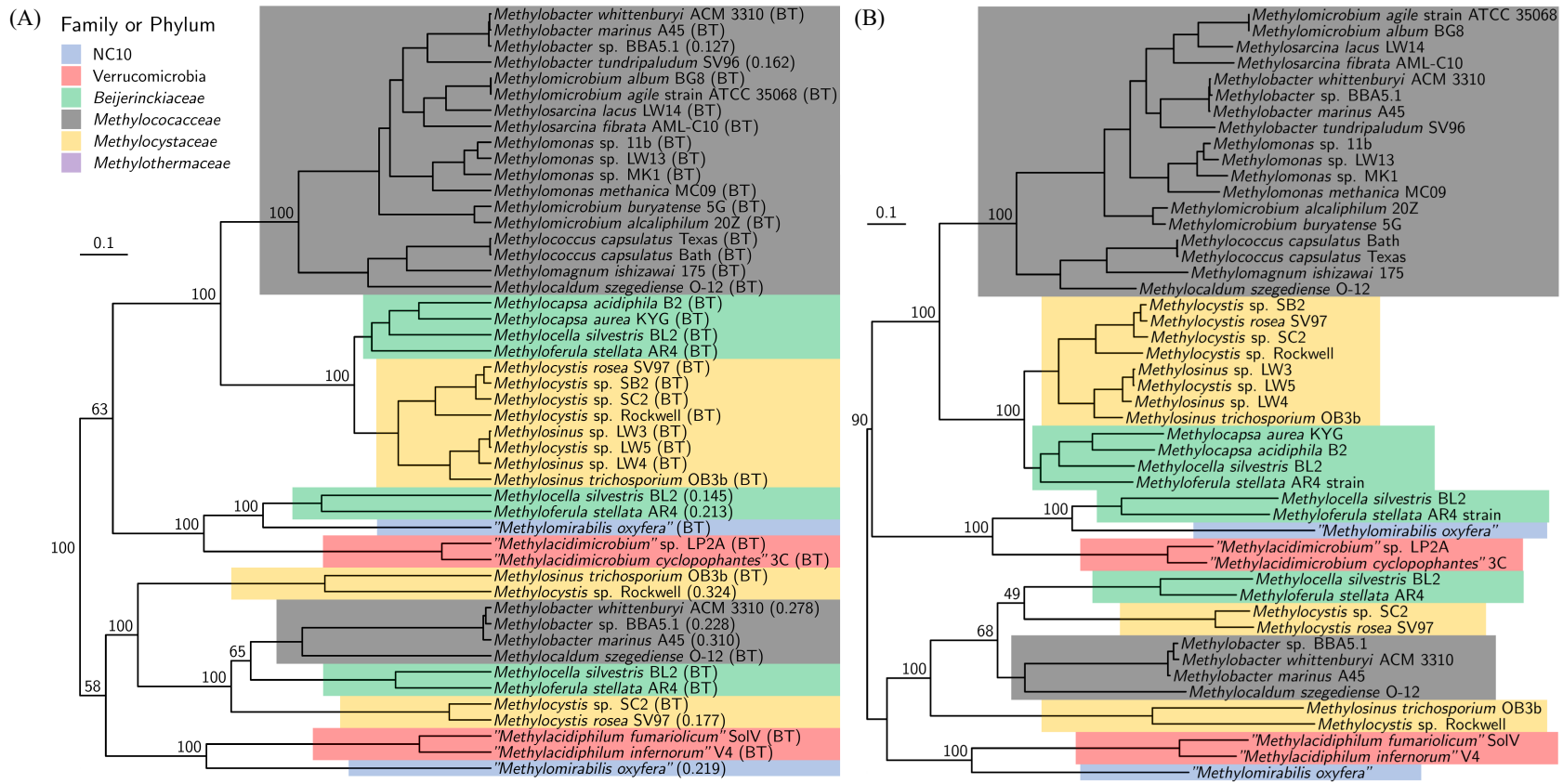

Figure 3.6. Phylogeny based on *xoxFJ*. (A) Bayesian *xoxFJ* based phylogeny of aerobic methanotrophs. The tree was constructed using the general time-reversible model with invariant sites and four distinct gamma categories (GTR+I+G) under a strict clock with a minimum nucleotide sequence length of 2604. Node values indicate posterior probabilities based on 10,000,000 iterations with a burn-in of 25%. The scale bar represents changes per nucleotide position. Alien Hunter D_{KL} values are provided in parentheses. BT indicates below threshold. (B) Maximum likelihood concatenated *xoxFJ* based phylogeny of aerobic methanotrophs. The tree was constructed using the general time-reversible model with four categories in a discrete gamma model of site variability and was midpoint rooted (minimum of 2604 nucleotides). Node values are based on 100 bootstrap replicates. The scale bar represents 0.1 changes per nucleotide position.

Despite evidence for LGT of some *xox* genes, the data suggest that genes encoding Xox-MeDH in methanotrophic genomes were present before the acquisition of MMO. First, the D_{KL} values for *xoxFJ* in many species were (as found for *mxaFJGI*) below the detection threshold of Alien Hunter, and CodonW agreed with these results (Table 3.1 and Table 3.2). Second, although divergence is evident when comparing phylogenetic trees based on 16S rRNA and *xoxFJ*, there are also some intriguing similarities. That is, the phylogenetic grouping of *xoxFJ* for the *Methylococcaceae*, *Methylocystaceae* and *Beijerinckiaceae* at the top of Figure 3.6A is similar to that observed in 16S rRNA phylogeny (Figure 3.2A) and almost all (28/30) of these *xoxFJ* sequences had D_{KL} values below the threshold of Alien Hunter (as noted in Figure 3.6A). The other groupings at the bottom of Figure 3.6A appear to have been influenced by several LGT events, and many of these copies exhibit significant D_{KL} values (based on Alien Hunter). Thus, it appears that both forms of MeDH were ancestral, but some genes for Xox-MeDH were subsequently laterally transferred across multiple species.

3.4. Evidence of LGT of additional genes involved in carbon oxidation and assimilation

Previously, phylogenetic analyses focusing on *Alphaproteobacteria* methanotrophs indicated that genes involved in carbon oxidation and assimilation were vertically inherited in these microbes (Tamas et al., 2014). We extended these analyses to examine the compositional divergence and phylogenetic relationships of *sga* (encoding serine-glyoxylate aminotransaminase), *fdh* and *fds* (encoding the tungsten and molybdenum dependent forms of formate dehydrogenase, respectively) for other phylogenetic groups of methanotrophs. As shown in Figure 3.1, Table 3.1, and Table 3.2, little sequence divergence of these genes was calculated using either Alien Hunter or CodonW for any family/phylum of methanotrophs. Further, phylogenetic trees based on these sequences (Figure 3.7 and Figure 3.9) were similar to 16S rRNA phylogenetic analysis (Figure 3.2). Such data indicate that not only were multiple forms of MeDH likely vertically inherited, so were other aspects of C_1 metabolism, i.e., methanotrophs likely arose from methylotrophs.

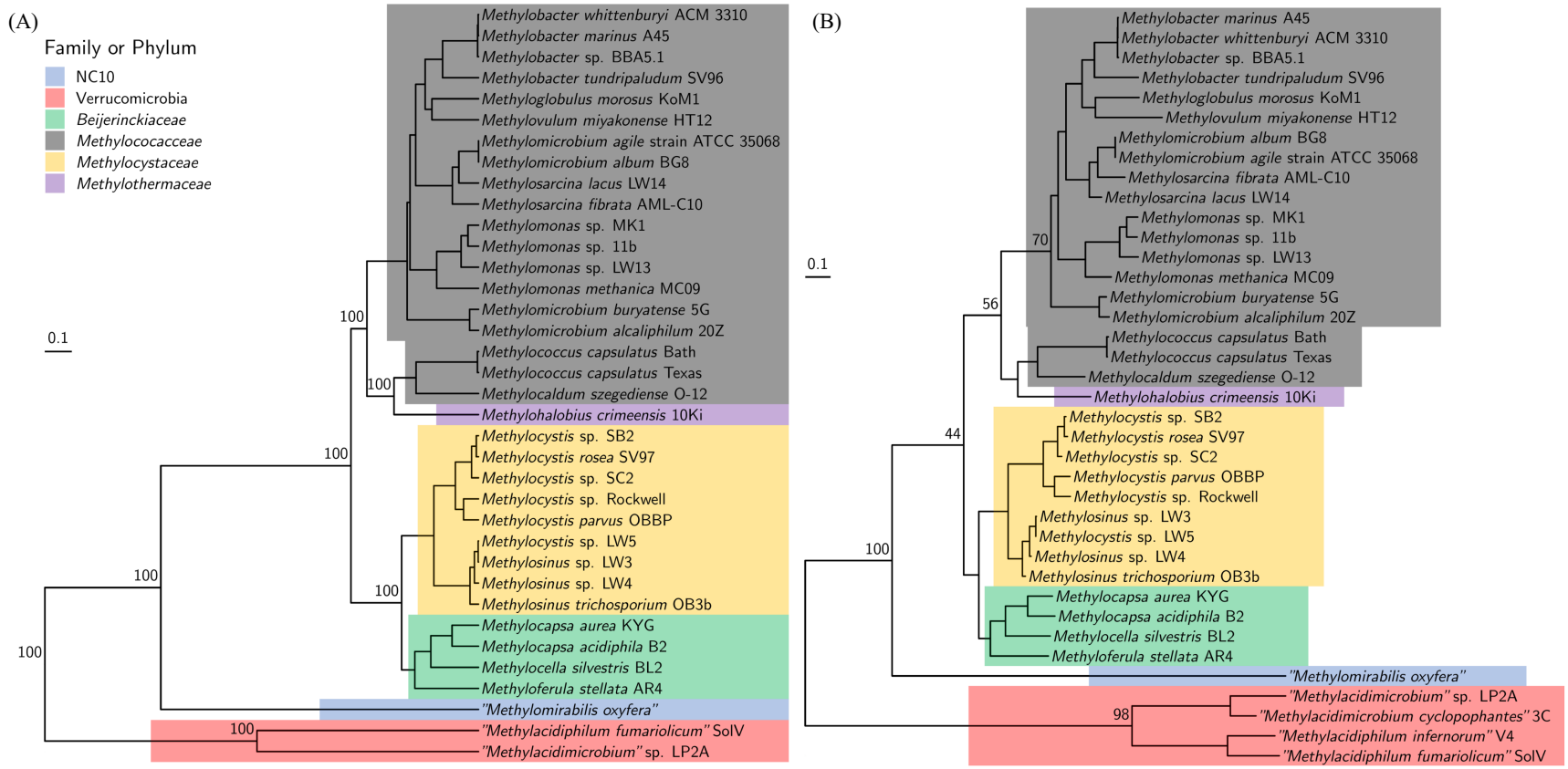

Figure 3.7. Phylogeny based on *sgaA*. (A) Bayesian *sgaA* based phylogeny of aerobic methanotrophs. The tree was constructed using the general time-reversible model with invariant sites and four distinct gamma categories (GTR+I+G) under a strict clock with a minimum nucleotide sequence length of 1005. Node values indicate posterior probabilities based on 10,000,000 iterations with a burn-in of 25%. The scale bar represents 0.1 changes per nucleotide position. (B) Maximum likelihood *sgaA* based phylogeny of aerobic methanotrophs. The tree was constructed using the general time-reversible model with four categories in a discrete gamma model of site variability and was midpoint rooted (minimum of 1005 nucleotides). Node values are based on 100 bootstrap replicates. The scale bar represents 0.1 changes per nucleotide position.

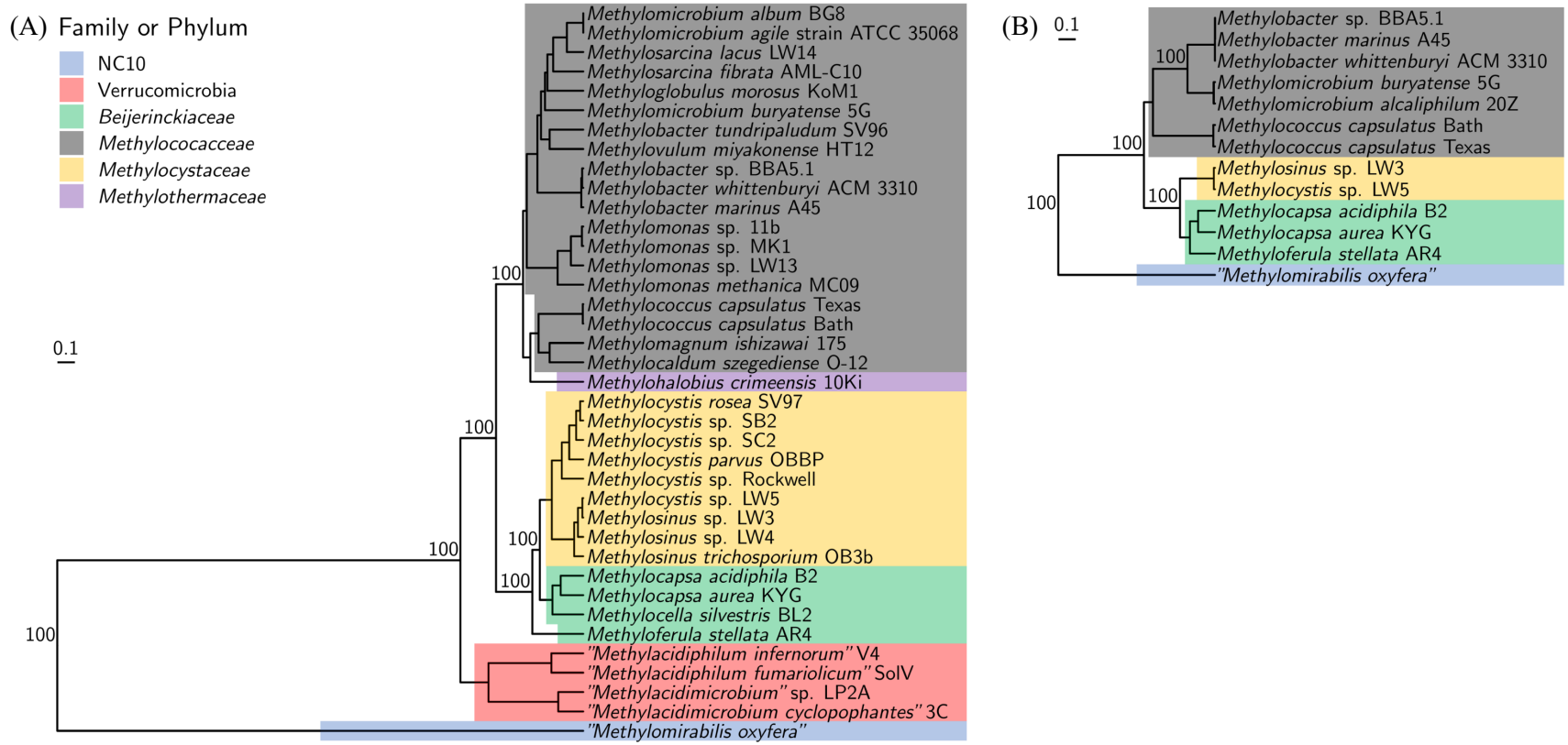

Figure 3.8. Bayesian concatenated (A) *fdsBA* and (B) *fdhBA* based phylogenies of aerobic methanotrophs. The trees were constructed using the general time-reversible model with invariant sites and four distinct gamma categories (GTR+I+G) under a strict clock with a minimum nucleotide sequence length of 4092. Node values indicate posterior probabilities based on 10,000,000 iterations with a burn-in of 25%. The scale bars are identical and represent 0.1 changes per nucleotide position.

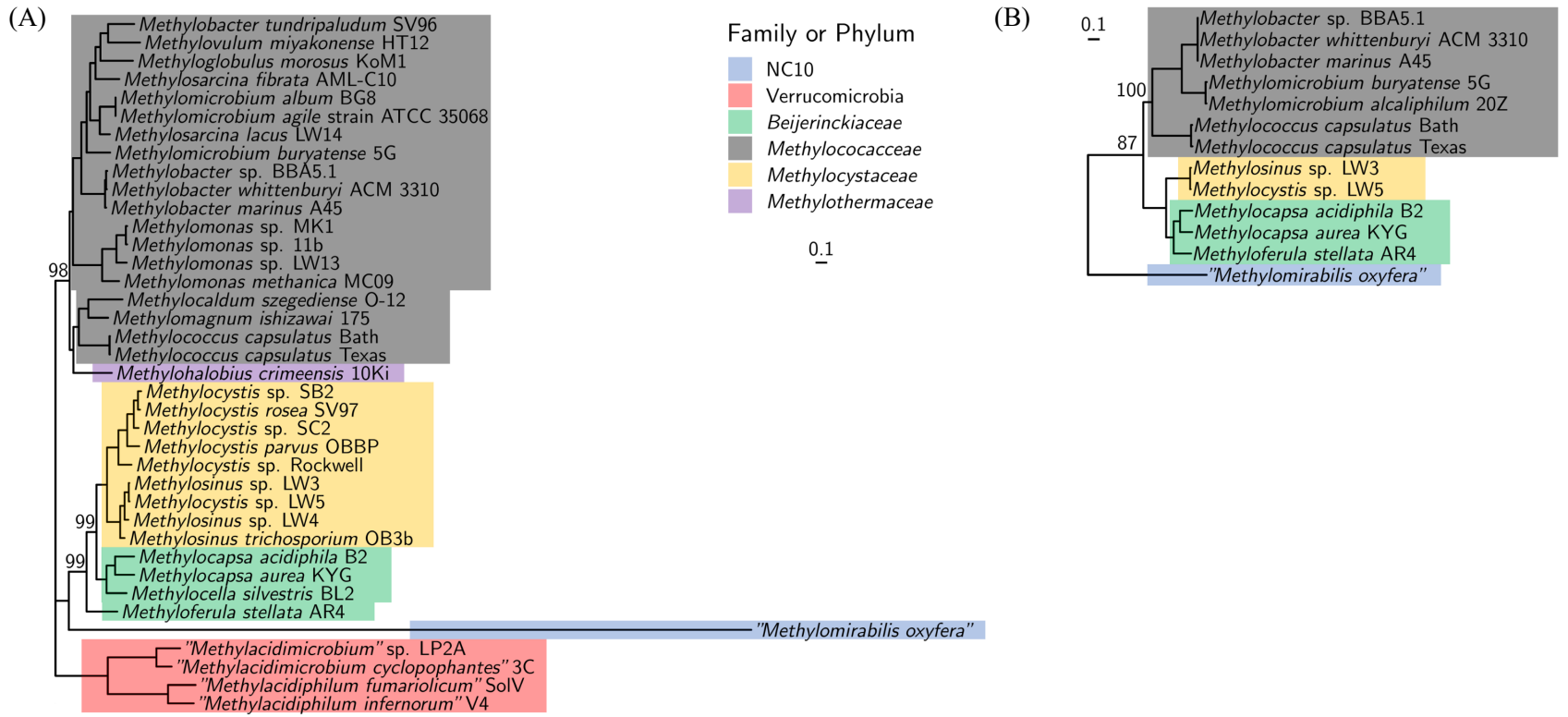

Figure 3.9. Maximum likelihood concatenated (A) *fdsBA* and (B) *fdhBA* based phylogenies of aerobic methanotrophs. The trees were constructed using the general time-reversible model with four categories in a discrete gamma model of site variability and was rooted at the Verrucomicrobia node or midpoint, respectively (minimum of 4092 nucleotides). Node values are based on 100 bootstrap replicates. The scale bars are identical and represent 0.1 changes per nucleotide position.

3.5. Origin of copper uptake systems in methanotrophs

The existence of copper uptake systems in methanotrophs was screened by conducting BLAST searches for genes encoding the copper-binding peptides MB, MopE, CorA, and CopCD (Table 1.2, pg. 19). Genes encoding for MB (*mbnABCM*) were observed only in methanotrophs from the *Methylocystaceae*, while MopE and CorA (both with their surface associated cytochrome *c* peroxidases) were found only in methanotrophs affiliated with *Methylococcaceae*. Evidence of CopCD was found in most methanotrophs, with Verrucomicrobia methanotrophs being the only exception. Very little compositional divergence for *mopE* and its surface associated cytochrome c peroxidase were found, nor for *corA* and its surface associated cytochrome *c* peroxidase (Figure 3.1). These data suggest these genes did not arise from a recent LGT, and were present prior to the acquisition of MMO. MB genes, however, showed a greater range of D_{KL} values, with some methanotrophs having D_{KL} values below the threshold of Alien Hunter indicating an LGT being unlikely, while others had values greater than 0.2, suggestive of an LGT. Finally, compositional divergence of *copCD* indicated that this copper uptake system was not the result of an LGT event for most methanotrophs. For those methanotrophs with multiple copies of *copCD* (of the *Methylocystaceae* and *Beijerinckiaceae* families), although Alien Hunter typically calculated divergence values below threshold for both copies, CodonW indicated that one copy had D_{KL} values two-three times greater than the other. These data suggest that the second copy of *copCD* in these species may have arisen as a result of LGT, and Bayesian and Maximum likelihood phylogenetic trees based on *copCD* (Figure 3.10) support this finding.

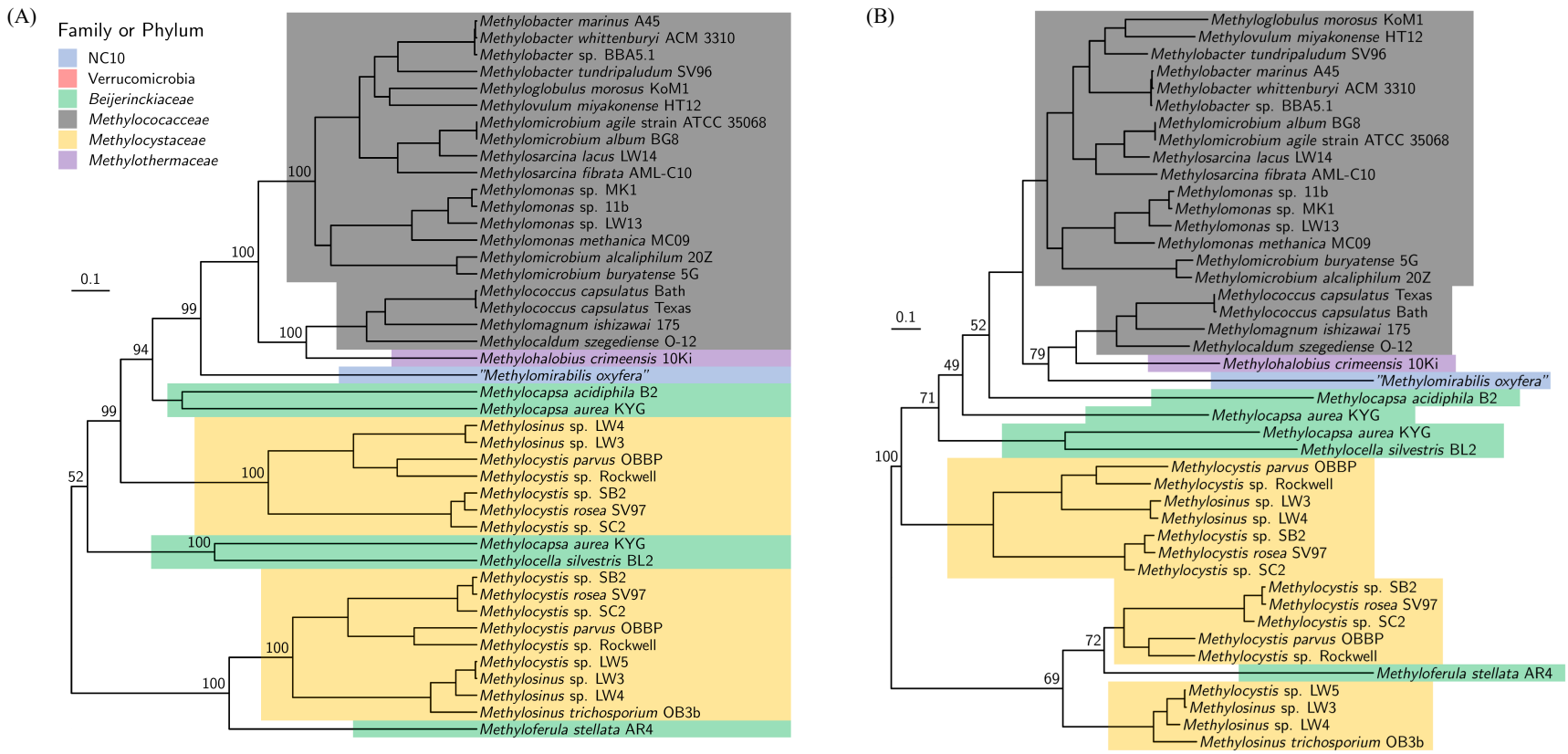

Figure 3.10. Phylogeny based on *copCD*. (A) Bayesian *copCD* based phylogeny of aerobic methanotrophs. The tree was constructed using the general time-reversible model with invariant sites and four distinct gamma categories (GTR+I+G) under a strict clock with a minimum nucleotide sequence length of 1351. Node values indicate posterior probabilities based on 10,000,000 iterations with a burn-in of 25%. The scale bar represents changes per nucleotide position. (B) Maximum likelihood concatenated *copCD* based phylogeny of aerobic methanotrophs. The tree was constructed using the general time-reversible model with four categories in a discrete gamma model of site variability and was midpoint rooted (minimum of 1351 nucleotides). Node values are based on 100 bootstrap replicates. The scale bar represents 0.1 changes per nucleotide position.

3.6. Diversity of methanobactin

Although much has been learned about MB, there are still many more questions than answers. Thus, great opportunity exists for further research to elucidate the pathway(s) of MB biosynthesis as well as the diversity of MB made my methanotrophs. Indeed, a phylogenetic tree based on concatenated *mbnABCM* sequences (Figure 3.11A; note that methanotrophs with structurally characterized MBs are identified with a *) not only support the original division of MBs into two general groups, but also suggests these may be further divided into multiple subgroups.

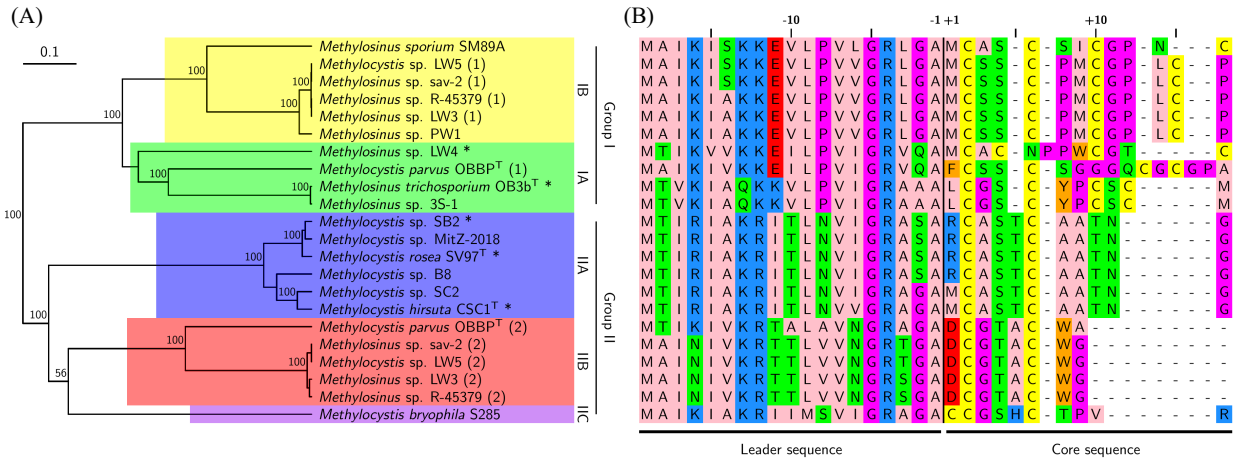

Figure 3.11. Phylogeny of *mbnABCM* and MbnA sequence alignment. (A) Bayesian *mbnABCM*-based phylogeny. The tree was constructed using the general time-reversible model with invariant sites and four distinct gamma categories (GTR + I + G) under a strict clock with a minimum nucleotide sequence length of 2715. Node values indicate posterior probabilities based on 10,000,000 iterations with a burn-in of 25%. The scale bar represents changes per nucleotide position. (B) Predicted amino acid sequence of MbnA from corresponding methanotrophs. Note that MbnA has both a leader sequence (not observed in characterized MBs) and a core sequence (found in characterized MBs denoted by *).

Within Group I MBs, based on *mbnABCM* sequence comparison, there appear to be two subpopulations – Group IA and IB. Group IA MBs include that from *Msn. trichosporium* OB3b and *Methylosinus* sp. LW4 that have been structurally characterized. One MB gene cluster in *Mct. parvus* OBBP and that from *Methylosinus* sp. 3S-1 are also included in this subgroup.

Group IB MBs include several from a number of methanotrophs with multiple gene clusters (i.e., various *Methylosinus* and *Methylocystis* species), as well as the *mbn* genes of *Msn. sporium* SM89A. MB of *Msn. sporium* SM89A is more distantly related in comparison with the relatively tight clustering of the rest of the group and may possibly encode for a different form of MB. It would be worthwhile to determine if these methanotrophs (particularly *Msn. sporium* SM89A) produce MBs, and if so, how structurally similar they are to known MBs. It is important to note that a partial *mbnA* gene sequence is available for *Msn. sporium* NR3K (Baslé et al., 2018). When comparing the predicted MbnA sequence o*f Msn. sporium* NR3K to that of *Msn. sporium* SM89A, there is remarkable similarity (only the first amino acid of the core peptide is different; LCASCSICGPNC vs MCASCSICGPNC, respectively). This suggests that different *Msn. sporium* strains may make near-identical MBs.

On the other hand, there are three general subgroups within the Group II MBs based on *mbnABCM* sequence comparison. The only identified Group II MBs are from Group IIA, i.e., various *Methylocystis* species that have significant gene synteny, phylogeny and MbnA sequences (Figure 1.20, pg. 57 and Figure 3.11). One can postulate the presence of an additional subgroup (Group IIB) but MB has not been purified/characterized from any methanotrophs in this group, although it appears that both *Methylocystis* and *Methylosinus* species may produce MBs of this type. The possibility that these strains may produce a novel form of MB is supported by the fact these *mbn* gene clusters lack *mbnS*, putatively encoding for a sulfotransferase (Figure 1.20, pg. 57). It is also interesting to note that those putative Group II MB gene clusters lacking *mbnS* appear to have the C-terminal ring of MB formed from either an Alanine-Cysteine or Histidine-Cysteine dipeptide (Figure 3.11B) rather than Threonine-Cysteine as found in Group IIA MBs. The predicted core polypeptide sequence of *mbnA* from these

clusters includes a threonine elsewhere, but apparently these are not sulfonated, possibly because they are not involved in ring formation. MB has not been isolated/characterized from any of these methanotrophs, and so it is unknown if these threonines are sulfonated or not, but if so, it would seem that a sulfotransferase encoded elsewhere in the genome is responsible. This appears unlikely, however, as no evidence of any gene with significant similarity to *mbnS* from *Methylocystis* sp. SB2 was found in the genomes of methanotrophs putatively making IIB MBs. One should keep in mind, however, that a novel sulfotransferase may be present in these genomes as a large fraction of any genome encodes for genes of unknown function.

Finally, bioinformatic interrogation of available methanotroph genomes suggest that *Methylocystis bryophila* S285 (Group IIC) may make a novel form of MB (Figure 3.11A). The predicted core peptide of this putative MB has significant differences as compared to other MBs (Figure 3.11B), e.g., other MBs are predicted to either have two or four cysteines in the core peptide (Group II and I MBs, respectively), but MB from *Mct. bryophila* S285 appears to have three. This methanotroph, isolated from a sphagnum peat bog with a pH of 4.2 (Belova et al., 2013; Han et al., 2018), may make a modified acid-stable form of MB as other forms of MB are easily digested in dilute acid solutions, especially the oxazolone rings of *Msn. trichosporium* OB3b and *Methylocystis* sp. SB2 MBs. We hasten to stress this is highly speculative, however, and provide these comments in the interest of stimulating further discussion and research into MB.

3.7. Lanmodulin in methanotrophs

The occurrence of LanM and LanM-like protein in different microorganisms was searched via protein BLAST using three major criteria, (1) contains four EF hands, (2) have 11~13 residues between each EF hand, and (3) the protein is less than 200 residues long. A total of 266 possible proteins were identified, of which only one was *Gammaproteobacteria* (*Moraxellaceae* family) and the rest *Alphaproteobacteria* (Figure 3.12). Of the 265 *Alphaproteobacteria*, 113 were nonmethanotrophic methylotrophs (7 *Acetobacteraceae*, 1 *Bradyrhizobiaceae*, 9 *Hyphomicrobiaceae*, 94 *Methylobacteriaceae*, 2 *Xanthobacteraceae*) and 28 methanotrophs (10 *Beijerinckiaceae*, 17 *Methylocystaceae*, 1 unclassified Rhizobiales). From this list of LanM-like proteins, a more stringent screen was applied, where only those with four EF hands with the motif BPDXDXXXDXXE were selected to identify LanMs that are more similar to that found in *Mrr. extorquens* AM1. 36 such proteins were found, and the majority occurred in *Methylobacteriaceae*, followed by *Hyphomicrobiaceae* family (Figure 3.13). It is interesting to note that both families are nonmethanotrophic methylotrophs, and no methanotrophs were found to have this superior LanM.

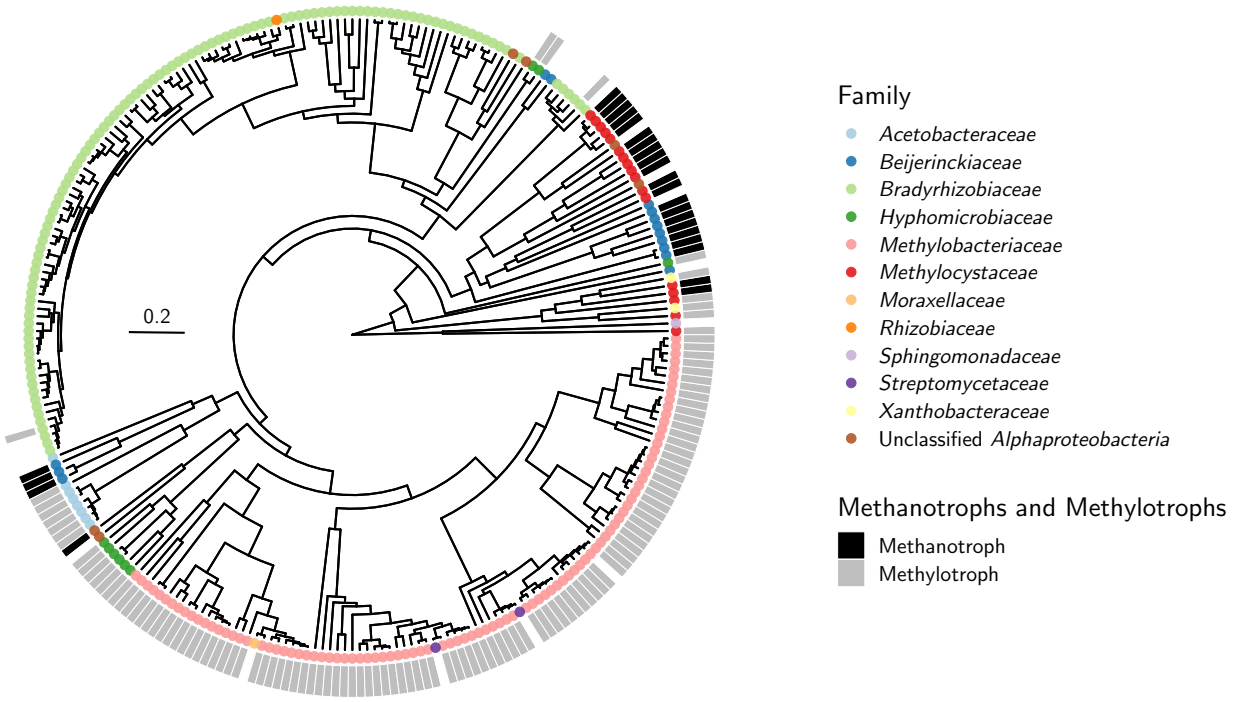

Figure 3.12. Bayesian phylogeny based on LanM and LanM-like proteins. The tree was constructed using the general time-reversible model with invariant sites and four distinct gamma categories (GTR+I+G) under a strict clock with a minimum amino acid sequence length of 101. Node values indicate posterior probabilities based on 10,000,000 iterations with a burn-in of 25%. The scale bar represents 0.2 changes per amino acid position.

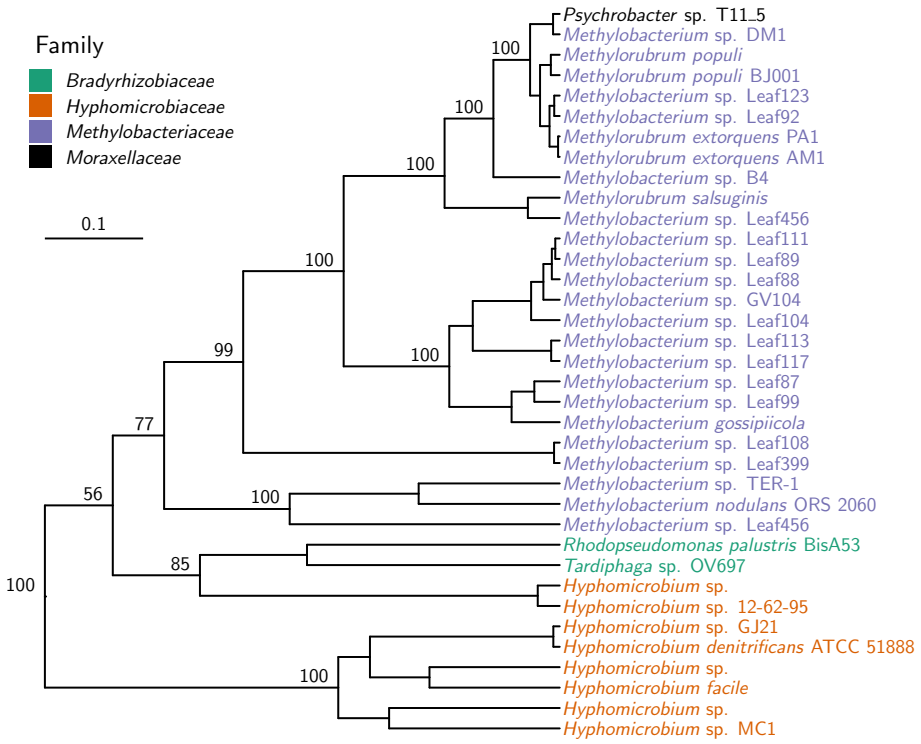

Figure 3.13. Bayesian LanM based phylogeny. The tree was constructed using the general time-reversible model with invariant sites and four distinct gamma categories (GTR+I+G) under a strict clock with a minimum amino acid sequence length of 103. Node values indicate posterior probabilities based on 10,000,000 iterations with a burn-in of 25%. The scale bar represents 0.1 changes per amino acid position.

In fact, in methanotrophs, the proline residue in the second position of EF hands, identified as a key characteristic responsible for enhanced selectivity for REE over Ca^{2+} (Cotruvo et al., 2018), is highly conserved only in the third EF hand (Figure 1.22, pg. 63, and Figure 3.14). In addition, instead of an aspartate residue in the ninth position, the third EF hands include threonine or serine residue at this position. These observations collectively suggest that the proline residue in the third EF hand is essential for binding REEs in methanotrophs. The deviation from the model LanM found in *M. extorquens* AM1 and other nonmethanotrophic methylotrophs may suggest that the sensitivity to sense and/or bind REEs via LanM in methanotrophs is weaker compared to nonmethanotrophic methylotrophs. Moreover, *lanM* is

only found in *Alphaproteobacteria* and have a relatively low nucleotide compositional bias with respect to methanotroph genomes (BT, 0.0301 ~ 0.0486), suggesting vertical inheritance of this gene.

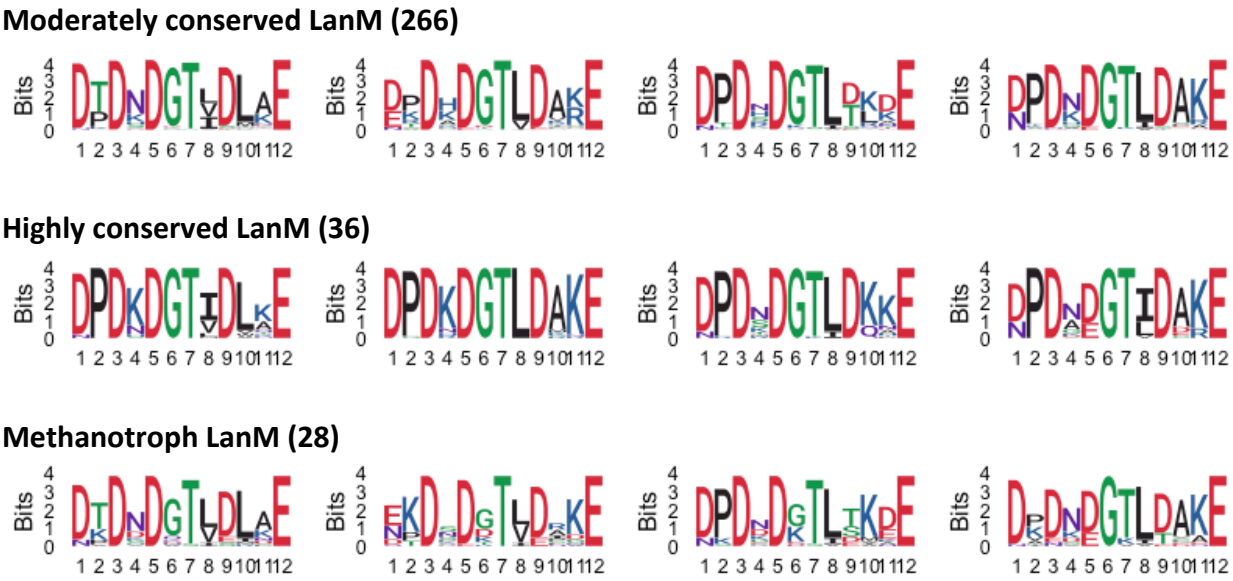

Figure 3.14. Sequence logos of EF hands in LanM, number of proteins aligned is provided in parentheses.

Another important fact to note is the gene synteny found proximate to *lanM* in methanotrophs and nonmethanotrophic methylotrophs. There are genes encoding for a TonB-dependent receptor and ABC transporter upstream of *lanM* in *Mrr. extorquens* AM1 (Figure 3.15). These genes are also found in most *Methylocystis* species, except the ABC transporter genes are found downstream of *lanM*, and in their place, genes for a two-component regulatory system consisting of histidine kinase and LuxR type regulator are found. Interestingly, the gene for TonB-dependent receptor is not found near *lanM* in *Methylosinus* species. It has been shown that this TonB-dependent receptor is crucial for REE uptake in *Mrr. extorquens* PA1 and AM1 (Ochsner et al., 2019; Roszczenko-Jasińska et al., 2020), so it is likely that the gene is encoded elsewhere on the chromosome of *Methylosinus* species containing *lanM*. Upstream of *lanM* in *Beijerinckiaceae* methanotrophs are genes encoding for components of TonB-dependent transporter (i.e., receptor, TonB, and ExbBD), and downstream those encoding for a lone histidine kinase and transaldolase. Genes for ABC transporter are not found near any of the *lanM* here.

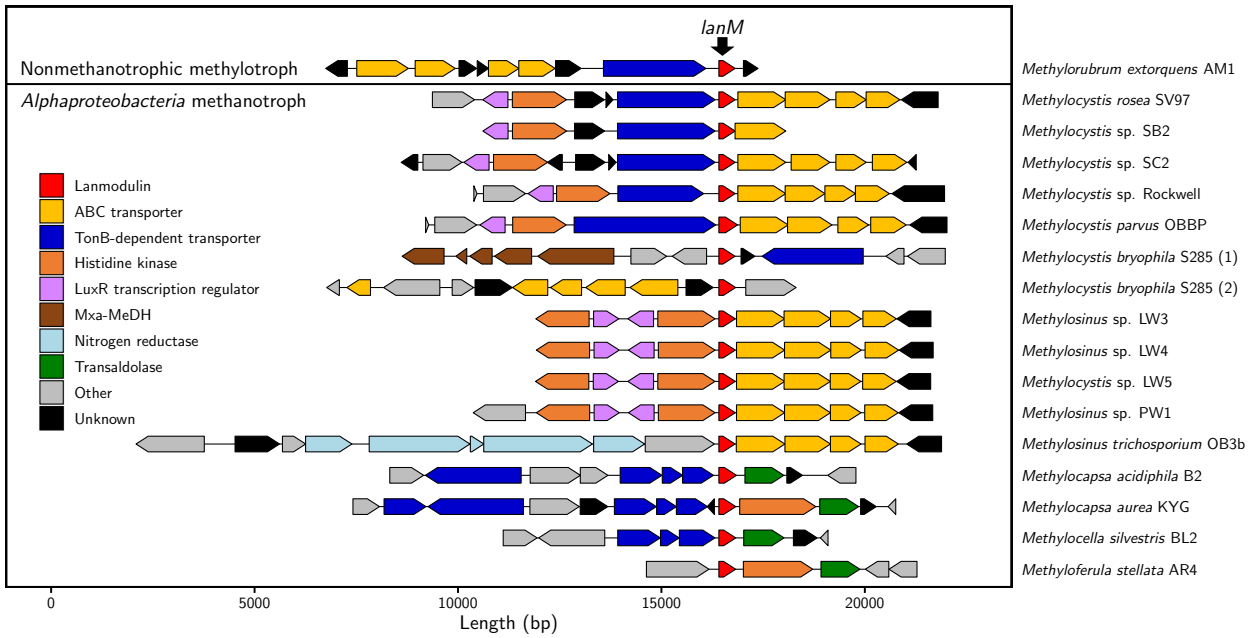

Figure 3.15. Lanmodulin gene and related regulatory and transporter genes from methanotrophs with available genome sequences.

3.8. Discussion

It has been speculated, based on the complexity hypothesis (Jain et al., 1999), that methanotrophy arose from LGT of MMO-encoding genes to methylotrophs (Tamas et al., 2014). If true, one would expect to find greater compositional divergence of MMO-encoding genes than of genes involved in further carbon oxidation or carbon assimilation. Indeed, all tested genes for methanol dehydrogenase, formate dehydrogenase and serine-glyoxylate aminotransaminase had low D_{KL} values as well as predicted phylogenies similar to that based on 16s rRNA sequence, suggesting that these genes were indeed present in the respective genomes before LGT acquisition of MMO.

Compositional and phylogenetic analyses of genes encoding Xox-MeDH indicate that this form, although likely ancestral, was more easily shared via LGT. That is, for those

methanotrophs with multiple copies of *xoxFJ*, often one copy had a nucleotide composition indistinguishable from the host genome, while a duplicate copy was appreciably different (Figure 3.1, Table 3.1 and Table 3.2). At this level of analysis, we cannot state with any certainty why one form of MeDH may be more amenable to LGT than another. One possibility may be that as rare earth elements are strong Lewis acids (Lim & Franklin, 2004), MeDH with rare earth elements are catalytically superior to calcium-containing MeDH (Keltjens et al., 2014). As a result, competition pressure may promote the acquisition of *xox* genes via LGT. Interestingly, it has been shown that methanotrophs expressing Xox-MeDH do not excrete methanol, but do when expressing Mxa-MeDH (Krause et al., 2017a). Thus acquisition/expression of Xox-MeDH may provide methanotrophs with a competitive growth advantage by limiting the loss of methanol.

In relation to Xox-MeDH and its REE requirement, the gene encoding for lanmodulin was only found in microbes belonging to *Alphaproteobacteria*, with the exception of one of *Gammaproteobacteria*. Interestingly, this finding indicates that *Gammaproteobacteria* methanotrophs with *xoxFJ* all lack *lanM*, suggesting *lanM* is not crucial for REE uptake/sensing or Xox-MeDH activity, or takes on a secondary role. Indeed, deletion of *lanM* in *Mrr. extorquens* did not cause adverse effects on growth on methanol (Ochsner et al., 2019; Roszczenko-Jasińska et al., 2020). Thus, the role of *lanM* in methylotrophy is still unclear. In addition, the *lanM* found in *Alphaproteobacteria* methanotrophs contains EF hands lacking residues crucial for enhanced selectivity and affinity of LanM, though its REE binding efficiency would still likely be better than that of calmodulins (Cotruvo et al., 2018). Perhaps LanM is a periplasmic partner to an extracellular REE-binding molecule, or lanthanophore, to assist REE release and/or transport to other parts of the cell. This is greatly hypothetical, but future

investigation will help elucidate the role of LanM in REE uptake and regulation in methanotrophs.

The evidence that some methanotrophs have evolved via LGT of pMMO-encoding genes (and possibly sMMO-encoding genes) to methylotrophs raises the intriguing question of why aerobic methanotrophs have limited phylogenetic diversity, being largely restricted to the *Alpha*- and *Gammaproteobacteria*. That is, aerobic methylotrophs have been found in the *Alpha*-, *Beta*-, and *Gammaproteobacteria* as well as in the Actinobacteria, Firmicutes, and in some eukaryotes (Kolb, 2009). Why then are there no identified methanotrophs in these additional classes/phyla/domain? This question cannot be unequivocally answered at this time, but it may be that such metabolisms exist in these phylogenetic groups, but have yet to be discovered.

Alternatively, it may be that the ability of a methylotroph to become a methanotroph requires more than LGT of MMO genes. Specifically, it is well-known that copper strongly affects the expression and activity of both sMMO and pMMO (Green et al., 1985; Leak & Dalton, 1986b; Prior & Dalton, 1985; Semrau et al., 2010, 2013, 2018), suggesting that conversion from a methylotrophic to a methanotrophic lifestyle not only requires incorporation of MMO genes, but also the means to sense, collect, and respond to copper. If this were true, one would expect that copper likely played a key role in the physiology of the methanotrophic ancestor. In such a case, genes other than those involved in methane oxidation would be expected to be regulated by copper in methanotrophs. Indeed, it has been shown that varying copper not only affects expression of genes encoding polypeptides of sMMO and pMMO in *Msn. trichosporium* OB3b, but also *mxaF* (encoding the large subunit of Mxa-MeDH) and genes involved in cell synthesis and transcriptional regulation (Farhan Ul Haque et al., 2015a, 2017; Gu & Semrau, 2017). Further, copper affects the formation of intracytoplasmic membranes in

Mcc. capsulatus Bath (Choi et al., 2003), as well as the expression of genes involved in energy metabolism, cell synthesis, transcriptional regulation, and electron transport (Larsen & Karlsen, 2016).

If copper uptake were required for the evolution of methanotrophy from methylotrophy, it is reasonable then to expect that all known aerobic methanotrophs would have identified copper uptake systems. Methanotrophs have been shown to have multiple mechanisms for copper uptake, i.e., MB (found in the *Methylocystaceae*), MopE/CorA (found in the *Methylococcaceae*) and CopCD (found in the *Methylocystaceae*, *Methylococcaceae*, *Methylothermaceae, Beijerinckiaceae* and NC10). If one assumes that the ability to collect copper is a requirement for the evolution of methanotrophy from methylotrophy, then it is reasonable to expect that these genes would either be predicted to be part of the ancestral genome or have been incorporated into methanotrophic genomes in the same time frame as MMO genes. Of these copper uptake systems, *copCD* was present in all but the Verrucomicrobia methanotrophs, and at least one copy of *copCD* in each methanotroph examined had low divergence values. Genes encoding for MopE/CorA also had low D_{KL} values, suggesting that this copper uptake system was present in the genome of the ancestor of *Methylococcaceae* methanotrophs prior to LGT of MMO. On the other hand, MB appears to be ancestral for some methanotrophs of the α-Proteobacteria, and a product of LGT for others. What is also notable is that representative methylotrophs do not have genes for MB, MopE or CorA, although some appear to have *copCD* (Table 3.3). Collectively the presence of multiple copper uptake systems in methanotrophs juxtaposed with the absence of copper-uptake systems in many methylotrophs provides circumstantial evidence that the evolution of methanotrophy from methylotrophy not only required LGT of MMO genes, but also the means to sequester copper.

Table 3.3. Presence of select genes in the genomes of methylotrophs.

Class or Phylum	Strain	*mbnBC*	*mopE/ corA*	*copCD*	*lanM*
Actinobacteria	*Amycolatopsis methanolica* 239 AQUL.1	No	No	Yes	No
Alphaproteobacteria	*Azorhizobium caulinodans* ORS 571 NC_009937.1	No	No	No	No
	Bradyrhizobium diazoefficiens USDA 110 NZ_CP011360.1	No	No	Yes	Yes
	Hyphomicrobium denitrificans 1NES1 NC_021172.1	No	No	No	No
	Hyphomicrobium nitrativorans NL23 NC_022997.1	No	No	No	
	Methylobacterium extorquens AM1 META1.1	No	No	No	Yes
	Methylobacterium nodulans ORS 2060 NC_011894.1	No	No	Yes	Yes
	Methylopila sp. M107 NZ_ARWB.1	No	No	Yes	No
	Paracoccus pantotrophus KS1 QOZU.1	No	No	No	No
	Rhodobacter sphaeroides ATH 2.4.1 NC_007493.2; NC_007494.2	No	No	No	No
	Sagittula stellata E-37 NZ_AAYA.1	No	No	No	No
	Xanthomonas campestris pv. *campestris* ATCC 33913 NC_003902.1	No	No	No	No
Betaproteobacteria	*Methylibium petroleiphilum* PM1 NC_008825.1	No	No	No	No
	Methylobacillus flagellatus KT NC_007947.1	No	No	Yes	No
	Methylobacillus glycogenes JCM 2850 NZ_BAMT.1	No	No	No	No
	Methylophilus sp. 1[a] NZ_ARFK.1	No	No	No	No
	Methylophilus methylotrophus DSM 46235[a] NZ_ARJW.1	No	No	Yes	No
	Methylotenera mobilis JLW8 NC_012968.1	No	No	No	No
	Methylotenera versatilis 79 NZ_ARVX.1	No	No	No	
	Methyloversatilis thermotolerans NVD 3tT[a] M3TT.1	No	No	No	No
	Methyloversatilis universalis FAM5[a] AFHG.2	No	No	Yes	No
	Methylovorus glucosetrophus SIP3-4 NC_012972.1	No	No	Yes	No
	Methylovorus sp. MP688 NC_014733.1	No	No	No	No
Firmicutes	*Bacillus methanolicus* PB1 AFEU.1	No	No	No	No
Gammaproteobacteria	*Methylophaga aminisulfidivorans* MP[a] NZ_AFIG.1	No	No	No	No
	Methylophaga lonarensis MPL[a] NZ_APHR.1	No	No	No	No

[a]contains assembly gaps

It should be noted, however, that none of these copper uptake systems was found in Verrucomicrobia methanotrophs, although it also appears that MMO genes in these methanotrophs were the result of an LGT. At this time, it is unknown why these methanotrophs lack known copper uptake systems, but it may be due to copper availability not being an issue in the conditions these microbes grow. That is, in extremely low pH and metal-rich geothermal environments favored by these microbes (Op den Camp et al., 2009), metal availability is high as metal solubility increases with increasing H^+ concentrations. Further, at this time, it is unclear why *Methylocella* and *Methyloferula* species that cannot express pMMO have the CopCD copper uptake system as they would appear to have little need for collecting copper for pMMO activity, and copper uptake can inhibit sMMO expression. It has been suggested earlier that these methanotrophs likely once had *pmo* genes, but subsequently lost them (Tamas *et al*. 2014). In this case, the presence of *copCD* may be an evolutionary artefact. In addition, it may be that *copCD* expression is low in these strains, limiting copper uptake. We stress, however, that such statements should be considered speculative as no transcriptomic data have been published for these methanotrophs.

It is likely that aerobic methanotrophs evolved from methylotrophs via LGT of MMO genes, and that this has occurred several times independently (Khadka *et al*. 2018; Osborne and Haritos 2018). Here we present evidence that genes involved in carbon oxidation/carbon assimilation were present in the genomes of the receptor organisms before these LGT events, although additional copies of Xox-MeDH-encoding genes were later acquired by many methanotrophs via LGT. Transformation of an aerobic methylotroph to a methanotroph, however, not only required LGT of genes encoding for MMOs, but also the presence of a copper-uptake system(s), particularly for mesophilic aerobic methanotrophs. One or more copper

uptake systems appear to have been encoded in the genomes of the receptor organisms prior to LGT of MMO-encoding genes.

There has been great interest in engineering methanotrophy in other microbes to valorize methane, currently a relatively inexpensive carbon source, into precursors of bioplastics and biofuels (Khmelenina *et al*. 2015; Strong *et al*. 2016; Strong *et al*. 2015). To date only limited success has been reported for the heterologous expression of methane monooxygenases in non-methylotrophs (Jahng *et al*. 1996; Jahng and Wood 1994; Sun and Wood 1996), with expression being difficult to maintain. It is recommended that future efforts to engineer methanotrophy in foreign hosts also consider incorporating a copper-uptake system to ensure sufficient quantities of copper are available for optimal expression/activity, particularly of the pMMO. In such an event, net copper uptake must be carefully controlled, however, to ensure that copper does not build up to toxic levels i.e., due to copper's high redox activity and binding to iron-sulfur proteins (Semrau *et al*. 2018). Strategies to regulate copper toxicity could include incorporation of copper efflux systems, e.g., *cusA*, and/or copper storage proteins found in methanotrophs (Gu and Semrau 2017; Vita *et al*. 2016; Vita *et al*. 2015). Including such systems could also help optimize heterologous expression of sMMO.

Chapter 4 Competition for Copper Between Methanotrophs

4.1. Introduction

Aerobic methanotrophy is strongly controlled by copper, and methanotrophs are known to have multiple mechanisms for copper uptake. Some methanotrophs secrete a chalkophore called methanobactin (MB) (Kim et al., 2004; DiSpirito et al., 2016; Semrau et al., 2020) that binds copper with extremely high affinity (Semrau et al., 2018) while others utilize a surface-bound protein and a secreted form of it (MopE and MopE*, respectively) (Berson & Lidstrom, 1997; Fjellbirkeland et al., 2001; Karlsen et al., 2003; Helland et al., 2008; Ve et al., 2012) for copper collection. Finally, some *Methylocystaceae* methanotrophs lack both MB and the MopE/MopE* systems for copper uptake, suggesting that they collect copper by an as yet unknown system(s) (Table 1.2). As different methanotrophs have different means of sequestering copper, copper competition may significantly impact methanotrophic community composition and activity.

Given the importance of copper in methanotrophy, this raises several intriguing questions. First, do methanotrophs that express MB have a competitive advantage for copper sequestration? Competition between methanotrophs for copper is likely, with such competition affecting overall methanotrophic community composition, and by extension methanotrophic activity. Second, given that MB is secreted into the environment and then taken up after binding copper, can copper-MB complexes be "stolen" by other microbes? Such a phenomenon would require non-MB expressing microbes to have the uptake system identified for MB, i.e., MbnT, the TonB-dependent transporter required for MB uptake (Gu et al., 2016a; Dassama et al., 2016).

Such “theft” would not be unprecedented, as many microbes have been found to act as iron “cheaters” where they take up siderophores produced by others to meet their metabolic iron requirements (Champomier-Vergès et al., 1996; Guan et al., 2001; Cordero et al., 2012; Butaitė et al., 2017). Further, it has been found that methanotrophs that produce and take up MB are able to degrade the potent neurotoxin methylmercury through an as yet uncharacterized mechanism (Lu et al., 2017). If some methanotrophs act as “MB-cheaters”, does such “theft” enable these microbes to degrade methylmercury? Herein we describe experiments delineating copper uptake and gene expression in *Mmc. album* BG8, *Methylococcus capsulatus* Bath, and *Methylocystis* sp. strain Rockwell under varying conditions to determine: (1) if copper requirements of these methanotrophs can be met through “theft” of MB, (2) if such “theft” promotes the ability of non-MB producing methanotrophs to degrade methylmercury, and (3) if methanotrophs can collect copper via some novel mechanism.

4.2. Characterization of putative MbnTs identified in *Mmc. album* BG8, *Methylocystis* sp. strain Rockwell, and *Mcc. capsulatus* Bath

In *Mmc. album* BG8, one gene encoding for a putative TonB-dependent receptor was most similar to both OB3b-MbnT and SB2-MbnT (Metal_1282, or *mbnT-BG8*). Similarity was much greater, however, to OB3b-MbnT (2×10^{-145}, identity = 36%) than SB2-MbnT (1×10^{-12}, identity = 28%) as shown in Table 4.1. For *Methylocystis* sp. strain Rockwell, different genes were identified to be similar to OB3b-MbnT and SB2-MbnT (Table 4.1). Specifically, several genes encoding for putative TonB-dependent transporters similar to OB3b-MbnT were found in the genome of *Methylocystis* sp. strain Rockwell, of which MSPATv1_230027 (i.e., *mbnT1-Rockwell*) exhibited the highest similarity (E value = 1×10^{-136}, identity = 36%). Given this high similarity, expression of *mbnT1-Rockwell* was monitored under different growth conditions as described below. Two genes encoding for putative TonB-dependent transporters highly similar to SB2-MbnT (MSPATv1_550006 and MSPATv1_50173; E value = 0.0 for both) were found in the genome of *Methylocystis* sp. strain Rockwell. The identity of MSPATv1_550006 to SB2-MbnT, however, was much higher than that found for MSPATv1_50173, i.e., 65% vs. 42%. Expression of MSPATv1_550006 (or *mbnT2-Rockwell*) was thus measured via RT-qPCR as detailed below. For *Mcc. capsulatus* Bath, no TonB-dependent transporter was found to have significant similarity to either OB3b-MbnT or SB2-MbnT, the closest being MCA1957 to OB3b-MbnT (E value = 2×10^{-6}, identity = 21%) and MCA2074 to SB2-Mb (E value of 9×10^{-13}, identity = 28%). Nonetheless, expression of MCA1957 in *Mcc. capsulatus* Bath (hereafter labeled *mbnT-Bath*) was monitored under different growth conditions as described below.

Table 4.1. Putative MbnTs and Csps in *Mmc. album* BG8, *Mcc. capsulatus* Bath, and *Methylocystis* sp. strain Rockwell as identified by blastp comparison to MbnT and Csp of either *Msn. trichosporium* OB3b or *Methylocystis* sp. SB2.

Query	Subject	Locus	Identity (%)	E value	Annotated Function
Msn. trichosporium OB3b MbnT (ADVE02_V2_13651)	*Mmc. album* BG8	Metal_1282	36	2×10^{-145}	TonB-dependent siderophore receptor
		Metal_2337	27	7×10^{-68}	TonB-dependent siderophore receptor
	Mcc. capsulatus Bath	MCA1957	21	2×10^{-6}	TonB-dependent receptor
	Methylocystis sp. strain Rockwell	MSPATv1_230027	36	1×10^{-136}	Putative TonB-dependent receptor protein
		MSPATv1_180067	34	1×10^{-111}	Putative TonB-dependent receptor protein
		MSPATv1_410017	29	7×10^{-89}	Putative TonB-dependent receptor protein
		MSPATv1_180015	31	1×10^{-84}	Putative TonB-dependent receptor protein
		MSPATv1_20363	25	2×10^{-53}	TonB-dependent siderophore receptor
Methylocystis sp. SB2 MbnT (MSB2v1_460017)	*Mmc. album* BG8	Metal_1282	28	1×10^{-12}	TonB-dependent siderophore receptor
		Metal_2337	20	1×10^{-12}	TonB-dependent siderophore receptor
	Mcc. capsulatus Bath	MCA2074	25	9×10^{-13}	TonB domain-containing protein
		MCA1957	23	2×10^{-3}	TonB-dependent receptor
	Methylocystis sp. strain Rockwell	MSPATv1_550006	65	0.0	Putative TonB-dependent receptor protein
		MSPATv1_50173	42	0.0	TonB-dependent receptor
		MSPATv1_180067	25	4×10^{-11}	TonB-dependent siderophore receptor
		MSPATv1_20363	21	8×10^{-11}	TonB-dependent siderophore receptor
		MSPATv1_10115	23	2×10^{-9}	TonB-dependent receptor
	Methylocystis sp. strain Rockwell	MSPATv1_280020	62	4×10^{-61}	Conserved exported protein of unknown function

4.3. Growth of *Mmc. album* BG8 wild-type and Δ*mbnT* mutant

Growth of *Mmc. album* BG8 wildtype was strongly dependent on the availability of copper as described previously (Collins et al., 1991). That is, growth clearly occurred in the presence of 1 µM copper, but was significantly reduced when an inoculum grown in the presence of copper was transferred to NMS medium with no added copper (final OD_{600} of 0.60 ± 0.03 vs. 0.24 ± 0.10; $p = 0.018$) (Figure 4.1A and Figure 4.2A). Growth was abolished when this culture was transferred a second time to copper-free medium, indicating that original growth was likely due to the transfer of a small amount of copper with the initial inoculum. Such a result is not unexpected as *Mmc. album* BG8 can only express pMMO that requires copper for its activity.

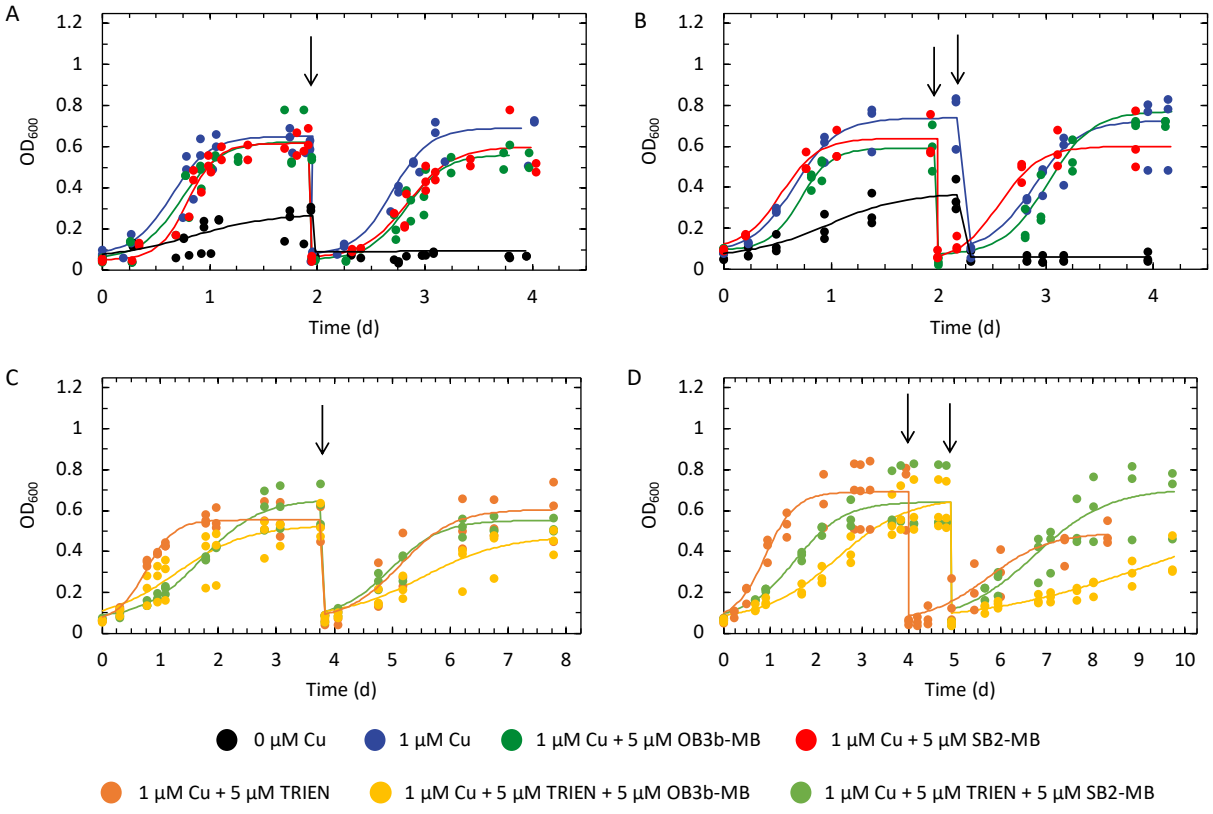

Figure 4.1. Growth of *Mmc. album* BG8 in the presence of varying amounts of copper, MBs, and TRIEN. Growth of the (a) wild-type and (b) Δ*mbnT* mutant with and without copper and MB. Growth of the (c) wild-type and (d) Δ*mbnT* mutant with and without copper, TRIEN, and MB. Solid lines indicate data fitted to logistic growth curve using growthcurver (Sprouffske & Wagner, 2016), and arrows indicate the beginning of second growth cycle.

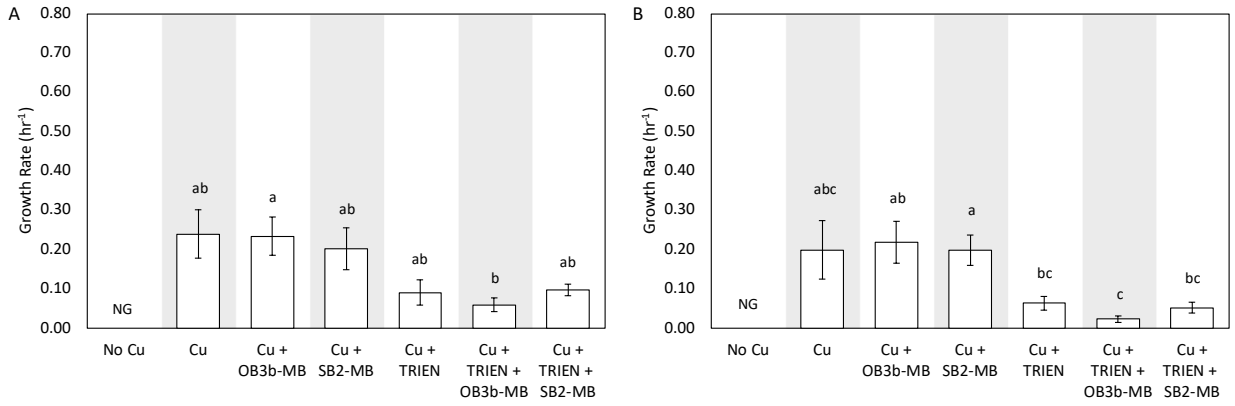

Figure 4.2. Growth rates of the second growth cycle as determined via growthcurver (Sprouffske & Wagner, 2016) of *Mmc. album* BG8 (a) wildtype and (b) Δ*mbnT* with or without 1 μM Cu, 5 μM MB, and 5 μM TRIEN. Error bar indicates standard error of biological triplicates and letters above bars indicate statistically significant difference determined through Student's t-test with Bonferroni correction ($p < 0.05$). NG indicates no growth.

The addition of either 5 μM OB3b-MB (a Group I MB) or SB2-MB (a Group II MB) in the presence of 1 μM copper did not affect growth of *Mmc. album* BG8 as compared to growth in the presence of 1 μM copper only, indicating that neither form of MB inhibited copper uptake (Figure 4.1A and Figure 4.2A). This was confirmed by measuring copper associated with biomass at the end of the second growth cycle - no significant difference was found for cultures of *Mmc. album* BG8 grown with copper and either OB3b-MB or SB2-MB (Figure 4.3A). Further, expression of various genes involved either in copper storage (*csp3*), carbon oxidation (*pmoA* and *mxaF*), or putative MB uptake (*mbnT-BG8*) was not significantly affected by the addition of either type of MB (Figure 4.4). Growth of the *Mmc. album* BG8 Δ*mbnT* mutant was comparable to that of wildtype under all conditions tested (Figure 4.1B and Figure 4.2B). Copper uptake by *Mmc. album* BG8 Δ*mbnT* was also not affected by the addition of either form of MB, nor was expression of various genes involved in methane oxidation or copper storage (Figure 4.3B and Figure 4.5).

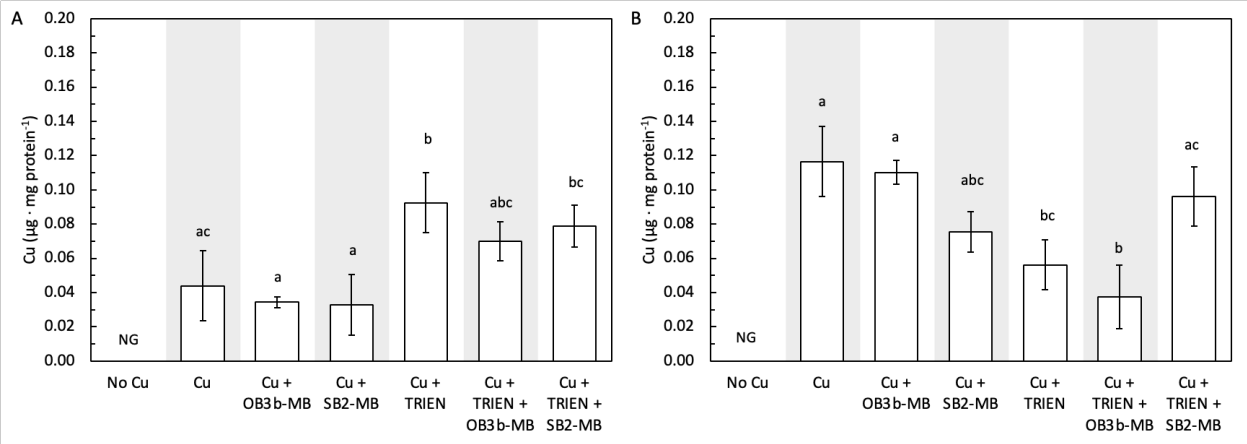

Figure 4.3. Copper associated with the biomass of *Mmc. album* BG8 (a) wildtype and (b) Δ*mbnT* mutant at the end of growth with 0 µM Cu, 1 µM Cu, 1 µM Cu and 5 µM OB3b-MB, 1 µM Cu and 5 µM SB2-MB, 1 µM Cu and 5 µM TRIEN, 1 µM Cu, 5 µM TRIEN and 5 µM OB3b-MB, and 1 µM Cu, 5 µM TRIEN and 5 µM SB2-MB. NG indicates no growth.

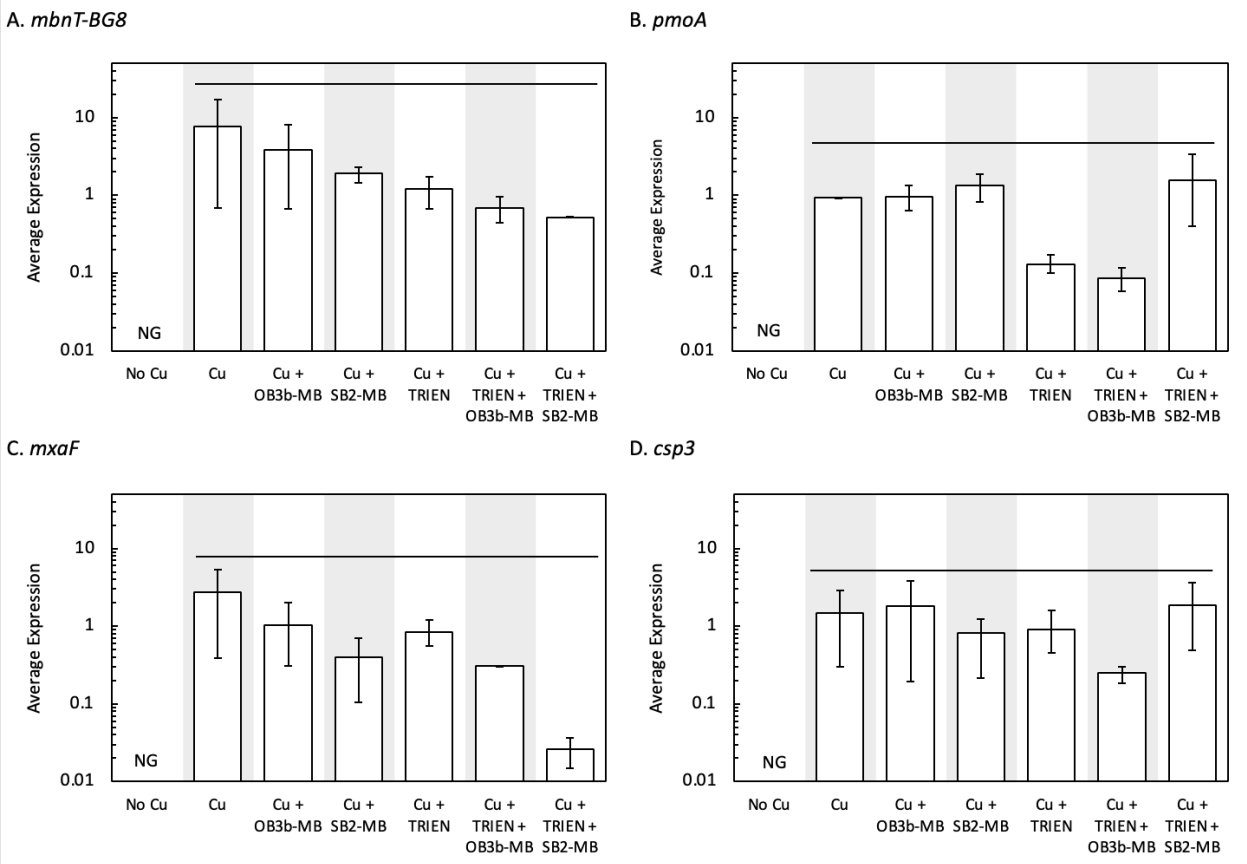

Figure 4.4. RT-qPCR of (a) *mbnT-BG8*, (b) *pmoA*, (c) *mxaF*, and (d) *csp3* in *Mmc. album* BG8 wildtype grown with or without 1 µM Cu, 5 µM MB, and/or 5 µM TRIEN. Error bar indicates range of biological duplicate or triplicate samples. Line over bars indicate no significant differences determined by Tukey's HSD test ($p < 0.05$). NG indicates no growth.

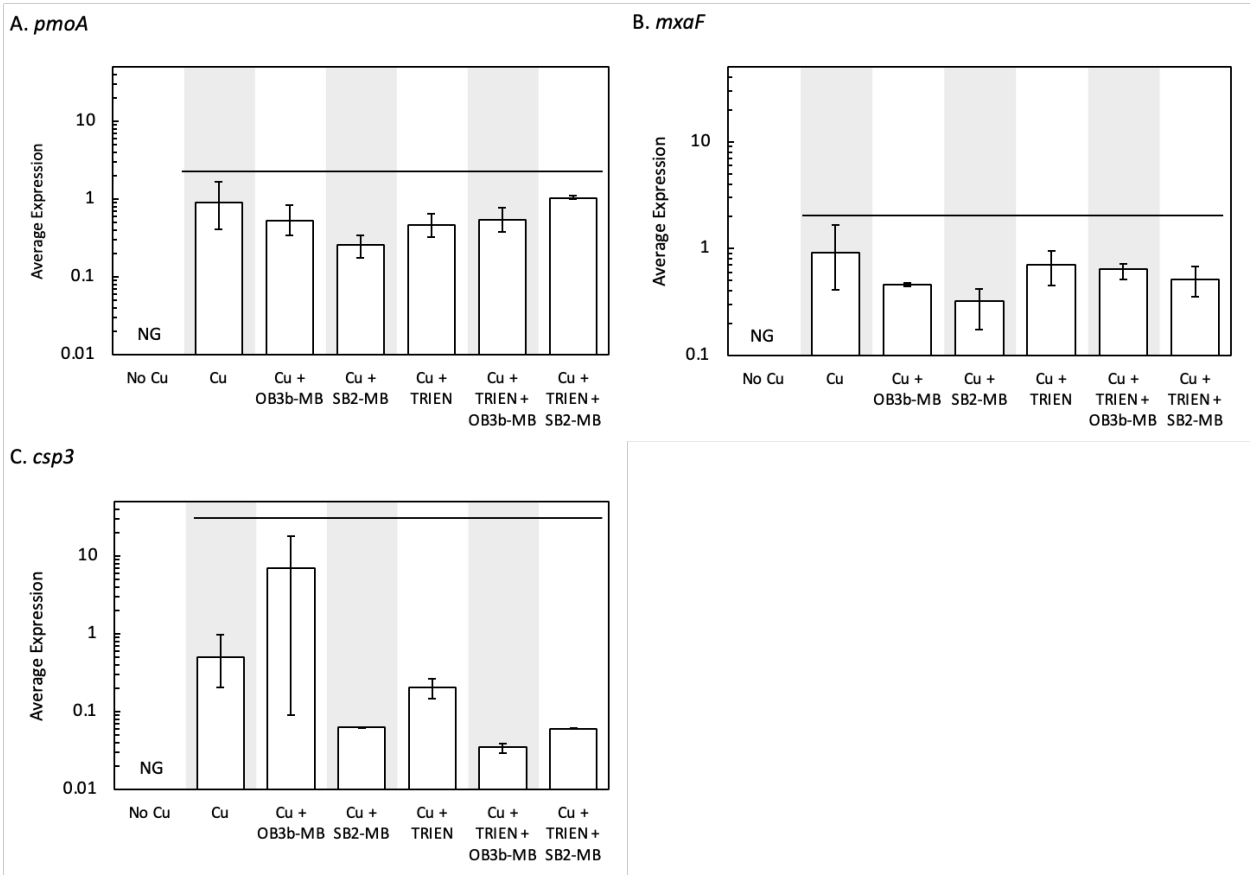

Figure 4.5. RT-qPCR of (a) *pmoA*, (b) *mxaF*, and (c) *csp3* of *Mmc. album* BG8 Δ*mbnT* grown with or without 1 μM Cu, 5 μM MB, and/or 5 μM TRIEN. Error bar indicates range of biological duplicate or triplicate samples. Line over bars indicate no significant differences determined by Tukey's HSD test ($p < 0.05$). NG indicates no growth.

The addition of 5 μM TRIEN in the presence of 1 μM copper significantly inhibited the growth of *Mmc. album* BG8 wildtype as compared to growth in the presence of copper alone (Figure 4.1C and Figure 4.2A). The addition of either form of MB did not improve growth of *Mmc. album* BG8 wildtype in the presence of copper and TRIEN (Figure 4.1C and Figure 4.2A). Expression of various genes involved in methane/methanol oxidation (*pmoA*, *mxaF*) or copper storage (*csp3*) were not significantly affected in *Mmc. album BG8* grown in the presence of TRIEN, copper and/or either form of MB (Figure 4.4), nor was copper uptake (Figure 4.3A). Growth of *Mmc. album BG8 ΔmbnT* was reduced in the presence of copper and TRIEN as

compared to copper alone, but not significantly so (Figure 4.1D and Figure 4.2B). Interestingly, the addition of OB3b-MB in conjunction with TRIEN did reduce the growth of *Mmc. album BG8 ΔmbnT* as compared to the presence of copper alone or copper plus TRIEN (Figure 4.1D and Figure 4.2B). Expression of various genes involved in methane/methanol oxidation (*pmoA*, *mxaF*) or copper storage (*csp3*) were not significantly affected in *Mmc. album BG8 ΔmbnT* (Figure 4.5), nor was copper uptake when the mutant was grown in the presence of TRIEN with or without either form of MB, although the mutant appeared to collect more copper in the presence of SB2-MB vs. OB3b-MB (Figure 4.3B).

4.4. Growth of *Methylocystis* sp. strain Rockwell

Like *Mmc. album* BG8, *Methylocystis* sp. strain Rockwell cannot express sMMO, and so requires copper for growth. As expected, growth of *Methylocystis* sp. strain Rockwell was inhibited in the absence of copper as compared to the presence of 1 μM copper (Figure 4.6A, C). Addition of SB2-MB in the presence of copper did not impact the growth of *Methylocystis* sp. strain Rockwell, whereas OB3b-MB significantly reduced its growth (Figure 4.6A, C). Expression of various genes involved in carbon assimilation (*pmoA, mxaF*), copper storage (*csp1*), or putative MB uptake (*mbnT1-Rockwell*, *mbnT2-Rockwell*) in *Methylocystis* sp. strain Rockwell was not affected by the addition of either MB (Figure 4.7). 5 μM TRIEN significantly inhibited the growth of *Methylocystis* sp. strain Rockwell in the presence of 1 μM copper, which was resolved only in the presence of 5 μM SB2-MB (Figure 4.6B, C). Copper uptake by *Methylocystis* sp. strain Rockwell was significantly reduced in the presence of OB3b-MB, but not in the presence of SB2-MB, regardless if TRIEN was present or not (Figure 4.8). Expression of *mbnT1-Rockwell* and *csp1* of *Methylocystis* sp. strain Rockwell only marginally increased in the presence of copper, TRIEN, and OB3b-MB as compared to that under 1 μM copper (Figure 4.7)

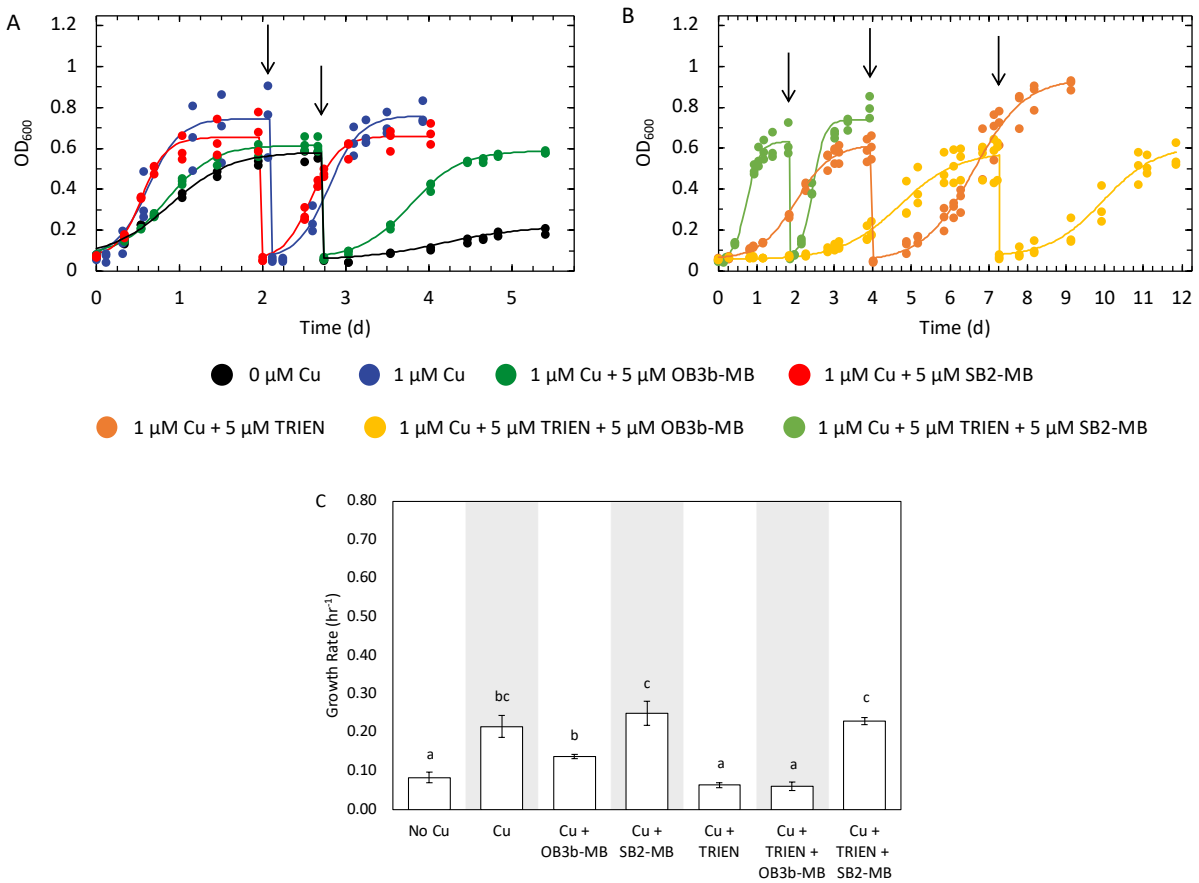

Figure 4.6. Growth of *Methylocystis* sp. strain Rockwell in the presence of varying amounts of copper, MBs, and TRIEN. Growth with and without copper, TRIEN, and MB. Solid lines indicate data fitted to a logistic growth curve using growthcurver (Sprouffske & Wagner, 2016), and arrows indicate the beginning of second growth cycle. (c) Growth rates of the second growth cycle as determined by growthcurver. Error bar indicates standard error of biological triplicates and letters above bars indicate statistically significant difference determined through Student's t-test with Bonferroni correction ($p < 0.05$).

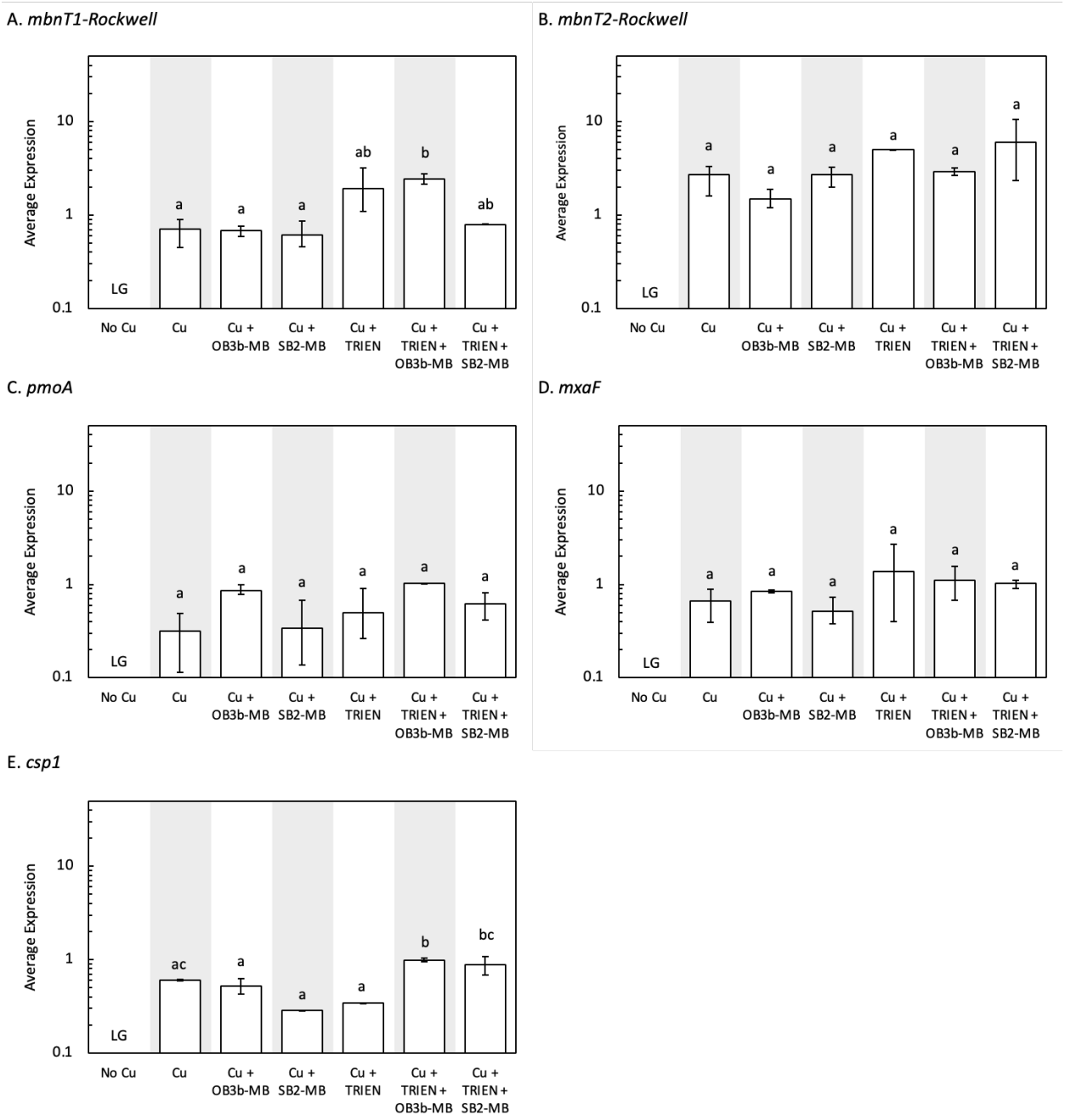

Figure 4.7. RT-qPCR of (a) *mbnT1-Rockwell*, (b) *mbnT2-Rockwell*, (c) *pmoA*, (d) *mxaF*, and (e) *csp1* in *Methylocystis* sp. strain Rockwell grown with or without 1 μM Cu, 5 μM MB, or 5 μM TRIEN. Error bar indicates range of biological duplicate or triplicate samples. Letters over bars indicate no significant differences determined by Tukey's HSD test ($p < 0.05$). LG indicates low growth.

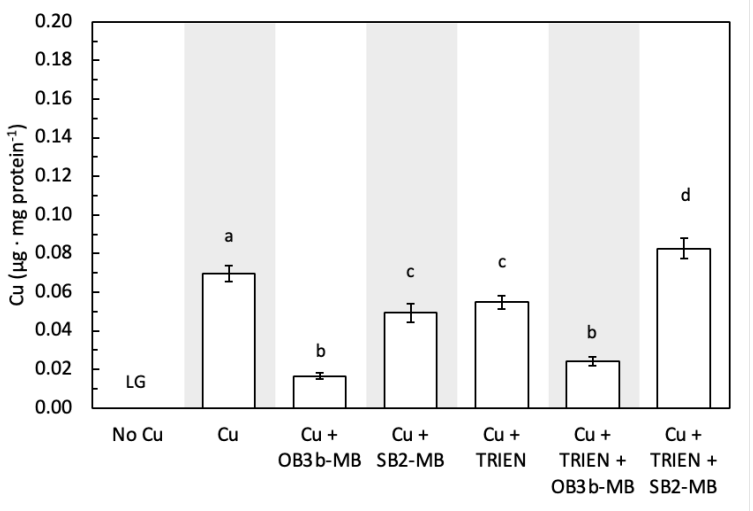

Figure 4.8. Copper associated with the biomass of *Methylocystis* sp. strain Rockwell at the end of growth with 0 µM Cu, 1 µM Cu, 1 µM Cu and 5 µM OB3b-MB, 1 µM Cu and 5 µM SB2-MB, 1 µM Cu and 5 µM TRIEN, 1 µM Cu, 5 µM TRIEN and 5 µM OB3b-MB, and 1 µM Cu, 5 µM TRIEN and 5 µM SB2-MB. LG indicates low growth.

4.5. Growth of *Mcc. capsulatus* Bath

Mcc. capsulatus Bath grows in both the presence and absence of copper as it can express both forms of MMO (Figure 4.9). Growth was faster and more extensive in the presence of copper, indicating that, as found earlier (Leak & Dalton, 1986a), *Mcc. capsulatus* Bath has greater carbon conversion efficiency under pMMO-expressing conditions. Addition of either OB3b-MB or SB2-MB in the presence of copper did not affect growth (Figure 4.9). Copper uptake by *Mcc. capsulatus* Bath was also not affected by the presence of either MB (Figure 4.10). Further, expression of various genes by *Mcc. capsulatus* Bath was not affected by the addition of MB including a putative MB uptake system (*mbnT-Bath*; Figure 4.11). Rather only the presence/absence of copper had any significant effect on gene expression, and then only on *mmoX* (encoding for a subunit of the sMMO) and *mopE* (encoding for a copper uptake protein). Activity of sMMO was also not affected by the presence of either MB, i.e., activity via the naphthalene assay was only evident in the absence of copper (Figure 4.12).

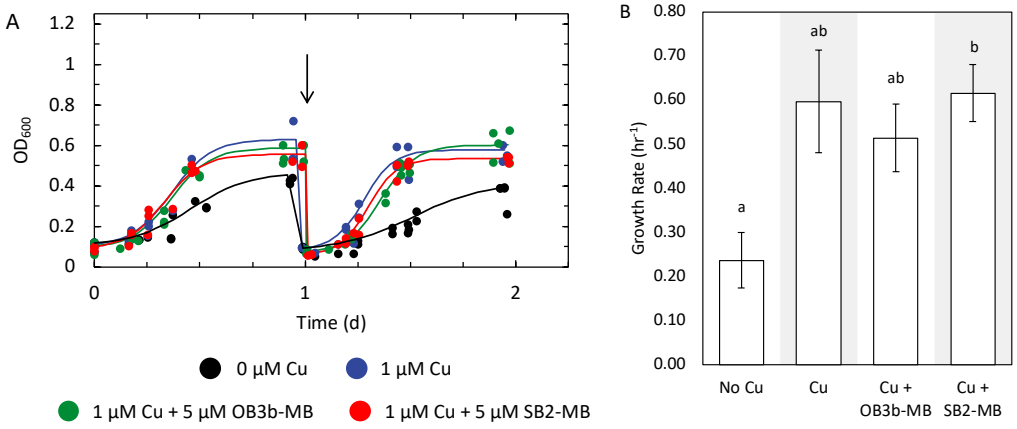

Figure 4.9. Growth of *Mcc. capsulatus* Bath with and without copper and MB. (a) Solid lines indicate data fitted to a logistic growth curve using growthcurver (Sprouffske & Wagner, 2016), and arrow indicates the beginning of second growth cycle. (b) Growth rates of the second growth cycle as determined via growthcurver. Error bar indicates standard error of biological triplicates and letters above bars indicate statistically significant difference determined through Student's t-test with Bonferroni correction ($p < 0.05$).

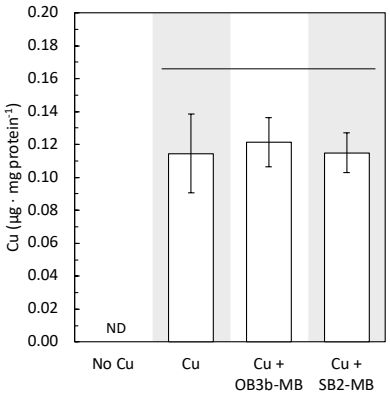

Figure 4.10. Copper associated with the biomass of *Mcc. capsulatus* Bath at the end of the second growth cycle with 0 μM Cu, 1 μM Cu, 1 μM Cu and 5 μM OB3b-MB, and 1 μM Cu and 5 μM SB2-MB. Error bar indicates standard deviation of biological triplicate samples. Lines over bars indicate no significant differences determined by Tukey's HSD test ($p < 0.05$). No detected (ND) copper associated with biomass is indicated.

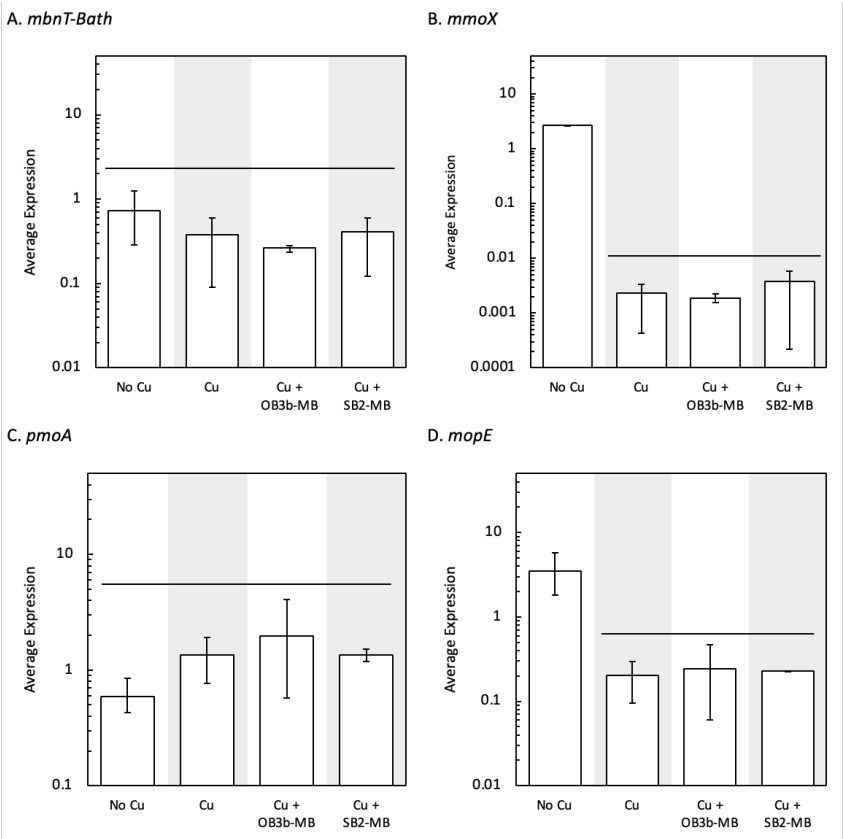

Figure 4.11. RT-qPCR of (a) *mbnT-Bath*, (b) *mmoX*, (c) *pmoA*, and (d) *mopE* in *Mcc. capsulatus* Bath grown with or without 1 μM Cu and 5 μM MB. Error bar indicates range of biological duplicate or triplicate samples. Line over bars indicate no significant differences determined by Tukey's HSD test ($p < 0.05$).

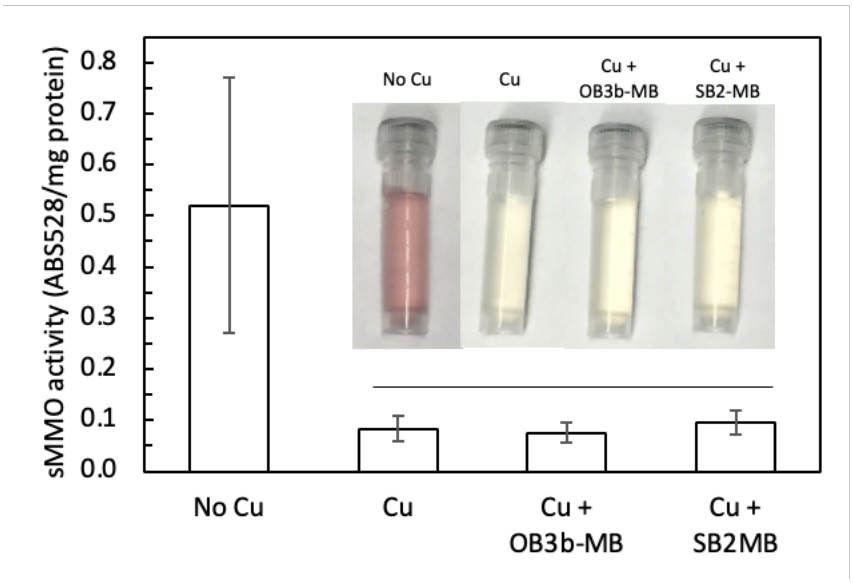

Figure 4.12. Naphthalene assay of *Mcc. capsulatus* Bath grown in the presence and absence of 1 μM Cu and 5 μM MB. Error bar indicates standard deviation of biological triplicate samples. Line over bars indicate no significant differences determined by Tukey's HSD test ($p < 0.05$).

4.6. Localization of MB via immunoblotting in *Mmc. album* BG8

To determine if methanotrophs can take up foreign MB, immunoblotting assays were first performed. Monoclonal antibodies were successfully raised to OB3b-MB, but attempts to do so for SB2-MB were unsuccessful (data not shown). Control immunoblots showed successful monoclonal antibody hybridization to OB3b-MB, but not to lysozyme or *E. coli* cell extracts (Figure 4.13). Interestingly, the monoclonal OB3b-MB antibody (10B10) cross-hybridized with cell extracts of *Mmc. album* BG8 grown in the presence of 1 μM copper and absence of OB3b-MB over two growth cycles, perhaps to a novel chalkophore as described above. Greater hybridization to *Mmc. album* BG8 cell extract was observed in the presence of 1 μM copper + 5 μM OB3b-MB than in the absence of OB3b-MB (Figure 4.13) but very little hybridization was observed in the spent medium or wash buffer when *Mmc. album* BG8 was grown in the presence of OB3b-MB (Figure 4.13). These data suggest that *Mmc. album* BG8 produces some compound analogous to OB3b-MB, but this methanotroph also takes up OB3b-MB as evidenced by greater hybridization signal in the cell extract and low signal in the spent medium and wash buffer when *Mmc. album* BG8 was grown in the presence of OB3b-MB. Due to the evidence of cross-hybridization of monoclonal OB3b-MB antibodies in *Mmc. album* BG8 and the inability to raise monoclonal antibodies to SB2-MB, these experiments were not replicated in other methanotrophs.

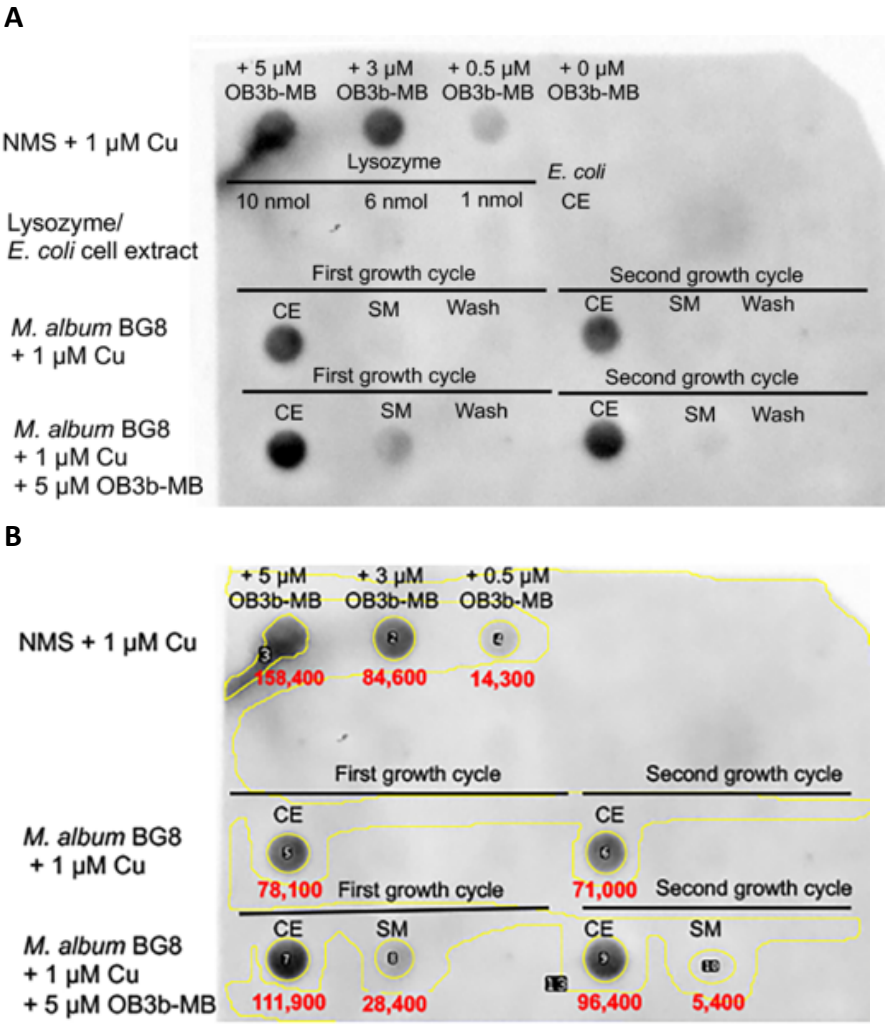

Figure 4.13. Immunoblot assay for the determination of uptake of OB3b-MB by *Mmc. album* BG8 (a). 10B10 antibody was used as described earlier. Lysozyme/*E. coli* cell extracts were used as negative controls while purified OB3b-MB suspended in NMS medium with 1 µM copper was used as a positive control. Measured signal intensity of antibody-MB hybridizations (b). Only those hybridizations with detectable signal above background shown. CE = Cell extract; SM = Spent medium; Wash = Cell wash buffer.

4.7. Evidence of a novel chalkophore from *Mmc. album* BG8

Given the findings that (1) neither form of MB had any measurable effect on *Mmc. album* BG8 wildtype or the *ΔmbnT* mutant and (2) the monoclonal OB3b-MB antibody cross-hybridized to cell extracts of *Mmc. album* BG8, further investigation as to whether *Mmc. album* BG8 can make some copper binding compound akin to MB was pursued. Earlier efforts indicated that *Mmc. album* BG8 does secrete some sort of chalkophore, but under standard growth conditions produces very little of it, making characterization difficult (Choi et al., 2010). *Mmc. album* BG8 was grown in the presence of TRIEN, a strong abiotic chelator of copper, to determine if copper limitation could induce production of this putative chalkophore. Indeed, when *Mmc. album* BG8 was grown in the presence of 1 μM copper + 5 μM TRIEN, growth was visibly reduced (Figure 4.1A and Figure 4.2A) and the spent medium became yellow (Figure 4.14). Such coloration was not observed when *Mmc. album* BG8 was grown in the presence of copper only, indicating that *Mmc. album* BG8 secretes some yellowish substance when copper availability is reduced through the addition of TRIEN. It should be noted that when methanotrophs such as *Msn. trichosporium* OB3b actively produce MB, the spent medium also appears yellow (Bandow et al., 2011). The isolated chalkophore from *Mmc. album* BG8 showed a molecular mass of 649.95 (Figure 4.15A) or 653.29 Da (Figure 4.15B) as determined by MALDI-TOF or ESI-MS, respectively. Following the addition of $CuCl_2$, the molecular mass shifted to 711.35 (Figure 4.15A) and 713.35 Da (Figure 4.15C) as determined by MALDI-TOF or ESI-MS, respectively, suggesting a 2 or $3H^+$ loss following copper binding (Figure 4.15). The UV-VIS spectrum of the isolated chalkophore did not have the characteristic peaks present in MBs (i.e., at ~340 and 394 nm), but did exhibit distinct absorption maxima at 396 nm and 402 nm with a molar extinction coefficient of 1.6 $mM^{-1}cm^{-1}$ at 402 nm (Figure 4.14B, C and Figure

4.16) with a discrete isobestic point at 340 nm at mole ratios of copper:*Mmc. album* BG8 chalkophore between 0 and 0.19 (Figure 4.16A). These peaks shifted to 404 nm at copper:chalkophore ratios between 0.2 and 0.45 (Figure 4.14 and Figure 4.16B) with discrete isobestic point at 398 nm and to 390 nm at copper:chalkophore ratios above 0.6 (Figure 4.14 and Figure 4.16C).

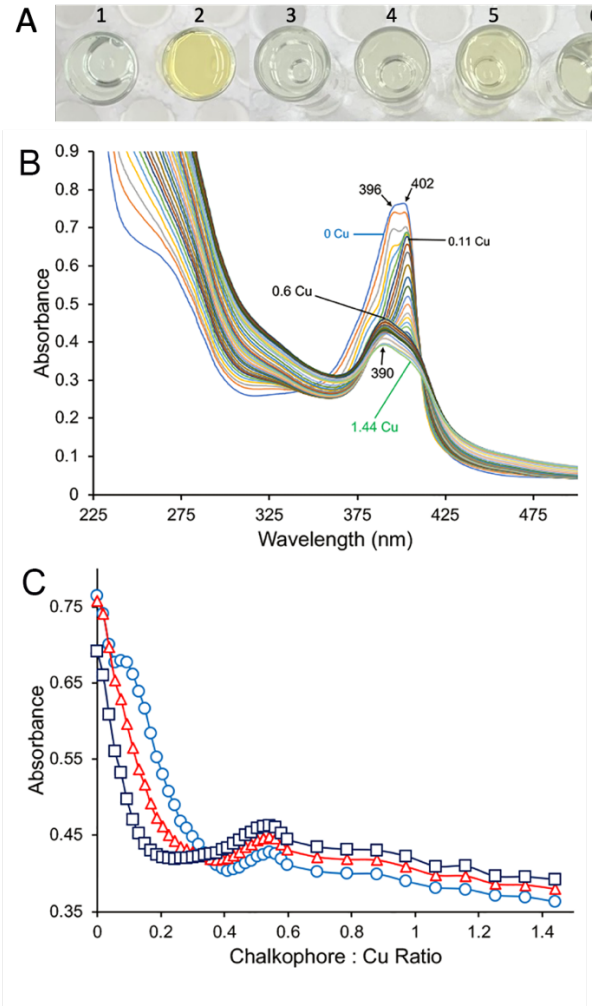

Figure 4.14. (a) Filtered spent medium of *Mmc. album* BG8 grown in the (1) presence of 1 µM copper and (2) 1 µM copper and 5 µM TRIEN, with abiotic controls (3) NMS, (4) NMS, 1 µM copper, and 5 µM TRIEN, (5) NMS and 5 µM OB3b-MB, (6) NMS and 5 µM SB2-MB. (b) UV-visible absorption spectra of 535 nmol of the chalkophore isolated from *Mmc. album* BG8 and following the addition of copper (as $CuCl_2$) initially in 10 nmol increments (up to 320 nmol) and then in 50 nmol increments (for an additional 450 nmol copper, or 770 nmol copper in total). (c) Absorbance changes at 402 nm (○), 396 nm (△), and 390 nm (□) following copper addition. Numbers in panel (a) refer to mole ratio of copper to *Mmc. album* BG8 chalkphore.

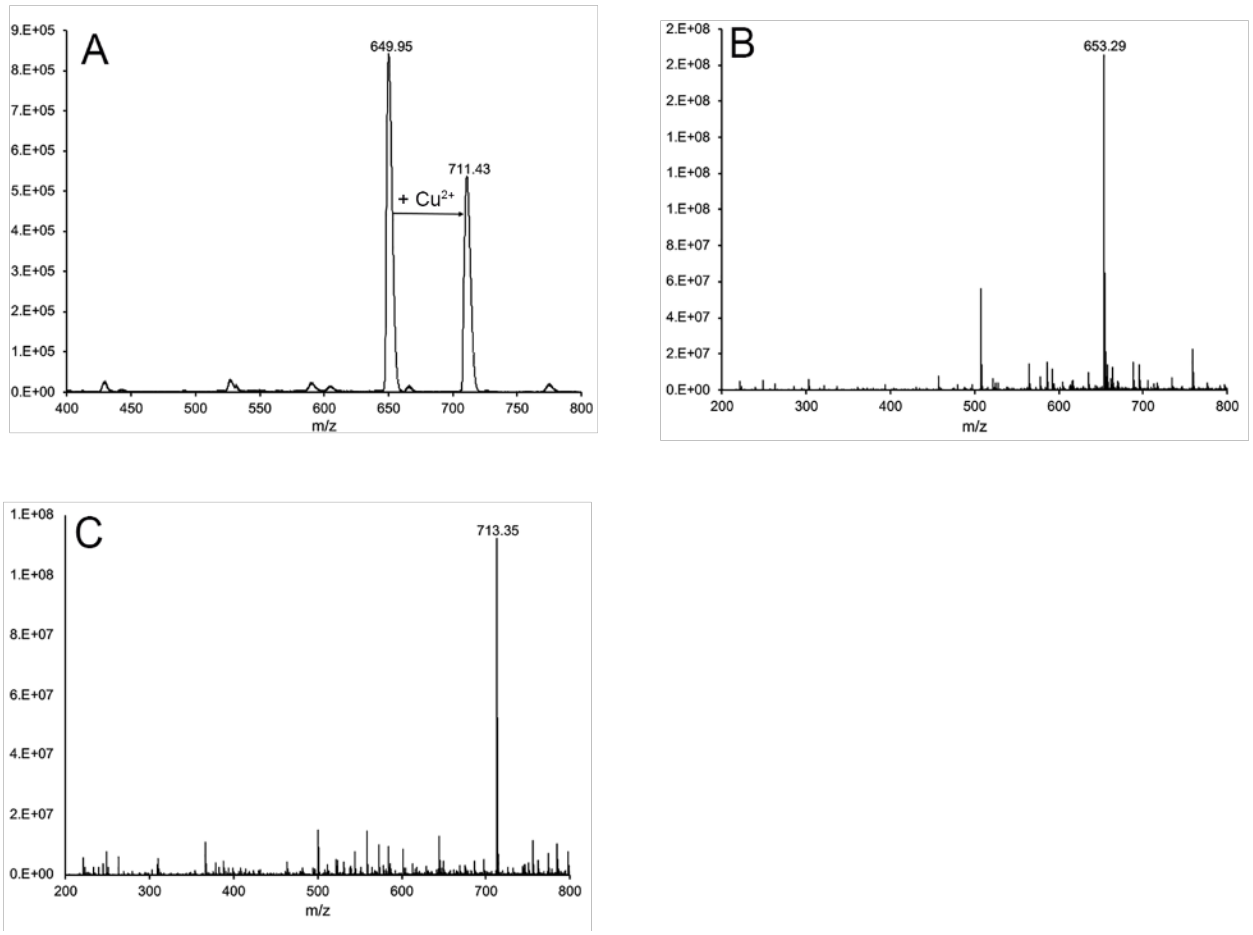

Figure 4.15. (a) MALDI-TOF of the chalkophore from *Mmc. album* BG8 following the addition of 0.5 molar addition of $CuCl_2$. (b) ESI-MS of the chalkophore isolated from *Mmc. album* BG8. (c) ESI-MS of the chalkophore isolated from *Mmc. album* BG8 following the addition of a molar excess of $CuCl_2$.

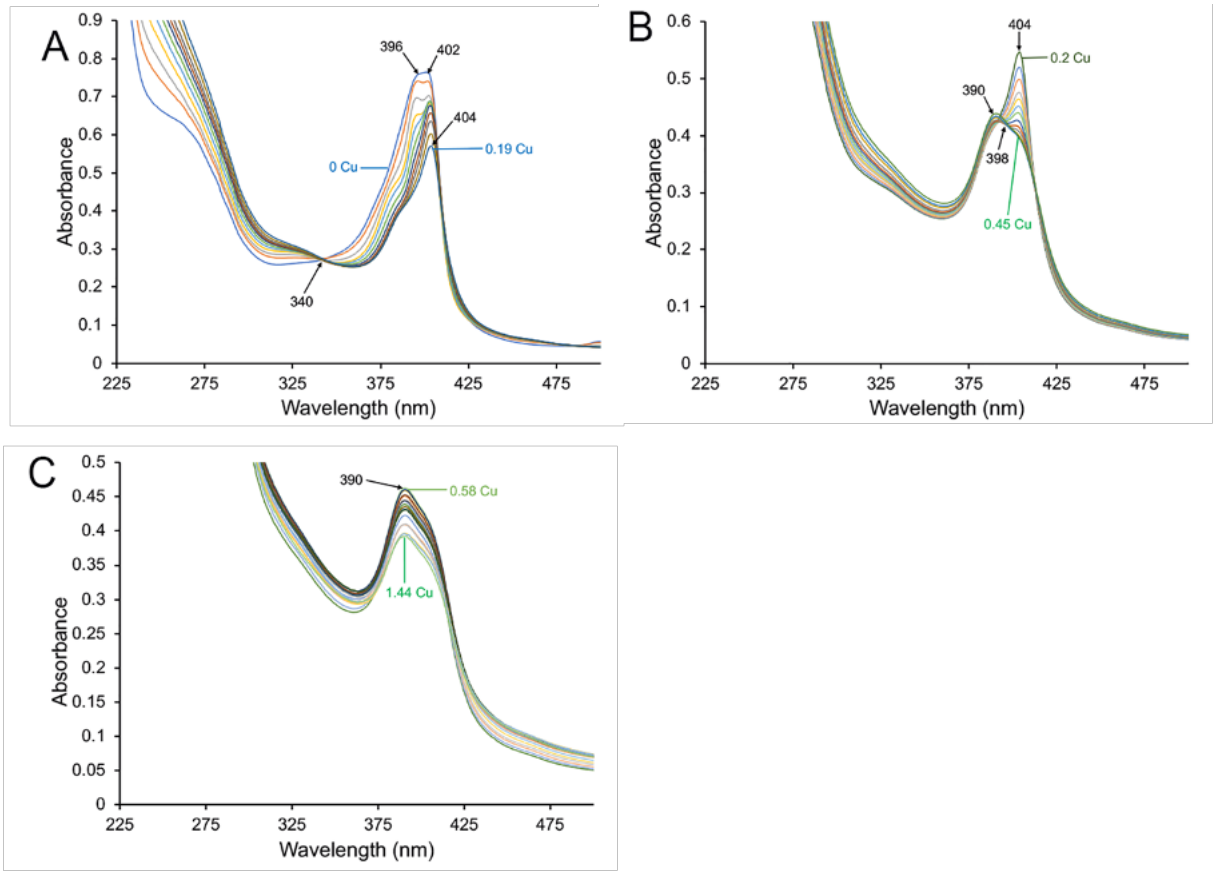

Figure 4.16. UV-visible absorption spectra of 535 nmol of the as isolated chalkophore and following the addition of copper (as $CuCl_2$) in copper:chalkophore ratios ranging from (a) 0 to 0.19, (b) 0.2 to 0.45, and (c) 0.58 to 1.44.

No such coloration in the spent medium was observed for *Methylocystis* sp. strain Rockwell under any condition (data not shown). An effort to identify novel chalkophore(s) in *Mcc. capsulatus* Bath was not attempted as this strain has already been clearly shown to produce both membrane-bound and secreted copper-binding polypeptides (i.e., MopE and MopE*, respectively) (Fjellbirkeland et al., 2001; Helland et al., 2008; Karlsen et al., 2003; Ve et al., 2012).

4.8. Effect of MB on methylmercury demethylation

Given the uncertainty of the immunoblot data and evidence that *Mmc. album* BG8 produces a competitive chalkophore, to further determine if MB "theft" occurs between methanotrophs, demethylation of methylmercury (MeHg) by *Mmc. album* BG8 wildtype and *ΔmbnT* mutant, *Methylocystis* sp. strain Rockwell, and *Mcc. capsulatus* Bath was monitored in the absence or presence of OB3b-MB and SB2-MB (Figure 4.17). These studies were pursued as our previous work has shown that only those methanotrophs expressing and taking up MB can degrade MeHg (Lu et al., 2017). That is, MB appears to serve as a device to deliver MeHg inside the cell where it is degraded, but not by the well-known organomercurial lyase as these microbes lack *merB*. Rather, data suggest that MeHg degradation may be carried out by the methanol dehydrogenase that all methanotrophs possess (Lu et al., 2017). If *Mmc. album* BG8, *Methylocystis* sp. strain Rockwell, and/or *Mcc. capsulatus* Bath can take up MB, one would expect that these methanotrophs would be able to degrade MeHg in the presence of MB but not in its absence. Indeed, relatively little MeHg degradation was observed in *Mmc. album* BG8 in the absence of MB (~10%), but this increased in the presence of both OB3b-MB and SB2-MB (32% and 61%, respectively; Figure 4.17). In the absence of either MB, MeHg degradation was observed in *Methylocystis* sp. strain Rockwell (40%), and the degradation again increased in the presence of both OB3b-MB and SB2-MB (57% and 75%, respectively). Interestingly, under no condition was MeHg degradation observed in *Mcc. capsulatus* Bath, nor was degradation of MeHg by the Δ*mbnT* mutant of *Mmc. album* BG8 significantly different in the presence or absence of either form of MB (Figure 4.17).

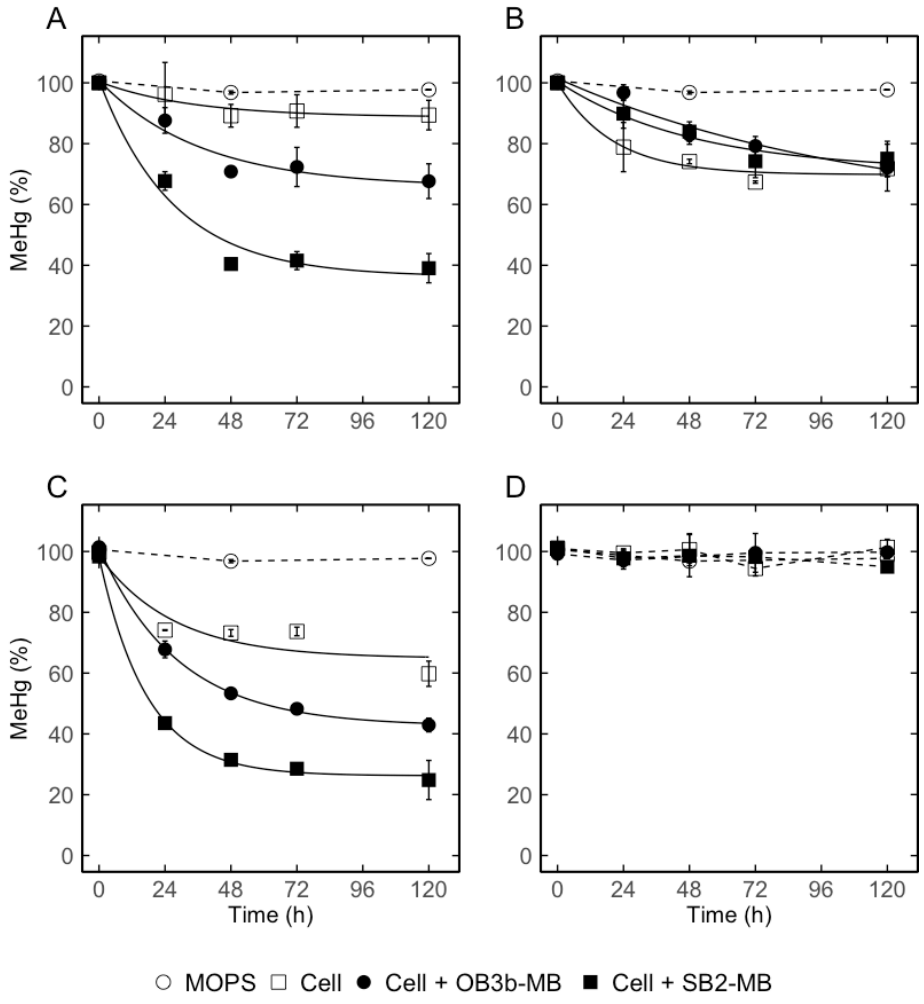

Figure 4.17. Degradation of MeHg over time by (a) *Mmc. album* BG8 wild-type, (b) *Mmc. album* BG8 Δ*mbnT*, (c) *Methylocystis* sp. strain Rockwell, and (d) *Mcc. capsulatus* Bath in MOPS buffer (5 mM), fitted to an exponential decay model with stabilization over time (solid line). The total added MeHg, methanobactin (MB), and cell concentrations were 5 nM, 45 μM, and 10^8 cells mL^{-1} at t = 0 h. Error bars represent standard deviation of at least biological duplicates.

4.9. Discussion

It has been well documented that microorganisms have active "social lives", i.e., microbes have been shown to exhibit a range of behaviors ranging from cooperation, competition and cheating (Griffin et al., 2004; West et al., 2006, 2007). Perhaps the best known example of social interactions between microbes is the finding that siderophores often serve as "public goods" in microbial communities. Iron availability commonly limits microbial growth due to the insolubility of Fe(III), and many microbes produce a variety of siderophores, or organic extracellular ferric iron chelating agents for iron solubilization and collection (Andrews et al., 2003; Ahmed & Holmström, 2014). Given that these compounds are secreted, they can be considered "public goods" i.e., although they are costly for the individual microorganism to make, they can be utilized by other microbes for iron collection, and thus promote the growth of the local microbial community (Griffin et al., 2004; West et al., 2006, 2007). A challenge that then arises is that microbes can and do develop "cheating" strategies, i.e., some microorganisms with the inability to produce siderophores "steal" them to meet their needs and such cheating strategies likely play important roles in the diversification and evolution of natural microbial communities (Champomier-Vergès et al., 1996; Guan et al., 2001; Butaitė et al., 2017; Cordero et al., 2012).

Previous studies suggest that methanotrophs do not utilize a "public good" for copper collection. That is, it has been reported that *Msn. trichosporium* OB3b outcompetes *Mmc. album* BG8 for copper, and as such predominates in mixed cultures (Graham et al., 1993). Such a conclusion, however, appears to be overstated as the *Mmc. album* BG8 is unequivocally present in large numbers in these experiments, suggesting that they have viable mechanism(s) to collect copper in the presence of MB-expressing methanotrophs.

Interestingly, although *Mmc. album* BG8 does not have genes encoding the polypeptide precursor of MB or enzymes required for conversion of this precursor to mature MB, it does express something akin to MB, i.e., it secretes a copper-binding compound, especially under copper-limiting conditions created when TRIEN is present, and appears to compete with MBs for copper. In addition, a mutant of *Mmc. album* BG8 deficient in the putative gene encoding for TonB-dependent transporter for MB uptake exhibited a wildtype phenotype, supporting the conclusion that the chalkophore expressed by *Mmc. album* BG8 is effective in competing for copper in the presence of MB. Nonetheless, data indicate that *Mmc. album* BG8, in addition to being able to effectively compete with MB by producing a novel chalkophore, also engages in MB "theft". That is, although TRIEN affected growth of both *Mmc. album* BG8 wildtype and *ΔmbnT* mutant, growth of *Mmc. album* BG8 wildtype was not further affected by the concurrent addition of OB3b-MB, but the *ΔmbnT* mutant was. It was also observed that MB enhanced MeHg demethylation in *Mmc. album BG8* wildtype, but not the Δ*mbnT* mutant, further implying that *Mmc. album* BG8 can indeed "steal" MB through expression of a TonB-dependent transporter that sequesters MB.

We were unable to identify any novel chalkophore produced by *Methylocystis* sp. strain Rockwell, but it does appear to act as a "cheater" by taking up MB - preferentially Group II MB - to meet its copper requirements as growth and copper uptake was inhibited in the presence of OB3b-MB (a group I MB), but not SB2-MB (a Group II MB). Such a conclusion is supported by the finding that the addition of TRIEN inhibited growth of *Methylocystis* sp. strain Rockwell, but the concurrent addition of SB2-MB relieved such inhibition. Although we could not directly determine SB2-MB uptake via immunoblots as we were unsuccessful in raising monoclonal

antibodies to SB2-MB, again, MeHg degradation data indicate that MB can be taken up by *Methylocystis* sp. strain Rockwell.

Mcc. capsulatus Bath appears to have an effective strategy to compete for copper against MB, as evidenced by the consistent growth, copper uptake, and gene expression in the presence vs. absence of MB. It is likely that this is attributable to MopE/MopE* that allows *Mcc. capsulatus* Bath to collect copper in the presence of MB, rather than MB "theft" (Berson & Lidstrom, 1997; Fjellbirkeland et al., 2001; Karlsen et al., 2003; Helland et al., 2008; Ve et al., 2012), as *Mcc. capsulatus* Bath cannot degrade MeHg under any conditions tested. Thus, MB may serve as a sort of "public good" to some methanotrophs, but is not of benefit to all methanotrophs. Given that methanotrophs use a variety of strategies to collect copper, these interactions likely are significant in structuring methanotrophic communities *in situ.*

While herein we report methanotrophic interactions based on competition for copper, including MB "theft", interspecies interactions have been documented earlier for methanotrophs, e.g., recognition of and response to acyl-homoserine lactone receptor/transcription factors and uptake of foreign MB by species that can make MB (i.e., examples of quorum sensing/cooperation between methanotrophs). Such interactions, however were within species of the same family, i.e., communication between closely related methanotrophic kin (Farhan Ul Haque et al., 2015b; Puri et al., 2019). Here we show potential social interactions not only between members of the same class of methanotrophs (i.e., *Alphaproteobacteria*), but also between members of different classes (i.e., *Alpha*- vs. *Gammaproteobacteria* methanotrophs). Such findings indicate that methanotrophic interactions can be phylogenetically far-ranging. It may be that the uptake of MB from the environment by non-MB producing methanotrophs not only enhances their ability to collect copper, but also gives them an advantage by acting as a MB

sink, thereby placing MB-producing methanotrophs at a relative disadvantage. Such a finding lends support to the conclusion that as competition for resources becomes more local, the influence of species relatedness for cooperation is reduced, thus decreasing altruism and allowing "cheating" to become more pronounced (Griffin et al., 2004; West et al., 2006, 2007). That is, as methanotrophs of different phylogenies co-habitate at the oxic-anoxic interface, kin recognition/discrimination becomes less effective for these microbes and MB can be more readily "stolen". These findings raise the intriguing question as what prevents "MB stealers" from overwhelming the population? As suggested for siderophores, it may be that MB production and distribution to non-MB producing methanotrophs provides both direct and indirect fitness benefits to MB-producers that outweigh the costs of MB synthesis and loss. The magnitude and distribution of such benefits, however, are likely to be highly dependent on environmental conditions (e.g., copper availability) and population density as suggested for siderophores (West et al., 2006).

While our data indicate MB "theft" between methanotrophs, it has been shown earlier that copper uptake by and activity of denitrifiers is strongly inhibited in the presence of either MB or MB-producing methanotrophs (Chang et al., 2018). That is, MB inhibited uptake of copper and activity of nitrous oxide reductase (NosZ, like pMMO has a high copper requirement) in a wide range of denitrifiers (*Pseudomonas stutzeri* DCP-Ps1, *Paracoccus denitrificans* ATCC17741, *Shewanella loihica* PV-4, and *Dechloromonas aromatica* RCB) in coculture experiments. As a result, in these situations, methanotrophic production of MB is an example of selfish behavior on the part of methanotrophs with the end result of increased nitrous oxide production by denitrifying microbes. As nitrous oxide is a much more potent greenhouse gas than methane, such "selfishness" for copper on the part of methanotrophs may have a major

impact on net greenhouse gas emissions. Thus, delineating how methanotrophs contend for copper with other methanotrophs as well as with non-methanotrophs – whether through cooperation, cheating, or selfishness – will likely provide insights as how best to manipulate microbial communities for enhanced methane and nitrous oxide removal from both anthropogenic and natural sources.

Finally, we also found that MB enhanced the ability of *Mmc. album* BG8 and *Methylocystis* sp. strain Rockwell, but not *Mcc. capsulatus* Bath or the Δ*mbnT* mutant of *Mmc. album* BG8 to degrade MeHg. The heterologous uptake or "theft" of MB thus enables MB non-producers to detoxify a highly toxic organic form of mercury, suggesting that methanotrophic-mediated MeHg detoxification may be more widespread than previously thought in the natural environment. Examining this in more detail will likely be very informative and will serve as key inputs for metabolic and reactive transport models that can be used to better predict net MeHg production and Hg biogeochemical cycling in the environment.

Chapter 5 Mechanism of Methylmercury Demethylation in Methanotrophs

5.1. Introduction

Methylmercury (MeHg) demethylation in the environment is typically carried out by microbes containing MerB, the canonical organomercurial lyase (Schaefer et al., 2004). MerB can cleave the carbon-metal bond within MeHg and produce methane and inorganic mercury, thereby decreasing the toxicity of the organic form of mercury (Eq. 1; Barkay et al., 2003). MerB has a pH optimum of greater than 9 and is active at micromolar substrate range (Begley et al., 1986a, 1986b). It has been found that methanotrophs are also able to degrade MeHg, not via MerB as evidenced by the lack of *merB* in genomes of methanotrophs capable of MeHg degradation, but rather through an as yet unknown process (Lu et al., 2017). Moreover, in contrast to MerB-mediated MeHg demethylation, degradation by methanotrophs occur at circumneutral pH and pico- to nanomolar substrate range, which are relevant to actual environmental conditions (Barkay & Wagner-Döbler, 2005; Lu et al., 2017). Therefore, understanding the mechanism of MeHg degradation by methanotrophs may provide a basis for promoting bioremediation in MeHg contaminated sites.

$$CH_3Hg^+ + H^+ \xrightarrow{\text{MerB}} CH_4 + Hg^{2+} \quad (1)$$

In a previous study, MeHg demethylation in model methanotrophs *Methylosinus trichosporium* OB3b, *Methylocystis* sp. SB2, *Methylocystis parvus* OBBP, and *Methylococcus capsulatus* Bath were investigated (Lu et al., 2017). It was found that methanobactin (MB) plays

a critical role in MeHg degradation, as only the non-MB producers and *Msn. trichosporium* OB3b deficient in MB production were unable to degrade MeHg (Lu et al., 2017). MB also strongly binds Hg(II) and can reduce it to Hg(0) (Vorobev et al., 2013; Baral et al., 2014), though it cannot degrade MeHg on its own (Lu et al., 2017). Collectively, these results suggested that MB may act as a mechanism to deliver MeHg into the cell, where degradation occurs. Lu et al. (2017) also investigated several candidates potentially responsible for MeHg demethylation in *Msn. trichosporium* OB3b, starting with methane monooxygenase (MMO). *Msn. trichosporium* OB3b did not show any difference in MeHg degradation rate when acetylene was used as an MMO inhibitor (Prior & Dalton, 1985), ruling out MMO as the enzyme that cleaves the carbon-metal bond (Figure 5.1; Lu et al., 2017). The methanol dehydrogenase (MeDH) was also considered, where methanol was added as a competitive inhibitor of MeDH. MeHg was completely inhibited when 5 mM of methanol was provided, suggesting that MeDH, in conjunction with MB, is critical for MeHg degradation by *Msn. trichosporium* OB3b (Figure 5.2; Lu et al., 2017).

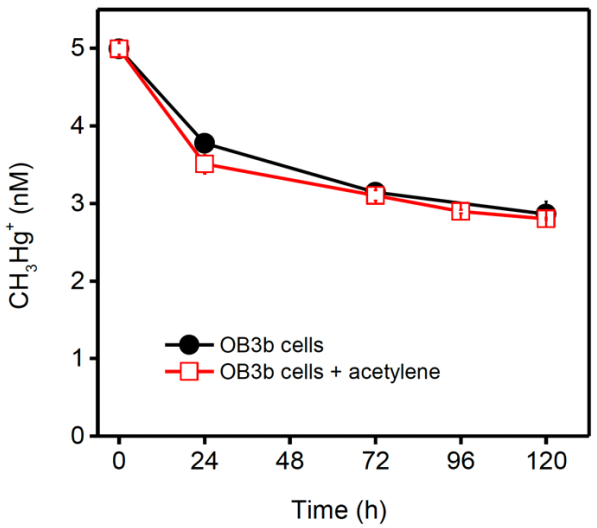

Figure 5.1. Effect of acetylene addition (as an inhibitor of MMOs) on methylmercury (MeHg) degradation by washed cells of *Msn. trichosporium* OB3b (10^8 cells mL^{-1}) in 5 mM MOPS buffer at 30 ºC (Lu et al., 2017). Cells were grown in the absence of copper ions. The initial added MeHg was 5 nM. Error bars represent one standard deviation of duplicate samples.

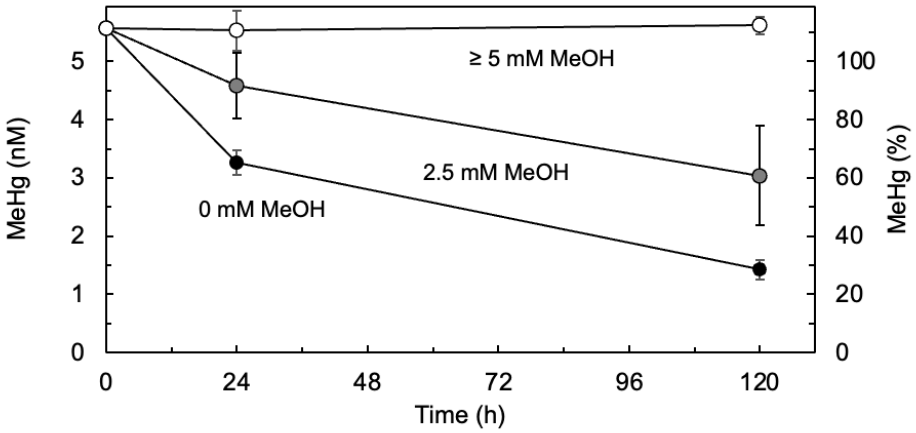

Figure 5.2. Effect of methanol addition on methylmercury (MeHg) degradation by washed cells of *Msn. trichosporium* OB3b (10^8 cells mL^{-1}) in 5 mM MOPS buffer at 30 ºC (adapted from Lu et al., 2017). The initial addition of MeHg was 5 nM. Error bars represent one standard deviation of triplicate samples.

However, it is important to note there are two forms of MeDH in *Msn. trichosporium* OB3b – the Ca^{2+}-dependent Mxa-MeDH and rare earth element (REE)-dependent Xox-MeDH – and one or both of them may be responsible for MeHg degradation. MeHg degradation by *Msn. trichosporium* OB3b was in fact enhanced in the presence of 25 µM cerium, supporting Xox-MeDH as the player in this process (Figure 5.3; unpublished data (Semrau et al.)).

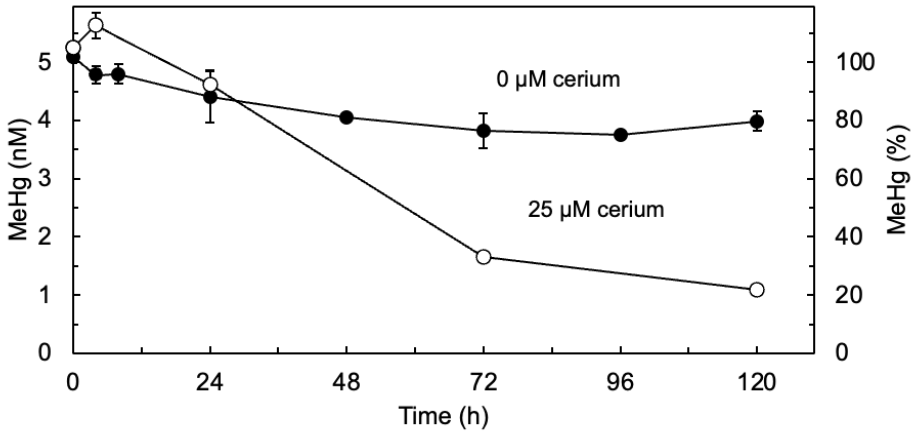

Figure 5.3. Effect of cerium on methylmercury (MeHg) degradation by washed cells of *Msn. trichosporium* OB3b (10^8 cells mL^{-1}) in 5 mM MOPS buffer at 30 ºC. The initial addition of MeHg was 5 nM. Error bar indicates standard deviation of biological triplicate.

Though it has been shown that MB and Xox-MeDH are required for methanotrophic-mediated MeHg degradation, more work is necessary to delineate the mechanism. There exists a gene that encodes for a putative organoarsenical lyase (*arsI*; ADVE02_v2_12724) in the genome of *Msn. trichosporium* OB3b that may be involved in the carbon-mercury bond cleavage. In addition, lanmodulin (LanM; ADVE02_v2_11067), a recently discovered periplasmic REE-binding protein, can also be found in the model methanotroph, and may be involved given the importance of Xox-MeDH in the process. Here we show that *arsI* in the model methanotroph *Msn. trichosporium* OB3b is not required for MeHg, but *lanM* is essential. We further provide additional evidence that MeHg degradation takes place in the periplasm of methanotrophs, where Xox-MeDH and LanM is located, by using spheroplasts prepared from *Msn. trichosporium* OB3b *mbnT*::Gm^r mutant.

5.2. Role of *arsI* in methylmercury demethylation

arsI encoding for a putative organoarsenical lyase in *Msn. trichosporium* OB3b was knocked out via markerless mutagenesis. The mutant was still able to degrade MeHg to levels comparable to the wildtype (Figure 5.4), suggesting that *arsI* has little role if any in degrading MeHg.

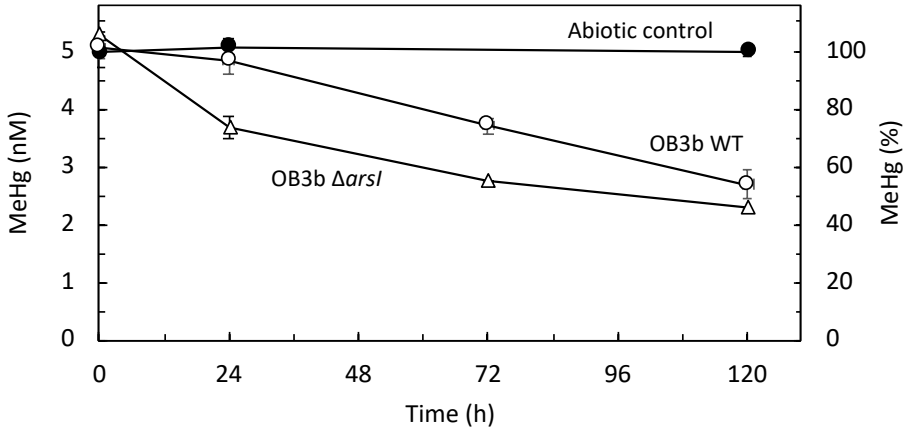

Figure 5.4. MeHg demethylation by *Msn. trichosporium* OB3b Δ*arsI*. Error bar indicates standard deviation of biological triplicate.

5.3. Role of *lanM* in methylmercury demethylation

In *Msn. trichosporium* OB3b, there are two complete *xox* operons (ADVE02_v2_12117-9, ADVE02_v2_11799-7) and an orphan *xoxF* gene (ADVE02_v2_12494). *xoxF1* (ADVE02_v2_12117) was targeted for markerless mutagenesis to further confirm the role of Xox-MeDH in MeHg degradation. However, *Msn. trichosporium* OB3b *ΔxoxF1* was not obtained (Section 2.4.1. pg. 95), suggesting that the deletion of *xoxF1* may be lethal. Given *Msn. trichosporium* OB3b contains multiple copies of *xoxF* and a *ΔxoxF1* mutant was not attainable, we proceeded to disrupt the potential REE uptake or signaling pathway to limit the activity of

Xox-MeDH. Specifically, *lanM* encoding for lanmodulin was deleted via markerless mutagenesis to produce *Msn. trichosporium* OB3b *ΔlanM* mutant.

Growth of the *Msn. trichosporium* OB3b *ΔlanM* mutant was compared to that of the wildtype in the presence and absence of copper and various REEs (Figure 5.5 and Figure 5.6). The *ΔlanM* mutant exhibited significantly higher growth rate than the wildtype in the absence of REE. In addition, the growth rate of the mutant was slightly slower in the presence of both copper and neodymium, the heaviest REE included in this study, as compared to that of the wildtype (Figure 5.5 and Figure 5.6). However, growth was variable between batches (data not shown), and may be attributable to the phosphate limitation of the modified NMS medium and variable inoculum.

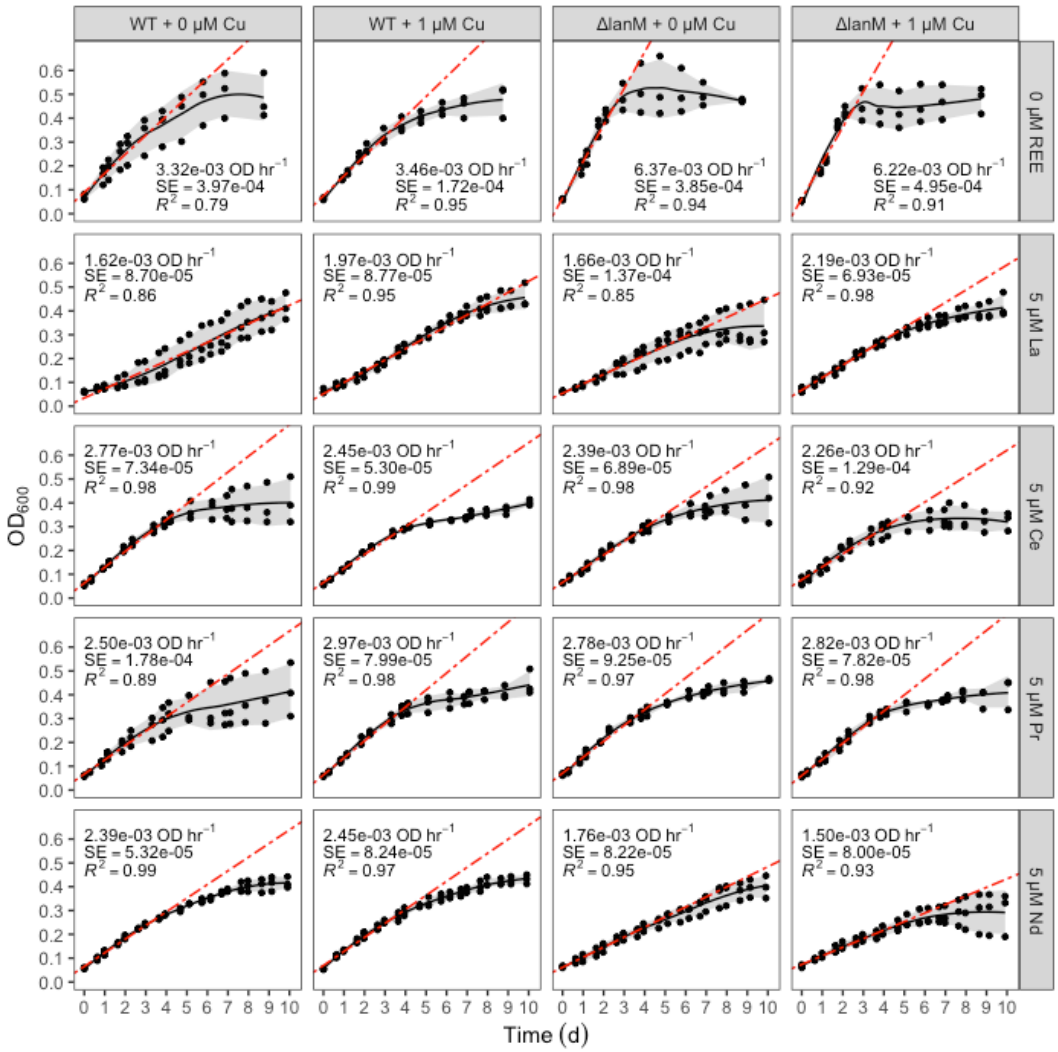

Figure 5.5. Growth of *Msn. trichosporium* OB3b wildtype and Δ*lanM* mutant in the presence and absence of copper and various REEs. Initial linear growth rate as determined by linear regression (dashed red line), standard error of growth rate, and R^2 value are provided in the panel.

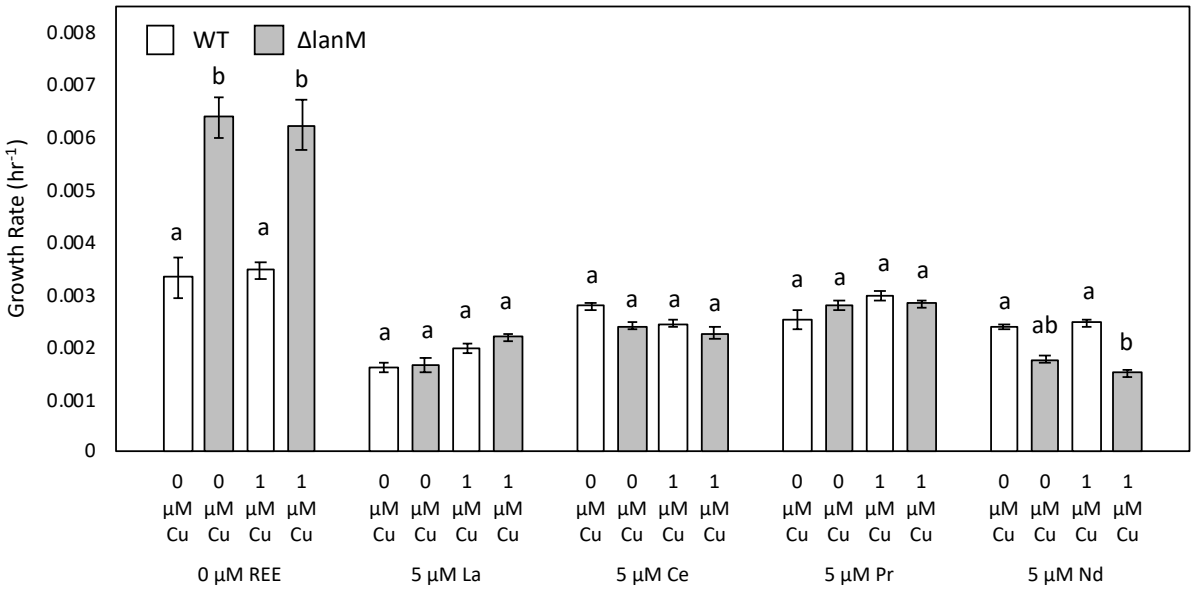

Figure 5.6. Growth rates of *Msn. trichosporium* OB3b wildtype and Δ*lanM* mutant in the presence and absence of copper and various REEs. Error bar indicates standard error of growth rate determined through linear regression. Line above bars indicate statistically significant difference within REE group determined through analysis of covariance (ANCOVA).

The copper and REE uptake rates were not affected by the deletion of *lanM*, as the amount of metals associated with the biomass of the wildtype and *ΔlanM* mutant was comparable (Figure 5.7). That is, significantly greater amount of copper was found associated with the biomass in the presence of copper with no REE, La, and Nd, for both wildtype and mutant. The only significantly different REE uptake rate is observed in the presence of Ce, where the wildtype uptakes more Ce in the presence of copper, whereas the *ΔlanM* mutant acquires comparable amount of Ce in both the absence and presence of copper.

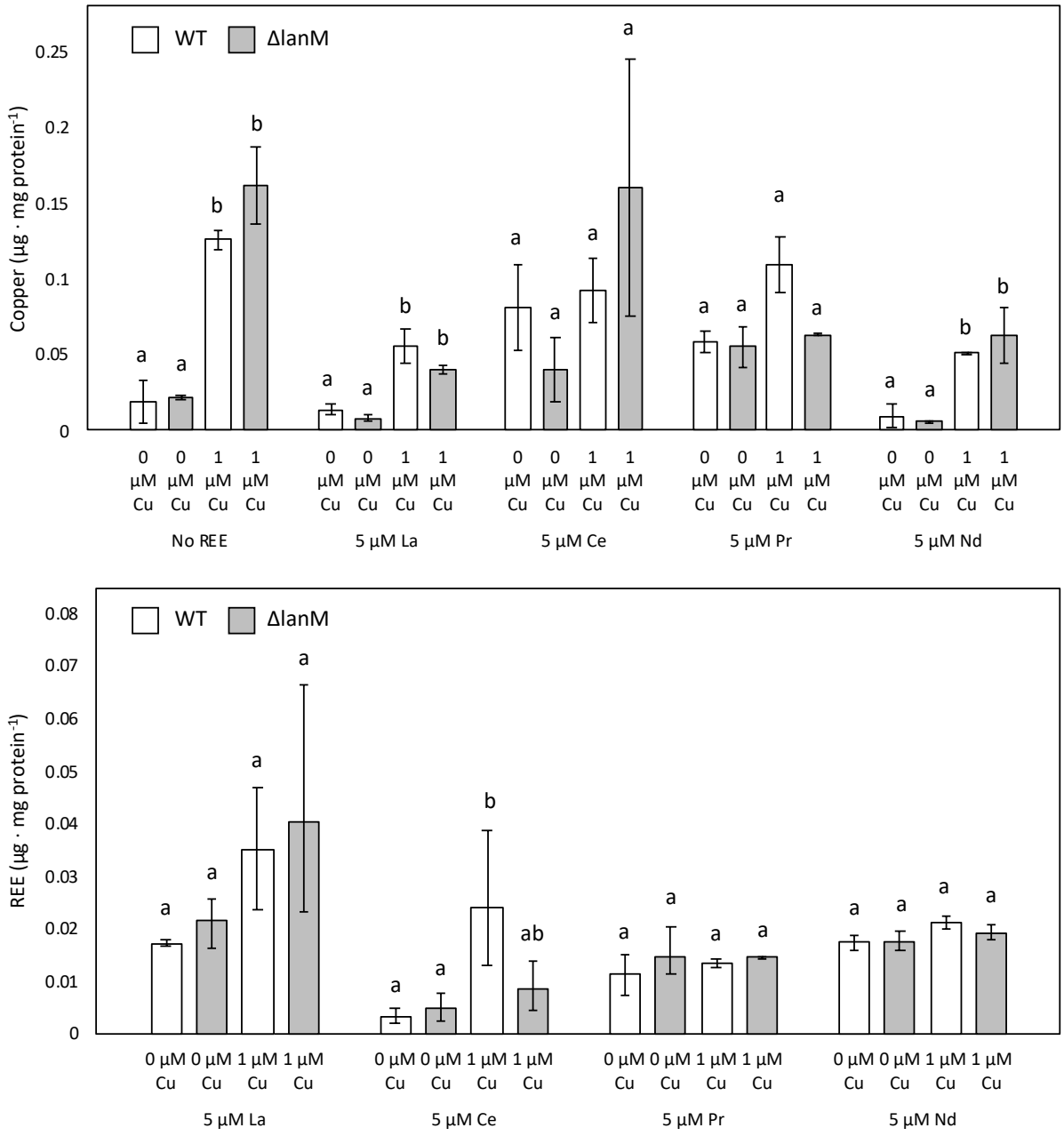

Figure 5.7. Metal uptake by *Msn. trichosporium* OB3b wildtype and Δ*lanM* mutant grown in the presence and absence of copper and various REEs. Error bar indicates range of biological duplicate or triplicate. Lines over bars indicate statistically significant difference determined through Tukey's HSD test ($p < 0.05$).

In addition, the deletion of *lanM* did not affect the copper switch, evidenced by the higher expression of *mmoX* and *mbnA* at low copper concentration and *pmoA* at higher copper concentration (Figure 5.8). Expression of *xoxF* was also unaffected. These results collectively suggest that *lanM* is not involved in REE uptake or the REE switch in *Msn. trichosporium* OB3b.

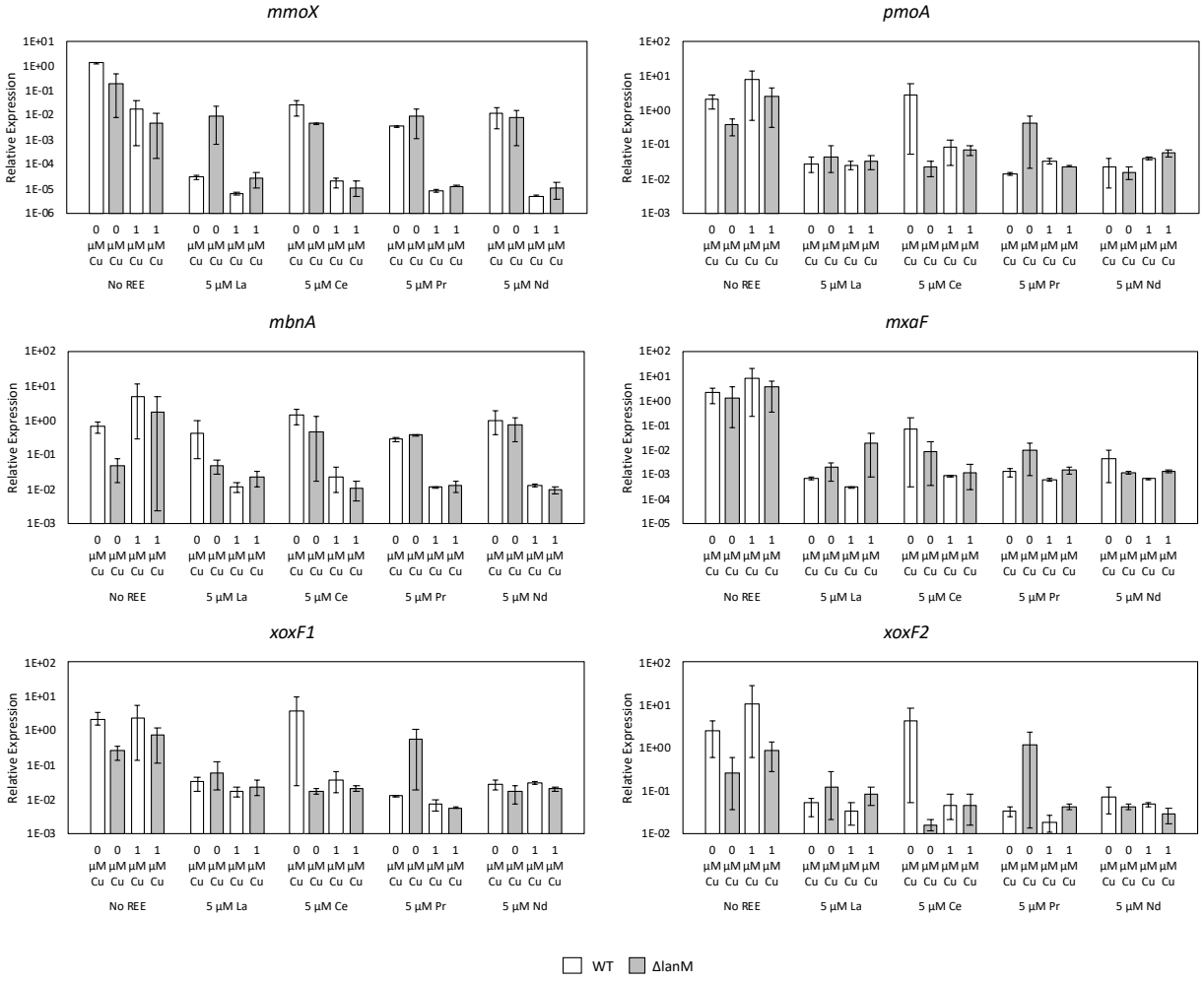

Figure 5.8. Change in gene expression in *Msn. trichosporium* OB3b wildtype and Δ*lanM* mutant grown in the presence and absence of copper and various REEs. Error bar indicates range of biological duplicate or triplicate.

Finally, the MeHg degradation rates of *Msn. trichosporium* OB3b wildtype and *ΔlanM* mutant were assessed. *Msn. trichosporium* OB3b wildtype continuously degraded MeHg over the course of 5 days to approximately 50% of the original MeHg, whereas the *ΔlanM* mutant was unable to degrade MeHg regardless of the addition of copper and/or cerium (Figure 5.9).

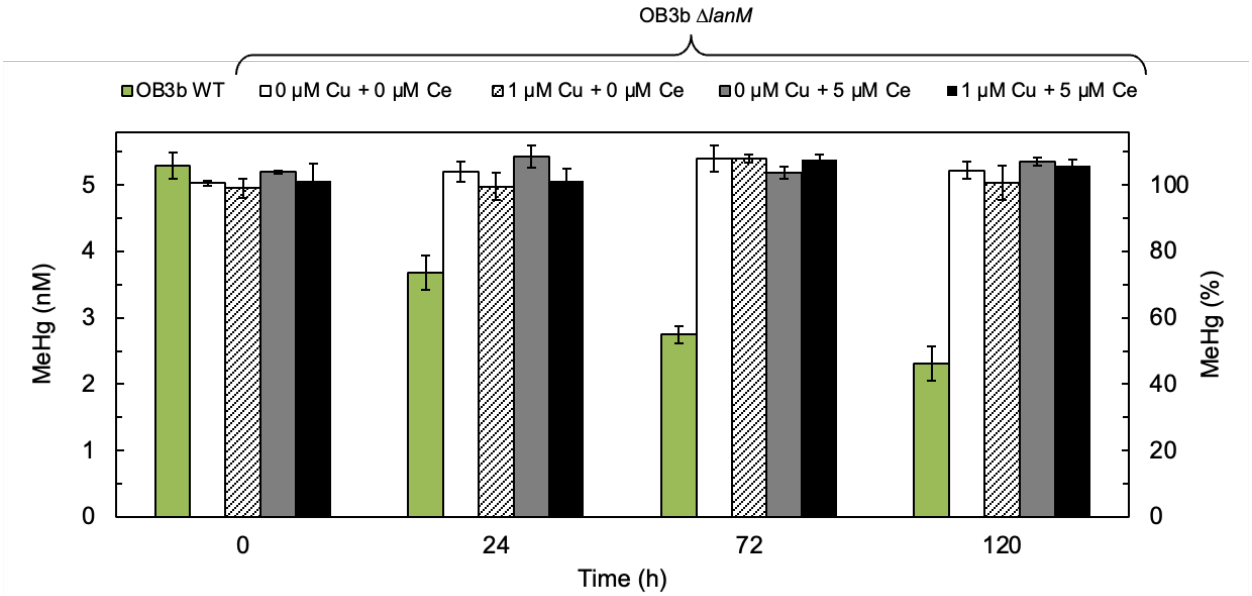

Figure 5.9. MeHg demethylation by *Msn. trichosporium* OB3b wildtype and Δ*lanM* mutant grown in the presence and absence of copper and cerium. Error bar indicates standard deviation of biological triplicate.

5.4. Methylmercury demethylation by spheroplasts of *Msn. trichosporium* OB3b *mbnT*::Gm^r

In order to further confirm whether one or more of the periplasmic constituents are responsible for MeHg degradation, spheroplasts of *Msn. trichosporium* OB3b *mbnT*::Gm^r were prepared via lysozyme and osmotic shock treatments, and then assayed for MeHg degradation. The *mbnT*::Gm^r mutant rather than the wildtype was selected for this purpose, as it was expected not to degrade MeHg due to deficiency in MB uptake (Gu et al., 2016a; Lu et al., 2017). However, since MB, Xox-MeDH, and LanM are required for methanotrophic-mediated MeHg degradation, the periplasmic fraction of the *mbnT*::Gm^r mutant, in theory, should be able to degrade MeHg. The formation of spheroplasts was confirmed via microscopy after staining the cells with crystal violet. After 4 h of treatment, spheroplasts were visible as round cells as opposed to the rod-shaped whole cells (Figure 5.10).

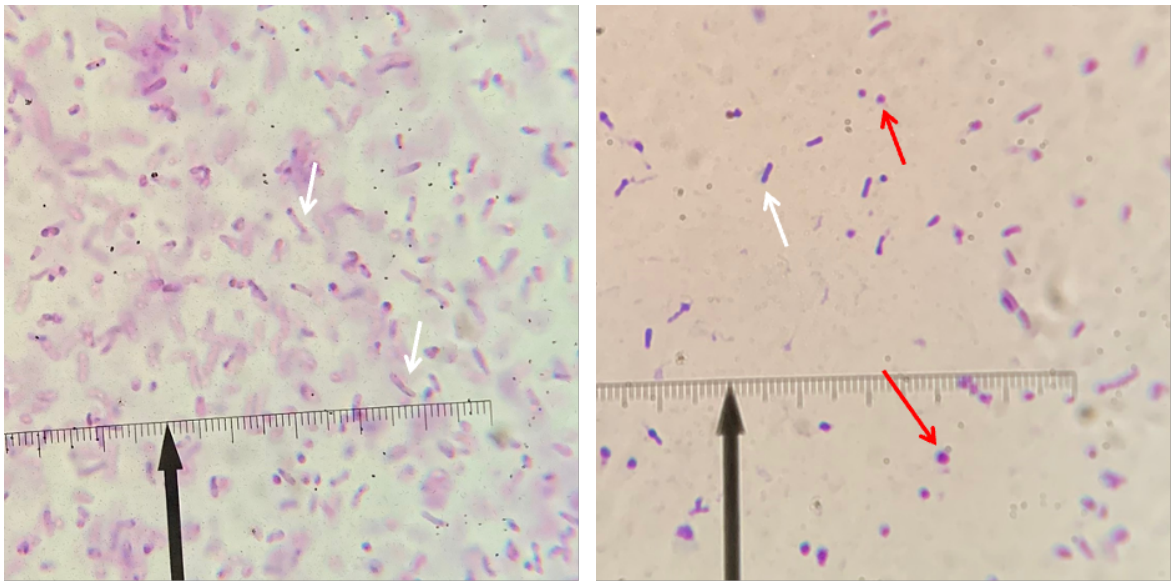

Figure 5.10. *Msn. trichosporium* OB3b *mbnT*::Gm^r before and after spheroplast formation at t = 0 h and t = 4 h, respectively, magnified to 400×. Intact cell and spheroplasts were stained with crystal violet and are indicated by white and red arrows, respectively.

Msn. trichosporium OB3b *mbnT*::Gm^r was able to degrade approximately 90% of the MeHg over 120 h regardless of the copper concentration (Figure 5.11). However, the spheroplast prepared from the same culture could only degrade ~30%, and no significant degradation was observed beyond 12 h. The fraction containing the periplasm and outer-membrane debris, in fact, exhibited a greater rate of MeHg degradation of approximately 60%-75% as compared to the spheroplast.

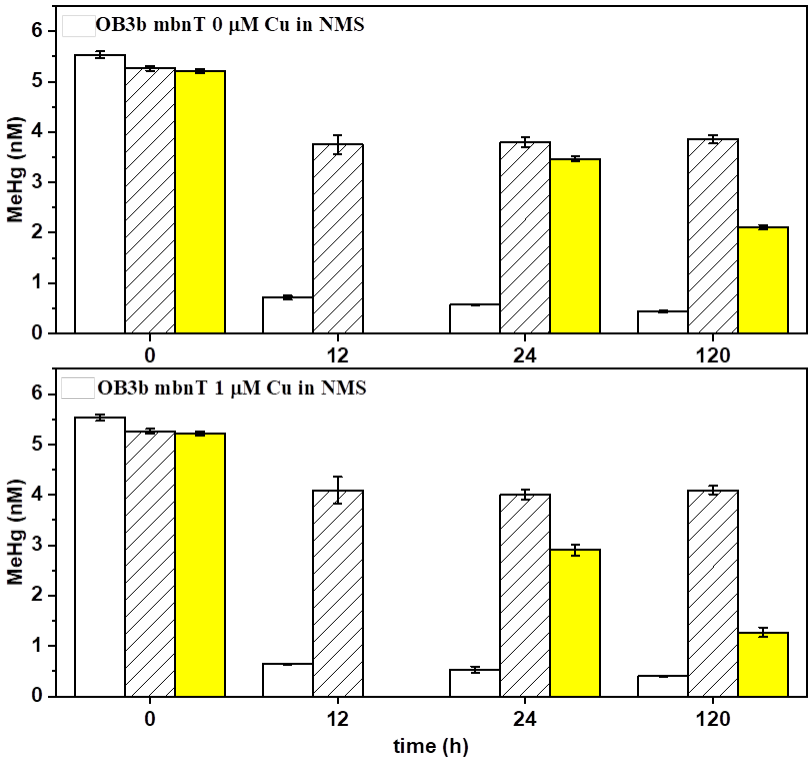

Figure 5.11. MeHg degradation by *Msn. trichosporium* OB3b *mbnT*::Gm^r grown in the absence and presence of 1 µM copper. Whole cell (☐), spheroplast (▨), and periplasm (▬) fractions.

5.5. Discussion

It has been shown that MB serves as a delivery mechanism for MeHg into the cell, and that Xox-MeDH has an important role in demethylating the delivered MeHg (Lu et al., 2017). Here we provide additional evidence for the mechanism of MeHg demethylation in methanotrophs by showing that the periplasm fraction is key in this process. *Msn. trichosporium* OB3b *mbnT*::Gm^r stripped of its periplasm, where Xox-MeDH and lanmodulin is located, had significantly lower rate of MeHg degradation (Figure 5.11). The amount of MeHg degradation by the spheroplasts can be attributed to incomplete spheroplast formation (Figure 5.10) or partial reconstitution of the periplasm and outer cell membrane after lysozyme and osmotic shock treatments. Also, surprisingly, whole cells of *Msn. trichosporium* OB3b *mbnT*::Gm^r was able to degrade MeHg despite the disrupted MB uptake system (Gu et al., 2016a). Nonetheless, it is important to note that the amount of MeHg degraded by the periplasm fraction is significantly greater than that of the spheroplasts. This indicates that one or more of the components residing in the periplasm, Xox-MeDH and most likely LanM, is important for MeHg degradation.

There exists another *mbnT* (ADVE02_v2_10210) on the chromosome of *Msn. trichosporium* OB3b that is highly similar (57.36% identity; E value = 0) to that found in *Methylocystis* sp. SB2 (MSB2v1_460017). The *Msn. trichosporium* OB3b mutant with this second *mbnT* deleted could not degrade MeHg, regardless of the absence or presence of MB (unpublished data; Peng et al., 2021). It may be that along with the uptake of MB, a signaling cascade mediated by MbnTs is involved in the MeHg degradation process. That is, it was shown that the two *mbnTs* found in *Msn. trichosporium* OB3b is critical for the "copper switch", as deletion of both broke the switch. The results of the spheroplast experiment using this mutant may provide further insight into the mechanism of MeHg degradation by methanotrophs.

The REE switch and uptake in *Msn. trichosporium* OB3b was not affected by the deletion of *lanM*, suggesting that LanM is not involved in these processes. These results agree with previous findings, where *lanM* mutants constructed in model methylotrophs *Methylorubrum extorquens* AM1 and PA1 did not exhibit any phenotypical difference compared to their wildtype counterparts (Ochsner et al., 2019; Roszczenko-Jasińska et al., 2020). Rather, the disruption of the TonB-dependent transporter and/or ABC-transporter associated with *lanM* affected REE uptake and REE-dependent growth on methanol (Ochsner et al., 2019; Roszczenko-Jasińska et al., 2020). However, *Msn. trichosporium* OB3b Δ*lanM* did completely lose its ability to degrade MeHg, suggesting that LanM is critical for MeHg degradation.

It is clear that LanM does not affect the REE switch and uptake. Another possibility that was not explored in detail here is that LanM may be involved in discriminating between early and late REEs in the cells, as previously suggested (Cotruvo et al., 2018). That is, lanthanum through samarium cause conformational change to LanM upon binding, and also induce expression of *xoxF1* in *Mrr. extorquens* (Vu et al., 2016). However, deletion of *lanM* did not affect uptake of REEs nor expression of MeDH in *Msn. trichosporium* OB3b, suggesting it does not have a regulatory role. An *in vitro* assay of Xox-MeDH activity using methanol and MeHg as substrates with LanM in the reaction matrix may help understand the exact role of LanM, as well as the mechanism of MeHg degradation.

Considering the importance of the periplasm and the role of Xox-MeDH in MeHg degradation, it may be that LanM is responsible for coordinating REEs for Xox-MeDH activity at least in *Msn. trichosporium* OB3b. However, this mechanism does not explain MeHg degradation by *Msn. trichosporium* OB3b observed in the absence of REEs (Figure 5.3; unpublished data), nor the lack of LanM in methanotrophs in classes other than

Alphaproteobacteria (Table 1.2) (Kang et al., 2019). Further investigation is required to delineate the underlying mechanism of MeHg degradation by methanotrophs.

Chapter 6 Methanotrophs Isolated from Mercury Contaminated Site

6.1. Introduction

The toxicity of mercury can vary depending on its speciation, where methylation can increase bioavailability which consequently increases toxicity (Tchounwou et al., 2012). Mercury speciation in the environment is influenced by various biotic and abiotic processes. Of these processes, methylation and demethylation by microorganisms have been extensively examined. That is, the two-gene cluster *hgcAB*, found in some anaerobic microbes, is responsible for mercury methylation (Gilmour et al., 2013; Parks et al., 2013; Smith et al., 2015), whereas *merB*, encoding for the canonical organomercurial lyase, is responsible for methylmercury (MeHg) demethylation (Weiss et al., 1977; Ogawa et al., 1984; Barkay et al., 2003; Schaefer et al., 2004).

In addition to the microbes harboring *hgcAB* and *merB*, methanotrophs have also been found to have intriguing interactions with mercury (Lu et al., 2017; Semrau et al., 2010, 2018). Specifically, some methanotrophs can produce ribosomally synthesized post-translationally modified polypeptide – methanobactin – that not only will bind Hg(II) in the environment to reduce its toxicity to the general microbial community, but can also bind the more toxic and bioavailable MeHg and deliver it into the periplasm where MeHg is then demethylated (Baral et al., 2014; Lu et al., 2017; Vorobev et al., 2013). However, the novel mechanism by which methanotrophs degrade MeHg does not involve the canonical MerB, but instead requires methanobactin and the rare earth element-dependent methanol dehydrogenase – Xox-MeDH (Lu et al., 2017). Methanotrophic-mediated MeHg degradation, unlike that facilitated by MerB,

occurs under environmentally relevant conditions, i.e., circumneutral pH, nM/pM range of MeHg (Lu et al., 2017). Thus, it appears methanotrophs may play an important role in controlling mercury speciation and toxicity in the environment, and characterizing methanotrophs in mercury-contaminated sites may provide insight into the significance of methanotrophic-mediated MeHg degradation and its impact *in situ*.

The Department of Energy (DOE) Y-12 National Security Complex in Oak Ridge, Tennessee, was built in the 1940s for metal isotope separation as part of the Manhattan Project during World War II (Brooks & Southworth, 2011). Mercury was extensively used in these metal separation processes at the Y-12 plant, and approximately 11,000 t of mercury was received there over the course of its operation (Brooks & Southworth, 2011), and resulted in the release of more than 200 t of mercury with the process water into the nearby watershed in the 1950s and 1960s (Barnett et al., 1997). Included in this watershed is the East Fork Poplar Creek (EFPC), where numerous efforts were made to assess mercury speciation and distribution (Revis et al., 1989; Barnett et al., 1995; Harris et al., 1996; Demers et al., 2018) and to remediate mercury contamination (Southworth et al., 2002; Brooks & Southworth, 2011; Peterson et al., 2018). The impact of geochemical properties on mercury cycling was also determined in later studies (Dong et al., 2010; Brooks et al., 2018), as well as the impact of mercury on microbial community in EFPC to identify potential mercury methylators (Vishnivetskaya et al., 2011; Mosher et al., 2012; Kim et al., 2021).

However, much work is still required to explain the role of methanotrophs in mercury speciation and toxicity in mercury-contaminated sites such as EFPC. Therefore, in this study, two strains of methanotrophs – *Methylomonas* sp. strain EFPC1 and *Methylococcus* sp. strain EFPC2 – were isolated from the stream of EFPC, and their genomes were subsequently

sequenced. Further characterization of these methanotrophs may provide insight into the mechanism of methanotrophic-mediated MeHg degradation as well as its ecological significance.

6.2. Microscopy of Gram-stained cell

Cells from pure cultures of *Methylomonas* sp. strain EFPC1 appeared rod-shaped, as summarized earlier for methanotrophs of the *Methylomonas* genus (Semrau et al., 2010), non-flagellated, and were Gram-negative (Figure 6.1). Cells of *Methylococcus* sp. strain EFPC2 were coccoid (Semrau et al., 2010), non-flagellated, and were Gram variable (Figure 6.2), though phylogenetically close neighbors *Methylococcus geothermalis* IM1 (Awala et al., 2020), *Methyloterricola oryzae* 73a (Frindte et al., 2017b), "*Candidatus* Methylospira mobilis" strain Shm1 (Danilova et al., 2016), *Methylococcus capsulatus* Bath (Foster & Davis, 1966), and *Methylocaldum marinum* S8 (Takeuchi et al., 2014a) all stain Gram-negative.

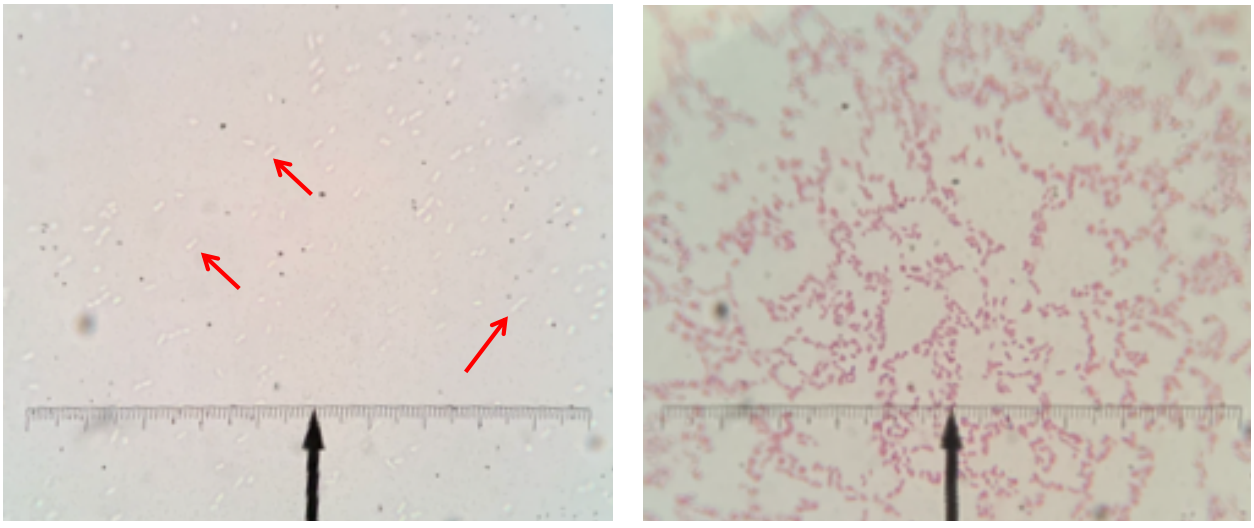

Figure 6.1. *Methylomonas* sp. strain EFPC1 before and after Gram-staining, magnified to 400×. Cells indicated by red arrows.

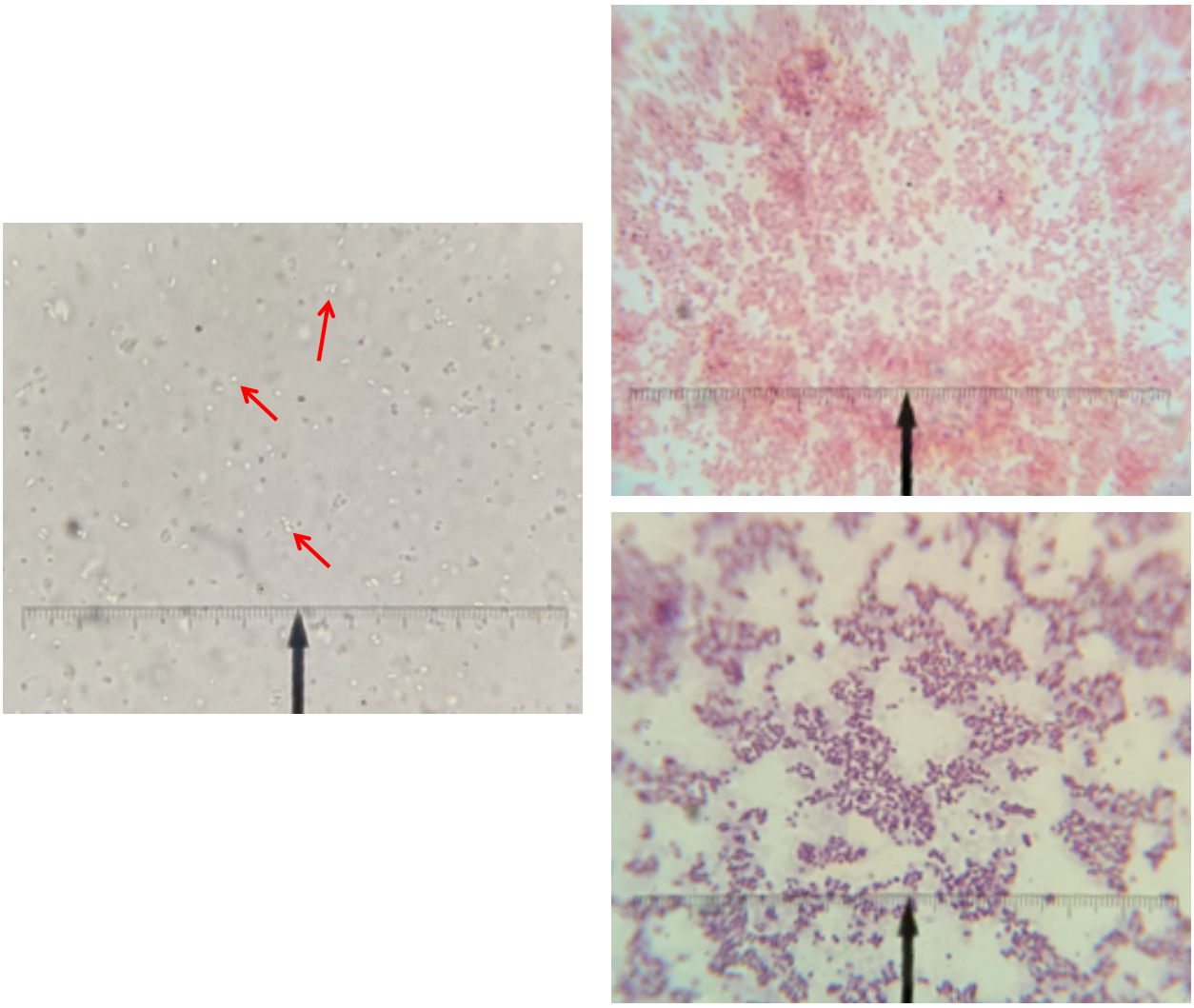

Figure 6.2. *Methylococcus* sp. strain EFPC2 before and after Gram-staining, magnified to 400×. Cells indicated by red arrows.

6.3. Genome assembly and annotation

The genomes of *Methylomonas* sp. strain EFPC1 and *Methylococcus* sp. strain EFPC2 were 4.99 Mbp and 4.56 Mbp (96% and 95.2% completion), consisting of either 1 chromosome + 1 plasmid (for *Methylomonas* sp. strain EFPC1; Figure 6.3) or 1 chromosome + 2 plasmids (for *Methylococcus* sp. strain EFPC2; Table 6.1, Figure 6.4 and Figure 6.5). All chromosomes and plasmids were circularized, then rotated according to the starting gene via Unicycler and were visually inspected using Bandage.

Table 6.1. General features of *Methylomonas* sp. strain EFPC1 and *Methylococcus* sp. strain EFPC2 genomes.

Feature	*Methylomonas* sp. strain EFPC1	*Methylococcus* sp. strain EFPC2
Complete genome size (bp)	4,993,755	4,558,902
Number of plasmids	1	2
Plasmid size (bp)	70,104	89,615 25,893
G+C (%)	51.8	61.2
Total # of coding sequences	4,488	3,891
# of features on plasmid(s)	163	231 61
No. of rRNA genes (16S, 23S, 5S)	9	9
No. of tRNA genes	47	50
Methane monooxygenases present	pMMO, pXMO, sMMO	pMMO
No. of Illumina reads (Accession number)	2,230,538 (SRX10121820)	2,379,682 (SRX10121822)
No. of GridION reads (Accession number)	232,890 (SRX10121821)	135,052 (SRX10121823)
N50 of GridION reads (bp)	51,070	50,620
GenBank accession numbers	CP070494, CP070495	CP070491, CP070492, CP070493
Closest neighbor based on 16S rRNA sequence	*Methylomonas* sp. LW13	*Methylococcus geothermalis* IM1^T
16S rRNA similarity with closest neighbor (%)	99.87	96.30
ANI with closest neighbor (%)[a]	95.20	72.70
dDDH with closest neighbor (%)[b]	64.60	20.00

[a] Average nucleotide identity
[b] Digital DNA-DNA hybridization

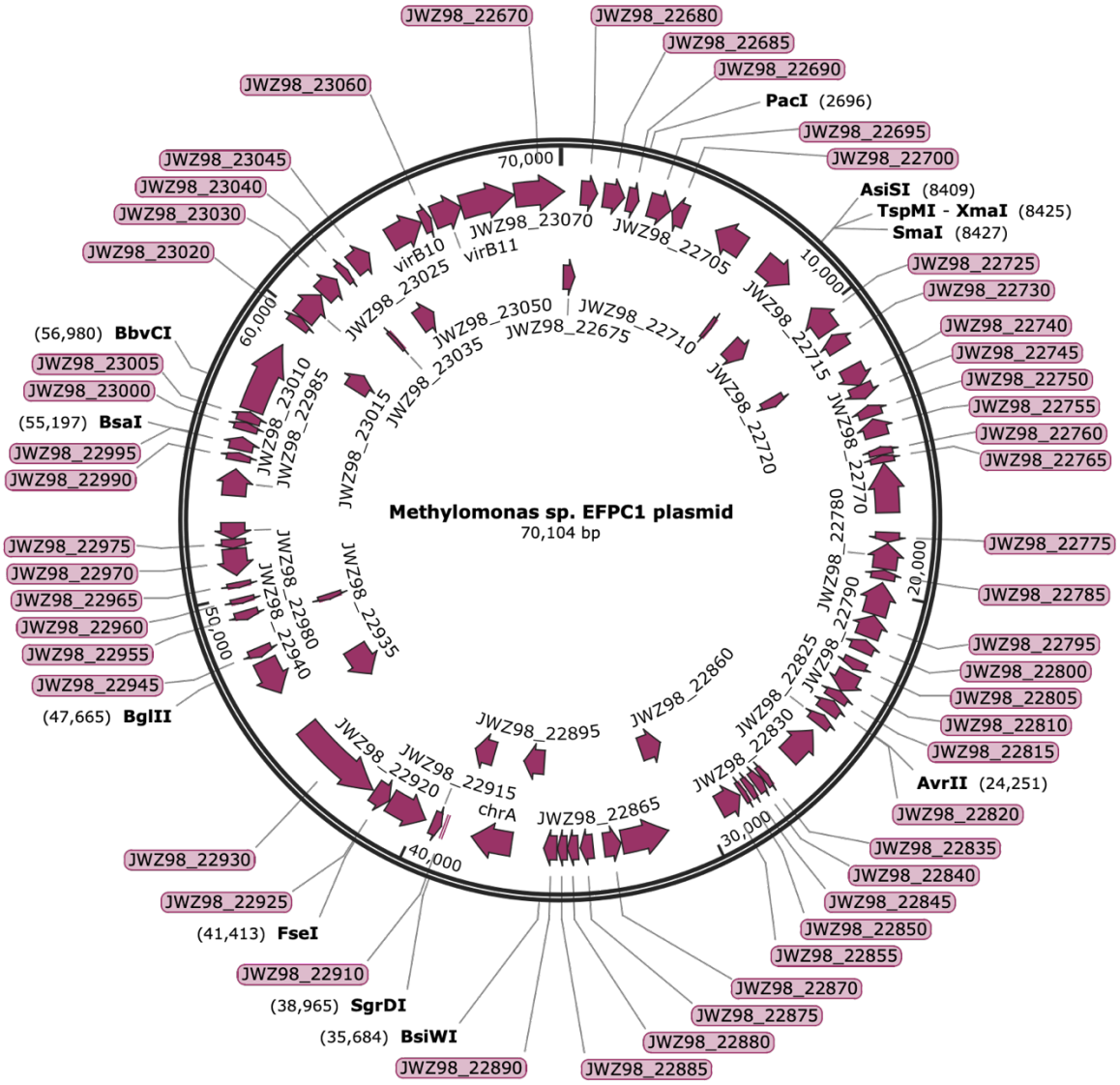

Figure 6.3. Map of plasmid in *Methylomonas* sp. strain EFPC1.

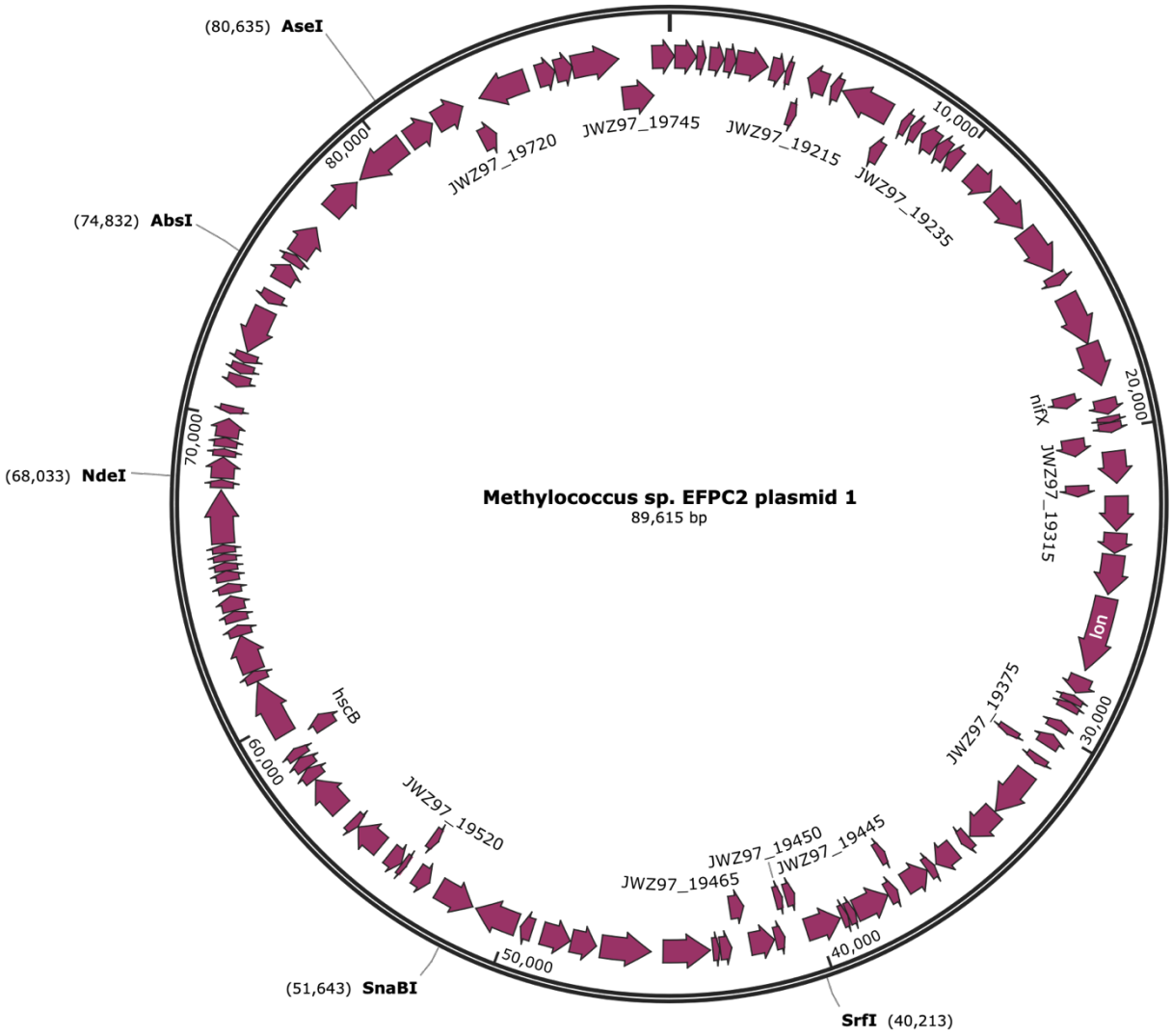

Figure 6.4. Map of plasmid 1 in *Methylococcus* sp. strain EFPC2.

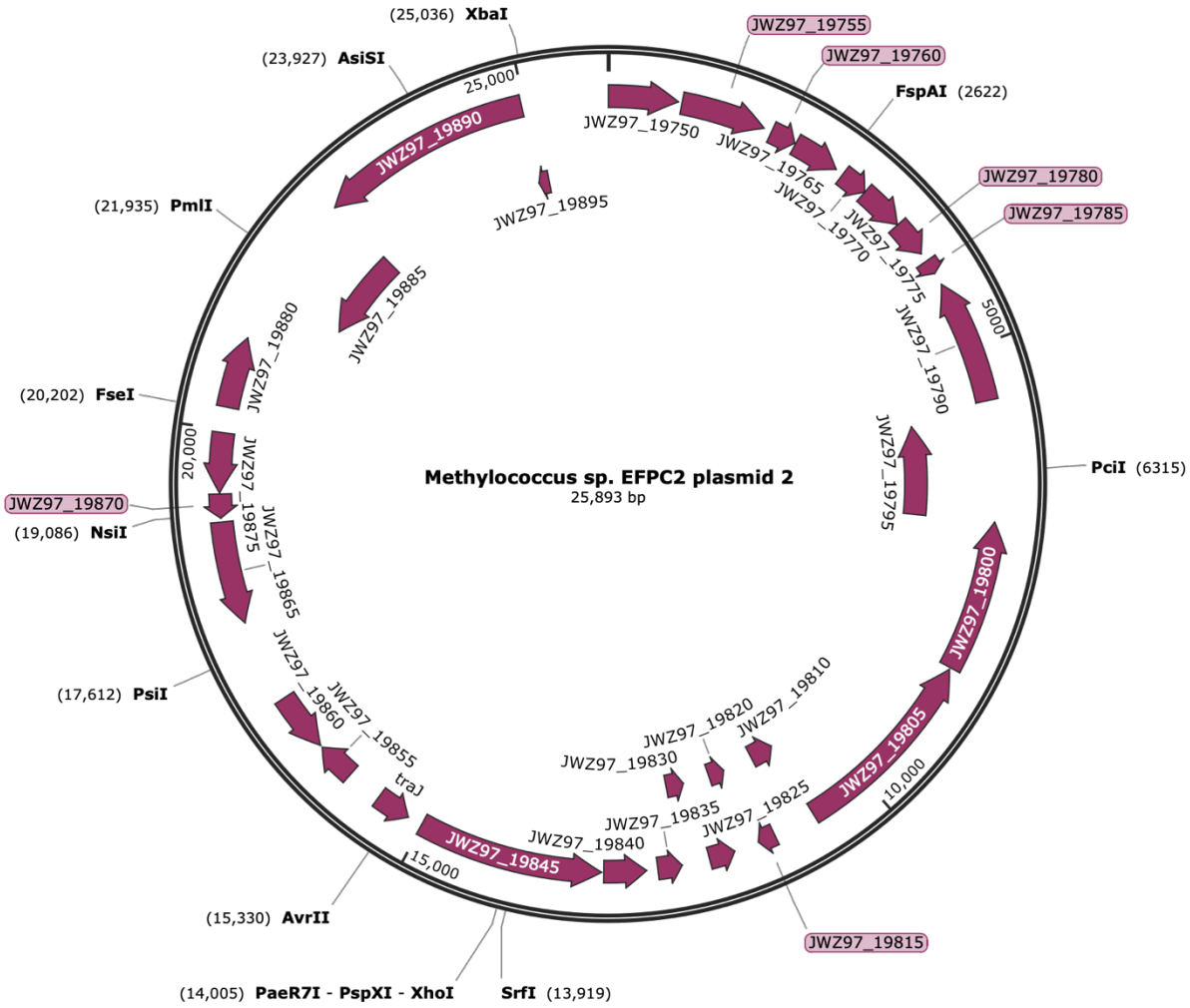

Figure 6.5. Map of plasmid 2 in *Methylococcus* sp. strain EFPC2.

6.4. Phylogenetic analysis of 16S rRNA and *pmoCAB*

16S rRNA sequences from the genome of *Methylomonas* sp. strain EFPC1 and *Methylococcus* sp. strain EFPC2 were used as queries for BLAST search to find those that are most similar. The results indicated that *Methylomonas* sp. strain EFPC1 was phylogenetically similar to *Methylomonas* sp. LW13 (Kalyuzhnaya et al., 2015a) (Table 6.2) and *Methylococcus* sp. strain EFPC2 was most similar to *Mcc. geothermalis* IM1 (Awala et al., 2020) (Table 6.3). Average nucleotide identity values between *Methylomonas* sp. strain EFPC1 with *Methylomonas* sp. LW13 and *Methylococcus* sp. strain EFPC2 with *Methylococcus* sp. IM1^{T} were approximately 95% and 73%, respectively (Yoon et al., 2017) (Table 6.1). Digital DNA-DNA hybridization values determined using the Genome Blast Distance Phylogeny algorithm (Meier-Kolthoff et al., 2013) were less than 70% between both novel isolates and their closest phylogenetic relatives (Table 6.1). These results indicate that *Methylococcus* sp. strain EFPC2 may be considered a new species.

Phylogeny constructed based on the 16S rRNA gene placed *Methylomonas* sp. strain EFPC1 with other methanotrophs of the *Methylomonas* genus, and *Methylococcus* sp. strain EFPC2 with those of the *Methylococcus* genus (Figure 6.6). *Methylomonas* sp. strain EFPC1 is most likely a variant strain and does not constitute a novel species. However, despite the fact that *Methylococcus* sp. strain EFPC2 did form a monophyletic group with other *Methylococcus* species, it was least similar to others with high bootstrap value (100%), even more so than the recently discovered novel species *Mcc. geothermalis* IM1 (Awala et al., 2020). The 16S rRNA gene based phylogeny therefore provides additional evidence to support that *Methylococcus* sp. strain EFPC2 is a novel species.

Table 6.2. Methanotrophs most similar to *Methylomonas* sp. strain EFPC1 as determined by BLAST search based on 16S rRNA gene sequence.

Organism	Total Score	E value	Identity (%)	Accession
Methylomonas sp. LW13	8468	0	99.87	CP033381.1
Methylomonas denitrificans FJG1	8368	0	99.48	CP014476.1
Methylomonas sp. Kb3	2713	0	99.53	KM995837.1
Methylomonas sp. R-45371	2706	0	99.53	FR798957.1
Methylomonas sp. R-45362	2706	0	99.53	FR798952.1
Methylomonas methanica	2706	0	99.40	AF150806.1
Methylomonas sp. R-45375	2702	0	99.46	FR798961.1
Methylomonas sp. LL1	8102	0	98.44	CP064653.1
Methylomonas sp. R-45372	2689	0	99.33	FR798958.1
Methylomonas sp. R-45363	2689	0	99.33	FR798953.1

Table 6.3. Methanotrophs most similar to *Methylococcus* sp. strain EFPC2 as determined by BLAST search based on 16S rRNA gene sequence.

Organism	Total Score	E value	Identity (%)	Accession
Methylococcus geothermalis IM1	5039	0	96.29	CP046565.1
Methyloterricola oryzae 73a	2481	0	95.84	MW390553.1
"*Candidatus* Methylospira mobilis" strain Shm1	7365	0	95.51	CP044205.1
Methylococcus capsulatus Bath	4855	0	95.25	AE017282.2
Methylococcus capsulatus Texas	2324	0	95.01	NR_042183.1
Methylococcus sp. strain BF19-07	2290	0	94.72	MT509869.1
Methylococcus capsulatus strain Cla	2246	0	94.86	JN166980.1
Methylococcus sp. RD4	2242	0	95.27	KU517778.1
Methylococcus capsulatus strain GDS2_4	2241	0	95.69	MN511721.1
Methylocaldum marinum S8	4316	0	92.03	AP017928.1

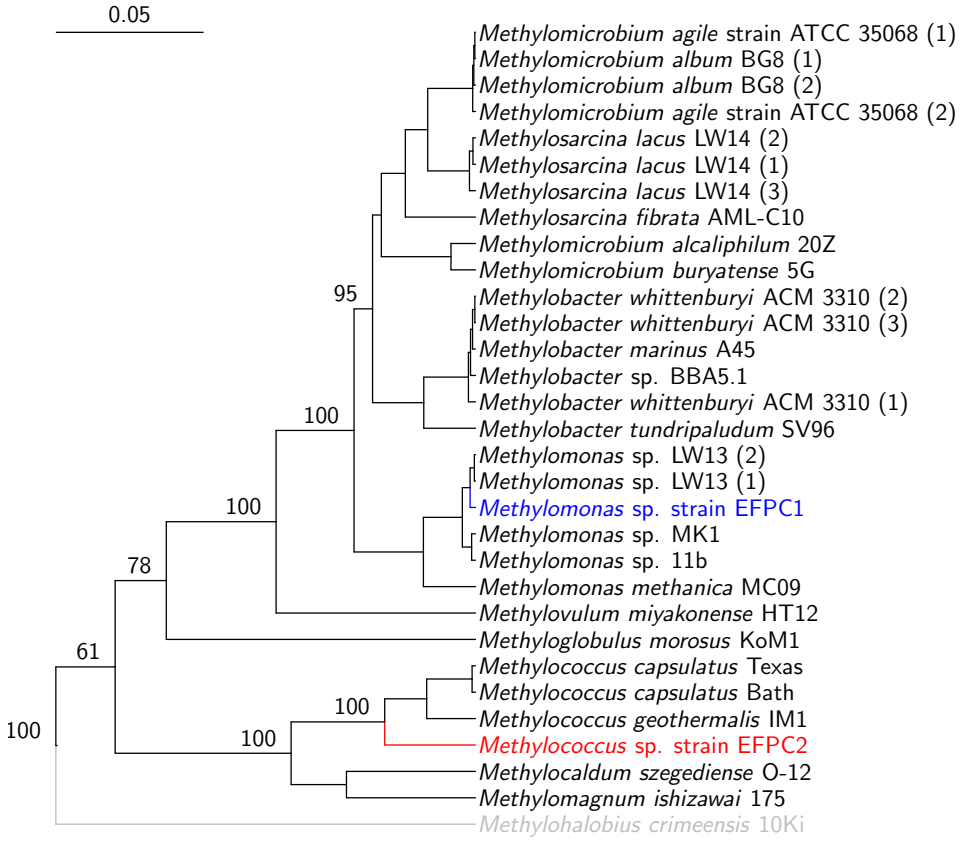

Figure 6.6. Bayesian phylogeny based on 16S rRNA gene. The tree was constructed using the general time-reversible model with invariant sites and four distinct gamma categories (GTR+I+G) under a strict clock with a minimum nucleotide sequence length of 1277. Node values indicate posterior probabilities based on 10,000,000 iterations with a burn-in of 25%. The scale bar represents 0.05 changes per nucleotide position. All methanotrophs belong to the *Methylococcaceae* family, except one from the *Methylothermaceae* family shown in gray.

Phylogeny constructed based on the concatenated *pmoCAB* sequence was similar to that of the 16S rRNA gene (Figure 6.7). However, there was a clear divergence that resulted in two distinct clades, which was not due to the absence of a significant outgroup as evidenced by identical structure found in a tree that included methanotrophs of other genera (Figure 3.3, pg. 117). Nonetheless, *Methylomonas* sp. strain EFPC1 formed a clade with other *Methylomonas* species. Both of the two *pmoCAB* operons found in *Methylococcus* sp. strain EFPC2, however,

formed a paraphyletic group with those from other *Methylococcus* species, and were more closely associated with *pmoCAB* operons from *Methylomagnum ishizawai* 175 with high bootstrap value (100%). Considering the fact that the topology of the phylogenetic tree based on 16S rRNA genes was conserved in the tree based on *pmoCAB* (Figure 3.2, pg. 116; Figure 3.3, pg. 117), the placement of *pmoCAB* from *Methylococcus* sp. strain EFPC2 in this tree (Figure 6.7) may again suggest that this methanotrophs is a novel species, distinct from others of the *Methylococcus* genus.

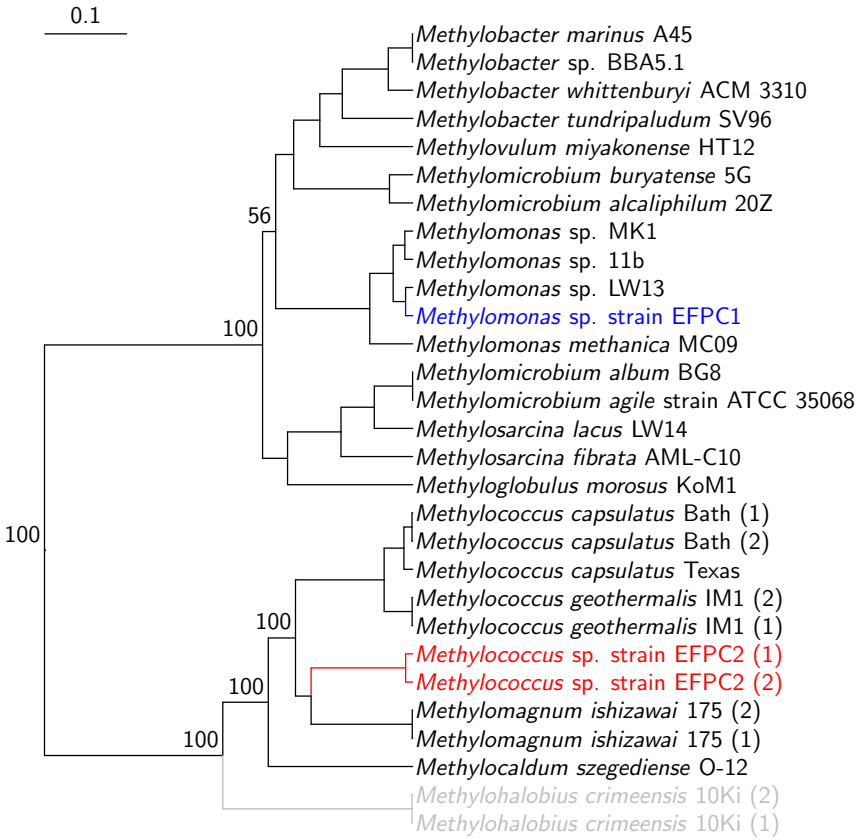

Figure 6.7. Bayesian phylogeny based on concatenated *pmoCAB*. The tree was constructed using the general time-reversible model with invariant sites and four distinct gamma categories (GTR+I+G) under a strict clock with a minimum nucleotide sequence length of 2085. Node values indicate posterior probabilities based on 10,000,000 iterations with a burn-in of 25%. The scale bar represents 0.1 changes per nucleotide position. All methanotrophs belong to the *Methylococcaceae* family, except one from the *Methylothermaceae* family shown in gray.

6.5. Genes and metabolic pathways

One copy of each genes encoding for particulate methane monooxygenase (*pmoCAB*) and soluble methane monooxygenase (*mmoXYBZDC*) were found in *Methylomonas* sp. strain EFPC1 for methane oxidation, along with one copy of the divergent form of the particulate methane monooxygenase (*pxmABC*) (Table 6.4). In *Methylococcus* sp. strain EFPC2, two copies of *pmoCAB* and an orphan copy of *pmoC* were found, but no evidence of genes for soluble methane monooxygenase was found. One copy of genes for methanol dehydrogenase (*mxaFJGI*) was found in both strains, but only *Methylococcus* sp. strain EFPC2 contained all genes for an alternative, lanthanide dependent methanol dehydrogenase (*xoxFJG*). Both genomes contained genes for the tetrahydromethanopterin (*fae*, *mtdA*, *fhcCDAB*, *mch*, *mtdB*) and tetrahydrofolate (*fhs*, *folD*, *mtdA*, *fch*) pathways for C_1 transfer, NAD-linked formate dehydrogenase (*fdsABGCD*), and the tricarboxylic acid cycle (Table 6.5 and Figure 6.8).

For carbon assimilation pathways, both genomes contained the complete ribulose monophosphate pathway (Table 6.5 and Figure 6.8). The serine cycle, however, was incomplete in both strains, as well as the CBB cycle.

Copper uptake and storage systems such as *corAB*/*mopE* + cytochrome *c* peroxidase, *mbnABCM*, and *csp*, and rare earth element-binding protein, *lanM*, were not found in either strain (Table 6.4). However, the periplasmic copper uptake system *copCD* was found in both strains. Putative TonB-dependent transporters similar to the methanobactin uptake protein, MbnT, were also identified (Table 6.6 and Table 6.7). Both isolates had putative MbnTs that were more similar to that of *Methylosinus trichosporium* OB3b than *Methylocystis* sp. SB2. In addition, *merB* encoding for the canonical organomercurial lyase was not found in either of the strains.

Table 6.4. Presence of select genes in *Methylomonas* sp. strain EFPC1 and *Methylococcus* sp. strain EFPC2.

Gene(s)	*Methylomonas* sp. strain EFPC1	*Methylococcus* sp. strain EFPC2
pmoCAB	JWZ98_20700 – 20690	JWZ97_03600 – 03610 JWZ97_16375 – 16385
Orphan *pmoC*	0	JWZ97_06950
pxmABC	JWZ98_21800 – 21790	0
mmoXYBZDC	JWZ98_21560 – 21585	0
xoxFJG/FGJ	0	JWZ97_15225 – 15235 (*xoxFJG*)
xoxFJ	JWZ98_17905 – 17910	JWZ97_07535 – 07540
Orphan xoxF	0	JWZ97_15975
mxaFJGI	JWZ98_12100 – 12085	JWZ97_00520 – 00535
Formate dehydrogenase	JWZ98_05300 (*fdsG*) JWZ98_05295 (*fdsB*) JWZ98_05290 (*fdhA*) JWZ98_05285 (*fdhD*) JWZ98_05280 (*fdsD*)	JWZ97_18590 (*fdsD*) JWZ97_18595 (*fdhD*) JWZ97_18600 (*fdsA*) JWZ97_18605 (*fdsB*) JWZ97_18610 (*fdsG*) JWZ97_13100 (*fdnG*) JWZ97_13145 (*fdsA*) JWZ97_13140 (*fdhB*) JWZ97_13135 (*fdhG*) JWZ97_13110 (*fdhE*)
lanM	0	0
copCD	JWZ98_04645-04640	JWZ97_18245-18240
csp	0	0
corAB	0	0
mopE + cyt *c* peroxidase	0	0
mbnABCM	0	0
nifH	JWZ98_18495	JWZ97_19265 (plasmid 1)

Table 6.5. Carbon metabolism pathways in *Methylomonas* sp. strain EFPC1 and *Methylococcus* sp. strain EFPC2.

Pathway/ Gene	Product	*Methylomonas* sp. strain EFPC1	*Methylococcus* sp. strain EFPC2
TCA Cycle		**Complete**	**Complete**
acn	Aconitate hydratase	JWZ98_11880	JWZ97_01820, JWZ97_04975
icd	Isocitrate dehydrogenase	JWZ98_20755	JWZ97_15995
odh	2-oxoglutarate dehydrogenase complex	JWZ98_13775 – 13780	JWZ97_13365 – 13370
suc	Succinyl-CoA ligase	JWZ98_03740 – 03735	JWZ97_01885 – 01890
sdh	Succinate dehydrogenase	JWZ98_13275 – 13270	JWZ97_13800 – 13805
fum	Fumarate hydratase	JWZ98_00170	JWZ97_07705
mdh	Malate dehydrogenase	JWZ98_08210	JWZ97_11655
-	Citrate synthase	JWZ98_07720, JWZ98_20850	JWZ97_16950, JWZ97_07185
RuMP Cycle		**Complete**	**Complete**
hps	6-Phospho-3-hexuloisomerase (EC 5.3.1.27)	JWZ98_20450, JWZ98_20135	JWZ97_14300
phi	-	JWZ98_20450	JWZ97_14295
pfk	6-Phosphofructokinase	JWZ98_02830	JWZ97_12490
fbaA	Fructose-1,6P aldolase	JWZ98_20430	JWZ97_14700
tkt	Transketolase	JWZ98_20130, JWZ98_20445	JWZ97_15635
tal	Transaldolase	JWZ98_20435	JWZ97_15630
rpe	Pentose-5-phosphate 3-epimerase	JWZ98_15340	JWZ97_14310
rpiA	Ribose 5-phosphate isomerase	JWZ98_04845	JWZ97_15710
Serine Cycle		**Incomplete**	**Incomplete**
glyA	Serine hydroxymethyltransferase	JWZ98_08195	JWZ97_02270
sgaA	Serine-glyoxylate aminotransferase	JWZ98_13285	JWZ97_01305
hprA	Hydroxypyruvate reductase	None	JWZ97_01295
gckA	Glycerate 2-kinase	JWZ98_08200	None
eno	Enolase	JWZ98_05230	JWZ97_11545
ppcA	Phosphoenolpyruvate carboxylase	JWZ98_08730	JWZ97_03325
mdh	Malate dehydrogenase	JWZ98_08210	JWZ97_11655
mtk	Malate thiokinase	None	None
mclA	Malyl coenzyme A lyase	JWZ98_13280	JWZ97_01880

Table 6.5. Continued.

Pathway/ Gene	Product	*Methylomonas* sp. strain EFPC1	*Methylococcus* sp. strain EFPC2
CBB Cycle		**Incomplete**	**Incomplete**
cbbL	Ribulose bisphosphate carboxylase/oxygenase, large subunit	None	JWZ97_14195
cbbS	Ribulose bisphosphate carboxylase/oxygenase, small subunit	None	None
H_4MPT Pathway		**Complete**	**Complete**
fae	Formaldehyde-activating enzyme	JWZ98_02300, JWZ98_04730, JWZ98_12555, JWZ98_13865	JWZ97_13880, JWZ97_16230
mtdA	NADP-Specific H_4MPT dehydrogenase	JWZ98_08205	JWZ97_02310
mtdB	NAD(P)-Dependent methylene-H_4MPT dehydrogenase	JWZ98_15865, JWZ98_15870	JWZ97_16350, JWZ97_16355
mch	Methenyl-H_4MPT cyclohydrolase	JWZ98_13880	JWZ97_16215
ftr	Formyltransferase	JWZ98_18885	JWZ97_17405
fhc	Ftr/hydrolase complex	JWZ98_18875 (*fhcB*) JWZ98_18880 (*fhcA*) JWZ98_18885 (*fhcD*) JWZ98_18890 (*fhcC*)	JWZ97_17395 (*fhcB*) JWZ97_17400 (*fhcA*) JWZ97_17405 (*fhcD*) JWZ97_17410 (*fhcC*)
H_4F Pathway		**Complete**	**Complete**
folD	Bifunctional methylene-H_4F dehydrogenase/cyclohydrolase	None	None
mtdA	NADP-Specific H_4F dehydrogenase	JWZ98_08205	JWZ97_02310
fhs (*ftfL*)	Formyl-H_4F synthetase (formyl-H_4F ligase)	JWZ98_08805	JWZ97_03895
purU	Formyl-H_4F deformylase	None	None
fch	Formiminotetrahydrofolate cyclodeaminase (EC 4.3.1.4)	JWZ98_16990	JWZ97_02315

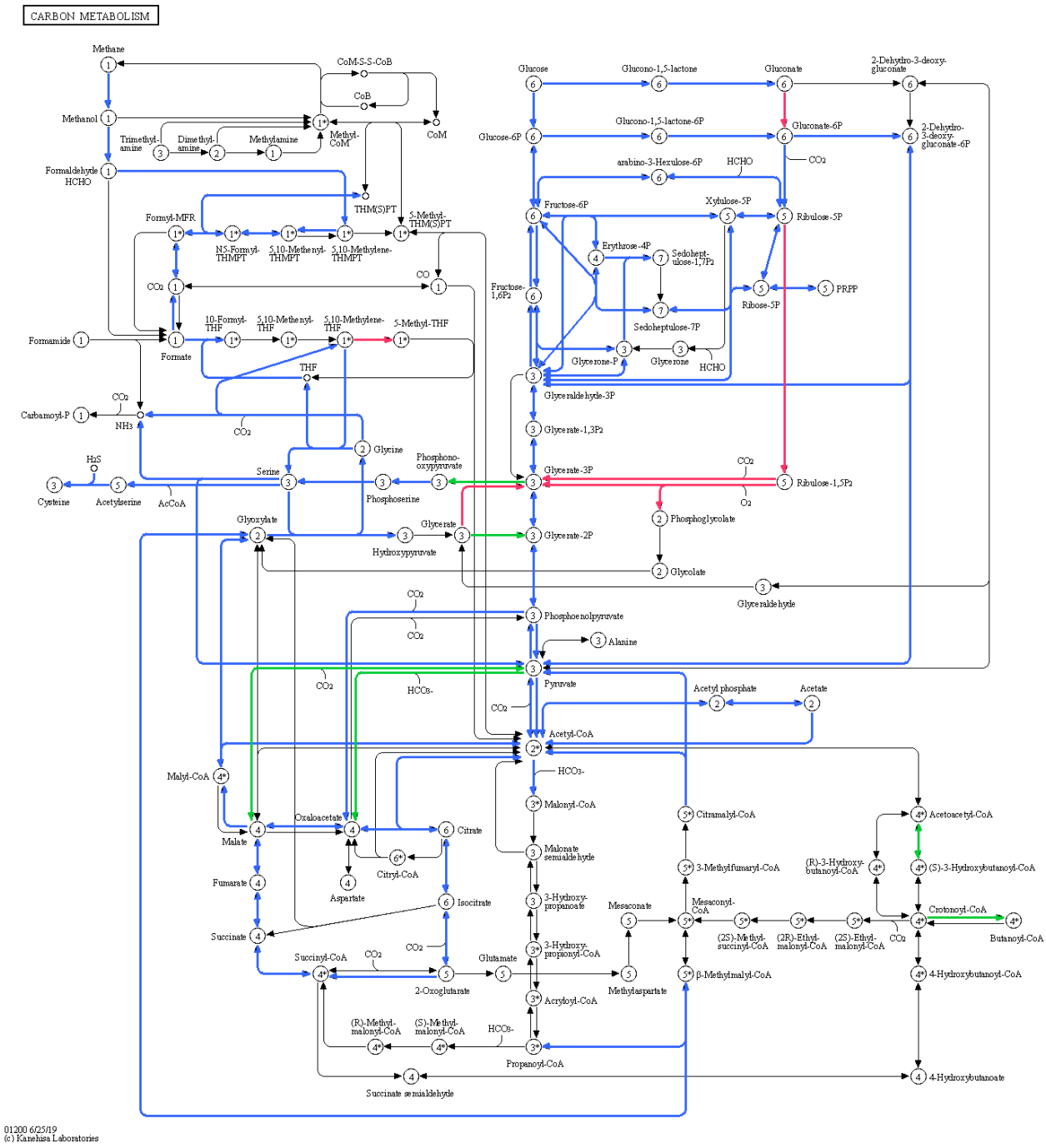

Figure 6.8. Carbon metabolism pathways in *Methylomonas* sp. strain EFPC1 (green), *Methylococcus* sp. strain EFPC2 (red), or both (blue). Amino acid sequence data were annotated using BlastKOALA, and subsequently mapped against KEGG databases (Kanehisa & Sato, 2020).

Table 6.6. Putative MbnTs in *Methylomonas* sp. strain EFPC1 identified via blastp.

Locus Tag	Total Score	Query Cover (%)	E value[a]	Identity (%)
Msn. trichosporium OB3b MbnT (ADVE02_v2_13650)				
JWZ98_21415	595	95	0	41.99
JWZ98_21285	527	95	6.00×10^{-177}	38.56
JWZ98_21250	514	99	4.00×10^{-172}	38.55
JWZ98_05020	459	99	1.00×10^{-150}	34.81
JWZ98_12165	458	99	2.00×10^{-150}	34.57
JWZ98_21345	451	95	8.00×10^{-148}	37.61
JWZ98_21265	441	95	2.00×10^{-143}	35.23
JWZ98_13005	439	99	6.00×10^{-143}	34.91
JWZ98_06185	431	95	5.00×10^{-140}	33.84
JWZ98_04990	421	94	1.00×10^{-135}	34.8
JWZ98_07325	419	95	2.00×10^{-135}	35.93
JWZ98_13025	402	95	7.00×10^{-129}	34.24
JWZ98_21325	369	95	2.00×10^{-116}	33.01
JWZ98_14830	368	95	6.00×10^{-116}	33.05
JWZ98_15215	187	81	2.00×10^{-50}	26.27
JWZ98_18630	170	92	1.00×10^{-44}	27.09
JWZ98_15170	166	84	1.00×10^{-43}	25.41
JWZ98_08595	118	43	5.00×10^{-16}	31.75
JWZ98_21305	107	64	5.00×10^{-10}	24.9
Methylocystis sp. SB2 MbnT (MSB2v1_460017)				
JWZ98_16195	60.5	29	4.00×10^{-10}	25.86
JWZ98_16065	106	41	7.00×10^{-9}	25.35
JWZ98_21305	100	59	3.00×10^{-7}	30.46
JWZ98_04990	50.8	31	3.00×10^{-7}	25.88
JWZ98_20820	49.7	51	7.00×10^{-7}	22.22
JWZ98_13025	49.7	31	7.00×10^{-7}	23.95

[a] E value threshold of 1×10^{-6}

Table 6.7. Putative MbnTs in *Methylococcus* sp. strain EFPC1 identified via blastp.

Locus Tag	Total Score	Query Cover (%)	E value[a]	Identity (%)
Msn. trichosporium OB3b MbnT (ADVE02_v2_13650)				
JWZ97_07565	555	94	0	40.63
JWZ97_15280	463	95	1.00×10^{-152}	36.78
JWZ97_10965	459	95	6.00×10^{-151}	37.79
JWZ97_12245	457	96	5.00×10^{-150}	36.78
JWZ97_15250	442	95	1.00×10^{-143}	34.29
JWZ97_15245	403	95	2.00×10^{-129}	33.37
JWZ97_12265	181	38	9.00×10^{-52}	35.28
JWZ97_17285	179	82	5.00×10^{-48}	25.65
JWZ97_17280	173	81	4.00×10^{-46}	27.07
Methylocystis sp. SB2 MbnT (MSB2v1_460017)				
JWZ97_17285	71.2	93	2.00×10^{-13}	20.71
JWZ97_12220	114	62	6.00×10^{-13}	31.63
JWZ97_13575	55.5	35	1.00×10^{-8}	25.24

[a] E value threshold of 1×10^{-6}

Next, genes that may be of interest were identified on the plasmids of *Methylomonas* sp. strain EFPC1 and *Methylococcus* sp. strain EFPC2. Partial operons for mercury and chromate resistance (*merRTP* and *chrBA*) and type IV secretion system for DNA and protein substrate exchange (*virB*) were found on the plasmid of *Methylomonas* sp. strain EFPC1 (CP070495) (Table 6.8 and Figure 6.3) (Barkay et al., 2003; Branco et al., 2008; Christie, 2004). In addition, a complete operon for cobalt/zinc/cadmium efflux pump (*czcCBAD*) was also found on the same plasmid (Rensing et al., 1997). Genes related to nitrogen fixation (*nifHDKENX*, *nifQ*, *nifT*, *nifZ*, *nifBA*, *nifL*, *nifVW*) were found on the larger of the two plasmids in *Methylococcus* sp. strain EFPC2 (CP070492) (Figure 6.4 and Figure 6.5), as well as those encoding for a putative electron transport complex for the nitrogenase (*rnfABCDGEH*) (Table 6.8) (Jeong & Jouanneau, 2000; Koo, 2003; Kumagai et al., 1997; Schmehl et al., 1993).

Table 6.8. Presence of select genes on the plasmids of *Methylomonas* sp. strain EFPC1 and *Methylococcus* sp. strain EFPC2.

Predicted Function	Gene(s)	Locus Tag
***Methylomonas* sp. strain EFPC1 plasmid**		
Mercury resistance	*merRTP*	JWZ98_22875 – 22885
Chromate resistance	*chrBA*	JWZ98_22900 – 22895
Type IV secretion system	*virB2-5*,	JWZ98_23000 – 23015
	virB6	JWZ98_23025
	virB8-10	JWZ98_23045 – 23055
	virB11	JWZ98_23065
Cobalt/Zinc/Cadmium efflux pump	*czcCBAD*	JWZ98_22940 – 22925
***Methylococcus* sp. strain EFPC2 plasmid 1**		
Nitrogen fixation	*nifHDKENX*	JWZ97_19265 – 19395
	nifQ	JWZ97_19315
	nifT	JWZ97_19435
	nifZ	JWZ97_19455
	nifBA	JWZ97_19477 – 19476
	nifL	JWZ97_19535
	nifVW	JWZ97_19580 – 19585
Electron transport complex for nitrogenase	*rnfABCDGEH*	JWZ97_19730 – 19745
		JWZ97_19180 – 19185

6.6. Discussion

Two strains of methanotrophs from the *Gammaproteobacteria* class – *Methylomonas* sp. strain EFPC1 and *Methylococcus* sp. strain EFPC2 – were isolated from the mercury-contaminated stream of East Fork Poplar Creek. *Methylomonas* sp. strain EFPC1 is rod-shaped and Gram-negative, whereas *Methylococcus* sp. strain EFPC2 is coccoid and Gram-variable, which is in line with other methanotrophs of the respective genera. Of these two, *Methylococcus* sp. strain EFPC2 presents as a novel species based on phylogenetic analysis and comparison with other closely related methanotrophs.

Both isolates did not contain the core genes for methanobactin, nor genes for other copper uptake systems except for *copCD*. In case of *Methylomonas* sp. strain EFPC1, this would not pose an issue as it contains the genes for soluble methane monooxygenase and can circumvent the copper requirement. However, *Methylococcus* sp. strain EFPC2 only has *pmoCAB* encoding for the particulate methane monooxygenase. Perhaps this methanotroph has a strategy to participate in chalkophore piracy in the environment, though this is highly speculative at this stage of analysis. In addition, as current evidence suggests, these methanotrophs would not be able to degrade MeHg on their own – i.e., they would have to "steal" non-native MeHg-methanobactin complexes from the environment into the periplasm. The presence of putative MbnTs that are highly similar to that found in *Msn. trichosporium* OB3b suggests that both strains have the potential to take up methanobactin and could contribute to MeHg degradation. Therefore, it will be of interest to investigate the extent of MeHg degradation by these methanotrophs.

It is also interesting to note that both methanotrophs isolated in this study belongs to the *Methylococcaceae* family. Reads that mapped to *pmoA* sequences from representative

methanotrophs of the *Beijerinckiaceae*, *Methylococcaceae*, and *Methylocystaceae* families as well as the candidate phylum NC10 were found in metagenome sequences obtained from cores sampled from EFPC at 0-3 cm and 9-12 cm depths (data not shown) (Kim et al., 2021). No reads mapped to a representative methanotroph belonging to the Verrucomicrobia phylum from cores taken from any depth, or to the *Beijerinckiaceae* at 9-12 cm depth, which may be attributable to the acidophilic nature of these methanotrophs (Dedysh et al., 2000; Dunfield et al., 2003, 2007; Vorobev et al., 2011). It was surprising to find the most reads (100 out of 200,408,672 total reads) mapped to a methanotroph belonging to the candidate phylum NC10 in the core sampled from 9-12 cm, as this methanotroph is an obligate anaerobe. However, the abundance of methanotrophs in these samples were not analyzed, and therefore the significance of these findings may be uncertain at this point. Nonetheless, despite the fact that methanotrophs of various phylogenetic groups are present in samples taken from the EFPC, only those in the *Methylococcaceae* family was isolated in this study.

Furthermore, it has been shown that 23 phyla, including Proteobacteria, Cyanobacteria, Acidobacteria, Verrucomicrobia, and unclassified bacteria, were found in the surface stream sediments of EFPC (Vishnivetskaya et al., 2011). The relative composition of the microbial community, as determined by 16S rRNA gene sequencing, was significantly correlated with seasonal and geochemical factors, and some members within the Proteobacteria and Verrucomicrobia phyla (both of which methanotrophs can be found in) appeared to be positively associated with mercury and MeHg (Vishnivetskaya et al., 2011). Thus, it may be the case that composition of methanotrophs at EFPC also vary with season. Isolation and characterization of diverse methanotrophs from mercury-contaminated environment in the future may help elucidate the mechanism of methanotrophic-mediated MeHg degradation.

Chapter 7 Conclusions and Future Work

The general objective of this study was to understand the relationship between metals and methanotrophs and how this interaction affects the environment. That is, elucidating the effect of copper, rare earth elements (REEs), as well as various species of mercury on methanotrophs and vice versa will further our comprehension of methanotrophic-mediated metal distribution *in situ*. The consequence of this interaction is not limited to the methanotrophic community, but may also apply to other groups of microorganisms co-habitating the environment.

First, bioinformatic analyses were conducted to study the evolutionary origin of methanotrophs to better understand metal uptake systems in the context of methanotrophy. Evolutionary trees were constructed for methanotrophs, and genome compositional analysis was conducted to identify foreign or relatively recently acquired genes in methanotrophs. In this study, we found that ancient methylotrophs with a preexisting copper uptake system likely evolved into methanotrophs, again providing evidence that copper is a critical component in methanotrophy. In addition, Xox-methanol dehydrogenase (MeDH) was more easily shared via lateral gene transfer as compared to Mxa-MeDH, possibly influenced by the superior catalytic efficiency of Xox-MeDH providing a competitive advantage. In relation to REE, a gene encoding for a putative lanmodulin (LanM), a periplasmic REE-binding protein, was found in all *Alphaproteobacteria* methanotrophs, but not in any belonging to the *Gammaproteobacteria* class.

Second, competition between methanotrophs for copper was investigated. As noted in earlier chapters, some but not all methanotrophs produce the copper chelator, methanobactin

(MB). Thus, those that do may be able to predominate in copper-poor environments. However, we have found that many methanotrophs, despite not being able to make MB, have the necessary machinery to take it up. That is, some methanotrophs can and do "steal" MB made by others to meet their copper requirements. In this study, model methanotrophs with and without a gene encoding for a putative TonB-dependent transporter for MB (*mbnT*) were selected and investigated for "cheating" behavior by challenging with Group I and Group II MBs from *Methylosinus trichosporium* OB3b and *Methylocystis* sp. SB2. *Methylococcus capsulatus* Bath, a *Gammaproteobacteria* methanotroph, was able to overcome copper limitation imposed by MBs using its own copper chelator, MopE/MopE*. *Methylocystis* sp. strain Rockwell, belonging to the *Alphaproteobacteria* class, preferentially took up Group II MB, and was inhibited by Group I MB. *Methylomicrobium album* BG8, another *Gammaproteobacteria*, was able to take up MB, but also had a novel chalkophore that could compete for copper against MBs. The results of this study demonstrated that a phylogenetically long-range MB piracy may occur in the environment, and also identified a novel chalkophore yet to be characterized.

Finally, the mechanism of methylmercury (MeHg) demethylation by methanotrophs was investigated by targeting several candidates that may be involved in this process. An organoarsenical lyase (ArsI), responsible for cleaving carbon-arsenic bonds, was found not to be involved in the process of MeHg degradation by *Msn. trichosporium* OB3b. The role of Xox-MeDH in MeHg degradation was assessed by generating spheroplasts of *Msn. trichosporium* OB3b Δ*mbnT* lacking the periplasm, where Xox-MeDH is located, and monitoring its MeHg degradation rates. As expected, when spheroplasts were incubated with MeHg, the rate of demethylation was drastically decreased as compared to whole cells, and the periplasmic fraction exhibited higher degradation rates, providing evidence that the periplasmic constituents are

important for MeHg degradation. Moreover, *Msn. trichosporium* OB3b Δ*lanM* mutant completely lost its ability to degrade MeHg, indicating that LanM is critical for MeHg degradation. This supports the findings from assessing spheroplasts, as LanM also resides in the periplasm. LanM may be responsible for coordinating REEs for Xox-MeDH activity, but more research is necessary to unravel the exact mechanism of MeHg degradation. As an effort to characterize methanotrophs from mercury-contaminated sites, two methanotrophs were isolated from mercury-contaminated stream in Oak Ridge Tennessee and subsequently sequenced. Both strains do not contain the canonical organomercurial lyase, MerB, so further characterization will provide insight into MeHg degradation by methanotrophs.

In this study, the significance of copper and REEs in methanotrophy was explored using bioinformatic tools, copper competition between methanotrophs was investigated, and important players in methanotrophic-mediated MeHg degradation were identified. However, much is still unknown about copper competition *in situ* as well as the exact mechanism of MeHg degradation by methanotrophs. Therefore, future studies should address the unknowns in order to establish a complete understanding of the interaction between metals, methanotrophs, and other groups of microbes sharing the habitat.

It has been shown that methanotrophs have a significant impact on the availability of copper, which in turn affects the activities of other groups of microorganisms. Specifically, it has been shown that competition for copper between MB-producing methanotrophs and denitrifiers leads to increased nitrous oxide production by denitrifiers. The copper limitation imposed by MB prevents denitrifiers from acquiring copper for the nitrous oxide reductase (NosZ), a critical enzyme that converts nitrous oxide to dinitrogen. Nitrous oxide is a much more potent greenhouse gas than methane, so understanding copper availability is essential to

minimize greenhouse gas emissions. Ammonia-oxidizing bacteria also requires copper – in fact, the ammonia monooxygenase in these bacteria is homologous to the particulate methane monooxygenase (pMMO) in methanotrophs. Ammonia-oxidizing bacteria have been associated with increased nitrous oxide emissions, especially with the application of fertilizers (Soares et al., 2016). Investigating microbial community copper availability and, particularly, copper competition between methanotrophs and ammonia-oxidizing bacteria and the resulting greenhouse gas flux will provide insight into engineering solutions for mitigating emissions from agriculture, a main anthropogenic source of nitrous oxide.

Similar to the copper competition facilitated by methanotrophs, mercury speciation may also be affected by methanotrophs in the environment. We show here that some non-MB producing methanotrophs may act as a "cheater," whereby they take up foreign MB, possibly MeHg-MB complexes, and subsequently degrade the MeHg. Therefore, we may augment methanotrophy in MeHg-contaminated sites in an attempt to reduce the toxicity of mercury by converting the more toxic organic form of mercury to inorganic mercury. Zhou et al. (2020) has found that adding copper to paddy soil samples to promote methanotrophy subsequently enhanced MeHg degradation, providing preliminary data for exploiting methanotrophy for MeHg remediation. However, there is a possibility that this may inadvertently increase mercury methylation by some anaerobes, because Group I MB may also act as a vehicle for delivering Hg(II) into these microbes for greater methylation (Yin et al., 2020). Therefore, it is critical to understand the role of methanotrophs in the mercury cycle *in situ* before designing solutions for MeHg degradation.

An extension to the future works mentioned above could be to conduct a survey of MB in environmental samples to determine the prevalence of MB. This could involve designing

universal primers that target MB to enable rapid screening of metabolic potential, or better yet to establish a streamlined proteomics protocol to detect MB peptides in high throughput. Properties of the site (e.g. microbial community, metal speciation, greenhouse gas flux) juxtaposed to the MB distribution data will provide insight into the environmental significance of methanotrophs and MB.

Appendix

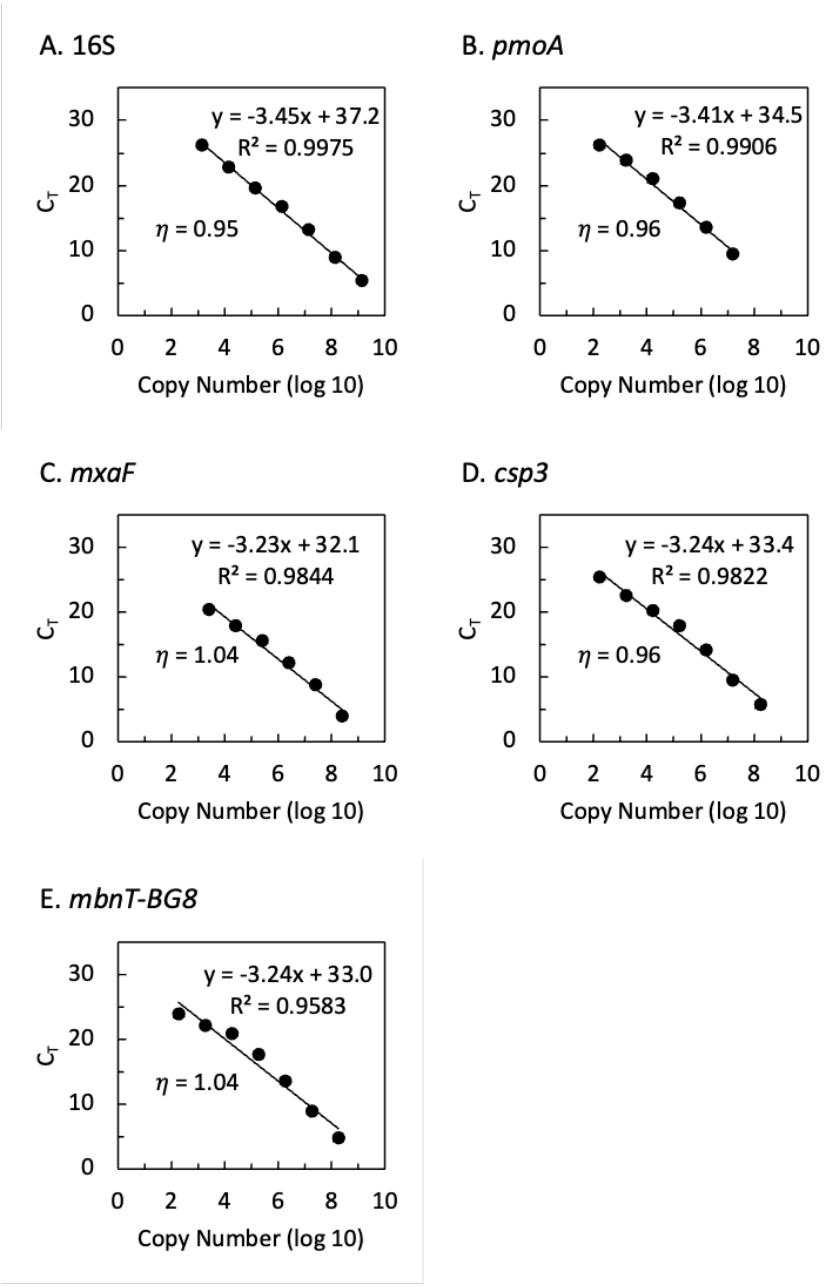

Figure A.1. Calibration curves of the qPCR standards of select genes involved in methane/methanol oxidation, copper storage and putative methanobactin uptake in *Mmc. album* BG8.

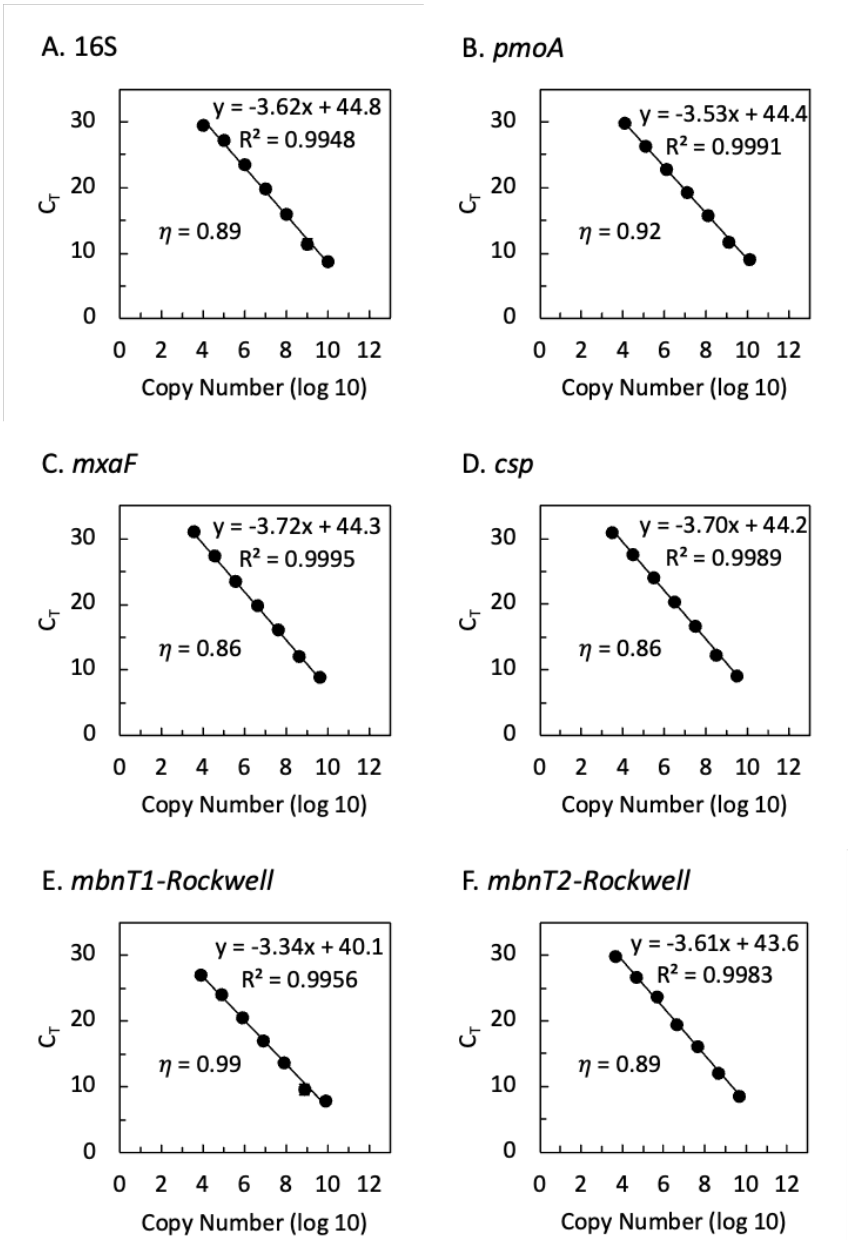

Figure A.2. Calibration curves of the qPCR standards of select genes involved in methane/methanol oxidation, copper storage and putative methanobactin uptake in *Methylocystis* sp. strain Rockwell.

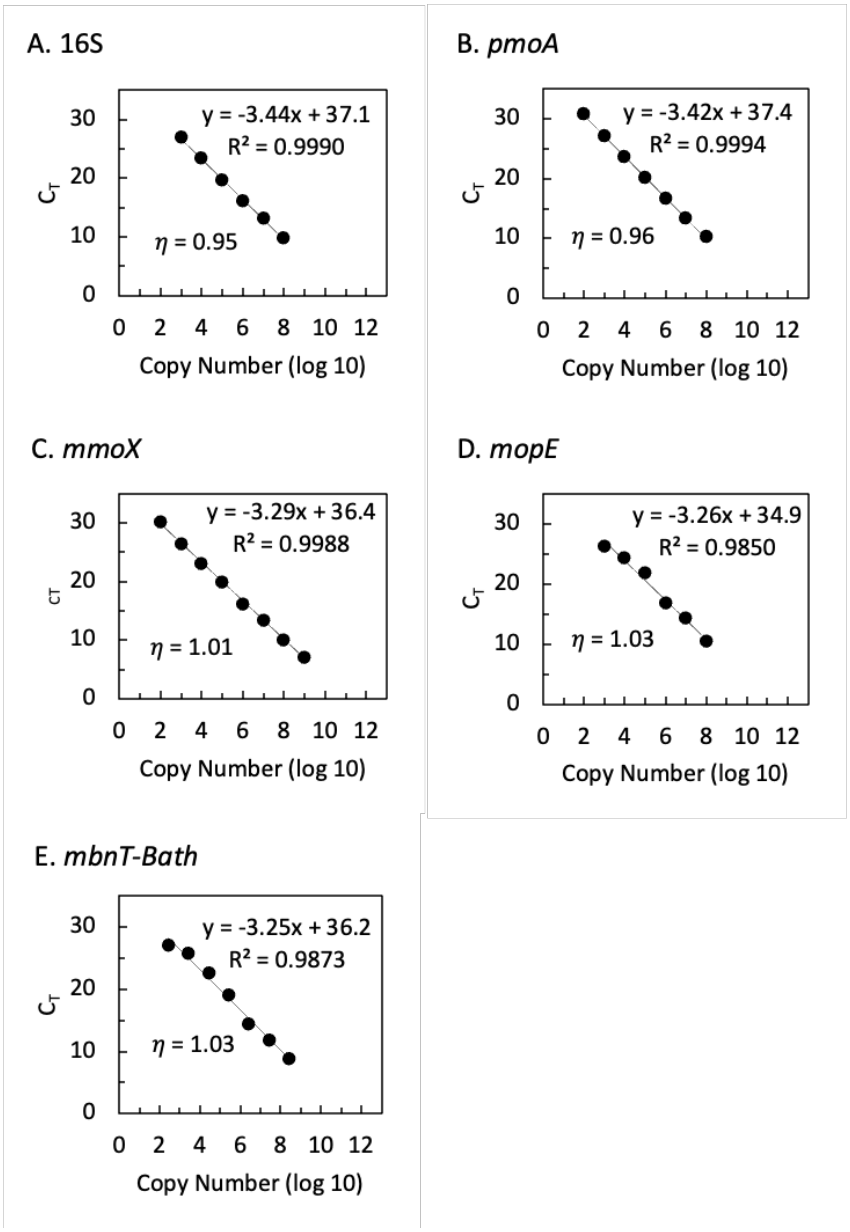

Figure A.3. Calibration curves of the qPCR standards of select genes involved in methane/methanol oxidation, copper storage and putative methanobactin uptake in *Mcc. capsulatus* Bath.

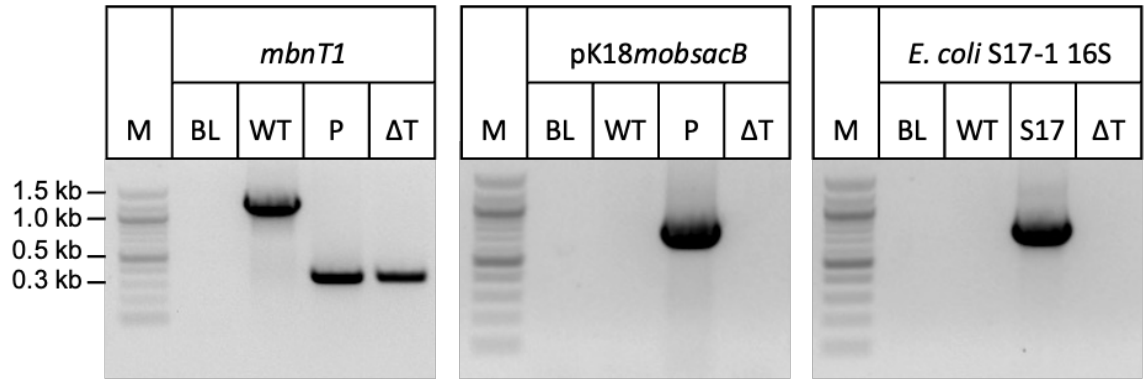

Figure A.4. Confirmation of construction of *Mmc. album* BG8 Δ*mbnT* mutant. M, molecular weight marker; BL, blank; WT, *Mmc. album* BG8 wild-type; P, plasmid; S17, *E. coli* S17-1 gDNA; ΔT, *Mmc. album* BG8 Δ*mbnT*.

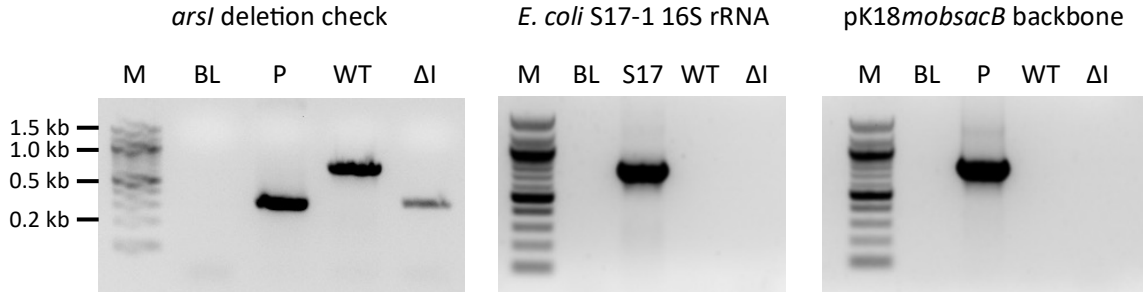

Figure A.5. Confirmation of construction of *Msn. trichosporium* OB3b Δ*arsI* mutant. M, molecular weight marker; BL, blank; WT, *Msn. trichosporium* OB3b wildtype; P, plasmid; S17, *E. coli* S17-1 gDNA; ΔI, *Msn. trichosporium* OB3b Δ*arsI*.

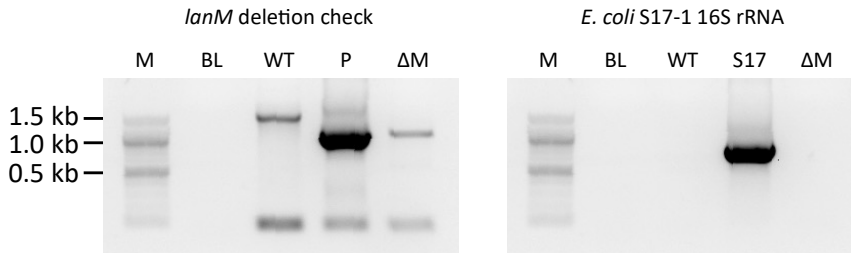

Figure A.6. Confirmation of construction of *Msn. trichosporium* OB3b Δ*lanM* mutant. M, molecular weight marker; BL, blank; WT, *Msn. trichosporium* OB3b wildtype; P, plasmid; S17, *E. coli* S17-1 gDNA; ΔM, *Msn. trichosporium* OB3b Δ*lanM*.

References

Adachi, O., Matsushita, K., Shinagawa, E., & Ameyama, M. (1990). Calcium in Quinoprotein Methanol Dehydrogenase Can Be Replaced by Strontium. *Agricultural and Biological Chemistry*, *54*(11), 2833–2837. https://doi.org/10.1080/00021369.1990.10870441

Afolabi, P. R., Mohammed, F., Amaratunga, K., Majekodunmi, O., Dales, L., Gill, R., Thompson, D., Cooper, B., Wood, P., Goodwin, M., & Anthony, C. (2001). Site-Directed Mutagenesis and X-ray Crystallography of the PQQ-Containing Quinoprotein Methanol Dehydrogenase and Its Electron Acceptor, Cytochrome c_L. *Biochemistry*, *40*(33), 9799–9809. https://doi.org/10.1021/bi0029321

Ahmed, E., & Holmström, S. J. M. (2014). Siderophores in environmental research: Roles and applications: Siderophores in environmental research. *Microbial Biotechnology*, *7*(3), 196–208. https://doi.org/10.1111/1751-7915.12117

Akberdin, I. R., Thompson, M., Hamilton, R., Desai, N., Alexander, D., Henard, C. A., Guarnieri, M. T., & Kalyuzhnaya, M. G. (2018). Methane utilization in *Methylomicrobium alcaliphilum* 20Z R: a systems approach. *Scientific Reports*, *8*(1), 1–13. https://doi.org/10.1038/s41598-018-20574-z

Ala, A., Walker, A. P., Ashkan, K., Dooley, J. S., & Schilsky, M. L. (2007). Wilson's disease. *The Lancet*, *369*(9559), 397–408. https://doi.org/10.1016/S0140-6736(07)60196-2

Alber, B. E., Spanheimer, R., Ebenau-Jehle, C., & Fuchs, G. (2006). Study of an alternate glyoxylate cycle for acetate assimilation by *Rhodobacter sphaeroides*. *Molecular Microbiology*, *61*(2), 297–309. https://doi.org/10.1111/j.1365-2958.2006.05238.x

Altschul, S. F., Gish, W., Miller, W., Myers, E. W., & Lipman, D. J. (1990). Basic local alignment search tool. *Journal of Molecular Biology*, *215*(3), 403–410. https://doi.org/10.1016/S0022-2836(05)80360-2

An, J., Zhang, L., Lu, X., Pelletier, D. A., Pierce, E. M., Johs, A., Parks, J. M., & Gu, B. (2019). Mercury Uptake by *Desulfovibrio desulfuricans* ND132: Passive or Active? *Environmental Science & Technology*, *53*(11), 6264–6272. https://doi.org/10.1021/acs.est.9b00047

Andersson, K., Froland, W. A., Lee, S.-K., & Lipscomb, J. D. (1991). Dioxygen independent oxygenation of hydrocarbons by methane monooxygenae hydroxylase component. *New Journal of Chemistry*, *15*, 411–415.

Andrews, S. (2010). *FastQC: A Quality Control Tool for High Throughput Sequence Data*. http://www.bioinformatics.babraham.ac.uk/projects/fastqc/

Andrews, S. C., Robinson, A. K., & Rodríguez-Quiñones, F. (2003). Bacterial iron homeostasis. *FEMS Microbiology Reviews*, *27*(2–3), 215–237. https://doi.org/10.1016/S0168-6445(03)00055-X

Anthony, C. (1982). *The biochemistry of methylotrophs*. Academic Press.

Anthony, C. (1992). The *c*-type cytochromes of methylotrophic bacteria. *Biochimica et Biophysica Acta (BBA) - Bioenergetics*, *1099*(1), 1–15. https://doi.org/10.1016/0005-2728(92)90181-Z

Anthony, C. (1993). Methanol Dehydrogenase in Gram-Negative Bacteria. In V. L. Davidson (Ed.), *Principles and applications of quinoproteins* (pp. 17–46). M. Dekker.

Anthony, C. (2004). The quinoprotein dehydrogenases for methanol and glucose. *Archives of Biochemistry and Biophysics*, *428*(1), 2–9. https://doi.org/10.1016/j.abb.2004.03.038

Anthony, C. (2011). How Half a Century of Research was Required to Understand Bacterial Growth on C_1 and C_2 Compounds; the Story of the Serine Cycle and the Ethylmalonyl-CoA Pathway. *Science Progress*, *94*(2), 109–137. https://doi.org/10.3184/003685011X13044430633960

Anthony, C., & Ghosh, M. (1998). The structure and function of the PQQ-containing quinoprotein dehydrogenases. *Progress in Biophysics and Molecular Biology*, *69*(1), 1–21. https://doi.org/10.1016/S0079-6107(97)00020-5

Anthony, C., Ghosh, M., & Blake, C. C. (1994). The structure and function of methanol dehydrogenase and related quinoproteins containing pyrrolo-quinoline quinone. *Biochemical Journal*, *304*(Pt 3), 665–674.

Anthony, C., & Williams, P. (2003). The structure and mechanism of methanol dehydrogenase. *Biochimica et Biophysica Acta (BBA) - Proteins and Proteomics*, *1647*(1), 18–23. https://doi.org/10.1016/S1570-9639(03)00042-6

Anthony, C., & Zatman, L. J. (1964a). The microbial oxidation of methanol. 1. Isolation and properties of *Pseudomonas* sp. M27. *Biochemical Journal*, *92*(3), 609–614.

Anthony, C., & Zatman, L. J. (1964b). The microbial oxidation of methanol. 2. The methanol-oxidizing enzyme of *Pseudomonas* sp. M27. *Biochemical Journal*, *92*(3), 614–621.

Anthony, C., & Zatman, L. J. (1967). The microbial oxidation of methanol. *Biochemical Journal*, *104*(3), 960–969.

Anvar, S. Y., Frank, J., Pol, A., Schmitz, A., Kraaijeveld, K., den Dunnen, J. T., & Op den Camp, H. J. (2014). The genomic landscape of the verrucomicrobial methanotroph *Methylacidiphilum fumariolicum* SolV. *BMC Genomics*, *15*(1), 914. https://doi.org/10.1186/1471-2164-15-914

Arnesano, F., Banci, L., Bertini, I., Mangani, S., & Thompsett, A. R. (2003). A redox switch in CopC: An intriguing copper trafficking protein that binds copper(I) and copper(II) at different sites. *Proceedings of the National Academy of Sciences*, *100*(7), 3814–3819. https://doi.org/10.1073/pnas.0636904100

Arps, P. J., Fulton, G. F., Minnich, E. C., & Lidstrom, M. E. (1993). Genetics of serine pathway enzymes in *Methylobacterium extorquens* AM1: Phosphoenolpyruvate carboxylase and malyl coenzyme A lyase. *Journal of Bacteriology*, *175*(12), 3776–3783. https://doi.org/10.1128/jb.175.12.3776-3783.1993

Asenjo, J. A., & Suk, J. S. (1986). Microbial Conversion of Methane into poly-β-hydroxybutyrate (PHB): Growth and intracellular product accumulation in a type II methanotroph. *Journal of Fermentation Technology*, *64*(4), 271–278. https://doi.org/10.1016/0385-6380(86)90118-4

Attwood, M. M. (1990). Formaldehyde dehydrogenases from methylotrophs. In *Methods in Enzymology* (Vol. 188, pp. 314–327). Academic Press. https://doi.org/10.1016/0076-6879(90)88049-G

Awala, S. I., Bellosillo, L. A., Gwak, J.-H., Nguyen, N.-L., Kim, S.-J., Lee, B.-H., & Rhee, S.-K. (2020). *Methylococcus geothermalis* sp. Nov., a methanotroph isolated from a geothermal field in the Republic of Korea. *International Journal of Systematic and Evolutionary Microbiology*, *70*(10), 5520–5530. https://doi.org/10.1099/ijsem.0.004442

Baani, M., & Liesack, W. (2008). Two isozymes of particulate methane monooxygenase with different methane oxidation kinetics are found in *Methylocystis* sp. Strain SC2. *Proceedings of the National Academy of Sciences*, *105*(29), 10203–10208. https://doi.org/10.1073/pnas.0702643105

Balasubramanian, R., Kenney, G. E., & Rosenzweig, A. C. (2011). Dual Pathways for Copper Uptake by Methanotrophic Bacteria. *Journal of Biological Chemistry*, *286*(43), 37313–37319. https://doi.org/10.1074/jbc.M111.284984

Balasubramanian, R., & Rosenzweig, A. C. (2008). Copper methanobactin: A molecule whose time has come. *Current Opinion in Chemical Biology*, *12*(2), 245–249. https://doi.org/10.1016/j.cbpa.2008.01.043

Balasubramanian, R., Smith, S. M., Rawat, S., Yatsunyk, L. A., Stemmler, T. L., & Rosenzweig, A. C. (2010). Oxidation of methane by a biological dicopper centre. *Nature*, *465*(7294), 115–119. https://doi.org/10.1038/nature08992

Bandow, N. L. (2014). Isolation and binding properties of methanobactin from the facultative methanotroph *Methylocystis* strain SB2. *Graduate Theses and Dissertations*. https://doi.org/10.31274/etd-180810-3137

Bandow, N. L., Gallagher, W. H., Behling, L., Choi, D. W., Semrau, J. D., Hartsel, S. C., Gilles, V. S., & DiSpirito, A. A. (2011). Isolation of Methanobactin from the Spent Media of Methane-Oxidizing Bacteria. In *Methods in Enzymology* (Vol. 495, pp. 259–269). Elsevier. https://doi.org/10.1016/B978-0-12-386905-0.00017-6

Banerjee, R., Meier, K. K., Münck, E., & Lipscomb, J. D. (2013). Intermediate P* from Soluble Methane Monooxygenase Contains a Diferrous Cluster. *Biochemistry*, *52*(25), 4331–4342. https://doi.org/10.1021/bi400182y

Banerjee, R., Proshlyakov, Y., Lipscomb, J. D., & Proshlyakov, D. A. (2015). Structure of the key species in the enzymatic oxidation of methane to methanol. *Nature*, *518*(7539), 431–434. https://doi.org/10.1038/nature14160

Baral, B. S., Bandow, N. L., Vorobev, A., Freemeier, B. C., Bergman, B. H., Herdendorf, T. J., Fuentes, N., Ellias, L., Turpin, E., Semrau, J. D., & DiSpirito, A. A. (2014). Mercury binding by methanobactin from *Methylocystis* strain SB2. *Journal of Inorganic Biochemistry*, *141*, 161–169. https://doi.org/10.1016/j.jinorgbio.2014.09.004

Barkay, T., Miller, S. M., & Summers, A. O. (2003). Bacterial mercury resistance from atoms to ecosystems. *FEMS Microbiology Reviews*, *27*(2–3), 355–384. https://doi.org/10.1016/S0168-6445(03)00046-9

Barkay, T., & Wagner-Döbler, I. (2005). Microbial Transformations of Mercury: Potentials, Challenges, and Achievements in Controlling Mercury Toxicity in the Environment. In *Advances in Applied Microbiology* (Vol. 57, pp. 1–52). Elsevier. https://doi.org/10.1016/S0065-2164(05)57001-1

Barnett, M. O., Harris, L. A., Turner, R. R., Henson, T. J., Melton, R. E., & Stevenson, R. J. (1995). Characterization of mercury species in contaminated floodplain soils. *Water, Air, & Soil Pollution*, *80*(1–4), 1105–1108. https://doi.org/10.1007/BF01189771

Barnett, M. O., Harris, L. A., Turner, R. R., Stevenson, R. J., Henson, T. J., Melton, R. C., & Hoffman, D. P. (1997). Formation of Mercuric Sulfide in Soil. *Environmental Science & Technology*, *31*(11), 3037–3043. https://doi.org/10.1021/es960389j

Baslé, A., El Ghazouani, A., Lee, J., & Dennison, C. (2018). Insight into Metal Removal from Peptides that Sequester Copper for Methane Oxidation. *Chemistry – A European Journal*, *24*(18), 4515–4518. https://doi.org/10.1002/chem.201706035

Basu, P., Katterle, B., Andersson, K. K., & Dalton, H. (2003). The membrane-associated form of methane mono-oxygenase from *Methylococcus capsulatus* (Bath) is a copper/iron protein. *Biochemical Journal*, *369*(2), 417–427. https://doi.org/10.1042/bj20020823

Baxter, N. J., Hirt, R. P., Bodrossy, L., Kovacs, K. L., Embley, M. T., Prosser, J. I., & Murrell, J. C. (2002). The ribulose-1,5-bisphosphate carboxylase/oxygenase gene cluster of *Methylococcus capsulatus* (Bath). *Archives of Microbiology*, *177*(4), 279–289. https://doi.org/10.1007/s00203-001-0387-x

Begley, T. P., Walts, A. E., & Walsh, C. T. (1986a). Bacterial organomercurial lyase: Overproduction, isolation, and characterization. *Biochemistry*, *25*(22), 7186–7192. https://doi.org/10.1021/bi00370a063

Begley, T. P., Walts, A. E., & Walsh, C. T. (1986b). Mechanistic studies of a protonolytic organomercurial cleaving enzyme: Bacterial organomercurial lyase. *Biochemistry*, *25*(22), 7192–7200. https://doi.org/10.1021/bi00370a064

Behling, L. A., Hartsel, S. C., Lewis, D. E., DiSpirito, A. A., Choi, D. W., Masterson, L. R., Veglia, G., & Gallagher, W. H. (2008). NMR, Mass Spectrometry and Chemical Evidence Reveal a Different Chemical Structure for Methanobactin That Contains Oxazolone Rings. *Journal of the American Chemical Society*, *130*(38), 12604–12605. https://doi.org/10.1021/ja804747d

Belova, S. E., Kulichevskaya, I. S., Bodelier, P. L. E., & Dedysh, S. N. (2013). *Methylocystis bryophila* sp. Nov., a facultatively methanotrophic bacterium from acidic Sphagnum peat, and emended description of the genus *Methylocystis* (ex Whittenbury et al. 1970) Bowman et al. 1993. *International Journal of Systematic and Evolutionary Microbiology*, *63*(Pt_3), 1096–1104. https://doi.org/10.1099/ijs.0.043505-0

Bender, M., & Conrad, R. (1992). Kinetics of CH_4 oxidation in oxic soils exposed to ambient air or high CH_4 mixing ratios. *FEMS Microbiology Letters*, *101*(4), 261–270. https://doi.org/10.1111/j.1574-6968.1992.tb05783.x

Berson, O., & Lidstrom, M. E. (1997). Cloning and characterization of *corA*, a gene encoding a copper-repressible polypeptide in the type I methanotroph, *Methylomicrobium albus* BG8. *FEMS Microbiology Letters*, *148*(2), 169–174. https://doi.org/10.1111/j.1574-6968.1997.tb10284.x

Bodrossy, L., Holmes, E. M., Holmes, A. J., Kovács, K. L., & Murrell, J. C. (1997). Analysis of 16S rRNA and methane monooxygenase gene sequences reveals a novel group of thermotolerant and thermophilic methanotrophs, *Methylocaldum* gen. Nov. *Archives of Microbiology*, *168*(6), 493–503. https://doi.org/10.1007/s002030050527

Bolger, A. M., Lohse, M., & Usadel, B. (2014). Trimmomatic: A flexible trimmer for Illumina sequence data. *Bioinformatics*, *30*(15), 2114–2120. https://doi.org/10.1093/bioinformatics/btu170

Bordel, S., Crombie, A. T., Muñoz, R., & Murrell, J. C. (2020). Genome Scale Metabolic Model of the versatile methanotroph *Methylocella silvestris*. *Microbial Cell Factories*, *19*(1), 144. https://doi.org/10.1186/s12934-020-01395-0

Bordel, S., Rodríguez, Y., Hakobyan, A., Rodríguez, E., Lebrero, R., & Muñoz, R. (2019a). Genome scale metabolic modeling reveals the metabolic potential of three Type II methanotrophs of the genus *Methylocystis*. *Metabolic Engineering*, *54*, 191–199. https://doi.org/10.1016/j.ymben.2019.04.001

Bordel, S., Rojas, A., & Muñoz, R. (2019b). Reconstruction of a Genome Scale Metabolic Model of the polyhydroxybutyrate producing methanotroph *Methylocystis parvus* OBBP. *Microbial Cell Factories*, *18*(1), 104. https://doi.org/10.1186/s12934-019-1154-5

Borodina, E., Nichol, T., Dumont, M. G., Smith, T. J., & Murrell, J. C. (2007). Mutagenesis of the "Leucine Gate" To Explore the Basis of Catalytic Versatility in Soluble Methane Monooxygenase. *Applied and Environmental Microbiology*, *73*(20), 6460–6467. https://doi.org/10.1128/AEM.00823-07

Bosch, G., Wang, T., Latypova, E., Kalyuzhnaya, M. G., Hackett, M., & Chistoserdova, L. (2009). Insights into the physiology of *Methylotenera mobilis* as revealed by metagenome-based shotgun proteomic analysis. *Microbiology, 155*(4), 1103–1110. https://doi.org/10.1099/mic.0.024968-0

Bothe, H., Møller Jensen, K., Mergel, A., Larsen, J., Jørgensen, C., Bothe, H., & Jørgensen, L. (2002). Heterotrophic bacteria growing in association with *Methylococcus capsulatus* (Bath) in a single cell protein production process. *Applied Microbiology and Biotechnology*, *59*(1), 33–39. https://doi.org/10.1007/s00253-002-0964-1

Bowman, J. P., McCammon, S. A., & Skerrat, J. H. (1997). *Methylosphaera hansonii* gen. Nov., sp. Nov., a psychrophilic, group I methanotroph from Antarctic marine-salinity, meromictic lakes. *Microbiology*, *143*(4), 1451–1459. https://doi.org/10.1099/00221287-143-4-1451

Bowman, J. P., SLY, L. I., & STACKEBRANDT, E. (1995). The Phylogenetic Position of the Family *Methylococcaceae*. *International Journal of Systematic and Evolutionary Microbiology, 45*(1), 182–185. https://doi.org/10.1099/00207713-45-1-182

Brady, D. C., Crowe, M. S., Turski, M. L., Hobbs, G. A., Yao, X., Chaikuad, A., Knapp, S., Xiao, K., Campbell, S. L., Thiele, D. J., & Counter, C. M. (2014). Copper is required for oncogenic BRAF signalling and tumorigenesis. *Nature*, *509*(7501), 492–496. https://doi.org/10.1038/nature13180

Branco, R., Chung, A. P., Johnston, T., Gurel, V., Morais, P., & Zhitkovich, A. (2008). The Chromate-Inducible *chrBACF* Operon from the Transposable Element TnOtChr Confers Resistance to Chromium(VI) and Superoxide. *Journal of Bacteriology*, *190*(21), 6996–7003. https://doi.org/10.1128/JB.00289-08

Brantner, C. A., Remsen, C. C., Owen, H. A., Buchholz, L. A., & Collins, M. (2002). Intracellular localization of the particulate methane monooxygenase and methanol dehydrogenase in *Methylomicrobium album* BG8. *Archives of Microbiology*, *178*(1), 59–64. https://doi.org/10.1007/s00203-002-0426-2

Brazeau, B. J., & Lipscomb, J. D. (2003). Key Amino Acid Residues in the Regulation of Soluble Methane Monooxygenase Catalysis by Component B. *Biochemistry*, *42*(19), 5618–5631. https://doi.org/10.1021/bi027429i

Brazeau, B. J., Wallar, B. J., & Lipscomb, J. D. (2001). Unmasking of Deuterium Kinetic Isotope Effects on the Methane Monooxygenase Compound Q Reaction by Site-Directed Mutagenesis of Component B. *Journal of the American Chemical Society*, *123*(42), 10421–10422. https://doi.org/10.1021/ja016632i

Brewer, G. J. (2014). Alzheimer's disease causation by copper toxicity and treatment with zinc. *Frontiers in Aging Neuroscience*, *6*. https://doi.org/10.3389/fnagi.2014.00092

Brooks, S. C., Lowe, K. A., Mehlhorn, T. L., Olsen, T. A., Yin, X. L., Fortner, A. M., & Peterson, M. J. (2018). *Intraday Water Quality Patterns in East Fork Poplar Creek with*

an Emphasis on Mercury and Monomethylmercury (ORNL/TM--2018/812, 1439147; p. ORNL/TM--2018/812, 1439147). https://doi.org/10.2172/1439147

Brooks, S. C., & Southworth, G. R. (2011). History of mercury use and environmental contamination at the Oak Ridge Y-12 Plant. *Environmental Pollution*, *159*(1), 219–228. https://doi.org/10.1016/j.envpol.2010.09.009

Brown, K., Tegoni, M., Prudêncio, M., Pereira, A. S., Besson, S., Moura, J. J., Moura, I., & Cambillau, C. (2000). A novel type of catalytic copper cluster in nitrous oxide reductase. *Nature Structural Biology*, *7*(3), 191–195. https://doi.org/10.1038/73288

Brown, L. R., Strawinski, R. J., & McCleskey, C. S. (1964). The Isolation and Characterization of *Methanomonas methanooxidans* Brown and Strawinski. *Canadian Journal of Microbiology*, *10*(5), 791–799. https://doi.org/10.1139/m64-100

Brusseau, G. A., Tsien, H.-C., Hanson, R. S., & Wackett, L. P. (1990). Optimization of trichloroethylene oxidation by methanotrophs and the use of a colorimetric assay to detect soluble methane monooxygenase activity. *Biodegradation*, *1*(1), 19–29. https://doi.org/10.1007/BF00117048

Burrows, K. J., Cornish, A., Scott, D., & Higgins, I. J. (1984). Substrate Specificities of the Soluble and Particulate Methane Mono-oxygenases of *Methylosinus trichosporium* OB3b. *Microbiology, 130*(12), 3327–3333. https://doi.org/10.1099/00221287-130-12-3327

Bush, A. I. (2008). Drug Development Based on the Metals Hypothesis of Alzheimer's Disease. *Journal of Alzheimer's Disease*, *15*(2), 223–240. https://doi.org/10.3233/JAD-2008-15208

Butaitė, E., Baumgartner, M., Wyder, S., & Kümmerli, R. (2017). Siderophore cheating and cheating resistance shape competition for iron in soil and freshwater *Pseudomonas* communities. *Nature Communications*, *8*(1), 414. https://doi.org/10.1038/s41467-017-00509-4

Caldwell, S. L., Laidler, J. R., Brewer, E. A., Eberly, J. O., Sandborgh, S. C., & Colwell, F. S. (2008). Anaerobic Oxidation of Methane: Mechanisms, Bioenergetics, and the Ecology of Associated Microorganisms. *Environmental Science & Technology*, *42*(18), 6791–6799. https://doi.org/10.1021/es800120b

Cao, L., Caldararu, O., Rosenzweig, A. C., & Ryde, U. (2018). Quantum Refinement Does Not Support Dinuclear Copper Sites in Crystal Structures of Particulate Methane Monooxygenase. *Angewandte Chemie International Edition*, *57*(1), 162–166. https://doi.org/10.1002/anie.201708977

Cardy, D. L. N., Laidler, V., Salmond, G. P. C., & Murrell, J. C. (1991). The methane monooxygenase gene cluster of *Methylosinus trichosporium*: Cloning and sequencing of the *mmoC* gene. *Archives of Microbiology*, *156*(6), 477–483. https://doi.org/10.1007/BF00245395

Cha, J.-S., & Cooksey, D. A. (1993). Copper Hypersensitivity and Uptake in *Pseudomonas syringae* Containing Cloned Components of the Copper Resistance Operon. *Applied and Environmental Microbiology*, *59*(5), 1671–1674.

Champomier-Vergès, M.-C., Stintzi, A., & Meyer, J.-M. (1996). Acquisition of iron by the non-siderophore-producing *Pseudomonas fragi*. *Microbiology*, *142*(5), 1191–1199. https://doi.org/10.1099/13500872-142-5-1191

Chan, S. I., Chen, K. H.-C., Yu, S. S.-F., Chen, C.-L., & Kuo, S. S.-J. (2004). Toward Delineating the Structure and Function of the Particulate Methane Monooxygenase from

Methanotrophic Bacteria. *Biochemistry*, *43*(15), 4421–4430. https://doi.org/10.1021/bi0497603

Chan, S. I., Lu, Y.-J., Nagababu, P., Maji, S., Hung, M.-C., Lee, M. M., Hsu, I.-J., Minh, P. D., Lai, J. C.-H., Ng, K. Y., Ramalingam, S., Yu, S. S.-F., & Chan, M. K. (2013). Efficient Oxidation of Methane to Methanol by Dioxygen Mediated by Tricopper Clusters. *Angewandte Chemie International Edition*, *52*(13), 3731–3735. https://doi.org/10.1002/anie.201209846

Chan, S. I., Wang, V. C.-C., Lai, J. C.-H., Yu, S. S.-F., Chen, P. P.-Y., Chen, K. H.-C., Chen, C.-L., & Chan, M. K. (2007). Redox Potentiometry Studies of Particulate Methane Monooxygenase: Support for a Trinuclear Copper Cluster Active Site. *Angewandte Chemie International Edition*, *46*(12), 1992–1994. https://doi.org/10.1002/anie.200604647

Chang, J., Gu, W., Park, D., Semrau, J. D., DiSpirito, A. A., & Yoon, S. (2018). Methanobactin from *Methylosinus trichosporium* OB3b inhibits N_2O reduction in denitrifiers. *The ISME Journal*, *12*(8), 2086–2089. https://doi.org/10.1038/s41396-017-0022-8

Chatwood, L. L., Müller, J., Gross, J. D., Wagner, G., & Lippard, S. J. (2004). NMR Structure of the Flavin Domain from Soluble Methane Monooxygenase Reductase from *Methylococcus capsulatus* (Bath). *Biochemistry*, *43*(38), 11983–11991. https://doi.org/10.1021/bi049066n

Chen, Y., Crombie, A., Rahman, M. T., Dedysh, S. N., Liesack, W., Stott, M. B., Alam, M., Theisen, A. R., Murrell, J. C., & Dunfield, P. F. (2010). Complete Genome Sequence of the Aerobic Facultative Methanotroph *Methylocella silvestris* BL2. *Journal of Bacteriology*, *192*(14), 3840–3841. https://doi.org/10.1128/JB.00506-10

Cherny, R. A., Atwood, C. S., Xilinas, M. E., Gray, D. N., Jones, W. D., McLean, C. A., Barnham, K. J., Volitakis, I., Fraser, F. W., Kim, Y.-S., Huang, X., Goldstein, L. E., Moir, R. D., Lim, J. T., Beyreuther, K., Zheng, H., Tanzi, R. E., Masters, C. L., & Bush, A. I. (2001). Treatment with a Copper-Zinc Chelator Markedly and Rapidly Inhibits β-Amyloid Accumulation in Alzheimer's Disease Transgenic Mice. *Neuron*, *30*(3), 665–676. https://doi.org/10.1016/S0896-6273(01)00317-8

Chi Fru, E., Gray, N. D., McCann, C., Baptista, J. de C., Christgen, B., Talbot, H. M., El Ghazouani, A., Dennison, C., & Graham, D. W. (2011). Effects of copper mineralogy and methanobactin on cell growth and sMMO activity in *Methylosinus trichosporium* OB3b. *Biogeosciences*, *8*(10), 2887–2894. https://doi.org/10.5194/bg-8-2887-2011

Chistoserdova, L. V. (2011). Modularity of methylotrophy, revisited. *Environmental Microbiology*, *13*(10), 2603–2622. https://doi.org/10.1111/j.1462-2920.2011.02464.x

Chistoserdova, L. V., Chen, S.-W., Lapidus, A., & Lidstrom, M. E. (2003). Methylotrophy in *Methylobacterium extorquens* AM1 from a Genomic Point of View. *Journal of Bacteriology*, *185*(10), 2980–2987. https://doi.org/10.1128/JB.185.10.2980-2987.2003

Chistoserdova, L. V., & Lidstrom, M. E. (1992). Cloning, mutagenesis, and physiological effect of a hydroxypyruvate reductase gene from *Methylobacterium extorquens* AM1. *Journal of Bacteriology*, *174*(1), 71–77. https://doi.org/10.1128/jb.174.1.71-77.1992

Chistoserdova, L. V., & Lidstrom, M. E. (1994a). Genetics of the serine cycle in *Methylobacterium extorquens* AM1: Identification of *sgaA* and *mtdA* and sequences of *sgaA*, *hprA*, and *mtdA*. *Journal of Bacteriology*, *176*(7), 1957–1968. https://doi.org/10.1128/jb.176.7.1957-1968.1994

Chistoserdova, L. V., & Lidstrom, M. E. (1994b). Genetics of the serine cycle in *Methylobacterium extorquens* AM1: Cloning, sequence, mutation, and physiological effect of *glyA*, the gene for serine hydroxymethyltransferase. *Journal of Bacteriology*, *176*(21), 6759–6762. https://doi.org/10.1128/jb.176.21.6759-6762.1994

Chistoserdova, L. V., & Lidstrom, M. E. (1994c). Genetics of the serine cycle in *Methylobacterium extorquens* AM1: Identification, sequence, and mutation of three new genes involved in C_1 assimilation, *orf4*, *mtkA*, and *mtkB*. *Journal of Bacteriology*, *176*(23), 7398–7404. https://doi.org/10.1128/jb.176.23.7398-7404.1994

Chistoserdova, L. V., & Lidstrom, M. E. (1997a). Molecular and mutational analysis of a DNA region separating two methylotrophy gene clusters in *Methylobacterium extorquens* AM1. *Microbiology, 143*(5), 1729–1736. https://doi.org/10.1099/00221287-143-5-1729

Chistoserdova, L. V., & Lidstrom, M. E. (1997b). Identification and mutation of a gene required for glycerate kinase activity from a facultative methylotroph, *Methylobacterium extorquens* AM1. *Journal of Bacteriology*, *179*(15), 4946–4948. https://doi.org/10.1128/jb.179.15.4946-4948.1997

Chistoserdova, L. V., & Lidstrom, M. E. (2013). Aerobic Methylotrophic Prokaryotes. *The Prokaryotes*, 267–285. https://doi.org/10.1007/978-3-642-30141-4_68

Chistoserdova, L. V., Vorholt, J. A., & Lidstrom, M. E. (2005). A genomic view of methane oxidation by aerobic bacteria and anaerobic archaea. *Genome Biology*, *6*(2), 208. https://doi.org/10.1186/gb-2005-6-2-208

Chistoserdova, L. V., Vorholt, J. A., Thauer, R. K., & Lidstrom, M. E. (1998). C_1 Transfer Enzymes and Coenzymes Linking Methylotrophic Bacteria and Methanogenic Archaea. *Science*, *281*(5373), 99–102. https://doi.org/10.1126/science.281.5373.99

Choi, D. W., Bandow, N. L., McEllistrem, M. T., Semrau, J. D., Antholine, W. E., Hartsel, S. C., Gallagher, W., Zea, C. J., Pohl, N. L., Zahn, J. A., & DiSpirito, A. A. (2010). Spectral and thermodynamic properties of methanobactin from γ-proteobacterial methane oxidizing bacteria: A case for copper competition on a molecular level. *Journal of Inorganic Biochemistry*, *104*(12), 1240–1247. https://doi.org/10.1016/j.jinorgbio.2010.08.002

Choi, D. W., Kunz, R. C., Boyd, E. S., Semrau, J. D., Antholine, W. E., Han, J.-I., Zahn, J. A., Boyd, J. M., Mora, A. M. de la, & DiSpirito, A. A. (2003). The Membrane-Associated Methane Monooxygenase (pMMO) and pMMO-NADH:Quinone Oxidoreductase Complex from *Methylococcus capsulatus* Bath. *Journal of Bacteriology*, *185*(19), 5755–5764. https://doi.org/10.1128/JB.185.19.5755-5764.2003

Choi, D. W., Zea, C. J., Do, Y. S., Semrau, J. D., Antholine, W. E., Hargrove, M. S., Pohl, N. L., Boyd, E. S., Geesey, G. G., Hartsel, S. C., Shafe, P. H., McEllistrem, M. T., Kisting, C. J., Campbell, D., Rao, V., de la Mora, A. M., & DiSpirito, A. A. (2006). Spectral, Kinetic, and Thermodynamic Properties of Cu(I) and Cu(II) Binding by Methanobactin from *Methylosinus trichosporium* OB3b. *Biochemistry*, *45*(5), 1442–1453. https://doi.org/10.1021/bi051815t

Choi, J. M., Kim, H. G., Kim, J.-S., Youn, H.-S., Eom, S. H., Yu, S.-L., Kim, S. W., & Lee, S. H. (2011). Purification, crystallization and preliminary X-ray crystallographic analysis of a methanol dehydrogenase from the marine bacterium *Methylophaga aminisulfidivorans* MPT. *Acta Crystallographica Section F: Structural Biology and Crystallization Communications*, *67*(4), 513–516. https://doi.org/10.1107/S1744309111006713

Christie, P. J. (2004). Type IV secretion: The *Agrobacterium* VirB/D4 and related conjugation systems. *Biochimica et Biophysica Acta (BBA) - Molecular Cell Research*, *1694*(1–3), 219–234. https://doi.org/10.1016/j.bbamcr.2004.02.013

Chu, F., Beck, D. A. C., & Lidstrom, M. E. (2016). MxaY regulates the lanthanide-mediated methanol dehydrogenase switch in *Methylomicrobium buryatense*. *PeerJ*, *4*, e2435. https://doi.org/10.7717/peerj.2435

Cohen, S. N., Chang, A. C. Y., & Hsu, L. (1972). Nonchromosomal Antibiotic Resistance in Bacteria: Genetic Transformation of *Escherichia coli* by R-Factor DNA. *Proceedings of the National Academy of Sciences*, *69*(8), 2110–2114. https://doi.org/10.1073/pnas.69.8.2110

Colby, J., & Dalton, H. (1976). Some properties of a soluble methane mono-oxygenase from *Methylococcus capsulatus* strain Bath. *Biochemical Journal*, *157*(2), 495–497. https://doi.org/10.1042/bj1570495

Colby, J., Stirling, D. I., & Dalton, H. (1977). The soluble methane mono-oxygenase of *Methylococcus capsulatus* (Bath). Its ability to oxygenate *n*-alkanes, *n*-alkenes, ethers, and alicyclic, aromatic and heterocyclic compounds. *Biochemical Journal*, *165*(2), 395–402.

Collins, M. L., Buchholz, L. A., & Remsen, C. C. (1991). Effect of Copper on *Methylomonas albus* BG8. *Applied and Environmental Microbiology*, *57*(4), 1261–1264. https://doi.org/10.1128/AEM.57.4.1261-1264.1991

Conrad, R. (2009). The global methane cycle: Recent advances in understanding the microbial processes involved. *Environmental Microbiology Reports*, *1*(5), 285–292. https://doi.org/10.1111/j.1758-2229.2009.00038.x

Conrado, R. J., & Gonzalez, R. (2014). Envisioning the Bioconversion of Methane to Liquid Fuels. *Science*, *343*(6171), 621–623. https://doi.org/10.1126/science.1246929

Cook, E. C., Featherston, E. R., Showalter, S. A., & Cotruvo, J. A. (2019). Structural Basis for Rare Earth Element Recognition by *Methylobacterium extorquens* Lanmodulin. *Biochemistry*, *58*(2), 120–125. https://doi.org/10.1021/acs.biochem.8b01019

Coppi, M. V., O'Neil, R. A., Leang, C., Kaufmann, F., Methe, B. A., Nevin, K. P., Woodard, T. L., Liu, A., & Lovley, D. R. (2007). Involvement of *Geobacter sulfurreducens* SfrAB in acetate metabolism rather than intracellular, respiration-linked Fe(III) citrate reduction. *Microbiology*, *153*(10), 3572–3585. https://doi.org/10.1099/mic.0.2007/006478-0

Cordero, O. X., Ventouras, L.-A., DeLong, E. F., & Polz, M. F. (2012). Public good dynamics drive evolution of iron acquisition strategies in natural bacterioplankton populations. *Proceedings of the National Academy of Sciences*, *109*(49), 20059–20064. https://doi.org/10.1073/pnas.1213344109

Costello, A. M., & Lidstrom, M. E. (1999). Molecular Characterization of Functional and Phylogenetic Genes from Natural Populations of Methanotrophs in Lake Sediments. *Applied and Environmental Microbiology*, *65*(11), 5066–5074. https://doi.org/10.1128/AEM.65.11.5066-5074.1999

Cotruvo, J. A. (2019). The Chemistry of Lanthanides in Biology: Recent Discoveries, Emerging Principles, and Technological Applications. *ACS Central Science*, *5*(9), 1496–1506. https://doi.org/10.1021/acscentsci.9b00642

Cotruvo, J. A., Featherston, E. R., Mattocks, J. A., Ho, J. V., & Laremore, T. N. (2018). Lanmodulin: A Highly Selective Lanthanide-Binding Protein from a Lanthanide-

Utilizing Bacterium. *Journal of the American Chemical Society*, *140*(44), 15056–15061. https://doi.org/10.1021/jacs.8b09842

Crosa, J. H., & Walsh, C. T. (2002). Genetics and Assembly Line Enzymology of Siderophore Biosynthesis in Bacteria. *Microbiology and Molecular Biology Reviews*, *66*(2), 223–249. https://doi.org/10.1128/MMBR.66.2.223-249.2002

Crossman, L. C., Moir, J. W. B., Enticknap, J. J., Richardson, D. J., & Spiro, S. (1997). Heterologous expression of heterotrophic nitrification genes. *Microbiology, 143*(12), 3775–3783. https://doi.org/10.1099/00221287-143-12-3775

Crowther, G. J., Kosály, G., & Lidstrom, M. E. (2008). Formate as the Main Branch Point for Methylotrophic Metabolism in *Methylobacterium extorquens* AM1. *Journal of Bacteriology*, *190*(14), 5057–5062. https://doi.org/10.1128/JB.00228-08

Crumbley, A. M., & Gonzalez, R. (2018). Cracking "Economies of Scale": Biomanufacturing on Methane-Rich Feedstock. In M. G. Kalyuzhnaya & X.-H. Xing (Eds.), *Methane Biocatalysis: Paving the Way to Sustainability* (pp. 271–292). Springer International Publishing. https://doi.org/10.1007/978-3-319-74866-5_17

Csáki, R., Bodrossy, L., Klem, J., Murrell, J. C., & Kovács, K. L. (2003). Genes involved in the copper-dependent regulation of soluble methane monooxygenase of *Methylococcus capsulatus* (Bath): Cloning, sequencing and mutational analysis. *Microbiology, 149*(7), 1785–1795. https://doi.org/10.1099/mic.0.26061-0

Culpepper, M. A., & Rosenzweig, A. C. (2014). Structure and Protein–Protein Interactions of Methanol Dehydrogenase from *Methylococcus capsulatus* (Bath). *Biochemistry*, *53*(39), 6211–6219. https://doi.org/10.1021/bi500850j

Daniel, M.-C., & Astruc, D. (2004). Gold Nanoparticles: Assembly, Supramolecular Chemistry, Quantum-Size-Related Properties, and Applications toward Biology, Catalysis, and Nanotechnology. *Chemical Reviews*, *104*(1), 293–346. https://doi.org/10.1021/cr030698+

Danilova, O. V., Suzina, N. E., Van De Kamp, J., Svenning, M. M., Bodrossy, L., & Dedysh, S. N. (2016). A new cell morphotype among methane oxidizers: A spiral-shaped obligately microaerophilic methanotroph from northern low-oxygen environments. *The ISME Journal*, *10*(11), 2734–2743. https://doi.org/10.1038/ismej.2016.48

Dassama, L. M. K., Kenney, G. E., Ro, S. Y., Zielazinski, E. L., & Rosenzweig, A. C. (2016). Methanobactin transport machinery. *Proceedings of the National Academy of Sciences*, *113*(46), 13027–13032. https://doi.org/10.1073/pnas.1603578113

Daumann, L. J. (2019). Essential and Ubiquitous: The Emergence of Lanthanide Metallobiochemistry. *Angewandte Chemie International Edition*, *58*(37), 12795–12802. https://doi.org/10.1002/anie.201904090

Davis, J. B., Coty, V. F., & Stanley, J. P. (1964). Atmospheric Nitrogen Fixation by Methane-Oxidizing Bacteria. *Journal of Bacteriology*, *88*(2), 468–472.

Dawson, M. J., & Jones, C. W. (1981). Energy Conservation in the Terminal Region of the Respiratory Chain of the Methylotrophic Bacterium *Methylophilus methylotrophus*. *European Journal of Biochemistry*, *118*(1), 113–118. https://doi.org/10.1111/j.1432-1033.1981.tb05492.x

de la Torre, A., Metivier, A., Chu, F., Laurens, L. M. L., Beck, D. A. C., Pienkos, P. T., Lidstrom, M. E., & Kalyuzhnaya, M. G. (2015). Genome-scale metabolic reconstructions and theoretical investigation of methane conversion in *Methylomicrobium buryatense* strain 5G(B1). *Microbial Cell Factories*, *14*(1), 188. https://doi.org/10.1186/s12934-015-0377-3

Dedysh, S. N., Khmelenina, V. N., Suzina, N. E., Trotsenko, Y. A., Semrau, J. D., Liesack, W., & Tiedje, J. M. (2002). *Methylocapsa acidiphila* gen. Nov., sp. Nov., a novel methane-oxidizing and dinitrogen-fixing acidophilic bacterium from Sphagnum bog. *International Journal of Systematic and Evolutionary Microbiology*, *52*(1), 251–261. https://doi.org/10.1099/00207713-52-1-251

Dedysh, S. N., Liesack, W., Khmelenina, V. N., Suzina, N. E., Trotsenko, Y. A., Semrau, J. D., Bares, A. M., Panikov, N. S., & Tiedje, J. M. (2000). *Methylocella palustris* gen. Nov., sp. Nov., a new methane-oxidizing acidophilic bacterium from peat bogs, representing a novel subtype of serine-pathway methanotrophs. *International Journal of Systematic and Evolutionary Microbiology*, *50*(3), 955–969. https://doi.org/10.1099/00207713-50-3-955

Dedysh, S. N., Naumoff, D. G., Vorobev, A. V., Kyrpides, N., Woyke, T., Shapiro, N., Crombie, A. T., Murrell, J. C., Kalyuzhnaya, M. G., Smirnova, A. V., & Dunfield, P. F. (2015). Draft Genome Sequence of *Methyloferula stellata* AR4, an Obligate Methanotroph Possessing Only a Soluble Methane Monooxygenase. *Genome Announcements*, *3*(2). https://doi.org/10.1128/genomeA.01555-14

Dedysh, S. N., Panikov, N. S., & Tiedje, J. M. (1998). Acidophilic Methanotrophic Communities from Sphagnum Peat Bogs. *Applied and Environmental Microbiology*, *64*(3), 922–929.

Delmotte, N., Knief, C., Chaffron, S., Innerebner, G., Roschitzki, B., Schlapbach, R., von Mering, C., & Vorholt, J. A. (2009). Community proteogenomics reveals insights into the physiology of phyllosphere bacteria. *Proceedings of the National Academy of Sciences*, *106*(38), 16428–16433. https://doi.org/10.1073/pnas.0905240106

Demers, J. D., Blum, J. D., Brooks, S. C., Donovan, P. M., Riscassi, A. L., Miller, C. L., Zheng, W., & Gu, B. (2018). Hg isotopes reveal in-stream processing and legacy inputs in East Fork Poplar Creek, Oak Ridge, Tennessee, USA. *Environmental Science: Processes & Impacts*, *20*(4), 686–707. https://doi.org/10.1039/C7EM00538E

Deng, Y. W., Ro, S. Y., & Rosenzweig, A. C. (2018). Structure and function of the lanthanide-dependent methanol dehydrogenase XoxF from the methanotroph *Methylomicrobium buryatense* 5GB1C. *JBIC Journal of Biological Inorganic Chemistry*, *23*(7), 1037–1047. https://doi.org/10.1007/s00775-018-1604-2

Dennis, J. J., & Zylstra, G. J. (1998). Plasposons: Modular self-cloning minitransposon derivatives for rapid genetic analysis of gram-negative bacterial genomes. *Applied and Environmental Microbiology*, *64*(7), 2710–2715. https://doi.org/10.1128/AEM.64.7.2710-2715.1998

Dennison, C., David, S., & Lee, J. (2018). Bacterial copper storage proteins. *Journal of Biological Chemistry*, *293*(13), 4616–4627. https://doi.org/10.1074/jbc.TM117.000180

DeRose, V. J., Liu, K. E., Kurtz, D. M., Hoffman, B. M., & Lippard, S. J. (1993). Proton ENDOR identification of bridging hydroxide ligands in mixed-valent diiron centers of proteins: Methane monooxygenase and semimet azidohemerythrin. *Journal of the American Chemical Society*, *115*(14), 6440–6441. https://doi.org/10.1021/ja00067a081

Deutzmann, J. S., Hoppert, M., & Schink, B. (2014). Characterization and phylogeny of a novel methanotroph, *Methyloglobulus morosus* gen. Nov., spec. Nov. *Systematic and Applied Microbiology*, *37*(3), 165–169. https://doi.org/10.1016/j.syapm.2014.02.001

Dianou, D., & Adachi, K. (1999). Characterization of methanotrophic bacteria isolated from a subtropical paddy field. *FEMS Microbiology Letters*, *173*(1), 163–173. https://doi.org/10.1111/j.1574-6968.1999.tb13498.x

DiSpirito, A. A., Kunz, R. C., Choi, D., & Zahn, J. A. (2004a). Chapter 7: Respiration in Methanotrophs. In D. Zannoni (Ed.), *Respiration in Archaea and Bacteria: Diversity of Prokaryotic Respiratory Systems* (pp. 149–168). Springer Netherlands. https://doi.org/10.1007/978-1-4020-3163-2_7

DiSpirito, A. A., Semrau, J. D., Murrell, J. C., Gallagher, W. H., Dennison, C., & Vuilleumier, S. (2016). Methanobactin and the Link between Copper and Bacterial Methane Oxidation. *Microbiology and Molecular Biology Reviews*, *80*(2), 387–409. https://doi.org/10.1128/MMBR.00058-15

DiSpirito, A. A., Zahn, J. A., Graham, D. W., Kim, H. J., Alterman, M., & Larive, C. (2004b). *Methanobactin: A copper binding compound having antibiotic and antioxidant activity isolated from methanotrophic bacteria* (World Intellectual Property Organization Patent No. WO2004056849A2). https://patents.google.com/patent/WO2004056849A2/en

DiSpirito, A. A., Zahn, J. A., Graham, D. W., Kim, H. J., Larive, C. K., Derrick, T. S., Cox, C. D., & Taylor, A. (1998). Copper-Binding Compounds from *Methylosinus trichosporium* OB3b. *Journal of Bacteriology*, *180*(14), 3606–3613. https://doi.org/10.1128/JB.180.14.3606-3613.1998

Dong, W., Liang, L., Brooks, S., Southworth, G., & Gu, B. (2010). Roles of dissolved organic matter in the speciation of mercury and methylmercury in a contaminated ecosystem in Oak Ridge, Tennessee. *Environmental Chemistry*, *7*(1), 94. https://doi.org/10.1071/EN09091

Duine, J. A., & Frank, J. (1980). The prosthetic group of methanol dehydrogenase. Purification and some of its properties. *Biochemical Journal*, *187*(1), 221–226. https://doi.org/10.1042/bj1870221

Duine, J. A., Frank, J., & Westerling, J. (1978). Purification and properties of methanol dehydrogenase from *Hyphomicrobium* X. *Biochimica et Biophysica Acta*, *524*(2), 277–287. https://doi.org/10.1016/0005-2744(78)90164-x

Dunfield, P. F., Khmelenina, V. N., Suzina, N. E., Trotsenko, Y. A., & Dedysh, S. N. (2003). *Methylocella silvestris* sp. Nov., a novel methanotroph isolated from an acidic forest cambisol. *International Journal of Systematic and Evolutionary Microbiology*, *53*(5), 1231–1239. https://doi.org/10.1099/ijs.0.02481-0

Dunfield, P. F., Yimga, M. T., Dedysh, S. N., Berger, U., Liesack, W., & Heyer, J. (2002). Isolation of a *Methylocystis* strain containing a novel *pmo A*-like gene. *FEMS Microbiology Ecology*, *41*(1), 17–26. https://doi.org/10.1111/j.1574-6941.2002.tb00962.x

Dunfield, P. F., Yuryev, A., Senin, P., Smirnova, A. V., Stott, M. B., Hou, S., Ly, B., Saw, J. H., Zhou, Z., Ren, Y., Wang, J., Mountain, B. W., Crowe, M. A., Weatherby, T. M., Bodelier, P. L. E., Liesack, W., Feng, L., Wang, L., & Alam, M. (2007). Methane oxidation by an extremely acidophilic bacterium of the phylum *Verrucomicrobia*. *Nature*, *450*(7171), 879–882. https://doi.org/10.1038/nature06411

El Ghazouani, A., Baslé, A., Firbank, S. J., Knapp, C. W., Gray, J., Graham, D. W., & Dennison, C. (2011). Copper-Binding Properties and Structures of Methanobactins from *Methylosinus trichosporium* OB3b. *Inorganic Chemistry*, *50*(4), 1378–1391. https://doi.org/10.1021/ic101965j

El Ghazouani, A., Baslé, A., Gray, J., Graham, D. W., Firbank, S. J., & Dennison, C. (2012). Variations in methanobactin structure influences copper utilization by methane-oxidizing bacteria. *Proceedings of the National Academy of Sciences*, *109*(22), 8400–8404. https://doi.org/10.1073/pnas.1112921109

Elahi, N., Kamali, M., & Baghersad, M. H. (2018). Recent biomedical applications of gold nanoparticles: A review. *Talanta*, *184*, 537–556. https://doi.org/10.1016/j.talanta.2018.02.088

Elango, N. A., Radhakrishnan, R., Froland, W. A., Wallar, B. J., Earhart, C. A., Lipscomb, J. D., & Ohlendorf, D. H. (1997). Crystal structure of the hydroxylase component of methane monooxygenase from *Methylosinus trichosporium* OB3b. *Protein Science*, *6*(3), 556–568. https://doi.org/10.1002/pro.5560060305

Erb, T. J., Berg, I. A., Brecht, V., Müller, M., Fuchs, G., & Alber, B. E. (2007). Synthesis of C_5-dicarboxylic acids from C_2-units involving crotonyl-CoA carboxylase/reductase: The ethylmalonyl-CoA pathway. *Proceedings of the National Academy of Sciences*, *104*(25), 10631–10636. https://doi.org/10.1073/pnas.0702791104

Erb, T. J., Fuchs, G., & Alber, B. E. (2009). (2S)-Methylsuccinyl-CoA dehydrogenase closes the ethylmalonyl-CoA pathway for acetyl-CoA assimilation. *Molecular Microbiology*, *73*(6), 992–1008. https://doi.org/10.1111/j.1365-2958.2009.06837.x

Erb, T. J., Rétey, J., Fuchs, G., & Alber, B. E. (2008). Ethylmalonyl-CoA Mutase from *Rhodobacter sphaeroides* Defines a New Subclade of Coenzyme B_{12}-dependent Acyl-CoA Mutases. *Journal of Biological Chemistry*, *283*(47), 32283–32293. https://doi.org/10.1074/jbc.M805527200

Erikstad, H.-A., & Birkeland, N.-K. (2015). Draft Genome Sequence of "*Candidatus* Methylacidiphilum kamchatkense" Strain Kam1, a Thermoacidophilic Methanotrophic Verrucomicrobium. *Genome Announcements*, *3*(2), e00065-15, /ga/3/2/e00065-15.atom. https://doi.org/10.1128/genomeA.00065-15

Erikstad, H.-A., Jensen, S., Keen, T. J., & Birkeland, N.-K. (2012). Differential expression of particulate methane monooxygenase genes in the verrucomicrobial methanotroph 'Methylacidiphilum kamchatkense' Kam1. *Extremophiles*, *16*(3), 405–409. https://doi.org/10.1007/s00792-012-0439-y

Eshinimaev, B. Ts., Medvedkova, K. A., Khmelenina, V. N., Suzina, N. E., Osipov, G. A., Lysenko, A. M., & Trotsenko, Yu. A. (2004). New Thermophilic Methanotrophs of the Genus Methylocaldum. *Microbiology*, *73*(4), 448–456. https://doi.org/10.1023/B:MICI.0000036991.31677.13

Ettwig, K. F., Alen, T. van, Pas-Schoonen, K. T. van de, Jetten, M. S. M., & Strous, M. (2009). Enrichment and Molecular Detection of Denitrifying Methanotrophic Bacteria of the NC10 Phylum. *Applied and Environmental Microbiology*, *75*(11), 3656–3662. https://doi.org/10.1128/AEM.00067-09

Ettwig, K. F., Butler, M. K., Paslier, D. L., Pelletier, E., Mangenot, S., Kuypers, M. M. M., Schreiber, F., Dutilh, B. E., Zedelius, J., Beer, D. de, Gloerich, J., Wessels, H. J. C. T., Alen, T. van, Luesken, F., Wu, M. L., Pas-Schoonen, K. T. van de, Camp, H. J. M. O. den, Janssen-Megens, E. M., Francoijs, K.-J., … Strous, M. (2010). Nitrite-driven anaerobic methane oxidation by oxygenic bacteria. *Nature*, *464*(7288), 543–548. https://doi.org/10.1038/nature08883

Ettwig, K. F., Shima, S., Pas-Schoonen, K. T. V. D., Kahnt, J., Medema, M. H., Camp, H. J. M. O. D., Jetten, M. S. M., & Strous, M. (2008). Denitrifying bacteria anaerobically oxidize methane in the absence of Archaea. *Environmental Microbiology*, *10*(11), 3164–3173. https://doi.org/10.1111/j.1462-2920.2008.01724.x

Farhan Ul Haque, M., Gu, W., Baral, B. S., DiSpirito, A. A., & Semrau, J. D. (2017). Carbon source regulation of gene expression in *Methylosinus trichosporium* OB3b. *Applied*

Microbiology and Biotechnology, *101*(9), 3871–3879. https://doi.org/10.1007/s00253-017-8121-z

Farhan Ul Haque, M., Gu, W., DiSpirito, A. A., & Semrau, J. D. (2016). Marker Exchange Mutagenesis of *mxaF*, Encoding the Large Subunit of the Mxa Methanol Dehydrogenase, in *Methylosinus trichosporium* OB3b. *Applied and Environmental Microbiology*, *82*(5), 1549–1555. https://doi.org/10.1128/AEM.03615-15

Farhan Ul Haque, M., Kalidass, B., Bandow, N., Turpin, E. A., DiSpirito, A. A., & Semrau, J. D. (2015a). Cerium Regulates Expression of Alternative Methanol Dehydrogenases in *Methylosinus trichosporium* OB3b. *Applied and Environmental Microbiology*, *81*(21), 7546–7552. https://doi.org/10.1128/AEM.02542-15

Farhan Ul Haque, M., Kalidass, B., Vorobev, A., Baral, B. S., DiSpirito, A. A., & Semrau, J. D. (2015b). Methanobactin from *Methylocystis* sp. Strain SB2 Affects Gene Expression and Methane Monooxygenase Activity in *Methylosinus trichosporium* OB3b. *Applied and Environmental Microbiology*, *81*(7), 2466–2473. https://doi.org/10.1128/AEM.03981-14

Fassel, T. A., Buchholz, L. A., Collins, M. L., & Remsen, C. C. (1992). Localization of methanol dehydrogenase in two strains of methylotrophic bacteria detected by immunogold labeling. *Applied and Environmental Microbiology*, *58*(7), 2302–2307.

Fei, Q., Guarnieri, M. T., Tao, L., Laurens, L. M. L., Dowe, N., & Pienkos, P. T. (2014). Bioconversion of natural gas to liquid fuel: Opportunities and challenges. *Biotechnology Advances*, *32*(3), 596–614. https://doi.org/10.1016/j.biotechadv.2014.03.011

Ferenci, P. (2005). Wilson's Disease. *Clinical Gastroenterology and Hepatology*, *3*(8), 726–733. https://doi.org/10.1016/S1542-3565(05)00484-2

Ferenci, T., Strøm, T., & Quayle, J. R. (1974). Purification and properties of 3-hexulose phosphate synthase and phospho-3-hexuloisomerase from *Methylococcus capsulatus*. *Biochemical Journal*, *144*(3), 477–486. https://doi.org/10.1042/bj1440477

Fitriyanto, N. A., Fushimi, M., Matsunaga, M., Pertiwiningrum, A., Iwama, T., & Kawai, K. (2011). Molecular structure and gene analysis of Ce^{3+}-induced methanol dehydrogenase of *Bradyrhizobium* sp. MAFF211645. *Journal of Bioscience and Bioengineering*, *111*(6), 613–617. https://doi.org/10.1016/j.jbiosc.2011.01.015

Fjellbirkeland, A., Kleivdal, H., Joergensen, C., Thestrup, H., & Jensen, H. B. (1997). Outer membrane proteins of *Methylococcus capsulatus* (Bath). *Archives of Microbiology*, *168*(2), 128–135. https://doi.org/10.1007/s002030050478

Fjellbirkeland, A., Kruger, P. G., Bemanian, V., Høgh, B. T., Murrell, C. J., & Jensen, H. B. (2001). The C-terminal part of the surface-associated protein MopE of the methanotroph *Methylococcus capsulatus* (Bath) is secreted into the growth medium. *Archives of Microbiology*, *176*(3), 197–203. https://doi.org/10.1007/s002030100307

Foster, J. W., & Davis, R. H. (1966). A Methane-Dependent Coccus, with Notes on Classification and Nomenclature of Obligate, Methane-Utilizing Bacteria. *Journal of Bacteriology*, *91*(5), 1924–1931.

Fox, B. G., Froland, W. A., Dege, J. E., & Lipscomb, J. D. (1989). Methane monooxygenase from *Methylosinus trichosporium* OB3b. Purification and properties of a three-component system with high specific activity from a type II methanotroph. *Journal of Biological Chemistry*, *264*(17), 10023–10033.

Franklin, S. J. (2001). Lanthanide-mediated DNA hydrolysis. *Current Opinion in Chemical Biology*, *5*(2), 201–208. https://doi.org/10.1016/S1367-5931(00)00191-5

Frindte, K., Kalyuzhnaya, M. G., Bringel, F., Dunfield, P. F., Jetten, M. S. M., Khmelenina, V. N., Klotz, M. G., Murrell, J. C., Op den Camp, H. J. M., Sakai, Y., Semrau, J. D., Shapiro, N., DiSpirito, A. A., Stein, L. Y., Svenning, M. M., Trotsenko, Y. A., Vuilleumier, S., Woyke, T., & Knief, C. (2017a). Draft Genome Sequences of Two Gammaproteobacterial Methanotrophs Isolated from Rice Ecosystems. *Genome Announcements*, *5*(33). https://doi.org/10.1128/genomeA.00526-17

Frindte, K., Maarastawi, S. A., Lipski, A., Hamacher, J., & Knief, C. (2017b). Characterization of the first rice paddy cluster I isolate, *Methyloterricola oryzae* gen. Nov., sp. Nov. And amended description of *Methylomagnum ishizawai*. *International Journal of Systematic and Evolutionary Microbiology, 67*(11), 4507–4514. https://doi.org/10.1099/ijsem.0.002319

Fu, Y., He, L., Reeve, J., Beck, D. A. C., & Lidstrom, M. E. (2019). Core Metabolism Shifts during Growth on Methanol versus Methane in the Methanotroph *Methylomicrobium buryatense* 5GB1. *MBio*, *10*(2). https://doi.org/10.1128/mBio.00406-19

Gaggelli, E., Kozlowski, H., Valensin, D., & Valensin, G. (2006). Copper Homeostasis and Neurodegenerative Disorders (Alzheimer's, Prion, and Parkinson's Diseases and Amyotrophic Lateral Sclerosis). *Chemical Reviews*, *106*(6), 1995–2044. https://doi.org/10.1021/cr040410w

Gamez, P., & Caballero, A. B. (2015). Copper in Alzheimer's disease: Implications in amyloid aggregation and neurotoxicity. *AIP Advances*, *5*(9), 092503. https://doi.org/10.1063/1.4921314

Geymonat, E., Ferrando, L., & Tarlera, S. E. (2011). *Methylogaea oryzae* gen. Nov., sp. Nov., a mesophilic methanotroph isolated from a rice paddy field. *International Journal of Systematic and Evolutionary Microbiology*, *61*(11), 2568–2572. https://doi.org/10.1099/ijs.0.028274-0

Ghosh, M., Anthony, C., Harlos, K., Goodwin, M. G., & Blake, C. (1995). The refined structure of the quinoprotein methanol dehydrogenase from *Methylobacterium extorquens* at 1.94 Å. *Structure*, *3*(2), 177–187. https://doi.org/10.1016/S0969-2126(01)00148-4

Gifford, J. L., Walsh, M. P., & Vogel, H. J. (2007). Structures and metal-ion-binding properties of the Ca^{2+}-binding helix–loop–helix EF-hand motifs. *Biochemical Journal*, *405*(2), 199–221. https://doi.org/10.1042/BJ20070255

Gilmour, C. C., Podar, M., Bullock, A. L., Graham, A. M., Brown, S. D., Somenahally, A. C., Johs, A., Hurt, R. A., Bailey, K. L., & Elias, D. A. (2013). Mercury Methylation by Novel Microorganisms from New Environments. *Environmental Science & Technology*, *47*(20), 11810–11820. https://doi.org/10.1021/es403075t

Good, N. M., Moore, R. S., Suriano, C. J., & Martinez-Gomez, N. C. (2019). Contrasting *in vitro* and *in vivo* methanol oxidation activities of lanthanide-dependent alcohol dehydrogenases XoxF1 and ExaF from *Methylobacterium extorquens* AM1. *Scientific Reports*, *9*(1), 1–12. https://doi.org/10.1038/s41598-019-41043-1

Goodwin, M. G., & Anthony, C. (1996). Characterization of a novel methanol dehydrogenase containing a Ba^{2+} ion at the active site. *Biochemical Journal*, *318*(2), 673–679. Scopus. https://doi.org/10.1042/bj3180673

Goodwin, M. G., Avezoux, A., Dales, S. L., & Anthony, C. (1996). Reconstitution of the quinoprotein methanol dehydrogenase from inactive Ca^{2+}-free enzyme with Ca^{2+}, Sr^{2+} or Ba^{2+}. *Biochemical Journal*, *319*(3), 839–842. https://doi.org/10.1042/bj3190839

Graf, J. S., Mayr, M. J., Marchant, H. K., Tienken, D., Hach, P. F., Brand, A., Schubert, C. J., Kuypers, M. M. M., & Milucka, J. (2018). Bloom of a denitrifying methanotroph, '*Candidatus* Methylomirabilis limnetica', in a deep stratified lake. *Environmental Microbiology*, *20*(7), 2598–2614. https://doi.org/10.1111/1462-2920.14285

Graham, D. W., Chaudhary, J. A., Hanson, R. S., & Arnold, R. G. (1993). Factors affecting competition between type I and type II methanotrophs in two-organism, continuous-flow reactors. *Microbial Ecology*, *25*(1), 1–17. https://doi.org/10.1007/BF00182126

Green, J., Prior, S. D., & Dalton, H. (1985). Copper ions as inhibitors of protein C of soluble methane monooxygenase of *Methylococcus capsulatus* (Bath). *European Journal of Biochemistry*, *153*(1), 137–144. https://doi.org/10.1111/j.1432-1033.1985.tb09279.x

Griffin, A. S., West, S. A., & Buckling, A. (2004). Cooperation and competition in pathogenic bacteria. *Nature*, *430*(7003), 1024–1027. https://doi.org/10.1038/nature02744

Griffiths, R. I., Whiteley, A. S., O'Donnell, A. G., & Bailey, M. J. (2000). Rapid Method for Coextraction of DNA and RNA from Natural Environments for Analysis of Ribosomal DNA- and rRNA-Based Microbial Community Composition. *Applied and Environmental Microbiology*, *66*(12), 5488–5491. https://doi.org/10.1128/AEM.66.12.5488-5491.2000

Groom, J. D., Ford, S. M., Pesesky, M. W., & Lidstrom, M. E. (2019). A Mutagenic Screen Identifies a TonB-Dependent Receptor Required for the Lanthanide Metal Switch in the Type I Methanotroph "*Methylotuvimicrobium buryatense*" 5GB1C. *Journal of Bacteriology*, *201*(15), e00120-19, /jb/201/15/JB.00120-19.atom. https://doi.org/10.1128/JB.00120-19

Gu, W., Baral, B. S., DiSpirito, A. A., & Semrau, J. D. (2017a). An Aminotransferase Is Responsible for the Deamination of the N-Terminal Leucine and Required for Formation of Oxazolone Ring A in Methanobactin of *Methylosinus trichosporium* OB3b. *Applied and Environmental Microbiology*, *83*(1). https://doi.org/10.1128/AEM.02619-16

Gu, W., Farhan Ul Haque, M., Baral, B. S., Turpin, E. A., Bandow, N. L., Kremmer, E., Flatley, A., Zischka, H., DiSpirito, A. A., & Semrau, J. D. (2016a). A TonB-Dependent Transporter Is Responsible for Methanobactin Uptake by *Methylosinus trichosporium* OB3b. *Applied and Environmental Microbiology*, *82*(6), 1917–1923. https://doi.org/10.1128/AEM.03884-15

Gu, W., Farhan Ul Haque, M., DiSpirito, A. A., & Semrau, J. D. (2016b). Uptake and effect of rare earth elements on gene expression in *Methylosinus trichosporium* OB3b. *FEMS Microbiology Letters*, *363*(13). https://doi.org/10.1093/femsle/fnw129

Gu, W., Farhan Ul Haque, M., & Semrau, J. D. (2017b). Characterization of the role of *copCD* in copper uptake and the 'copper-switch' in *Methylosinus trichosporium* OB3b. *FEMS Microbiology Letters*, *364*(10). https://doi.org/10.1093/femsle/fnx094

Gu, W., & Semrau, J. D. (2017). Copper and cerium-regulated gene expression in *Methylosinus trichosporium* OB3b. *Applied Microbiology and Biotechnology*, *101*(23), 8499–8516. https://doi.org/10.1007/s00253-017-8572-2

Guan, L. L., Kanoh, K., & Kamino, K. (2001). Effect of Exogenous Siderophores on Iron Uptake Activity of Marine Bacteria under Iron-Limited Conditions. *Applied and Environmental Microbiology*, *67*(4), 1710–1717. https://doi.org/10.1128/AEM.67.4.1710-1717.2001

Guindon, S., Dufayard, J.-F., Lefort, V., Anisimova, M., Hordijk, W., & Gascuel, O. (2010). New Algorithms and Methods to Estimate Maximum-Likelihood Phylogenies: Assessing the Performance of PhyML 3.0. *Systematic Biology*, *59*(3), 307–321. https://doi.org/10.1093/sysbio/syq010

Hagemeier, C. H., Bartoschek, S., Griesinger, C., Thauer, R. K., & Vorholt, J. A. (2001). Re-face stereospecificity of NADP dependent methylenetetrahydromethanopterin dehydrogenase from *Methylobacterium extorquens* AM1 as determined by NMR spectroscopy. *FEBS Letters*, *494*(1–2), 95–98. https://doi.org/10.1016/S0014-5793(01)02306-7

Hagemeier, C. H., Chistoserdova, L., Lidstrom, M. E., Thauer, R. K., & Vorholt, J. A. (2000). Characterization of a second methylene tetrahydromethanopterin dehydrogenase from *Methylobacterium extorquens* AM1. *European Journal of Biochemistry*, *267*(12), 3762–3769. https://doi.org/10.1046/j.1432-1327.2000.01413.x

Han, D., Dedysh, S. N., & Liesack, W. (2018). Unusual Genomic Traits Suggest *Methylocystis bryophila* S285 to Be Well Adapted for Life in Peatlands. *Genome Biology and Evolution*, *10*(2), 623–628. https://doi.org/10.1093/gbe/evy025

Han, J.-I., Lontoh, S., & Semrau, J. D. (1999). Degradation of chlorinated and brominated hydrocarbons by *Methylomicrobium album* BG8. *Archives of Microbiology*, *172*(6), 393–400. https://doi.org/10.1007/s002030050776

Hanson, R. S., & Hanson, T. E. (1996). Methanotrophic bacteria. *Microbiological Reviews*, *60*(2), 439–471.

Hanson, R. S., Tsien, H. C., Tsuji, K., Brusseau, G. A., & Wackett, L. P. (1990). Biodegradation of low-molecular-weight halogenated hydrocarbons by methanotrophic bacteria. *FEMS Microbiology Reviews*, *7*(3–4), 273–278. https://doi.org/10.1111/j.1574-6968.1990.tb04924.x

Harris, L. A., Henson, T. J., Combs, D., Melton, R. E., Steele, R. R., & Marsh, G. C. (1996). Imaging and microanalyses of mercury in flood plain soils of East Fork Poplar Creek. *Water, Air, and Soil Pollution*, *86*(1–4), 51–69. https://doi.org/10.1007/BF00279145

Helland, R., Fjellbirkeland, A., Karlsen, O. A., Ve, T., Lillehaug, J. R., & Jensen, H. B. (2008). An Oxidized Tryptophan Facilitates Copper Binding in *Methylococcus capsulatus*-secreted Protein MopE. *Journal of Biological Chemistry*, *283*(20), 13897–13904. https://doi.org/10.1074/jbc.M800340200

Hemmann, J. L., Saurel, O., Ochsner, A. M., Stodden, B. K., Kiefer, P., Milon, A., & Vorholt, J. A. (2016). The One-carbon Carrier Methylofuran from *Methylobacterium extorquens* AM1 Contains a Large Number of α- and γ-Linked Glutamic Acid Residues. *Journal of Biological Chemistry*, *291*(17), 9042–9051. https://doi.org/10.1074/jbc.M116.714741

Hemmann, J. L., Wagner, T., Shima, S., & Vorholt, J. A. (2019). Methylofuran is a prosthetic group of the formyltransferase/hydrolase complex and shuttles one-carbon units between two active sites. *Proceedings of the National Academy of Sciences*, *116*(51), 25583–25590. https://doi.org/10.1073/pnas.1911595116

Heyer, J., Berger, U., Hardt, M., & Dunfield, P. F. (2005). *Methylohalobius crimeensis* gen. Nov., sp. Nov., a moderately halophilic, methanotrophic bacterium isolated from hypersaline lakes of Crimea. *International Journal of Systematic and Evolutionary Microbiology*, *55*(5), 1817–1826. https://doi.org/10.1099/ijs.0.63213-0

Hibi, Y., Asai, K., Arafuka, H., Hamajima, M., Iwama, T., & Kawai, K. (2011). Molecular structure of La^{3+}-induced methanol dehydrogenase-like protein in *Methylobacterium radiotolerans*. *Journal of Bioscience and Bioengineering*, *111*(5), 547–549. https://doi.org/10.1016/j.jbiosc.2010.12.017

Hirayama, H., Abe, M., Miyazaki, M., Nunoura, T., Furushima, Y., Yamamoto, H., & Takai, K. (2014). *Methylomarinovum caldicuralii* gen. Nov., sp. Nov., a moderately thermophilic methanotroph isolated from a shallow submarine hydrothermal system, and proposal of

the family *Methylothermaceae* fam. Nov. *International Journal of Systematic and Evolutionary Microbiology*, *64*(3), 989–999. https://doi.org/10.1099/ijs.0.058172-0

Hirayama, H., Fuse, H., Abe, M., Miyazaki, M., Nakamura, T., Nunoura, T., Furushima, Y., Yamamoto, H., & Takai, K. (2013). *Methylomarinum vadi* gen. Nov., sp. Nov., a methanotroph isolated from two distinct marine environments. *International Journal of Systematic and Evolutionary Microbiology*, *63*(3), 1073–1082. https://doi.org/10.1099/ijs.0.040568-0

Hoefman, S., van der Ha, D., Iguchi, H., Yurimoto, H., Sakai, Y., Boon, N., Vandamme, P., Heylen, K., & De Vos, P. (2014). *Methyloparacoccus murrellii* gen. Nov., sp. Nov., a methanotroph isolated from pond water. *International Journal of Systematic and Evolutionary Microbiology*, *64*(Pt 6), 2100–2107. https://doi.org/10.1099/ijs.0.057760-0

Holmes, A. J., Costello, A., Lidstrom, M. E., & Murrell, J. C. (1995). Evidence that particulate methane monooxygenase and ammonia monooxygenase may be evolutionarily related. *FEMS Microbiology Letters*, *132*(3), 203–208. https://doi.org/10.1111/j.1574-6968.1995.tb07834.x

Holmes, A. J., Roslev, P., McDonald, I. R., Iversen, N., Henriksen, K., & Murrell, J. C. (1999). Characterization of Methanotrophic Bacterial Populations in Soils Showing Atmospheric Methane Uptake. *Applied and Environmental Microbiology*, *65*(8), 3312–3318. https://doi.org/10.1128/AEM.65.8.3312-3318.1999

Hou, S., Makarova, K. S., Saw, J. H., Senin, P., Ly, B. V., Zhou, Z., Ren, Y., Wang, J., Galperin, M. Y., Omelchenko, M. V., Wolf, Y. I., Yutin, N., Koonin, E. V., Stott, M. B., Mountain, B. W., Crowe, M. A., Smirnova, A. V., Dunfield, P. F., Feng, L., … Alam, M. (2008). Complete genome sequence of the extremely acidophilic methanotroph isolate V4, *Methylacidiphilum infernorum*, a representative of the bacterial phylum *Verrucomicrobia*. *Biology Direct*, *3*(1), 26. https://doi.org/10.1186/1745-6150-3-26

Huber-Humer, M., Gebert, J., & Hilger, H. (2008). Biotic systems to mitigate landfill methane emissions. *Waste Management & Research*, *26*(1), 33–46. https://doi.org/10.1177/0734242X07087977

Huelsenbeck, J. P. (2001). Bayesian Inference of Phylogeny and Its Impact on Evolutionary Biology. *Science*, *294*(5550), 2310–2314. https://doi.org/10.1126/science.1065889

Hutchens, E., Radajewski, S., Dumont, M. G., McDonald, I. R., & Murrell, J. C. (2003). Analysis of methanotrophic bacteria in Movile Cave by stable isotope probing: Methanotrophs in Movile Cave. *Environmental Microbiology*, *6*(2), 111–120. https://doi.org/10.1046/j.1462-2920.2003.00543.x

Iguchi, H., Yurimoto, H., & Sakai, Y. (2010). Soluble and particulate methane monooxygenase gene clusters of the type I methanotroph *Methylovulum miyakonense* HT12. *FEMS Microbiology Letters*, *312*(1), 71–76. https://doi.org/10.1111/j.1574-6968.2010.02101.x

Iguchi, H., Yurimoto, H., & Sakai, Y. (2011). *Methylovulum miyakonense* gen. Nov., sp. Nov., a type I methanotroph isolated from forest soil. *International Journal of Systematic and Evolutionary Microbiology*, *61*(4), 810–815. https://doi.org/10.1099/ijs.0.019604-0

Im, J., Lee, S.-W., Yoon, S., DiSpirito, A. A., & Semrau, J. D. (2011). Characterization of a novel facultative *Methylocystis* species capable of growth on methane, acetate and ethanol. *Environmental Microbiology Reports*, *3*(2), 174–181. https://doi.org/10.1111/j.1758-2229.2010.00204.x

IPCC. (2014). *Climate Change 2014: Synthesis Report* (R. K. Pachauri, L. Mayer, & Intergovernmental Panel on Climate Change, Eds.). Intergovernmental Panel on Climate Change.

Islam, T., Jensen, S., Reigstad, L. J., Larsen, Ø., & Birkeland, N.-K. (2008). Methane oxidation at 55°C and pH 2 by a thermoacidophilic bacterium belonging to the *Verrucomicrobia* phylum. *Proceedings of the National Academy of Sciences*, *105*(1), 300–304. https://doi.org/10.1073/pnas.0704162105

Jain, R., Rivera, M. C., & Lake, J. A. (1999). Horizontal gene transfer among genomes: The complexity hypothesis. *Proceedings of the National Academy of Sciences*, *96*(7), 3801–3806. https://doi.org/10.1073/pnas.96.7.3801

Jeong, H. S., & Jouanneau, Y. (2000). Enhanced nitrogenase activity in strains of *Rhodobacter capsulatus* that overexpress the *rnf* genes. *Journal of Bacteriology*, *182*(5), 1208–1214. https://doi.org/10.1128/jb.182.5.1208-1214.2000

Jiang, Y., Wilkins, P. C., & Dalton, H. (1993). Activation of the hydroxylase of sMMO from *Methylococcus capsulatus* (Bath) by hydrogen peroxide. *Biochimica et Biophysica Acta (BBA) - Protein Structure and Molecular Enzymology*, *1163*(1), 105–112. https://doi.org/10.1016/0167-4838(93)90285-Y

Johnson, C. (2006). Methanobactin: A potential novel biopreservative for use against the foodborne pathogen *Listeria monocytogenes*. *Retrospective Theses and Dissertations*. https://doi.org/10.31274/rtd-180813-11479

Johnson, K. A., Ve, T., Larsen, Ø., Pedersen, R. B., Lillehaug, J. R., Jensen, H. B., Helland, R., & Karlsen, O. A. (2014). CorA Is a Copper Repressible Surface-Associated Copper(I)-Binding Protein Produced in *Methylomicrobium album* BG8. *PLOS ONE*, *9*(2), e87750. https://doi.org/10.1371/journal.pone.0087750

Kalidass, B., Farhan Ul Haque, M., Baral, B. S., DiSpirito, A. A., & Semrau, J. D. (2015). Competition between Metals for Binding to Methanobactin Enables Expression of Soluble Methane Monooxygenase in the Presence of Copper. *Applied and Environmental Microbiology*, *81*(3), 1024–1031. https://doi.org/10.1128/AEM.03151-14

Kaluzhnaya, M., Khmelenina, V., Eshinimaev, B., Suzina, N., Nikitin, D., Solonin, A., Lin, J.-L., McDonald, I., Murrell, J. C., & Trotsenko, Y. (2001). Taxonomic Characterization of New Alkaliphilic and Alkalitolerant Methanotrophs from Soda Lakes of the Southeastern Transbaikal Region and description of *Methylomicrobium buryatense* sp. Nov. *Systematic and Applied Microbiology*, *24*(2), 166–176. https://doi.org/10.1078/0723-2020-00028

Kalyuzhnaya, M. G., Gomez, O. A., & Murrell, J. C. (2019). The Methane-Oxidizing Bacteria (Methanotrophs). In T. J. McGenity (Ed.), *Taxonomy, Genomics and Ecophysiology of Hydrocarbon-Degrading Microbes* (pp. 1–34). Springer International Publishing. https://doi.org/10.1007/978-3-319-60053-6_10-1

Kalyuzhnaya, M. G., Lamb, A. E., McTaggart, T. L., Oshkin, I. Y., Shapiro, N., Woyke, T., & Chistoserdova, L. (2015a). Draft Genome Sequences of Gammaproteobacterial Methanotrophs Isolated from Lake Washington Sediment. *Genome Announcements*, *3*(2), e00103-15, /ga/3/2/e00103-15.atom. https://doi.org/10.1128/genomeA.00103-15

Kalyuzhnaya, M. G., Puri, A. W., & Lidstrom, M. E. (2015b). Metabolic engineering in methanotrophic bacteria. *Metabolic Engineering*, *29*, 142–152. https://doi.org/10.1016/j.ymben.2015.03.010

Kalyuzhnaya, M. G., Yang, S., Rozova, O. N., Smalley, N. E., Clubb, J., Lamb, A., Gowda, G. A. N., Raftery, D., Fu, Y., Bringel, F., Vuilleumier, S., Beck, D. a. C., Trotsenko, Y. A.,

Khmelenina, V. N., & Lidstrom, M. E. (2013). Highly efficient methane biocatalysis revealed in a methanotrophic bacterium. *Nature Communications*, *4*(1), 1–7. https://doi.org/10.1038/ncomms3785

Kanehisa, M., & Sato, Y. (2020). KEGG Mapper for inferring cellular functions from protein sequences. *Protein Science*, *29*(1), 28–35. https://doi.org/10.1002/pro.3711

Kanehisa, M., Sato, Y., & Morishima, K. (2016). BlastKOALA and GhostKOALA: KEGG Tools for Functional Characterization of Genome and Metagenome Sequences. *Journal of Molecular Biology*, *428*(4), 726–731. https://doi.org/10.1016/j.jmb.2015.11.006

Kang, C. S., Dunfield, P. F., & Semrau, J. D. (2019). The origin of aerobic methanotrophy within the Proteobacteria. *FEMS Microbiology Letters*, *366*(9). https://doi.org/10.1093/femsle/fnz096

Kao, W.-C., Chen, Y.-R., Yi, E. C., Lee, H., Tian, Q., Wu, K.-M., Tsai, S.-F., Yu, S. S.-F., Chen, Y.-J., Aebersold, R., & Chan, S. I. (2004). Quantitative Proteomic Analysis of Metabolic Regulation by Copper Ions in *Methylococcus capsulatus* (Bath). *Journal of Biological Chemistry*, *279*(49), 51554–51560. https://doi.org/10.1074/jbc.M408013200

Karlsen, O. A., Berven, F. S., Stafford, G. P., Larsen, Ø., Murrell, J. C., Jensen, H. B., & Fjellbirkeland, A. (2003). The surface-associated and secreted MopE protein of *Methylococcus capsulatus* (Bath) responds to changes in the concentration of copper in the growth medium. *Applied and Environmental Microbiology*, *69*(4), 2386–2388. https://doi.org/10.1128/aem.69.4.2386-2388.2003

Karlsen, O. A., Kindingstad, L., Angelskår, S. M., Bruseth, L. J., Straume, D., Puntervoll, P., Fjellbirkeland, A., Lillehaug, J. R., & Jensen, H. B. (2005). Identification of a copper-repressible C-type heme protein of *Methylococcus capsulatus* (Bath). *The FEBS Journal*, *272*(24), 6324–6335. https://doi.org/10.1111/j.1742-4658.2005.05020.x

Karlsen, O. A., Larsen, Ø., & Jensen, H. B. (2010). Identification of a bacterial di-haem cytochrome *c* peroxidase from *Methylomicrobium album* BG8. *Microbiology, 156*(9), 2682–2690. https://doi.org/10.1099/mic.0.037119-0

Kaserer, H. (1905). Über die Oxidation des Wasserstoffes und des Methans durch Mikroorganismen. *Z. Landw. Versuchsw. in Österreich*, *8*, 789–792.

Keltjens, J. T., Pol, A., Reimann, J., & Op den Camp, H. J. M. (2014). PQQ-dependent methanol dehydrogenases: Rare-earth elements make a difference. *Applied Microbiology and Biotechnology*, *98*(14), 6163–6183. https://doi.org/10.1007/s00253-014-5766-8

Kemp, M. B. (1972). The hexose phosphate synthetase of *Methylococcus capsulatus*. *Biochemical Journal*, *127*(3), 64P-65P. https://doi.org/10.1042/bj1270064Pb

Kemp, M. B. (1974). Hexose phosphate synthetase from *Methylococcus capsulatus* makes d–arabino-3-hexulose phosphate. *Biochemical Journal*, *139*(1), 129–134. https://doi.org/10.1042/bj1390129

Kenney, G. E., Dassama, L. M. K., Pandelia, M.-E., Gizzi, A. S., Martinie, R. J., Gao, P., DeHart, C. J., Schachner, L. F., Skinner, O. S., Ro, S. Y., Zhu, X., Sadek, M., Thomas, P. M., Almo, S. C., Bollinger, J. M., Krebs, C., Kelleher, N. L., & Rosenzweig, A. C. (2018). The biosynthesis of methanobactin. *Science*, *359*(6382), 1411–1416. https://doi.org/10.1126/science.aap9437

Kenney, G. E., Goering, A. W., Ross, M. O., DeHart, C. J., Thomas, P. M., Hoffman, B. M., Kelleher, N. L., & Rosenzweig, A. C. (2016a). Characterization of Methanobactin from *Methylosinus* sp. LW4. *Journal of the American Chemical Society*, *138*(35), 11124–11127. https://doi.org/10.1021/jacs.6b06821

Kenney, G. E., & Rosenzweig, A. C. (2013). Genome mining for methanobactins. *BMC Biology*, *11*(1), 17. https://doi.org/10.1186/1741-7007-11-17

Kenney, G. E., & Rosenzweig, A. C. (2018). Chalkophores. *Annual Review of Biochemistry*, *87*(1), 645–676. https://doi.org/10.1146/annurev-biochem-062917-012300

Kenney, G. E., Sadek, M., & Rosenzweig, A. C. (2016b). Copper-responsive gene expression in the methanotroph *Methylosinus trichosporium* OB3b. *Metallomics*, *8*(9), 931–940. https://doi.org/10.1039/C5MT00289C

Khadem, A. F., Pol, A., Wieczorek, A., Mohammadi, S. S., Francoijs, K.-J., Stunnenberg, H. G., Jetten, M. S. M., & Camp, H. J. M. O. den. (2011). Autotrophic Methanotrophy in Verrucomicrobia: *Methylacidiphilum fumariolicum* SolV Uses the Calvin-Benson-Bassham Cycle for Carbon Dioxide Fixation. *Journal of Bacteriology*, *193*(17), 4438–4446. https://doi.org/10.1128/JB.00407-11

Khadem, A. F., Pol, A., Wieczorek, A. S., Jetten, M. S. M., & Op Den Camp, H. J. M. (2012a). Metabolic Regulation of "*Ca.* Methylacidiphilum Fumariolicum" SolV Cells Grown Under Different Nitrogen and Oxygen Limitations. *Frontiers in Microbiology*, *3*. https://doi.org/10.3389/fmicb.2012.00266

Khadem, A. F., Wieczorek, A. S., Pol, A., Vuilleumier, S., Harhangi, H. R., Dunfield, P. F., Kalyuzhnaya, M. G., Murrell, J. C., Francoijs, K.-J., Stunnenberg, H. G., Stein, L. Y., DiSpirito, A. A., Semrau, J. D., Lajus, A., Médigue, C., Klotz, M. G., Jetten, M. S. M., & Camp, H. J. M. O. den. (2012b). Draft Genome Sequence of the Volcano-Inhabiting Thermoacidophilic Methanotroph *Methylacidiphilum fumariolicum* Strain SolV. *Journal of Bacteriology*, *194*(14), 3729–3730. https://doi.org/10.1128/JB.00501-12

Khadka, R., Clothier, L., Wang, L., Lim, C. K., Klotz, M. G., & Dunfield, P. F. (2018). Evolutionary History of Copper Membrane Monooxygenases. *Frontiers in Microbiology*, *9*. https://doi.org/10.3389/fmicb.2018.02493

Khalifa, A., Lee, C. G., Ogiso, T., Ueno, C., Dianou, D., Demachi, T., Katayama, A., & Asakawa, S. (2015). *Methylomagnum ishizawai* gen. Nov., sp. Nov., a mesophilic type I methanotroph isolated from rice rhizosphere. *International Journal of Systematic and Evolutionary Microbiology*, *65*(10), 3527–3534. https://doi.org/10.1099/ijsem.0.000451

Khlebtsov, N. G., & Dykman, L. A. (2010). Optical properties and biomedical applications of plasmonic nanoparticles. *Journal of Quantitative Spectroscopy and Radiative Transfer*, *111*(1), 1–35. https://doi.org/10.1016/j.jqsrt.2009.07.012

Khmelenina, V. N., Kalyuzhnaya, M. G., Starostina, N. G., Suzina, N. E., & Trotsenko, Y. A. (1997). Isolation and Characterization of Halotolerant Alkaliphilic Methanotrophic Bacteria from Tuva Soda Lakes. *Current Microbiology*, *35*(5), 257–261. https://doi.org/10.1007/s002849900249

Khmelenina, V. N., Murrell, J. C., Smith, T. J., & Trotsenko, Y. A. (2018a). Physiology and Biochemistry of the Aerobic Methanotrophs. In F. Rojo (Ed.), *Aerobic Utilization of Hydrocarbons, Oils and Lipids* (pp. 1–25). Springer International Publishing. https://doi.org/10.1007/978-3-319-39782-5_4-1

Khmelenina, V. N., Rozova, O. N., Akberdin, I. R., Kalyuzhnaya, M. G., & Trotsenko, Y. A. (2018b). Pyrophosphate-Dependent Enzymes in Methanotrophs: New Findings and Views. In M. G. Kalyuzhnaya & X.-H. Xing (Eds.), *Methane Biocatalysis: Paving the Way to Sustainability* (pp. 83–98). Springer International Publishing. https://doi.org/10.1007/978-3-319-74866-5_6

Kim, H. J., Graham, D. W., DiSpirito, A. A., Alterman, M. A., Galeva, N., Larive, C. K., Asunskis, D., & Sherwood, P. M. A. (2004). Methanobactin, a Copper-Acquisition Compound from Methane-Oxidizing Bacteria. *Science*, *305*(5690), 1612–1615. https://doi.org/10.1126/science.1098322

Kim, M., Wilpiszeski, R. L., Wells, M., Wymore, A. M., Gionfriddo, C. M., Brooks, S. C., Podar, M., & Elias, D. A. (2021). Metagenome-Assembled Genome Sequences of Novel Prokaryotic Species from the Mercury-Contaminated East Fork Poplar Creek, Oak Ridge, Tennessee, USA. *Microbiology Resource Announcements*, *10*(17). https://doi.org/10.1128/MRA.00153-21

Kits, K. D., Campbell, D. J., Rosana, A. R., & Stein, L. Y. (2015a). Diverse electron sources support denitrification under hypoxia in the obligate methanotroph *Methylomicrobium album* strain BG8. *Frontiers in Microbiology*, *6*. https://doi.org/10.3389/fmicb.2015.01072

Kits, K. D., Klotz, M. G., & Stein, L. Y. (2015b). Methane oxidation coupled to nitrate reduction under hypoxia by the Gammaproteobacterium *Methylomonas denitrificans*, sp. Nov. Type strain FJG1. *Environmental Microbiology*, *17*(9), 3219–3232. https://doi.org/10.1111/1462-2920.12772

Knief, C., Lipski, A., & Dunfield, P. F. (2003). Diversity and Activity of Methanotrophic Bacteria in Different Upland Soils. *Applied and Environmental Microbiology*, *69*(11), 6703–6714. https://doi.org/10.1128/AEM.69.11.6703-6714.2003

Koay, M., Zhang, L., Yang, B., Maher, M. J., Xiao, Z., & Wedd, A. G. (2005). CopC Protein from *Pseudomonas syringae*: Intermolecular Transfer of Copper from Both the Copper(I) and Copper(II) Sites. *Inorganic Chemistry*, *44*(15), 5203–5205. https://doi.org/10.1021/ic0506198

Kolb, S. (2009). Aerobic methanol-oxidizing *Bacteria* in soil. *FEMS Microbiology Letters*, *300*(1), 1–10. https://doi.org/10.1111/j.1574-6968.2009.01681.x

Koo, M.-S. (2003). A reducing system of the superoxide sensor SoxR in *Escherichia coli*. *The EMBO Journal*, *22*(11), 2614–2622. https://doi.org/10.1093/emboj/cdg252

Kool, D. M., Zhu, B., Rijpstra, W. I. C., Jetten, M. S. M., Ettwig, K. F., & Damsté, J. S. S. (2012). Rare Branched Fatty Acids Characterize the Lipid Composition of the Intra-Aerobic Methane Oxidizer "*Candidatus* Methylomirabilis oxyfera." *Applied and Environmental Microbiology*, *78*(24), 8650–8656. https://doi.org/10.1128/AEM.02099-12

Kopp, D. A., Berg, E. A., Costello, C. E., & Lippard, S. J. (2003). Structural Features of Covalently Cross-linked Hydroxylase and Reductase Proteins of Soluble Methane Monooxygenase as Revealed by Mass Spectrometric Analysis. *Journal of Biological Chemistry*, *278*(23), 20939–20945. https://doi.org/10.1074/jbc.M301581200

Kornberg, H. L., & Madsen, N. B. (1957). Synthesis of C_4-dicarboxylic acids from acetate by a "glyoxylate bypass" of the tricarboxylic acid cycle. *Biochimica et Biophysica Acta*, *24*, 651–653. https://doi.org/10.1016/0006-3002(57)90268-8

Korotkova, N., Chistoserdova, L., Kuksa, V., & Lidstrom, M. E. (2002a). Glyoxylate Regeneration Pathway in the Methylotroph *Methylobacterium extorquens* AM1. *Journal of Bacteriology*, *184*(6), 1750–1758. https://doi.org/10.1128/JB.184.6.1750-1758.2002

Korotkova, N., Chistoserdova, L., & Lidstrom, M. E. (2002b). Poly-β-Hydroxybutyrate Biosynthesis in the Facultative Methylotroph *Methylobacterium extorquens* AM1:

Identification and Mutation of *gap11*, *gap20*, and *phaR*. *Journal of Bacteriology*, *184*(22), 6174–6181. https://doi.org/10.1128/JB.184.22.6174-6181.2002

Krause, S. M. B., Johnson, T., Karunaratne, Y. S., Fu, Y., Beck, D. A. C., Chistoserdova, L., & Lidstrom, M. E. (2017a). Lanthanide-dependent cross-feeding of methane-derived carbon is linked by microbial community interactions. *Proceedings of the National Academy of Sciences*, *114*(2), 358–363. https://doi.org/10.1073/pnas.1619871114

Krause, S. M. B., Johnson, T., Samadhi Karunaratne, Y., Fu, Y., Beck, D. A. C., Chistoserdova, L., & Lidstrom, M. E. (2017b). Lanthanide-dependent cross-feeding of methane-derived carbon is linked by microbial community interactions. *Proceedings of the National Academy of Sciences*, *114*(2), 358–363. https://doi.org/10.1073/pnas.1619871114

Krentz, B. D., Mulheron, H. J., Semrau, J. D., DiSpirito, A. A., Bandow, N. L., Haft, D. H., Vuilleumier, S., Murrell, J. C., McEllistrem, M. T., Hartsel, S. C., & Gallagher, W. H. (2010). A Comparison of Methanobactins from *Methylosinus trichosporium* OB3b and *Methylocystis* Strain SB2 Predicts Methanobactins Are Synthesized from Diverse Peptide Precursors Modified To Create a Common Core for Binding and Reducing Copper Ions. *Biochemistry*, *49*(47), 10117–10130. https://doi.org/10.1021/bi1014375

Kumagai, H., Fujiwara, T., Matsubara, H., & Saeki, K. (1997). Membrane Localization, Topology, and Mutual Stabilization of the *rnfABC* Gene Products in *Rhodobacter capsulatus* and Implications for a New Family of Energy-Coupling NADH Oxidoreductases. *Biochemistry*, *36*(18), 5509–5521. https://doi.org/10.1021/bi970014q

Lane, D. J. (1991). 16S/23S rRNA sequencing. In E. Stackebrandt & M. Goodfellow (Eds.), *Nucleic acid techniques in bacterial systematics* (pp. 125–175). Wiley.

Lapidus, A., Clum, A., LaButti, K., Kaluzhnaya, M. G., Lim, S., Beck, D. A. C., Rio, T. G. del, Nolan, M., Mavromatis, K., Huntemann, M., Lucas, S., Lidstrom, M. E., Ivanova, N., & Chistoserdova, L. (2011). Genomes of Three Methylotrophs from a Single Niche Reveal the Genetic and Metabolic Divergence of the *Methylophilaceae*. *Journal of Bacteriology*, *193*(15), 3757–3764. https://doi.org/10.1128/JB.00404-11

Large, P. J., Peel, D., & Quayle, J. (1961). Microbial growth on C_1 compounds. 2. Synthesis of cell constituents by methanol- and formate-grown *Pseudomonas* AM 1, and methanol-grown *Hyphomicrobium vulgare*. *Biochemical Journal*, *81*(3), 470–480. https://doi.org/10.1042/bj0810470

Large, P. J., Peel, D., & Quayle, J. R. (1962a). Microbial growth on C_1 compounds. 3. Distribution of radioactivity in metabolites of methanol-grown *Pseudomonas* AM1 after incubation with [^{14}C]methanol and [^{14}C]bicarbonate. *Biochemical Journal*, *82*(3), 483–488. https://doi.org/10.1042/bj0820483

Large, P. J., Peel, D., & Quayle, J. R. (1962b). Microbial growth on C_1 compounds. 4. Carboxylation of phosphoenolpyruvate in methanol-grown *Pseudomonas* AM1. *Biochemical Journal*, *85*(1), 243–250. https://doi.org/10.1042/bj0850243

Large, P. J., & Quayle, J. R. (1963). Microbial growth on C_1 compounds. 5. Enzyme activities in extracts of *Pseudomonas* AM1. *Biochemical Journal*, *87*(2), 386–396. https://doi.org/10.1042/bj0870386

Larsen, Ø., & Karlsen, O. A. (2016). Transcriptomic profiling of *Methylococcus capsulatus* (Bath) during growth with two different methane monooxygenases. *Microbiology Open*, *5*(2), 254–267. https://doi.org/10.1002/mbo3.324

Lawton, T. J., Kenney, G. E., Hurley, J. D., & Rosenzweig, A. C. (2016). The CopC Family: Structural and Bioinformatic Insights into a Diverse Group of Periplasmic Copper

Binding Proteins. *Biochemistry*, *55*(15), 2278–2290. https://doi.org/10.1021/acs.biochem.6b00175
Lawton, T. J., & Rosenzweig, A. C. (2016). Biocatalysts for methane conversion: Big progress on breaking a small substrate. *Current Opinion in Chemical Biology*, *35*, 142–149. https://doi.org/10.1016/j.cbpa.2016.10.001
Leahy, J. G., Batchelor, P. J., & Morcomb, S. M. (2003). Evolution of the soluble diiron monooxygenases. *FEMS Microbiology Reviews*, *27*(4), 449–479. https://doi.org/10.1016/S0168-6445(03)00023-8
Leak, D. J., & Dalton, H. (1983). *In vivo* Studies of Primary Alcohols, Aldehydes and Carboxylic Acids as Electron Donors for the Methane Mono-oxygenase in a Variety of Methanotrophs. *Microbiology*, *129*(11), 3487–3497. https://doi.org/10.1099/00221287-129-11-3487
Leak, D. J., & Dalton, H. (1986a). Growth yields of methanotrophs 1. Effect of copper on the energetics of methane oxidation. *Applied Microbiology and Biotechnology*, *23*(6), 470–476. https://doi.org/10.1007/BF02346062
Leak, D. J., & Dalton, H. (1986b). Growth yields of methanotrophs 2. A theoretical analysis. *Applied Microbiology and Biotechnology*, *23*(6), 477–481. https://doi.org/10.1007/BF02346063
Lee, S. J., McCormick, M. S., Lippard, S. J., & Cho, U.-S. (2013). Control of substrate access to the active site in methane monooxygenase. *Nature*, *494*(7437), 380–384. https://doi.org/10.1038/nature11880
Lee, S.-K., Fox, B. G., Froland, W. A., Lipscomb, J. D., & Munck, E. (1993). A transient intermediate of the methane monooxygenase catalytic cycle containing an $Fe^{IV}Fe^{IV}$ cluster. *Journal of the American Chemical Society*, *115*(14), 6450–6451. https://doi.org/10.1021/ja00067a086
Lee, S.-K., & Lipscomb, J. D. (1999). Oxygen Activation Catalyzed by Methane Monooxygenase Hydroxylase Component: Proton Delivery during the O−O Bond Cleavage Steps. *Biochemistry*, *38*(14), 4423–4432. https://doi.org/10.1021/bi982712w
Lee, S.-W., Keeney, D. R., Lim, D.-H., Dispirito, A. A., & Semrau, J. D. (2006). Mixed Pollutant Degradation by *Methylosinus trichosporium* OB3b Expressing either Soluble or Particulate Methane Monooxygenase: Can the Tortoise Beat the Hare? *Applied and Environmental Microbiology*, *72*(12), 7503–7509. https://doi.org/10.1128/AEM.01604-06
Lichtmannegger, J., Leitzinger, C., Wimmer, R., Schmitt, S., Schulz, S., Kabiri, Y., Eberhagen, C., Rieder, T., Janik, D., Neff, F., Straub, B. K., Schirmacher, P., DiSpirito, A. A., Bandow, N., Baral, B. S., Flatley, A., Kremmer, E., Denk, G., Reiter, F. P., … Zischka, H. (2016). Methanobactin reverses acute liver failure in a rat model of Wilson disease. *The Journal of Clinical Investigation*, *126*(7), 2721–2735. https://doi.org/10.1172/JCI85226
Lidstrom, M. E. (1988). Isolation and characterization of marine methanotrophs. *Antonie van Leeuwenhoek*, *54*(3), 189–199. https://doi.org/10.1007/BF00443577
Lieberman, R. L., & Rosenzweig, A. C. (2005a). Crystal structure of a membrane-bound metalloenzyme that catalyses the biological oxidation of methane. *Nature*, *434*(7030), 177–182. https://doi.org/10.1038/nature03311

Lieberman, R. L., & Rosenzweig, A. C. (2005b). The quest for the particulate methane monooxygenase active site. *Dalton Transactions*, *21*, 3390–3396. https://doi.org/10.1039/B506651D

Lieberman, R. L., Shrestha, D. B., Doan, P. E., Hoffman, B. M., Stemmler, T. L., & Rosenzweig, A. C. (2003). Purified particulate methane monooxygenase from *Methylococcus capsulatus* (Bath) is a dimer with both mononuclear copper and a copper-containing cluster. *Proceedings of the National Academy of Sciences*, *100*(7), 3820–3825. https://doi.org/10.1073/pnas.0536703100

Lieven, C., Petersen, L. A. H., Jørgensen, S. B., Gernaey, K. V., Herrgard, M. J., & Sonnenschein, N. (2018). A Genome-Scale Metabolic Model for *Methylococcus capsulatus* (Bath) Suggests Reduced Efficiency Electron Transfer to the Particulate Methane Monooxygenase. *Frontiers in Microbiology*, *9*. https://doi.org/10.3389/fmicb.2018.02947

Liew, E. F., Tong, D., Coleman, N. V., & Holmes, A. J. (2014). Mutagenesis of the hydrocarbon monooxygenase indicates a metal centre in subunit-C, and not subunit-B, is essential for copper-containing membrane monooxygenase activity. *Microbiology, 160*(6), 1267–1277. https://doi.org/10.1099/mic.0.078584-0

Lim, S., & Franklin, S. J. (2004). Lanthanide-binding peptides and the enzymes that Might Have Been. *Cellular and Molecular Life Sciences CMLS*, *61*(17), 2184–2188. https://doi.org/10.1007/s00018-004-4156-2

Lin, H., Lu, X., Liang, L., & Gu, B. (2015). Thiol-Facilitated Cell Export and Desorption of Methylmercury by Anaerobic Bacteria. *Environmental Science & Technology Letters*, *2*(10), 292–296. https://doi.org/10.1021/acs.estlett.5b00209

Lipscomb, J. D. (1994). Biochemistry of the soluble methane monooxygenase. *Annual Review of Microbiology*, *48*(1), 371–399. https://doi.org/10.1146/annurev.mi.48.100194.002103

Liu, Y., Nesheim, J. C., Lee, S.-K., & Lipscomb, J. D. (1995). Gating Effects of Component B on Oxygen Activation by the Methane Monooxygenase Hydroxylase Component. *Journal of Biological Chemistry*, *270*(42), 24662–24665. https://doi.org/10.1074/jbc.270.42.24662

Liu, Y.-R., Lu, X., Zhao, L., An, J., He, J.-Z., Pierce, E. M., Johs, A., & Gu, B. (2016). Effects of Cellular Sorption on Mercury Bioavailability and Methylmercury Production by *Desulfovibrio desulfuricans* ND132. *Environmental Science & Technology*, *50*(24), 13335–13341. https://doi.org/10.1021/acs.est.6b04041

Lontoh, S., DiSpirito, A. A., & Semrau, J. D. (1999). Dichloromethane and trichloroethylene inhibition of methane oxidation by the membrane-associated methane monooxygenase of *Methylosinus trichosporium* OB3b. *Archives of Microbiology*, *171*(5), 301–308. https://doi.org/10.1007/s002030050714

Lu, X., Gu, W., Zhao, L., Farhan Ul Haque, M., DiSpirito, A. A., Semrau, J. D., & Gu, B. (2017). Methylmercury uptake and degradation by methanotrophs. *Science Advances*, *3*(5), e1700041. https://doi.org/10.1126/sciadv.1700041

Lu, X., Liu, Y., Johs, A., Zhao, L., Wang, T., Yang, Z., Lin, H., Elias, D. A., Pierce, E. M., Liang, L., Barkay, T., & Gu, B. (2016). Anaerobic Mercury Methylation and Demethylation by *Geobacter bemidjiensis* Bem. *Environmental Science & Technology*, *50*(8), 4366–4373. https://doi.org/10.1021/acs.est.6b00401

Lund, J., & Dalton, H. (1985). Further characterisation of the FAD and Fe_2S_2 redox centres of component C, the NADH: acceptor reductase of the soluble methane monooxygenase of

Methylococcus capsulatus (Bath). *European Journal of Biochemistry*, *147*(2), 291–296. https://doi.org/10.1111/j.1432-1033.1985.tb08749.x

MacArthur, R., Sazinsky, M. H., Kühne, H., Whittington, D. A., Lippard, S. J., & Brudvig, G. W. (2002). Component B Binding to the Soluble Methane Monooxygenase Hydroxylase by Saturation-Recovery EPR Spectroscopy of Spin-Labeled MMOB. *Journal of the American Chemical Society*, *124*(45), 13392–13393. https://doi.org/10.1021/ja0279904

Mackenzie, C., Choudhary, M., Larimer, F. W., Predki, P. F., Stilwagen, S., Armitage, J. P., Barber, R. D., Donohue, T. J., Hosler, J. P., Newman, J. E., Shapleigh, J. P., Sockett, R. E., Zeilstra-Ryalls, J., & Kaplan, S. (2001). The home stretch, a first analysis of the nearly completed genome of *Rhodobacter sphaeroides* 2.4.1. *Photosynthesis Research*, *70*(1), 19–41. https://doi.org/10.1023/A:1013831823701

Maden, B. E. (2000). Tetrahydrofolate and tetrahydromethanopterin compared: Functionally distinct carriers in C_1 metabolism. *Biochemical Journal*, *350*(Pt 3), 609–629.

Mandel, M., & Higa, A. (1970). Calcium-dependent bacteriophage DNA infection. *Journal of Molecular Biology*, *53*(1), 159–162. https://doi.org/10.1016/0022-2836(70)90051-3

Marison, I. W., & Attwood, M. M. (1982). A Possible Alternative Mechanism for the Oxidation of Formaldehyde to Formate. *Microbiology*, *128*(7), 1441–1446. https://doi.org/10.1099/00221287-128-7-1441

Martin, H., & Murrell, J. C. (1995). Methane monooxygenase mutants of *Methylosinus trichosporium* constructed by marker-exchange mutagenesis. *FEMS Microbiology Letters*, *127*(3), 243–248. https://doi.org/10.1111/j.1574-6968.1995.tb07480.x

Martinho, M., Choi, D., DiSpirito, A. A., Antholine, W. E., Semrau, J. D., & Münck, E. (2007). Mössbauer Studies of the Membrane-Associated Methane Monooxygenase from *Methylococcus capsulatus* Bath: Evidence for a Diiron Center. *Journal of the American Chemical Society*, *129*(51), 15783–15785. https://doi.org/10.1021/ja077682b

Marx, C. J., Laukel, M., Vorholt, J. A., & Lidstrom, M. E. (2003). Purification of the Formate-Tetrahydrofolate Ligase from *Methylobacterium extorquens* AM1 and Demonstration of Its Requirement for Methylotrophic Growth. *Journal of Bacteriology*, *185*(24), 7169–7175. https://doi.org/10.1128/JB.185.24.7169-7175.2003

Masuda, S., Suzuki, Y., Fujitani, Y., Mitsui, R., Nakagawa, T., Shintani, M., & Tani, A. (2018). Lanthanide-Dependent Regulation of Methylotrophy in *Methylobacterium aquaticum* Strain 22A. *MSphere*, *3*(1), e00462-17. https://doi.org/10.1128/mSphere.00462-17

Mattocks, J. A., Ho, J. V., & Cotruvo, J. A. (2019). A Selective, Protein-Based Fluorescent Sensor with Picomolar Affinity for Rare Earth Elements. *Journal of the American Chemical Society*, *141*(7), 2857–2861. https://doi.org/10.1021/jacs.8b12155

Meier-Kolthoff, J. P., Auch, A. F., Klenk, H.-P., & Göker, M. (2013). Genome sequence-based species delimitation with confidence intervals and improved distance functions. *BMC Bioinformatics*, *14*(1), 60. https://doi.org/10.1186/1471-2105-14-60

Meister, M., Saum, S., Alber, B. E., & Fuchs, G. (2005). L-Malyl-Coenzyme A/β-Methylmalyl-Coenzyme A Lyase Is Involved in Acetate Assimilation of the Isocitrate Lyase-Negative Bacterium *Rhodobacter capsulatus*. *Journal of Bacteriology*, *187*(4), 1415–1425. https://doi.org/10.1128/JB.187.4.1415-1425.2005

Merkx, M., Kopp, D. A., Sazinsky, M. H., Blazyk, J. L., Müller, J., & Lippard, S. J. (2001). Dioxygen Activation and Methane Hydroxylation by Soluble Methane Monooxygenase: A Tale of Two Irons and Three Proteins. *Angewandte Chemie International Edition*,

40(15), 2782–2807. https://doi.org/10.1002/1521-3773(20010803)40:15<2782::AID-ANIE2782>3.0.CO;2-P

Miroshnikov, K. K., Didriksen, A., Naumoff, D. G., Huntemann, M., Clum, A., Pillay, M., Palaniappan, K., Varghese, N., Mikhailova, N., Mukherjee, S., Reddy, T. B. K., Daum, C., Shapiro, N., Ivanova, N., Kyrpides, N., Woyke, T., Dedysh, S. N., & Svenning, M. M. (2017). Draft Genome Sequence of *Methylocapsa palsarum* NE2T, an Obligate Methanotroph from Subarctic Soil. *Genome Announcements*, *5*(24). https://doi.org/10.1128/genomeA.00504-17

Mosher, J., Vishnivetskaya, T., Elias, D., Podar, M., Brooks, S., Brown, S., Brandt, C., & Palumbo, A. (2012). Characterization of the Deltaproteobacteria in contaminated and uncontaminated stream sediments and identification of potential mercury methylators. *Aquatic Microbial Ecology*, *66*(3), 271–282. https://doi.org/10.3354/ame01563

Müller, J.-C., Lichtmannegger, J., Zischka, H., Sperling, M., & Karst, U. (2018). High spatial resolution LA-ICP-MS demonstrates massive liver copper depletion in Wilson disease rats upon Methanobactin treatment. *Journal of Trace Elements in Medicine and Biology*, *49*, 119–127. https://doi.org/10.1016/j.jtemb.2018.05.009

Myronova, N., Kitmitto, A., Collins, R. F., Miyaji, A., & Dalton, H. (2006). Three-Dimensional Structure Determination of a Protein Supercomplex That Oxidizes Methane to Formaldehyde in *Methylococcus capsulatus* (Bath). *Biochemistry*, *45*(39), 11905–11914. https://doi.org/10.1021/bi061294p

Nagy, P. L., Marolewski, A., Benkovic, S. J., & Zalkin, H. (1995). Formyltetrahydrofolate hydrolase, a regulatory enzyme that functions to balance pools of tetrahydrofolate and one-carbon tetrahydrofolate adducts in *Escherichia coli*. *Journal of Bacteriology*, *177*(5), 1292–1298. https://doi.org/10.1128/jb.177.5.1292-1298.1995

Naizabekov, S., & Lee, E. Y. (2020). Genome-Scale Metabolic Model Reconstruction and in Silico Investigations of Methane Metabolism in *Methylosinus trichosporium* OB3b. *Microorganisms*, *8*(3). https://doi.org/10.3390/microorganisms8030437

Nakagawa, T., Mitsui, R., Tani, A., Sasa, K., Tashiro, S., Iwama, T., Hayakawa, T., & Kawai, K. (2012). A Catalytic Role of XoxF1 as La^{3+}-Dependent Methanol Dehydrogenase in *Methylobacterium extorquens* Strain AM1. *PLoS ONE*, *7*(11), e50480. https://doi.org/10.1371/journal.pone.0050480

Narayanan, K. B., & Sakthivel, N. (2010). Biological synthesis of metal nanoparticles by microbes. *Advances in Colloid and Interface Science*, *156*(1), 1–13. https://doi.org/10.1016/j.cis.2010.02.001

NCBI Resource Coordinators, Agarwala, R., Barrett, T., Beck, J., Benson, D. A., Bollin, C., Bolton, E., Bourexis, D., Brister, J. R., Bryant, S. H., Canese, K., Cavanaugh, M., Charowhas, C., Clark, K., Dondoshansky, I., Feolo, M., Fitzpatrick, L., Funk, K., Geer, L. Y., … Zbicz, K. (2018). Database resources of the National Center for Biotechnology Information. *Nucleic Acids Research*, *46*(D1), D8–D13. https://doi.org/10.1093/nar/gkx1095

Nielsen, A. K., Gerdes, K., & Murrell, J. C. (1997). Copper-dependent reciprocal transcriptional regulation of methane monooxygenase genes in *Methylococcus capsulatus* and *Methylosinus trichosporium*. *Molecular Microbiology*, *25*(2), 399–409. https://doi.org/10.1046/j.1365-2958.1997.4801846.x

Nojiri, M., Hira, D., Yamaguchi, K., Okajima, T., Tanizawa, K., & Suzuki, S. (2006). Crystal Structures of Cytochrome c_L and Methanol Dehydrogenase from *Hyphomicrobium*

denitrificans: Structural and Mechanistic Insights into Interactions between the Two Proteins. *Biochemistry*, *45*(11), 3481–3492. https://doi.org/10.1021/bi051877j

Notredame, C., Higgins, D. G., & Heringa, J. (2000). T-coffee: A novel method for fast and accurate multiple sequence alignment. *Journal of Molecular Biology*, *302*(1), 205–217. https://doi.org/10.1006/jmbi.2000.4042

Ochsner, A. M., Hemmerle, L., Vonderach, T., Nüssli, R., Bortfeld-Miller, M., Hattendorf, B., & Vorholt, J. A. (2019). Use of rare-earth elements in the phyllosphere colonizer *Methylobacterium extorquens* PA1. *Molecular Microbiology*, *111*(5), 1152–1166. https://doi.org/10.1111/mmi.14208

Ogawa, H. lyehara, Tolle, C. L., & Summers, A. O. (1984). Physical and genetic map of the organomercury resistance (Omr) and inorganic mercury resistance (Hgr) loci of the IncM plasmid R831b. *Gene*, *32*(3), 311–320. https://doi.org/10.1016/0378-1119(84)90006-4

Oldenhuis, R., Oedzes, J. Y., Waarde, J. J. van der, & Janssen, D. B. (1991). Kinetics of chlorinated hydrocarbon degradation by *Methylosinus trichosporium* OB3b and toxicity of trichloroethylene. *Applied and Environmental Microbiology*, *57*(1), 7–14.

Oldenhuis, R., Vink, R. L., Janssen, D. B., & Witholt, B. (1989). Degradation of chlorinated aliphatic hydrocarbons by *Methylosinus trichosporium* OB3b expressing soluble methane monooxygenase. *Applied and Environmental Microbiology*, *55*(11), 2819–2826.

Op den Camp, H. J. M., Islam, T., Stott, M. B., Harhangi, H. R., Hynes, A., Schouten, S., Jetten, M. S. M., Birkeland, N.-K., Pol, A., & Dunfield, P. F. (2009). Environmental, genomic and taxonomic perspectives on methanotrophic *Verrucomicrobia*. *Environmental Microbiology Reports*, *1*(5), 293–306. https://doi.org/10.1111/j.1758-2229.2009.00022.x

Orata, F. D., Meier-Kolthoff, J. P., Sauvageau, D., & Stein, L. Y. (2018). Phylogenomic Analysis of the Gammaproteobacterial Methanotrophs (Order *Methylococcales*) Calls for the Reclassification of Members at the Genus and Species Levels. *Frontiers in Microbiology*, *9*. https://doi.org/10.3389/fmicb.2018.03162

Osborne, C. D., & Haritos, V. S. (2018). Horizontal gene transfer of three co-inherited methane monooxygenase systems gave rise to methanotrophy in the Proteobacteria. *Molecular Phylogenetics and Evolution*, *129*, 171–181. https://doi.org/10.1016/j.ympev.2018.08.010

Oswald, K., Graf, J. S., Littmann, S., Tienken, D., Brand, A., Wehrli, B., Albertsen, M., Daims, H., Wagner, M., Kuypers, M. M., Schubert, C. J., & Milucka, J. (2017). *Crenothrix* are major methane consumers in stratified lakes. *The ISME Journal*, *11*(9), 2124–2140. https://doi.org/10.1038/ismej.2017.77

Park, Y. J., Kenney, G. E., Schachner, L. F., Kelleher, N. L., & Rosenzweig, A. C. (2018). Repurposed HisC Aminotransferases Complete the Biosynthesis of Some Methanobactins. *Biochemistry*, *57*(25), 3515–3523. https://doi.org/10.1021/acs.biochem.8b00296

Parks, J. M., Johs, A., Podar, M., Bridou, R., Hurt, R. A., Smith, S. D., Tomanicek, S. J., Qian, Y., Brown, S. D., Brandt, C. C., Palumbo, A. V., Smith, J. C., Wall, J. D., Elias, D. A., & Liang, L. (2013). The Genetic Basis for Bacterial Mercury Methylation. *Science*, *339*(6125), 1332–1335. https://doi.org/10.1126/science.1230667

Patel, R. N., Hou, C. T., Derelanko, P., & Felix, A. (1980). Purification and properties of a heme-containing aldehyde dehydrogenase from *Methylosinus trichosporium*. *Archives of Biochemistry and Biophysics*, *203*(2), 654–662. https://doi.org/10.1016/0003-9861(80)90223-4

Peden, J. (1999). *Analysis of Codon Usage* [Thesis]. Department of Genetics, University of Nottingham.

Peterson, M. J., Brooks, S. C., Mathews, T. J., Mayes, M. A., Johs, A., Watson, D. B., Muller, K. A., Gonez Rodriguez, L., Derolph, C. R., & Surendrannair, S. (2018). *Mercury Remediation Technology Development for Lower East Fort Poplar Creek—FY2018 Update* (ORNL/SPR--2018/912, 1490603; p. ORNL/SPR--2018/912, 1490603). https://doi.org/10.2172/1490603

Peyraud, R., Kiefer, P., Christen, P., Massou, S., Portais, J.-C., & Vorholt, J. A. (2009). Demonstration of the ethylmalonyl-CoA pathway by using ^{13}C metabolomics. *Proceedings of the National Academy of Sciences*, *106*(12), 4846–4851. https://doi.org/10.1073/pnas.0810932106

Pol, A., Barends, T. R. M., Dietl, A., Khadem, A. F., Eygensteyn, J., Jetten, M. S. M., & Camp, H. J. M. O. den. (2014). Rare earth metals are essential for methanotrophic life in volcanic mudpots. *Environmental Microbiology*, *16*(1), 255–264. https://doi.org/10.1111/1462-2920.12249

Pol, A., Heijmans, K., Harhangi, H. R., Tedesco, D., Jetten, M. S. M., & Camp, H. J. M. O. den. (2007). Methanotrophy below pH 1 by a new *Verrucomicrobia* species. *Nature*, *450*(7171), 874–878. https://doi.org/10.1038/nature06222

Pomper, B. K., Saurel, O., Milon, A., & Vorholt, J. A. (2002). Generation of formate by the formyltransferase/hydrolase complex (Fhc) from *Methylobacterium extorquens* AM1. *FEBS Letters*, *523*(1–3), 133–137. https://doi.org/10.1016/S0014-5793(02)02962-9

Pomper, B. K., & Vorholt, J. A. (2001). Characterization of the formyltransferase from *Methylobacterium extorquens* AM1. *European Journal of Biochemistry*, *268*(17), 4769–4775. https://doi.org/10.1046/j.1432-1327.2001.02401.x

Pomper, B. K., Vorholt, J. A., Chistoserdova, L., Lidstrom, M. E., & Thauer, R. K. (1999). A methenyl tetrahydromethanopterin cyclohydrolase and a methenyl tetrahydrofolate cyclohydrolase in *Methylobacterium extorquens* AM1. *European Journal of Biochemistry*, *261*(2), 475–480. https://doi.org/10.1046/j.1432-1327.1999.00291.x

Pourali, P., Badiee, S. H., Manafi, S., Noorani, T., Rezaei, A., & Yahyaei, B. (2017). Biosynthesis of gold nanoparticles by two bacterial and fungal strains, *Bacillus cereus* and *Fusarium oxysporum*, and assessment and comparison of their nanotoxicity *in vitro* by direct and indirect assays. *Electronic Journal of Biotechnology*, *29*, 86–93. https://doi.org/10.1016/j.ejbt.2017.07.005

Prior, S. D., & Dalton, H. (1985). Acetylene as a suicide substrate and active site probe for methane monooxygenase from *Methylococcus capsulatus* (Bath). *FEMS Microbiology Letters*, *29*(1–2), 105–109. https://doi.org/10.1111/j.1574-6968.1985.tb00843.x

Puri, A. W., Liu, D., Schaefer, A. L., Yu, Z., Pesesky, M. W., Greenberg, E. P., & Lidstrom, M. E. (2019). Interspecies Chemical Signaling in a Methane-Oxidizing Bacterial Community. *Applied and Environmental Microbiology*, *85*(7). https://doi.org/10.1128/AEM.02702-18

R Core Team. (2018). *R: A language and environment for statistical computing*. R Foundation for Statistical Computing. https://www.R-project.org/

Rahalkar, M., Bussmann, I., & Schink, B. (2007). *Methylosoma difficile* gen. Nov., sp. Nov., a novel methanotroph enriched by gradient cultivation from littoral sediment of Lake Constance. *International Journal of Systematic and Evolutionary Microbiology*, *57*(5), 1073–1080. https://doi.org/10.1099/ijs.0.64574-0

Rasigraf, O., Kool, D. M., Jetten, M. S. M., Damsté, J. S. S., & Ettwig, K. F. (2014). Autotrophic Carbon Dioxide Fixation via the Calvin-Benson-Bassham Cycle by the Denitrifying Methanotroph "*Candidatus* Methylomirabilis oxyfera." *Applied and Environmental Microbiology*, *80*(8), 2451–2460. https://doi.org/10.1128/AEM.04199-13

Rensing, C., Pribyl, T., & Nies, D. H. (1997). New functions for the three subunits of the CzcCBA cation-proton antiporter. *Journal of Bacteriology*, *179*(22), 6871–6879. https://doi.org/10.1128/jb.179.22.6871-6879.1997

Revis, N. W., Osborne, T. R., Holdsworth, G., & Hadden, C. (1989). Distribution of mercury species in soil from a mercury-contaminated site. *Water, Air, and Soil Pollution*, *45*, 105–113.

Richardson, I. W., & Anthony, C. (1992). Characterization of mutant forms of the quinoprotein methanol dehydrogenase lacking an essential calcium ion. *Biochemical Journal*, *287*(3), 709–715. https://doi.org/10.1042/bj2870709

Roberts, E. A. (2011). Wilson's disease. *Medicine*, *39*(10), 602–604. https://doi.org/10.1016/j.mpmed.2011.08.006

Rodrigues, J. D., Combrink, J., & Brandt, W. F. (1994). Derivatization of Polyvinylidene Difluoride Membranes for the Solid-Phase Sequence Analysis of a Phosphorylated Sea Urchin Embryo Histone H1 Peptide. *Analytical Biochemistry*, *216*(2), 365–372. https://doi.org/10.1006/abio.1994.1054

Rosenzweig, A. C., Frederick, C. A., Lippard, S. J., Auml, P., & Nordlund, R. (1993). Crystal structure of a bacterial non-haem iron hydroxylase that catalyses the biological oxidation of methane. *Nature*, *366*(6455), 537–543. https://doi.org/10.1038/366537a0

Rosenzweig, A. C., Nordlund, P., Takahara, P. M., Frederick, C. A., & Lippard, S. J. (1995). Geometry of the soluble methane monooxygenase catalytic diiron center in two oxidation states. *Chemistry & Biology*, *2*(6), 409–418. https://doi.org/10.1016/1074-5521(95)90222-8

Roslev, P., & Iversen, N. (1999). Radioactive Fingerprinting of Microorganisms That Oxidize Atmospheric Methane in Different Soils. *Applied and Environmental Microbiology*, *65*(9), 4064–4070. https://doi.org/10.1128/AEM.65.9.4064-4070.1999

Ross, M. O., MacMillan, F., Wang, J., Nisthal, A., Lawton, T. J., Olafson, B. D., Mayo, S. L., Rosenzweig, A. C., & Hoffman, B. M. (2019). Particulate methane monooxygenase contains only mononuclear copper centers. *Science*, *364*(6440), 566–570. https://doi.org/10.1126/science.aav2572

Ross, M. O., & Rosenzweig, A. C. (2017). A tale of two methane monooxygenases. *JBIC Journal of Biological Inorganic Chemistry*, *22*(2), 307–319. https://doi.org/10.1007/s00775-016-1419-y

Roszczenko-Jasińska, P., Vu, H. N., Subuyuj, G. A., Crisostomo, R. V., Cai, J., Lien, N. F., Clippard, E. J., Ayala, E. M., Ngo, R. T., Yarza, F., Wingett, J. P., Raghuraman, C., Hoeber, C. A., Martinez-Gomez, N. C., & Skovran, E. (2020). Gene products and processes contributing to lanthanide homeostasis and methanol metabolism in *Methylorubrum extorquens* AM1. *Scientific Reports*, *10*(1), 1–15. https://doi.org/10.1038/s41598-020-69401-4

Rozova, O. N., But, S. Y., Khmelenina, V. N., Reshetnikov, A. S., Mustakhimov, I. I., & Trotsenko, Y. A. (2017). Characterization of two recombinant 3-hexulose-6-phosphate synthases from the halotolerant obligate methanotroph *Methylomicrobium alcaliphilum*

20Z. *Biochemistry (Moscow)*, *82*(2), 176–185. https://doi.org/10.1134/S0006297917020092
Rozova, O. N., Khmelenina, V. N., Gavletdinova, J. Z., Mustakhimov, I. I., & Trotsenko, Y. A. (2015). Acetate kinase-an enzyme of the postulated phosphoketolase pathway in *Methylomicrobium alcaliphilum* 20Z. *Antonie van Leeuwenhoek*, *108*(4), 965–974. https://doi.org/10.1007/s10482-015-0549-5
Saidi-Mehrabad, A., He, Z., Tamas, I., Sharp, C. E., Brady, A. L., Rochman, F. F., Bodrossy, L., Abell, G. C., Penner, T., Dong, X., Sensen, C. W., & Dunfield, P. F. (2013). Methanotrophic bacteria in oilsands tailings ponds of northern Alberta. *The ISME Journal*, *7*(5), 908–921. https://doi.org/10.1038/ismej.2012.163
Salem, A. R., Hacking, A. J., & Quayle, J. R. (1973). Cleavage of malyl-coenzyme A into acetyl-coenzyme A and glyoxylate by *Pseudomonas* AM1 and other C_1-unit-utilizing bacteria. *Biochemical Journal*, *136*(1), 89–96. https://doi.org/10.1042/bj1360089
Salisbury, S. A., Forrest, H. S., Cruse, W. B. T., & Kennard, O. (1979). A novel coenzyme from bacterial primary alcohol dehydrogenases. *Nature*, *280*(5725), 843–844. https://doi.org/10.1038/280843a0
Sánchez, B., Zúñiga, M., González-Candelas, F., de los Reyes-Gavilán, C. G., & Margolles, A. (2010). Bacterial and Eukaryotic Phosphoketolases: Phylogeny, Distribution and Evolution. *Journal of Molecular Microbiology and Biotechnology*, *18*(1), 37–51. https://doi.org/10.1159/000274310
Sato, T., & Atomi, H. (2010). Microbial Inorganic Carbon Fixation. In *ELS*. American Cancer Society. https://doi.org/10.1002/9780470015902.a0021900
Sazinsky, M. H., Bard, J., Donato, A. D., & Lippard, S. J. (2004). Crystal Structure of the Toluene/*o*-Xylene Monooxygenase Hydroxylase from *Pseudomonas stutzeri* OX1. *Journal of Biological Chemistry*, *279*(29), 30600–30610. https://doi.org/10.1074/jbc.M400710200
Sazinsky, M. H., & Lippard, S. J. (2005). Product Bound Structures of the Soluble Methane Monooxygenase Hydroxylase from *Methylococcus capsulatus* (Bath): Protein Motion in the α-Subunit. *Journal of the American Chemical Society*, *127*(16), 5814–5825. https://doi.org/10.1021/ja044099b
Sazinsky, M. H., & Lippard, S. J. (2006). Correlating Structure with Function in Bacterial Multicomponent Monooxygenases and Related Diiron Proteins. *Accounts of Chemical Research*, *39*(8), 558–566. https://doi.org/10.1021/ar030204v
Scanlan, J., Dumont, M. G., & Murrell, J. C. (2009). Involvement of MmoR and MmoG in the transcriptional activation of soluble methane monooxygenase genes in *Methylosinus trichosporium* OB3b. *FEMS Microbiology Letters*, *301*(2), 181–187. https://doi.org/10.1111/j.1574-6968.2009.01816.x
Schaefer, J. K., Yagi, J., Reinfelder, J. R., Cardona, T., Ellickson, K. M., Tel-Or, S., & Barkay, T. (2004). Role of the Bacterial Organomercury Lyase (MerB) in Controlling Methylmercury Accumulation in Mercury-Contaminated Natural Waters. *Environmental Science & Technology*, *38*(16), 4304–4311. https://doi.org/10.1021/es049895w
Schäfer, A., Tauch, A., Jäger, W., Kalinowski, J., Thierbach, G., & Pühler, A. (1994). Small mobilizable multi-purpose cloning vectors derived from the *Escherichia coli* plasmids pK18 and pK19: Selection of defined deletions in the chromosome of *Corynebacterium glutamicum*. *Gene*, *145*(1), 69–73. https://doi.org/10.1016/0378-1119(94)90324-7

Schauer, K., Rodionov, D. A., & de Reuse, H. (2008). New substrates for TonB-dependent transport: Do we only see the 'tip of the iceberg'? *Trends in Biochemical Sciences*, *33*(7), 330–338. https://doi.org/10.1016/j.tibs.2008.04.012

Scheutz, C., Kjeldsen, P., Bogner, J. E., De Visscher, A., Gebert, J., Hilger, H. A., Huber-Humer, M., & Spokas, K. (2009). Microbial methane oxidation processes and technologies for mitigation of landfill gas emissions. *Waste Management & Research*, *27*(5), 409–455. https://doi.org/10.1177/0734242X09339325

Schilsky, M. L. (2001). Treatment of Wilson's disease: What are the relative roles of penicillamine, trientine, and zinc supplementation? *Current Gastroenterology Reports*, *3*(1), 54–59. https://doi.org/10.1007/s11894-001-0041-4

Schilsky, M. L. (2014). Liver transplantation for Wilson's disease. *Annals of the New York Academy of Sciences*, *1315*(1), 45–49. https://doi.org/10.1111/nyas.12454

Schmehl, M., Jahn, A., Meyer zu Vilsendorf, A., Hennecke, S., Masepohl, B., Schuppler, M., Marxer, M., Oelze, J., & Klipp, W. (1993). Identification of a new class of nitrogen fixation genes in *Rhodobacter capsalatus*: A putative membrane complex involved in electron transport to nitrogenase. *Molecular and General Genetics MGG*, *241–241*(5–6), 602–615. https://doi.org/10.1007/BF00279903

Schmidt, S., Christen, P., Kiefer, P., & Vorholt, J. A. (2010). Functional investigation of methanol dehydrogenase-like protein XoxF in *Methylobacterium extorquens* AM1. *Microbiology, 156*(8), 2575–2586. https://doi.org/10.1099/mic.0.038570-0

Schmittgen, T. D., & Livak, K. J. (2008). Analyzing real-time PCR data by the comparative C_T method. *Nature Protocols*, *3*(6), 1101–1108. https://doi.org/10.1038/nprot.2008.73

Sehnal, D., Rose, A., Koca, J., Burley, S., & Velankar, S. (2018). Mol*: Towards a Common Library and Tools for Web Molecular Graphics. *Workshop on Molecular Graphics and Visual Analysis of Molecular Data*, 5 pages. https://doi.org/10.2312/MOLVA.20181103

Semrau, J. D., & DiSpirito, A. A. (2019). Methanobactin: A Novel Copper-Binding Compound Produced by Methanotrophs. In E. Y. Lee (Ed.), *Methanotrophs: Microbiology Fundamentals and Biotechnological Applications* (pp. 205–229). Springer International Publishing. https://doi.org/10.1007/978-3-030-23261-0_7

Semrau, J. D., DiSpirito, A. A., Gu, W., & Yoon, S. (2018). Metals and Methanotrophy. *Applied and Environmental Microbiology*, *84*(6). https://doi.org/10.1128/AEM.02289-17

Semrau, J. D., DiSpirito, A. A., Obulisamy, P. K., & Kang-Yun, C. S. (2020). Methanobactin from methanotrophs: Genetics, structure, function and potential applications. *FEMS Microbiology Letters*, *367*(5). https://doi.org/10.1093/femsle/fnaa045

Semrau, J. D., DiSpirito, A. A., & Yoon, S. (2010). Methanotrophs and copper. *FEMS Microbiology Reviews*, *34*(4), 496–531. https://doi.org/10.1111/j.1574-6976.2010.00212.x

Semrau, J. D., Jagadevan, S., DiSpirito, A. A., Khalifa, A., Scanlan, J., Bergman, B. H., Freemeier, B. C., Baral, B. S., Bandow, N. L., Vorobev, A., Haft, D. H., Vuilleumier, S., & Murrell, J. C. (2013). Methanobactin and MmoD work in concert to act as the 'copper-switch' in methanotrophs. *Environmental Microbiology*, *15*(11), 3077–3086. https://doi.org/10.1111/1462-2920.12150

Shchukin, V. N., Khmelenina, V. N., Eshinimayev, B. Ts., Suzina, N. E., & Trotsenko, Yu. A. (2011). Primary characterization of dominant cell surface proteins of halotolerant methanotroph *Methylomicrobium alcaliphilum* 20Z. *Microbiology*, *80*(5), 608. https://doi.org/10.1134/S0026261711050122

Simão, F. A., Waterhouse, R. M., Ioannidis, P., Kriventseva, E. V., & Zdobnov, E. M. (2015). BUSCO: Assessing genome assembly and annotation completeness with single-copy orthologs. *Bioinformatics*, *31*(19), 3210–3212. https://doi.org/10.1093/bioinformatics/btv351

Simon, R., Priefer, U., & Pühler, A. (1983). A Broad Host Range Mobilization System for In Vivo Genetic Engineering: Transposon Mutagenesis in Gram Negative Bacteria. *Bio/Technology*, *1*(9), 784–791. https://doi.org/10.1038/nbt1183-784

Sirajuddin, S., & Rosenzweig, A. C. (2015). Enzymatic Oxidation of Methane. *Biochemistry*, *54*(14), 2283–2294. https://doi.org/10.1021/acs.biochem.5b00198

Skovran, E., Palmer, A. D., Rountree, A. M., Good, N. M., & Lidstrom, M. E. (2011). XoxF Is Required for Expression of Methanol Dehydrogenase in *Methylobacterium extorquens* AM1. *Journal of Bacteriology*, *193*(21), 6032–6038. https://doi.org/10.1128/JB.05367-11

Smith, S. D., Bridou, R., Johs, A., Parks, J. M., Elias, D. A., Hurt, R. A., Brown, S. D., Podar, M., & Wall, J. D. (2015). Site-Directed Mutagenesis of HgcA and HgcB Reveals Amino Acid Residues Important for Mercury Methylation. *Applied and Environmental Microbiology*, *81*(9), 3205–3217. https://doi.org/10.1128/AEM.00217-15

Smith, T. J., Slade, S. E., Burton, N. P., Murrell, J. C., & Dalton, H. (2002). Improved System for Protein Engineering of the Hydroxylase Component of Soluble Methane Monooxygenase. *Applied and Environmental Microbiology*, *68*(11), 5265–5273. https://doi.org/10.1128/AEM.68.11.5265-5273.2002

Soares, J. R., Cassman, N. A., Kielak, A. M., Pijl, A., Carmo, J. B., Lourenço, K. S., Laanbroek, H. J., Cantarella, H., & Kuramae, E. E. (2016). Nitrous oxide emission related to ammonia-oxidizing bacteria and mitigation options from N fertilization in a tropical soil. *Scientific Reports*, *6*(1), 30349. https://doi.org/10.1038/srep30349

Söhngen, N. L. (1906). Über Bakterien, welche Methan als Kohlenstoffnahrung und Energiequelle gebrauchen. *Centralbl. Bakt. Parasitenk. II. Abt.*, *15*, 513–517.

Sorokin, D. Yu., Jones, B. E., & Gijs Kuenen, J. (2000). An obligate methylotrophic, methane-oxidizing *Methylomicrobium* species from a highly alkaline environment. *Extremophiles*, *4*(3), 145–155. https://doi.org/10.1007/s007920070029

Southworth, G. R., Peterson, M. J., & Bogle, M. A. (2002). Effect of point source removal on mercury bioaccumulation in an industrial pond. *Chemosphere*, *49*(5), 455–460. https://doi.org/10.1016/S0045-6535(02)00249-7

Sowell, S. M., Abraham, P. E., Shah, M., Verberkmoes, N. C., Smith, D. P., Barofsky, D. F., & Giovannoni, S. J. (2011). Environmental proteomics of microbial plankton in a highly productive coastal upwelling system. *The ISME Journal*, *5*(5), 856–865. https://doi.org/10.1038/ismej.2010.168

Springer, A. L., Auman, A. J., & Lidstrom, M. E. (1998). Sequence and characterization of *mxaB*, a response regulator involved in regulation of methanol oxidation, and of *mxaW*, a methanol-regulated gene in *Methylobacterium extorquens* AM1. *FEMS Microbiology Letters*, *160*(1), 119–124. https://doi.org/10.1111/j.1574-6968.1998.tb12900.x

Springer, A. L., Morris, C. J., & Lidstrom, M. E. (1997). Molecular analysis of *mxbD* and *mxbM*, a putative sensor-regulator pair required for oxidation of methanol in *Methylobacterium extorquens* AM1. *Microbiology, 143*(5), 1737–1744. https://doi.org/10.1099/00221287-143-5-1737

Sprouffske, K., & Wagner, A. (2016). Growthcurver: An R package for obtaining interpretable metrics from microbial growth curves. *BMC Bioinformatics*, *17*(1), 172. https://doi.org/10.1186/s12859-016-1016-7

Squitti, R. (2012). Copper dysfunction in Alzheimer's disease: From meta-analysis of biochemical studies to new insight into genetics. *Journal of Trace Elements in Medicine and Biology*, *26*(2), 93–96. https://doi.org/10.1016/j.jtemb.2012.04.012

Squitti, R., Siotto, M., & Polimanti, R. (2014). Low-copper diet as a preventive strategy for Alzheimer's disease. *Neurobiology of Aging*, *35*, S40–S50. https://doi.org/10.1016/j.neurobiolaging.2014.02.031

Srinivas, V., Banerjee, R., Lebrette, H., Jones, J. C., Aurelius, O., Kim, I.-S., Pham, C. C., Gul, S., Sutherlin, K., Bhowmick, A., John, J., Bozkurt, E., Fransson, T., Aller, P., Butryn, A., Bogacz, I., Simon, P. S., Keable, S., Britz, A., … Högbom, M. (2020). High Resolution XFEL Structure of the Soluble Methane Monooxygenase Hydroxylase Complex with its Regulatory Component at Ambient Temperature in Two Oxidation States. *Journal of the American Chemical Society*, jacs.0c05613. https://doi.org/10.1021/jacs.0c05613

Stafford, G. P., Scanlan, J., McDonald, I. R., & Murrell, J. C. (2003). *RpoN*, *mmoR* and *mmoG*, genes involved in regulating the expression of soluble methane monooxygenase in *Methylosinus trichosporium* OB3b. *Microbiology*, *149*(7), 1771–1784. https://doi.org/10.1099/mic.0.26060-0

Stainthorpe, A. C., Lees, V., Salmond, G. P. C., Dalton, H., & Murrell, J. C. (1990). The methane monooxygenase gene cluster of *Methylococcus capsulatus* (Bath). *Gene*, *91*(1), 27–34. https://doi.org/10.1016/0378-1119(90)90158-N

Stanley, S. H., Prior, S. D., Leak, D. J., & Dalton, H. (1983). Copper stress underlies the fundamental change in intracellular location of methane mono-oxygenase in methane-oxidizing organisms: Studies in batch and continuous cultures. *Biotechnology Letters*, *5*(7), 487–492. https://doi.org/10.1007/BF00132233

Stoecker, K., Bendinger, B., Schöning, B., Nielsen, P. H., Nielsen, J. L., Baranyi, C., Toenshoff, E. R., Daims, H., & Wagner, M. (2006). Cohn's *Crenothrix* is a filamentous methane oxidizer with an unusual methane monooxygenase. *Proceedings of the National Academy of Sciences*, *103*(7), 2363–2367. https://doi.org/10.1073/pnas.0506361103

Stolyar, S., Costello, A. M., Peeples, T. L., & Lidstrom, M. E. (1999). Role of multiple gene copies in particulate methane monooxygenase activity in the methane-oxidizing bacterium *Methylococcus capsulatus* Bath. *Microbiology*, *145*(5), 1235–1244. https://doi.org/10.1099/13500872-145-5-1235

Stolyar, S., Franke, M., & Lidstrom, M. E. (2001). Expression of Individual Copies of *Methylococcus capsulatus* Bath Particulate Methane Monooxygenase Genes. *Journal of Bacteriology*, *183*(5), 1810–1812. https://doi.org/10.1128/JB.183.5.1810-1812.2001

Strøm, T., Ferenci, T., & Quayle, J. R. (1974). The carbon assimilation pathways of *Methylococcus capsulatus*, *Pseudomonas methanica* and *Methylosinus trichosporium* (OB3B) during growth on methane. *Biochemical Journal*, *144*(3), 465–476. https://doi.org/10.1042/bj1440465

Studer, A., McAnulla, C., Büchele, R., Leisinger, T., & Vuilleumier, S. (2002). Chloromethane-Induced Genes Define a Third C_1 Utilization Pathway in *Methylobacterium chloromethanicum* CM4. *Journal of Bacteriology*, *184*(13), 3476–3484. https://doi.org/10.1128/JB.184.13.3476-3484.2002

Takeguchi, M., Miyakawa, K., & Okura, I. (1998). Purification and properties of particulate methane monooxygenase from *Methylosinus trichosporium* OB3b. *Journal of Molecular Catalysis A: Chemical*, *132*(2), 145–153. https://doi.org/10.1016/S1381-1169(97)00275-6

Takeuchi, M., Kamagata, Y., Oshima, K., Hanada, S., Tamaki, H., Marumo, K., Maeda, H., Nedachi, M., Hattori, M., Iwasaki, W., & Sakata, S. (2014a). *Methylocaldum marinum* sp. Nov., a thermotolerant, methane-oxidizing bacterium isolated from marine sediments, and emended description of the genus *Methylocaldum*. *International Journal of Systematic and Evolutionary Microbiology*, *64*(Pt_9), 3240–3246. https://doi.org/10.1099/ijs.0.063503-0

Takeuchi, M., Katayama, T., Yamagishi, T., Hanada, S., Tamaki, H., Kamagata, Y., Oshima, K., Hattori, M., Marumo, K., Nedachi, M., Maeda, H., Suwa, Y., & Sakata, S. (2014b). *Methyloceanibacter caenitepidi* gen. Nov., sp. Nov., a facultatively methylotrophic bacterium isolated from marine sediments near a hydrothermal vent. *International Journal of Systematic and Evolutionary Microbiology*, *64*(Pt 2), 462–468. https://doi.org/10.1099/ijs.0.053397-0

Tamas, I., Smirnova, A. V., He, Z., & Dunfield, P. F. (2014). The (d)evolution of methanotrophy in the *Beijerinckiaceae*—A comparative genomics analysis. *The ISME Journal*, *8*(2), 369–382. https://doi.org/10.1038/ismej.2013.145

Tatusova, T., DiCuccio, M., Badretdin, A., Chetvernin, V., Nawrocki, E. P., Zaslavsky, L., Lomsadze, A., Pruitt, K. D., Borodovsky, M., & Ostell, J. (2016). NCBI prokaryotic genome annotation pipeline. *Nucleic Acids Research*, *44*(14), 6614–6624. https://doi.org/10.1093/nar/gkw569

Tavormina, P. L., Hatzenpichler, R., McGlynn, S., Chadwick, G., Dawson, K. S., Connon, S. A., & Orphan, V. J. (2015). *Methyloprofundus sedimenti* gen. Nov., sp. Nov., an obligate methanotroph from ocean sediment belonging to the 'deep sea-1' clade of marine methanotrophs. *International Journal of Systematic and Evolutionary Microbiology*, *65*(1), 251–259. https://doi.org/10.1099/ijs.0.062927-0

Tavormina, P. L., Orphan, V. J., Kalyuzhnaya, M. G., Jetten, M. S. M., & Klotz, M. G. (2011). A novel family of functional operons encoding methane/ammonia monooxygenase-related proteins in gammaproteobacterial methanotrophs. *Environmental Microbiology Reports*, *3*(1), 91–100. https://doi.org/10.1111/j.1758-2229.2010.00192.x

Taylor, S. C., Dalton, H., & Dow, C. S. (1981). Ribulose-1,5-bisphosphate Carboxylase/Oxygenase and Carbon Assimilation in *Methylococcus capsulatus* (Bath). *Microbiology*, *122*(1), 89–94. https://doi.org/10.1099/00221287-122-1-89

Tchounwou, P. B., Yedjou, C. G., Patlolla, A. K., & Sutton, D. J. (2012). *Heavy Metal Toxicity and the Environment*. Springer, Basel. https://doi.org/10.1007/978-3-7643-8340-4_6

Téllez, C. M., Gaus, K. P., Graham, D. W., Arnold, R. G., & Guzman, R. Z. (1998). Isolation of Copper Biochelates from *Methylosinus trichosporium* OB3b and Soluble Methane Monooxygenase Mutants. *Applied and Environmental Microbiology*, *64*(3), 1115–1122. https://doi.org/10.1128/AEM.64.3.1115-1122.1998

Timmers, P. H. A., Welte, C. U., Koehorst, J. J., Plugge, C. M., Jetten, M. S. M., & Stams, A. J. M. (2017). Reverse Methanogenesis and Respiration in Methanotrophic Archaea. *Archaea*, *2017*. http://dx.doi.org/10.1155/2017/1654237

Tinberg, C. E., & Lippard, S. J. (2010). Oxidation Reactions Performed by Soluble Methane Monooxygenase Hydroxylase Intermediates H_{peroxo} and Q Proceed by Distinct Mechanisms. *Biochemistry*, *49*(36), 7902–7912. https://doi.org/10.1021/bi1009375

Trotsenko, Y. A., & Murrell, J. C. (2008). Metabolic Aspects of Aerobic Obligate Methanotrophy. In *Advances in Applied Microbiology* (Vol. 63, pp. 183–229). Academic Press. https://doi.org/10.1016/S0065-2164(07)00005-6

Tsubota, J., Eshinimaev, B. Ts., Khmelenina, V. N., & Trotsenko, Y. A. (2005). *Methylothermus thermalis* gen. Nov., sp. Nov., a novel moderately thermophilic obligate methanotroph from a hot spring in Japan. *International Journal of Systematic and Evolutionary Microbiology*, *55*(5), 1877–1884. https://doi.org/10.1099/ijs.0.63691-0

Tveit, A. T., Hestnes, A. G., Robinson, S. L., Schintlmeister, A., Dedysh, S. N., Jehmlich, N., Bergen, M. von, Herbold, C., Wagner, M., Richter, A., & Svenning, M. M. (2019). Widespread soil bacterium that oxidizes atmospheric methane. *Proceedings of the National Academy of Sciences*, *116*(17), 8515–8524. https://doi.org/10.1073/pnas.1817812116

Ukaegbu, U. E., & Rosenzweig, A. C. (2009). Structure of the Redox Sensor Domain of *Methylococcus capsulatus* (Bath) MmoS. *Biochemistry*, *48*(10), 2207–2215. https://doi.org/10.1021/bi8019614

US EPA, O. (2020, February 4). *Inventory of U.S. Greenhouse Gas Emissions and Sinks: 1990-2018* [Reports and Assessments]. US EPA. https://www.epa.gov/ghgemissions/inventory-us-greenhouse-gas-emissions-and-sinks-1990-2018

Vallenet, D., Calteau, A., Dubois, M., Amours, P., Bazin, A., Beuvin, M., Burlot, L., Bussell, X., Fouteau, S., Gautreau, G., Lajus, A., Langlois, J., Planel, R., Roche, D., Rollin, J., Rouy, Z., Sabatet, V., & Médigue, C. (2019). MicroScope: An integrated platform for the annotation and exploration of microbial gene functions through genomic, pangenomic and metabolic comparative analysis. *Nucleic Acids Research*, gkz926. https://doi.org/10.1093/nar/gkz926

van Spanning, R. J., Wansell, C. W., De Boer, T., Hazelaar, M. J., Anazawa, H., Harms, N., Oltmann, L. F., & Stouthamer, A. H. (1991). Isolation and characterization of the *moxJ*, *moxG*, *moxI*, and *moxR* genes of *Paracoccus denitrificans*: Inactivation of *moxJ*, *moxG*, and *moxR* and the resultant effect on methylotrophic growth. *Journal of Bacteriology*, *173*(21), 6948–6961. https://doi.org/10.1128/JB.173.21.6948-6961.1991

van Teeseling, M. C. F., Pol, A., Harhangi, H. R., van der Zwart, S., Jetten, M. S. M., Op den Camp, H. J. M., & van Niftrik, L. (2014). Expanding the Verrucomicrobial Methanotrophic World: Description of Three Novel Species of *Methylacidimicrobium* gen. nov. *Applied and Environmental Microbiology*, *80*(21), 6782–6791. https://doi.org/10.1128/AEM.01838-14

Ve, T., Mathisen, K., Helland, R., Karlsen, O. A., Fjellbirkeland, A., Røhr, Å. K., Andersson, K. K., Pedersen, R.-B., Lillehaug, J. R., & Jensen, H. B. (2012). The *Methylococcus capsulatus* (Bath) Secreted Protein, MopE*, Binds Both Reduced and Oxidized Copper. *PLOS ONE*, *7*(8), e43146. https://doi.org/10.1371/journal.pone.0043146

Vernikos, G. S., & Parkhill, J. (2006). Interpolated variable order motifs for identification of horizontally acquired DNA: Revisiting the *Salmonella* pathogenicity islands. *Bioinformatics*, *22*(18), 2196–2203. https://doi.org/10.1093/bioinformatics/btl369

Versantvoort, W., Guerrero-Cruz, S., Speth, D. R., Frank, J., Gambelli, L., Cremers, G., van Alen, T., Jetten, M. S. M., Kartal, B., Op den Camp, H. J. M., & Reimann, J. (2018). Comparative Genomics of *Candidatus* Methylomirabilis Species and Description of *Ca.* Methylomirabilis Lanthanidiphila. *Frontiers in Microbiology*, *9*. https://doi.org/10.3389/fmicb.2018.01672

Vigliotta, G., Nutricati, E., Carata, E., Tredici, S. M., Stefano, M. D., Pontieri, P., Massardo, D. R., Prati, M. V., Bellis, L. D., & Alifano, P. (2007). *Clonothrix fusca* Roze 1896, a Filamentous, Sheathed, Methanotrophic γ-Proteobacterium. *Applied and Environmental Microbiology*, *73*(11), 3556–3565. https://doi.org/10.1128/AEM.02678-06

Vishnivetskaya, T. A., Mosher, J. J., Palumbo, A. V., Yang, Z. K., Podar, M., Brown, S. D., Brooks, S. C., Gu, B., Southworth, G. R., Drake, M. M., Brandt, C. C., & Elias, D. A. (2011). Mercury and Other Heavy Metals Influence Bacterial Community Structure in Contaminated Tennessee Streams. *Applied and Environmental Microbiology*, *77*(1), 302–311. https://doi.org/10.1128/AEM.01715-10

Vorholt, J. A. (2002). Cofactor-dependent pathways of formaldehyde oxidation in methylotrophic bacteria. *Archives of Microbiology*, *178*(4), 239–249. https://doi.org/10.1007/s00203-002-0450-2

Vorholt, J. A., Chistoserdova, L., Lidstrom, M. E., & Thauer, R. K. (1998). The NADP-Dependent Methylene Tetrahydromethanopterin Dehydrogenase in *Methylobacterium extorquens* AM1. *Journal of Bacteriology*, *180*(20), 5351–5356. https://doi.org/10.1128/JB.180.20.5351-5356.1998

Vorholt, J. A., Marx, C. J., Lidstrom, M. E., & Thauer, R. K. (2000). Novel Formaldehyde-Activating Enzyme in *Methylobacterium extorquens* AM1 Required for Growth on Methanol. *Journal of Bacteriology*, *182*(23), 6645–6650. https://doi.org/10.1128/JB.182.23.6645-6650.2000

Vorobev, A. V., Baani, M., Doronina, N. V., Brady, A. L., Liesack, W., Dunfield, P. F., & Dedysh, S. N. (2011). *Methyloferula stellata* gen. Nov., sp. Nov., an acidophilic, obligately methanotrophic bacterium that possesses only a soluble methane monooxygenase. *International Journal of Systematic and Evolutionary Microbiology*, *61*(10), 2456–2463. https://doi.org/10.1099/ijs.0.028118-0

Vorobev, A. V., Jagadevan, S., Baral, B. S., DiSpirito, A. A., Freemeier, B. C., Bergman, B. H., Bandow, N. L., & Semrau, J. D. (2013). Detoxification of Mercury by Methanobactin from *Methylosinus trichosporium* OB3b. *Applied and Environmental Microbiology*, *79*(19), 5918–5926. https://doi.org/10.1128/AEM.01673-13

Vu, H. N., Subuyuj, G. A., Vijayakumar, S., Good, N. M., Martinez-Gomez, N. C., & Skovran, E. (2016). Lanthanide-Dependent Regulation of Methanol Oxidation Systems in *Methylobacterium extorquens* AM1 and Their Contribution to Methanol Growth. *Journal of Bacteriology*, *198*(8), 1250–1259. https://doi.org/10.1128/JB.00937-15

Wagih, O. (2017). ggseqlogo: A versatile R package for drawing sequence logos. *Bioinformatics*, *33*(22), 3645–3647. https://doi.org/10.1093/bioinformatics/btx469

Wallar, B. J., & Lipscomb, J. D. (2001). Methane Monooxygenase Component B Mutants Alter the Kinetics of Steps Throughout the Catalytic Cycle. *Biochemistry*, *40*(7), 2220–2233. https://doi.org/10.1021/bi002298b

Wang, V. C.-C., Maji, S., Chen, P. P.-Y., Lee, H. K., Yu, S. S.-F., & Chan, S. I. (2017). Alkane Oxidation: Methane Monooxygenases, Related Enzymes, and Their Biomimetics. *Chemical Reviews*, *117*(13), 8574–8621. https://doi.org/10.1021/acs.chemrev.6b00624

Wang, W., Liang, A. D., & Lippard, S. J. (2015). Coupling Oxygen Consumption with Hydrocarbon Oxidation in Bacterial Multicomponent Monooxygenases. *Accounts of Chemical Research*, *48*(9), 2632–2639. https://doi.org/10.1021/acs.accounts.5b00312

Wang, Y., Graichen, M. E., Liu, A., Pearson, A. R., Wilmot, C. M., & Davidson, V. L. (2003). MauG, a Novel Diheme Protein Required for Tryptophan Tryptophylquinone Biogenesis. *Biochemistry*, *42*(24), 7318–7325. https://doi.org/10.1021/bi034243q

Wang, Y., Schaefer, J. K., Mishra, B., & Yee, N. (2016). Intracellular Hg(0) Oxidation in *Desulfovibrio desulfuricans* ND132. *Environmental Science & Technology*, *50*(20), 11049–11056. https://doi.org/10.1021/acs.est.6b03299

Wehrmann, M., Berthelot, C., Billard, P., & Klebensberger, J. (2019). Rare Earth Element (REE)-Dependent Growth of *Pseudomonas putida* KT2440 Relies on the ABC-Transporter PedA1A2BC and Is Influenced by Iron Availability. *Frontiers in Microbiology*, *10*. https://doi.org/10.3389/fmicb.2019.02494

Weiss, A. A., Murphy, S. D., & Silver, S. (1977). Mercury and Organomercurial Resistances Determined by Plasmids in Staphylococcus aureus. *Journal of Bacteriology*, *132*(1), 197–208. https://doi.org/10.1128/JB.132.1.197-208.1977

Wellner, A., Lurie, M. N., & Gophna, U. (2007). Complexity, connectivity, and duplicability as barriers to lateral gene transfer. *Genome Biology*, *8*(8), R156. https://doi.org/10.1186/gb-2007-8-8-r156

Wernersson, R. (2005). FeatureExtract—Extraction of sequence annotation made easy. *Nucleic Acids Research*, *33*(Web Server), W567–W569. https://doi.org/10.1093/nar/gki388

West, S. A., Diggle, S. P., Buckling, A., Gardner, A., & Griffin, A. S. (2007). The Social Lives of Microbes. *Annual Review of Ecology, Evolution, and Systematics*, *38*(1), 53–77. https://doi.org/10.1146/annurev.ecolsys.38.091206.095740

West, S. A., Griffin, A. S., Gardner, A., & Diggle, S. P. (2006). Social evolution theory for microorganisms. *Nature Reviews Microbiology*, *4*(8), 597–607. https://doi.org/10.1038/nrmicro1461

Whalen, S. C., & Reeburgh, W. S. (1990). Consumption of atmospheric methane by tundra soils. *Nature*, *346*(6280), 160–162. https://doi.org/10.1038/346160a0

White, S., Boyd, G., Mathews, F. S., Xia, Z. X., Dai, W. W., Zhang, Y. F., & Davidson, V. L. (1993). The active site structure of the calcium-containing quinoprotein methanol dehydrogenase. *Biochemistry*, *32*(48), 12955–12958. https://doi.org/10.1021/bi00211a002

Whittenbury, R., Davies, S. L., & Davey, J. F. (1970a). Exospores and cysts formed by methane-utilizing bacteria. *Journal of General Microbiology*, *61*(2), 219–226. https://doi.org/10.1099/00221287-61-2-219

Whittenbury, R., Phillips, K. C., & Wilkinson, J. F. (1970b). Enrichment, Isolation and Some Properties of Methane-utilizing Bacteria. *Journal of General Microbiology*, *61*(2), 205–218. https://doi.org/10.1099/00221287-61-2-205

Whittington, D. A., Rosenzweig, A. C., Frederick, C. A., & Lippard, S. J. (2001). Xenon and Halogenated Alkanes Track Putative Substrate Binding Cavities in the Soluble Methane Monooxygenase Hydroxylase. *Biochemistry*, *40*(12), 3476–3482. https://doi.org/10.1021/bi0022487

Wick, R. R. (2018, October 18). *Porechop: An adapter trimmer for Oxford Nanopore reads*. Porechop. https://github.com/rrwick/Porechop

Wick, R. R., Judd, L. M., Gorrie, C. L., & Holt, K. E. (2017). Unicycler: Resolving bacterial genome assemblies from short and long sequencing reads. *PLOS Computational Biology*, *13*(6), e1005595. https://doi.org/10.1371/journal.pcbi.1005595

Wick, R. R., Judd, L. M., & Holt, K. E. (2019). Performance of neural network basecalling tools for Oxford Nanopore sequencing. *Genome Biology*, *20*(1), 129. https://doi.org/10.1186/s13059-019-1727-y

Wick, R. R., Schultz, M. B., Zobel, J., & Holt, K. E. (2015). Bandage: Interactive visualization of *de novo* genome assemblies. *Bioinformatics*, *31*(20), 3350–3352. https://doi.org/10.1093/bioinformatics/btv383

Wijekoon, C. J. K., Young, T. R., Wedd, A. G., & Xiao, Z. (2015). CopC Protein from *Pseudomonas fluorescens* SBW25 Features a Conserved Novel High-Affinity Cu(II) Binding Site. *Inorganic Chemistry*, *54*(6), 2950–2959. https://doi.org/10.1021/acs.inorgchem.5b00031

Williams, P. A., Coates, L., Mohammed, F., Gill, R., Erskine, P. T., Coker, A., Wood, S. P., Anthony, C., & Cooper, J. B. (2005). The atomic resolution structure of methanol dehydrogenase from *Methylobacterium extorquens*. *Acta Crystallographica Section D: Biological Crystallography*, *61*(1), 75–79. https://doi.org/10.1107/S0907444904026964

Wise, M. G., McArthur, J. V., & Shimkets, L. J. (1999). Methanotroph Diversity in Landfill Soil: Isolation of Novel Type I and Type II Methanotrophs Whose Presence Was Suggested by Culture-Independent 16S Ribosomal DNA Analysis. *Applied and Environmental Microbiology*, *65*(11), 4887–4897.

Wise, M. G., McArthur, J. V., & Shimkets, L. J. (2001). *Methylosarcina fibrata* gen. Nov., sp. Nov. And *Methylosarcina quisquiliarum* sp. Nov., novel type I methanotrophs. *International Journal of Systematic and Evolutionary Microbiology*, 11.

Woodland, M. P., & Dalton, H. (1984). Purification and characterization of component A of the methane monooxygenase from *Methylococcus capsulatus* (Bath). *Journal of Biological Chemistry*, *259*(1), 53–59.

Wu, M. L., Ettwig, K. F., Jetten, M. S. M., Strous, M., Keltjens, J. T., & Niftrik, L. van. (2011). A new intra-aerobic metabolism in the nitrite-dependent anaerobic methane-oxidizing bacterium *Candidatus* 'Methylomirabilis oxyfera.' *Biochemical Society Transactions*, *39*(1), 243–248. https://doi.org/10.1042/BST0390243

Wu, M. L., Teeseling, M. C. F. van, Willems, M. J. R., Donselaar, E. G. van, Klingl, A., Rachel, R., Geerts, W. J. C., Jetten, M. S. M., Strous, M., & Niftrik, L. van. (2012). Ultrastructure of the Denitrifying Methanotroph "*Candidatus* Methylomirabilis oxyfera," a Novel Polygon-Shaped Bacterium. *Journal of Bacteriology*, *194*(2), 284–291. https://doi.org/10.1128/JB.05816-11

Wu, M. L., Wessels, H. J. C. T., Pol, A., Camp, H. J. M. O. den, Jetten, M. S. M., Niftrik, L. van, & Keltjens, J. T. (2015). XoxF-Type Methanol Dehydrogenase from the Anaerobic Methanotroph "*Candidatus* Methylomirabilis oxyfera." *Applied and Environmental Microbiology*, *81*(4), 1442–1451. https://doi.org/10.1128/AEM.03292-14

Xia, Z., Dai, W., Zhang, Y., White, S. A., Boyd, G. D., & Mathews, S. F. (1996). Determination of the Gene Sequence and the Three-dimensional Structure at 2.4 Å Resolution of Methanol Dehydrogenase from *Methylophilus* W3A1. *Journal of Molecular Biology*, *259*(3), 480–501. https://doi.org/10.1006/jmbi.1996.0334

Xia, Z. X., Dai, W. W., Xiong, J. P., Hao, Z. P., Davidson, V. L., White, S., & Mathews, F. S. (1992). The three-dimensional structures of methanol dehydrogenase from two methylotrophic bacteria at 2.6-Å resolution. *Journal of Biological Chemistry*, *267*(31), 22289–22297.

Xia, Z.-X., Dai, W.-W., He, Y.-N., White, S. A., Mathews, F. S., & Davidson, V. L. (2003). X-ray structure of methanol dehydrogenase from *Paracoccus denitrificans* and molecular modeling of its interactions with cytochrome *c*-551i. *JBIC Journal of Biological Inorganic Chemistry*, *8*(8), 843–854. https://doi.org/10.1007/s00775-003-0485-0

Yan, X., Chu, F., Puri, A. W., Fu, Y., & Lidstrom, M. E. (2016). Electroporation-Based Genetic Manipulation in Type I Methanotrophs. *Applied and Environmental Microbiology*, *82*(7), 2062–2069. https://doi.org/10.1128/AEM.03724-15

Yavitt, J. B., Downey, D. M., Lang, G. E., & Sexston, A. J. (1990). Methane consumption in two temperate forest soils. *Biogeochemistry*, *9*(1), 39–52. https://doi.org/10.1007/BF00002716

Yin, T., Cook, D., & Lawrence, M. (2012). ggbio: An R package for extending the grammar of graphics for genomic data. *Genome Biology*, *13*(8), R77. https://doi.org/10.1186/gb-2012-13-8-r77

Yin, X., Wang, L., Zhang, L., Chen, H., Liang, X., Lu, X., DiSpirito, A. A., Semrau, J. D., & Gu, B. (2020). Synergistic Effects of a Chalkophore, Methanobactin, on Microbial Methylation of Mercury. *Applied and Environmental Microbiology*, *86*(11). https://doi.org/10.1128/AEM.00122-20

Yoon, S., & Semrau, J. D. (2008). Measurement and modeling of multiple substrate oxidation by methanotrophs at 20 °C. *FEMS Microbiology Letters*, *287*(2), 156–162. https://doi.org/10.1111/j.1574-6968.2008.01314.x

Yoon, S.-H., Ha, S., Lim, J., Kwon, S., & Chun, J. (2017). A large-scale evaluation of algorithms to calculate average nucleotide identity. *Antonie van Leeuwenhoek*, *110*(10), 1281–1286. https://doi.org/10.1007/s10482-017-0844-4

Yu, G., Smith, D. K., Zhu, H., Guan, Y., & Lam, T. T. (2017). ggtree: An R package for visualization and annotation of phylogenetic trees with their covariates and other associated data. *Methods in Ecology and Evolution*, *8*(1), 28–36. https://doi.org/10.1111/2041-210X.12628

Zahn, J. A., Bergmann, D. J., Boyd, J. M., Kunz, R. C., & DiSpirito, A. A. (2001). Membrane-Associated Quinoprotein Formaldehyde Dehydrogenase from *Methylococcus capsulatus* Bath. *Journal of Bacteriology*, *183*(23), 6832–6840. https://doi.org/10.1128/JB.183.23.6832-6840.2001

Zahn, J. A., & DiSpirito, A. A. (1996). Membrane-associated methane monooxygenase from *Methylococcus capsulatus* (Bath). *Journal of Bacteriology*, *178*(4), 1018–1029. https://doi.org/10.1128/jb.178.4.1018-1029.1996

Zatman, L. (1981). A search for patterns in methylotrophic pathways. In H. Dalton (Ed.), *Microbial growth on C_1 compounds: Proceedings of the third international symposium held in Sheffield, UK 12-16 August 1980*. Heyden.

Zheng, Y.-J., Xia, Z., Chen, Z., Mathews, F. S., & Bruice, T. C. (2001). Catalytic mechanism of quinoprotein methanol dehydrogenase: A theoretical and x-ray crystallographic investigation. *Proceedings of the National Academy of Sciences*, *98*(2), 432–434. https://doi.org/10.1073/pnas.98.2.432

Zhou, X.-Q., Hao, Y.-Y., Gu, B., Feng, J., Liu, Y.-R., & Huang, Q. (2020). Microbial Communities Associated with Methylmercury Degradation in Paddy Soils. *Environmental Science & Technology*, *54*(13), 7952–7960. https://doi.org/10.1021/acs.est.0c00181

Zischka, H., Lichtmannegger, J., DiSpirito, A. A., & Semrau, J. D. (2017). *Means and methods for treating copper-related diseases* (World Intellectual Property Organization Patent No. WO2017103094A2). https://patents.google.com/patent/WO2017103094A2/en